FOREWORD

The research program summarized in this report was initiated 1 June 1962 by AF Flight Dynamics Laboratory, Research and Technology Division, Wright-Patterson Air Force Base, Ohio. The research effort consisted of converting RTD's Six-Degree-of-Freedom Flight Path generalized computer program from SOS to FORTRAN/FAP computer language and was undertaken as a portion of the study conducted by McDonnell Aircraft Corporation under USAF Contract No. AF33(657)-8829 during the period 1 June 1962 to 31 December 1963. This report, prepared by A. E. Combs, McDonnell Aircraft Corporation, is essentially the original formulation report (WADD TR-60-781, Part I) with the additions, modifications, and corrections made since its publication. Mr. B. R. Benson of the AF Flight Dynamics Laboratory has been the Air Force technical representative.

This report was prepared under Project 1431, "Flight Path Analysis", Task 143103, "Six-Degree-of-Freedom Flight Path Analysis".

The authors are indebted to Messrs. D. C. Bounds and K. D. Reside of the System Technology Division for contributions to the original analytical formulation and to the following members of the McDonnell Automation Center: Messrs. F. W. Seubert and N. E. Usher for design and modification of the computing program, and R. F. Vorwald for further modification, correction, and conversion of the machine language.

For ease of reading, the documentation of this project has been prepared in several parts. The total documentation is summarized as follows:

Part I

     Volume 1 - Basic Problem Formulation

     Volume 2 - Structural Loads Formulation

     Volume 3 - Optimization Problem Formulation

Part II

     Volume 1 - User's Manual for Part I, Volume 1

     Volume 2 - User's Manual for Part I, Volume 2

     Volume 3 - User's Manual for Part 1, Volume 3

ABSTRACT

A trajectory computation program is described for determining vehicle performance throughout the entire flight regime of speed and altitude in the atmosphere and gravity field of a non-spherical rotating planet. The program is formulated for seven options of varying refinement from the six-degree-of-freedom problem to the two-degree point mass problem. A reverse option for the aerodynamic analysis of flight test data, a punched card output, and a semi-automatic computational tie to an interplanetary trajectory computer program are included. The program is specifically oriented for computation on the IBM 7090/7094 digital computer using the FAP/FORTRAN2 machine language.

This technical documentary report has been reviewed and is approved.

Philip P. Antonatos
Philip P. Antonatos
Chief Flight Mechanics Division
AF Flight Dynamics Laboratory

TABLE OF CONTENTS

SYMBOLS AND NOMENCLATURE

The symbols and nomenclature used in the formulation of the Six-Degree-of-Freedom Flight-Path Study computer program are summarized in this section. Standard symbols, currently in use in the fields to which they are applied, have been used whenever such use does not result in conflicts. Duplicity of symbols has been allowed for derivation purposes; however, all quantities computed by the program have unique symbols assigned. The engineering notation and the normal units for each quantity are included with the definition. The symbols and definitions have been subdivided according to usage as follows:

SYMBOLS	DEFINITION AND UNITS

Wind Axes Forces - Pounds

D	Drag
Y	Side Force (also inertial or space-fixed coordinate system)
L	Lift (also summation of rolling moments in the body axes system)

Body Axes Forces - Pounds

a	Axial Force
y	Side Force (also body-axes coordinate system)
n_F	Normal Force

Aerodynamic Body Axes Moments - Foot-Pounds

l	Moment About the x Axis
m	Moment About the y Axis
n	Moment About the z Axis

Coefficients - Dimensionless

C_A	Axial Force Coefficient
C_y	Side Force Coefficient (body axis)
C_N	Normal Force Coefficient
C_l	Rolling Moment Coefficient
C_m	Pitching Moment Coefficient
C_n	Yawing Moment Coefficient
C_D	Drag Coefficient
C_Y	Side Force Coefficient (wind axis)
C_L	Lift Coefficient
C_f	Skin Friction Coefficient
C_P	Pressure Coefficient
$q*$	Dynamic Pressure - pounds/square foot
R_N	Reynolds Number
μ	Coefficient of Viscosity - slugs/foot-second (also gravitational potential constant)
C_A''	Axial Force Coefficient Defined in the Plane of $\alpha_{T_1} = a/q*S$
C_N''	Normal Force Coefficient Defined in the Plane of $\alpha_{T_1} = n_F''/q*S$
C_m''	Pitching Moment Coefficient Defined in the Plane of $\alpha_{T_1} = m''/q*Sd_1$

C_{N_p}'' Magnus Force Coefficient $= \partial C_N''/\partial \ (pd_1/2V_a)$

C_{m_p}'' Magnus Moment Coefficient $= \partial C_m''/\partial \ (pd_1/2V_a)$

C_{A_o} C_A at $\alpha = \beta = 0°$ - dimensionless

C_{A_α} $\partial C_A/\partial \alpha$ - per degree

$C_{A_{\alpha^2}}$ $\partial C_A/\partial \alpha^2$ - per degree^2

C_{A_β} $\partial C_A/\partial \beta$ - per degree

$C_{A_{\beta^2}}$ $\partial C_A/\partial \beta^2$ - per degree^2

$C_{A\delta_q}$ $\partial C_A/\partial \delta_q$ - per degree

$C_{A_{\delta_q^2}}$ $\partial C/\partial \delta_q^2$ - per degree^2

$C_{A_{\alpha\beta}}$ $\partial^2 C_A/\partial \alpha \partial \beta$ - per degree^2

$C_{A_{\alpha\delta_q}}$ $\partial^2 C_A/\partial \alpha \partial \delta_q$ - per degree^2

$C_{A_{\beta\delta_q}}$ $\partial^2 C_A/\partial \beta \partial \delta_q$ - per degree^2

$(C_A)_{\delta=0}$ C_A at $\delta_p = \delta_q = \delta_r = 0°$ - dimensionless

C_{N_o} C_N at $\alpha = \beta = 0°$ - dimensionless

C_{N_α} $\partial C_N/\partial \alpha$ - per degree

$C_{N_{\alpha^2}}$ $\partial C_N/\partial \alpha^2$ - per degree^2

C_{N_β} $\partial C_N/\partial \beta$ - per degree

$C_{N_{\beta^2}}$ $\partial C_N/\partial \beta^2$ - per degree^2

$C_{N\delta_q}$ $\partial C_N/\partial \delta_q$ - per degree

$C_{N_{\delta_q 2}}$ $\partial C_N/\partial \delta_q^2$ - per degree^2

$C_{N_{\alpha\beta}}$ $\partial^2 C_N/\partial \alpha \partial \beta$ - per degree^2

$C_{N_{\alpha\delta_q}}$ $\partial^2 C_N/\partial \alpha \partial \delta_q$ - per degree^2

$C_{N_{\beta\delta_q}}$ $\partial^2 C_N/\partial \beta \partial \delta_q$ - per degree^2

$C_{N_{\dot\alpha}}$ $\partial C_N/\partial (\dot\alpha d_1/2V_a)$ - per radian

$C_{N_{\dot\alpha_x}}$ $\partial^2 C_N/\partial (\dot\alpha d_1/2V_a)\partial x_{C.G.}$ - per radian per foot

c_{N_q} $\partial c_N / \partial (q d_1 / 2 V_a)$ - per radian

$c_{N_{q_x}}$ $\partial^2 c_N / \partial (q d_1 / 2 V_a) \partial x_{C.G.}$ - per radian per foot

$(c_N)_{\delta=0}$ c_N at $\delta_p = \delta_q = \delta_r = 0°$ - dimensionless

c_{y_o} c_y at $\alpha = \beta = 0°$ - dimensionless

c_{y_α} $\partial c_y / \partial \alpha$ - per degree

$c_{y_{\alpha^2}}$ $\partial c_y / \partial \alpha^2$ - per degree^2

c_{y_β} $\partial c_y / \partial \beta$ - per degree

$c_{y_{\beta^2}}$ $\partial c_y / \partial \beta^2$ - per degree^2

$c_{y_{\delta_r}}$ $\partial c_y / \partial \delta_r$ - per degree

$c_{y_{\delta_r 2}}$ $\partial c_y / \partial \delta_r 2$ - per degree^2

$c_{y_{\alpha \delta_r}}$ $\partial^2 c_y / \partial \alpha \partial \delta_r$ - per degree^2

$c_{y_{\alpha \beta}}$ $\partial^2 c_y / \partial \alpha \partial \beta$ - per degree^2

$c_{y_{\beta \delta_r}}$ $\partial^2 c_y / \partial \beta \partial \delta_r$ - per degree^2

$c_{y_{\dot{\beta}}}$ $\partial c_y / \partial (\dot{\beta} d_2 / 2 V_a)$ - per radian

$c_{y_{\dot{\beta}_x}}$ $\partial^2 c_y / \partial (\dot{\beta} d_2 / 2 V_a) \partial x_{C.G.}$ - per radian per foot

c_{y_r} $\partial c_y / \partial (r d_2 / 2 V_a)$ - per radian

$c_{y_{r_x}}$ $\partial^2 c_y / \partial (r d_2 / 2 V_a) \partial x_{C.G.}$ - per radian per foot

$(c_y)_{\delta=0}$ c_y at $\delta_p = \delta_q = \delta_r = 0°$ - dimensionless

c_{l_o} c_l at $\alpha = \beta = 0°$ - dimensionless

c_{l_α} $\partial c_l / \partial \alpha$ - per degree

$c_{l_{\alpha^2}}$ $\partial c_l / \partial \alpha^2$ - per degree^2

c_{l_β} $\partial c_l / \partial \beta$ - per degree

$c_{l_{\beta^2}}$ $\partial c_l / \partial \beta^2$ - per degree^2

$c_{l_{\delta_p}}$ $\partial c_l / \partial \delta_p$ - per degree

$c_{l_{\delta_p^2}}$ $\partial c_l / \partial \delta_p 2$ - per degree^2

xv

$C_{l_{\alpha\beta}}$ $\partial^2 C_l / \partial\alpha\partial\beta$ - per degree^2

$C_{l_{\alpha\delta_p}}$ $\partial^2 C_l / \partial\alpha\partial\delta_p$ - per degree^2

$C_{l_{\beta\delta_p}}$ $\partial^2 C_l / \partial\beta\partial\delta_p$ - per degree^2

C_{l_p} $\partial C_l / \partial(pd_2/2V_a)$ - per radian

C_{l_r} $\partial C_l / \partial(rd_2/2V_a)$ - per radian

$C_{l_{r_x}}$ $\partial^2 C_l / \partial(rd_2/2V_a)\partial x_{C.G.}$ - per radian per foot

$(C_l)_{\delta=0}$ C_l at $\delta_p = \delta_q = \delta_r = 0^o$ - dimensionless

C_{m_o} C_m at $\alpha = \beta = 0^o$ - dimensionless

C_{m_α} $\partial C_m / \partial\alpha$ - per degree

$C_{m_{\alpha^2}}$ $\partial C_m / \partial\alpha^2$ - per degree^2

C_{m_β} $\partial C_m / \partial\beta$ - per degree

$C_{m_{\beta^2}}$ $\partial C_m / \partial\beta^2$ - per degree^2

$C_{m\delta_q}$ $\partial C_m / \partial\delta_q$ - per degree

$C_{m\delta_q^2}$ $\partial C_m / \partial\delta_q^2$ - per degree^2

$C_{m_{\alpha\beta}}$ $\partial^2 C_m / \partial\alpha\partial\beta$ - per degree^2

$C_{m_{\alpha\delta_q}}$ $\partial^2 C_m / \partial\alpha\partial\delta_q$ - per degree^2

$C_{m_{\beta\delta_q}}$ $\partial^2 C_m / \partial\beta\partial\delta_q$ - per degree^2

$C_{m_{\dot\alpha}}$ $\partial C_m / \partial(\dot\alpha d_1/2V_a)$ - per radian

$C_{m_{\dot\alpha_x}}$ $\partial^2 C_m / \partial(\dot\alpha d_1/2V_a)\partial x_{C.G.}$ - per radian per foot

C_{m_q} $\partial C_m / \partial(qd_1/2V_a)$ - per radian

$C_{m_{q_x}}$ $\partial^2 C_m / \partial(qd_1/2V_a)\partial x_{C.G.}$ - per radian per foot

$(C_m)_{\delta=0}$ C_m at $\delta_p = \delta_q = \delta_r = 0^o$ - dimensionless

C_{n_o} C_n at $\alpha = \beta = 0^o$ - dimensionless

C_{n_α} $\partial C_n / \partial\alpha$ - per degree

$C_{n_{\alpha^2}}$ $\partial C_n / \partial\alpha^2$ - per degree^2

C_{n_β} $\partial C_n / \partial\beta$ - per degree

$C_{n_{\beta^2}}$ $\partial C_n / \partial\beta^2$ - per degree^2

$C_{n\delta_r}$	$\partial C_n / \partial \delta_r$ - per degree
$C_{n\delta_r^2}$	$\partial C_n / \partial \delta_r 2$ - per degree^2
$C_{n_{\alpha\beta}}$	$\partial^2 C_n / \partial \alpha \partial \beta$ - per degree^2
$C_{n_{\alpha\delta_r}}$	$\partial^2 C_n / \partial \alpha \partial \delta_r$ - per degree^2
$C_{n_{\beta\delta_r}}$	$\partial^2 C_n / \partial \beta \partial \delta_r$ - per degree^2
$C_{n_{\dot{\beta}}}$	$\partial C_n / \partial (\dot{\beta} d_2 / 2 V_a)$ - per radian
$C_{n_{\dot{\beta}x}}$	$\partial^2 C_n / \partial (\dot{\beta} d_2 / 2 V_a) \partial x_{C.G.}$ - per radian per foot
C_{n_r}	$\partial C_n / \partial (r d_2 / 2 V_a)$ - per radian
$C_{n_{rx}}$	$\partial^2 C_n / \partial (r d_2 / 2 V_a) \partial x_{C.G.}$ - per radian per foot
$(C_n)_{\delta=0}$	C_n at $\delta_p = \delta_q = \delta_r = 0^{\circ}$ - dimensionless

Aerothermoelastic Coefficients

A_1	First Order Elastic Coefficient in C'_{A_α} Equation - feet^2/pound
A_2	Second Order Elastic Coefficient in C'_{A_α} Equation - feet^4/pound^2
A_3	First Order Elastic Coefficient in $C'_{A\delta_q}$ Equation - feet^2/pound
A_4	Second Order Elastic Coefficient in $C'_{A\delta_q}$ Equation - feet^4/pound^2
A_5	First Order Elastic Coefficient in C'_{N_α} Equation - feet^2/pound
A_6	Second Order Elastic Coefficient in C'_{N_α} Equation - feet^4/pound^2
A_7	First Order Elastic Coefficient in $C'_{N\delta_q}$ Equation - feet^2/pound
A_8	Second Order Elastic Coefficient in $C'_{N\delta_q}$ Equation - feet^4/pound^2
A_9	First Order Elastic Coefficient in C'_{y_β} Equation - feet^2/pound
A_{10}	Second Order Elastic Coefficient in C'_{y_β} Equation - feet^4/pound^2

SYMBOLS	DEFINITION AND UNITS

A_{11} — First Order Elastic Coefficient in $C'_{y\delta_r}$ Equation - feet^2/pound

A_{12} — Second Order Elastic Coefficient in $C'_{y\delta_r}$ Equation - feet^4/pound^2

A_{13} — First Order Elastic Coefficient in C'_{l_α} Equation - feet^2/pound

A_{14} — Second Order Elastic Coefficient in C'_{l_α} Equation - feet^4/pound^2

A_{15} — First Order Elastic Coefficient in $C'_{l\delta_p}$ Equation - feet^2/pound

A_{16} — Second Order Elastic Coefficient in $C'_{l\delta_p}$ Equation - feet^4/pound^2

A_{17} — First Order Elastic Coefficient in C'_{m_α} Equation - feet^2/pound

A_{18} — Second Order Elastic Coefficient in C'_{m_α} Equation - feet^4/pound^2

A_{19} — First Order Elastic Coefficient in $C'_{m\delta_q}$ Equation - feet^2/pound

A_{20} — Second Order Elastic Coefficient in $C'_{m\delta_q}$ Equation - feet^4/pound^2

A_{21} — First Order Elastic Coefficient in C'_{n_β} Equation - feet^2/pound

A_{22} — Second Order Elastic Coefficient in C'_{n_β} Equation - feet^4/pound^2

A_{23} — First Order Elastic Coefficient in $C'_{n\delta_r}$ Equation - feet^2/pound

A_{24} — Second Order Elastic Coefficient in $C'_{n\delta_r}$ Equation - feet^4/pound^2

ϵ_1 — Error Multiplier for C_N - dimensionless

ϵ_2 — Incremental Error in C_N - dimensionless

ϵ_3 — Error Multiplier for C_A - dimensionless

ϵ_4 — Incremental Error in C_A - dimensionless

ϵ_5 — Error Multiplier for C_y - dimensionless

SYMBOLS	DEFINITION AND UNITS
ϵ_6	Incremental Error in C_y - dimensionless
ϵ_7	Error Multiplier for C_l - dimensionless
ϵ_8	Incremental Error in C_l - dimensionless
ϵ_9	Error Multiplier for C_m - dimensionless
ϵ_{10}	Incremental Error in C_m - dimensionless
ϵ_{11}	Error Multiplier for C_n - dimensionless
ϵ_{12}	Incremental Error in C_n - dimensionless

SYMBOLS	DEFINITION AND UNITS
$c_{p_{T_s=0}}$	Specific Heat at $T_s=0$ - BTU/pound $^\circ$R
c_{p_s}	Specific Heat of the Skin - BTU/pound $^\circ$R
C_p	Pressure Coefficient
D_1-D_6	Constants
D_7	Wedge Angle - degrees
H	Free Stream Enthalpy of Air - BTU/pound (also angular momentum and gravitational potential harmonic constant)
H^*	Reference Enthalpy - BTU/pound
H_{aw}	Adiabatic Wall Enthalpy - BTU/pound
H_e	Enthalpy Based on Equilibrium Stagnation Temperature - $^\circ$R
H_{ref}	Reference Enthalpy of Air at 540°R - BTU/pound
H_s	Skin Enthalpy - BTU/pound
H_T	Total Enthalpy - BTU/pound
H_{T_1}	Adiabatic Wall Enthalpy at the Stagnation Line of a Hemi-Cylinder Leading Edge - BTU/pound
H_2	Enthalpy Aft of the Shock Wave - BTU/pound
l_H	Characteristic Length to Skin Temperature Point - feet
M_{N_n}	Mach Number Normal to Shock Wave
M_{N_2}	Mach Number Aft of the Shock Wave
$(P_r^*)^{-2/3}$	Prandtl Number Based on Reference Enthalpy (raised to the -2/3 power)
P_2	Static Pressure Aft of Shock Wave - pounds/square foot
r_H	Constants Depending upon Reynolds Number
Y_H	
K_H	

SYMBOLS	DEFINITION AND UNITS
R_{N*}	Reynolds Number Based on Reference Enthalpy
$R_{N_{CRIT}}$	Critical Reynolds Number
R_{N_2}	Reynolds Number Aft of the Shock Wave (local)
T_e	Equilibrium Stagnation Temperature - ^{o}R
T_{H*}	Temperature Based on Reference Enthalpy - ^{o}R
T_r	Effective Temperature of Space - ^{o}R
T_s	Skin Temperature - ^{o}R
$\dot{T}_s$	Skin Temperature Rate of Change - $^{o}R/sec$
$T_{s_{est}}$	Estimated Skin Temperature - ^{o}R
T_2	Temperature Aft of the Shock Wave - ^{o}R
V_2	Velocity Aft of the Shock Wave - feet/second
α_H	Angle of Attack of Skin Surface - degrees
β	Shock Wave Angle (also sideslip angle) - degrees
δ_s	Skin Thickness - feet
ϵ_e	Emissivity of the Spherical Nose
ϵ_s	Emissivity of the Skin
$\epsilon_{s_{T_s=0}}$	Emissivity of the Skin at $T_s=0$
$d\epsilon_s/dT$	Derivative of Emissivity with Respect to Temperature
$\mu*$	Coefficient of Viscosity Based on Reference Enthalpy - pounds/foot-second
μ_2	Coefficient of Viscosity Aft of the Shock Wave - pounds/foot-second
ρ_s	Skin Density - pounds/foot^3
$\rho*$	Density Based on Reference Enthalpy - pounds/foot^3
σ	Stefan Boltzmann Constant (4.758×10^{-13}) BTU/second/foot^2/$^{o}R^4$ (also azimuth angle)

SYMBOLS	DEFINITION AND UNITS
A	Azimuth of Platform X_p Axis - degrees
B	Equatorial Angle Between Geocentric and Inertial Coordinate System - degrees
B_A	Bank Angle - degrees
B_p	Equatorial Angle Between Inertial and Platform Coordinates - degrees
α	Angle of Attack - degrees
α_T	Total Angle of Attack - degrees
β	Angle of Sideslip (also shock wave angle) - degrees
γ	Elevation Flight-Path Angle - degrees
γ_a	Elevation Flight-Path Angle Including Effect of Winds - degrees
γ_D	Geodetic Flight-Path Angle - degrees
δ_p	Control Deflection to Induce a Moment About the x Axis - degrees
δ_q	Control Deflection to Induce a Moment About the y Axis - degrees
δ_r	Control Deflection to Induce a Moment About the z Axis - degrees
$\delta_{1,2\ldots n}$	Control Surface Deflections - degrees
σ	Horizontal Flight-Path or Azimuth Angle (also Stefan-Boltzmann constant) - degrees
σ_a	Azimuth Angle Including Effect of Winds - degrees
σ_D	Geodetic Hotizontal Flight-Path Angle - degrees
ϕ_A	Aerodynamic Roll Angle - degrees
ϕ_{LP}	Platform Geocentric Latitude - degrees
ϕ_T	Angular Rotation of the Plane of Swivel of a Thrust Vectoring Nozzle About the x Axis - degrees

SYMBOLS	DEFINITION AND UNITS
λ_T	Angle of Swivel of a Thrust Vectoring Nozzle - degrees
ψ Θ ϕ	Euler Angles Between Body Axes and Local-Geocentric Horizon Coordinates. Set 1. Yaw-Pitch-Roll Rotation Sequence - degrees
Θ' ψ' ϕ'	Set 2. Pitch-Yaw-Roll Rotation Sequence - degrees
Θ'' ϕ'' ψ''	Set 3. Pitch-Roll-Yaw Rotation Sequence - degrees
ψ Θ ϕ	Euler Angles Between Body Axes and Inertial Coordinates in Degrees
Θ_m ϕ_m ψ_m	Measured Euler Angles Between Body Axes and Platform Axes System - degrees
ψ_p Θ_p ϕ_p	Euler Angles Between Body Axes and Platform Axes System. Set 1. Yaw-Pitch-Roll Rotation Sequence - degrees
Θ_p' ψ_p' ϕ_p'	Set 2. Pitch-Yaw-Roll Rotation Sequence - degrees
Θ_p'' ϕ_p'' ψ_p''	Set 3. Pitch-Roll-Yaw Rotation Sequence - degrees
ψ_r Θ_r ϕ_r	Angles Between Rotating Machinery Axes System and Body Axes System - degrees
ϕ_{T_c} λ_{T_c}	Autopilot Command Values of ϕ_T and λ_T - degrees

xxiii

ANGULAR VELOCITIES

SYMBOLS	DEFINITION AND UNITS
p q r	Inertial Angular Rates of Body About Its Axis System - radians/second
q_A r_A	Aeroelastic Inertial Angular Rates of Body About Its Axis System - degrees/second
p_e q_e r_e	Planet Referenced Angular Rates of Body About Its Axis System - radians/second
p_m q_m r_m	Measured Inertial Angular Rates of Body About Its Axis System - radians/second
ω_r	Rotation Rate of Machinery Within the Body About Its Axis System - RPM

ATMOSPHERE DATA

SYMBOLS	DEFINITION AND UNITS
H_{g_p}	Geopotential Altitude - geopotential meters
P	Atmosphere Pressure - pounds/foot^2
T	Temperature of the Atmosphere (also engine thrust) - $^{\circ}R$
T_M	Molecular-Scale Temperature of the Atmosphere - $^{\circ}R$
V_s	Speed of Sound - feet/second
ν	Kinematic Viscosity of the Atmosphere - feet^2/second
ρ	Atmosphere Density - slugs/foot^3

AXES SYSTEMS

SYMBOLS	DEFINITION AND UNITS
x y z	Body Axes Coordinate System or Displacements From a Specified Origin in that System (y also aerodynamic side force, body axes) - feet
X Y Z	Inertial or Space Fixed Coordinate System or Displacements from a Specific Origin in that System (Y also aerodynamic side force, wind axis) - feet
X_A Y_A Z_A	Wind Coordinate System or Displacements from a Specified Origin in that System - feet
X_e Y_e Z_e	Earth Reference Coordinate System or Displacements from a Specified Origin in that System - feet
X_g Y_g Z_g	Local-Geocentric-Horizon Coordinates or Displacements from a Specified Origin in that System - feet
X_{gl} Y_{gl} Z_{gl}	Local-Geodetic-Horizon Coordinates or Displacements from a Specified Origin in that System - feet
x_m y_m z_m	Measured Displacements in a Coordinate System Fixed to the Planet (radar coordinates) - feet
X_p Y_p Z_p	Platform Coordinate System or Displacements from a Specified Origin in that System - feet
x_r y_r z_r	Rotating-Machinery Axis System or Displacements from a Specified Origin in that System - feet

AXES SYSTEMS

INTERPLANETARY TRAJECTORY PROBLEM TIE-IN

SYMBOLS	DEFINITION AND UNITS
α_N	Right Ascension of Planet North Pole - degrees
Υ Λ Γ	Planetocentric Equatorial Coordinates Based Upon the Earth's Equatorial Plane and the Mean Vernal Equinox of Reference Date in Ephemeris Time or Displacement from a Specified Origin in that System - feet
δ_N	Declination of Planet North Pole - degrees
ν_N	Hour Angle of the Vernal Equinox. Referenced with the Intersection of the Planet Equatorial Plane and the Earth Equatorial Plane of Reference Date - radians
λ_N	Hour Angle of Launch-Site Meridian with a Plane Perpendicular to the Intersection of the Planet Equatorial Plane and the Earth Equatorial Plane of Reference Date - hours
μ_N	Hour Angle of the Vernal Equinox of Reference Date with Respect to the Launch Point at the Time of Launch - hours
t_Υ	Sidereal Time - hours
HA	Hour Angle of Planet's Prime Meridian Measured from the Meridian Passing Through the Vernal Equinox of the Reference Date - degrees

BODY PHYSICAL DATA

SYMBOLS	DEFINITION AND UNITS
b	Wing Span - feet
C.G.	Center of Gravity
d_1	Reference Length - Longitudinal Plane - feet
d_2	Reference Length - Lateral Plane - feet
E	Modulus of Elasticity - pounds/inch^2
I_{xr} I_{yr} I_{zr}	Moments of Inertia of Rotating Machinery Within the Body About Machinery-Axes System - slugs-feet^2
I_{xx} I_{yy} I_{zz}	Moments of Inertia About the Body Axes - slugs-feet^2
I_{xy} I_{xz} I_{yz}	Products of Inertia About the Body Axes - slugs-feet^2
l_1 l_m l_n	Characteristic Distances for Jet-Damping Moments - feet
l_y l_z	Characteristic Distances for Jet-Damping Forces - feet
m	Mass of the Body - slugs
m_f	Fuel Mass Consumed - slugs
r_n	Radius of Hemispherical Nose (stagnation region) - feet
S	Reference Area - feet^2
W_T	Weight of the Body - Equal to Mass Times Reference g - pounds
$x_{C.G.}$ $y_{C.G.}$ $z_{C.G.}$	Position Coordinates of the C.G. in Body Coordinates - feet
$\Delta x_{C.G.}$	$(x_{C.G.} - x_{C.G._{ref}})$ - feet

SYMBOLS	DEFINITION AND UNITS
ϵ_{15}	Incremental Error in Vehicle Mass - slugs
ϵ_{18}	Incremental Error in C.G. Location - feet
ϵ_{19}	Incremental Error in I_{xx} - slugs-feet^2
ϵ_{20}	Incremental Error in I_{yy} - slugs-feet^2
ϵ_{21}	Incremental Error in I_{zz} - slugs-feet^2
ϵ_{22}	Incremental Error in I_{xy} - slugs-feet^2
ϵ_{23}	Incremental Error in I_{xz} - slugs-feet^2
ϵ_{24}	Incremental Error in I_{yz} - slugs-feet^2

DIRECTION COSINES

SYMBOLS	DEFINITION AND UNITS

$\begin{matrix} a_1 a_2 a_3 \\ b_1 b_2 b_3 \\ c_1 c_2 c_3 \end{matrix}$ — Matrix of Direction Cosines. Used to Transfer Quantities from Inertial Axes System to Platform Axes System

$\begin{matrix} d_1 d_2 d_3 \\ e_1 e_2 e_3 \\ f_1 f_2 f_3 \end{matrix}$ — Matrix of Direction Cosines. Used to Transfer Quantities from Local-Geocentric Horizon Coordinate System to Body-Axes System Using Local Body Euler Angles and to Transfer Quantities from the Body Coordinate System to Platform Axes System Using Platform Euler Angles

$\begin{matrix} i_1 i_2 i_3 \\ j_1 j_2 j_3 \\ k_1 k_2 k_3 \end{matrix}$ — Matrix of Direction Cosines. Used to Transfer Quantities from Geocentric Horizon Coordinate System to Inertial Coordinate System

$\begin{matrix} i_{10} i_{20} i_{30} \\ j_{10} j_{20} j_{30} \\ k_{10} k_{20} k_{30} \end{matrix}$ — i, j, k, Direction Cosines with $\omega_p = 0$

$\begin{matrix} l_1 l_2 l_3 \\ m_1 m_2 m_3 \\ n_1 n_2 n_3 \end{matrix}$ — Matrix of Direction Cosines. Used to Transfer Quantities from Inertial Axes System to Body-Axes System

$\begin{matrix} o_1 o_2 o_3 \\ p_1 p_2 p_3 \\ q_1 q_2 q_3 \end{matrix}$ — Matrix of Direction Cosines. Used to Transfer Quantities from Wind Coordinates to the X_e, Y_e, Z_e System

$\begin{matrix} u_1 u_2 u_3 \\ v_1 v_2 v_3 \\ w_1 w_2 w_3 \end{matrix}$ — Matrix of Direction Cosines. Used to Transfer Quantities from Body Coordinates to Wind Coordinates

xxx

ENGINE DATA

SYMBOLS	DEFINITION AND UNITS
A_e	Engine Exit Area - square feet
L_T M_T N_T	Engine Thrust Moments in the Body-Axes System - foot/pounds
N	Throttle Setting (also moment in body-axes system)
T	Engine Thrust (also temperature) - pounds
T_{VAC}	Vacuum Engine Thrust (rocket motor) - pounds
T_{XA} T_{YA} T_{ZA}	Engine Thrust Forces in the Wind-Axes System - pounds
T_{X_e} T_{Y_e} T_{Z_e}	Engine Thrust Forces in the Earth Reference Axes System - pounds
T_x T_y T_z	Engine Thrust in Body Components - pounds
x_N y_N z_N	Engine-Nozzle Swivel Point from Reference Center of Gravity - feet
ϵ_{13}	Error Multiplier for Thrust Force - dimensionless
ϵ_{14}	Incremental Error in Thrust Force - pounds

FLIGHT-PLAN PROGRAMMER AND AUTOPILOT

SYMBOLS	DEFINITION AND UNITS
A_{X_p} A_{Y_p} A_{Z_p}	Indication of Platform Accelerometer - feet/second^2
a_x a_y a_z	Body Axes Components of Inertial Acceleration - feet/second^2
$B_1 - B_{30}$	Bias Values Used in Autopilot Equations
C_{A_c} C_{Y_c} C_{N_c} C_{D_c} C_{Y_c} C_{L_c} C_{q^*} C_α C_β C_γ $C_{\dot\gamma}$	Axial-Force Coefficient Command Side-Force Coefficient Command Normal-Force Coefficient Command Drag-Force Coefficient Command Side-Force Coefficient Command Lift Coefficient Command Gain Coefficients
$E_1 - E_{25}$	Auxiliary Variables Used for Solution of Autopilot Differential Equations
$K_A - K_Z$	Autopilot Gains (see defining equations)
$L_1 - L_{25}$	Limiter Values (see defining equations)
n_a n_ψ n_θ	Body Axes Load Factors - g's
n_{a_c} n_{ψ_c} n_{θ_c}	Body Axes Load Factors Commands - g's
n_v n_σ n_γ	Wind Axes Load Factors - g's
n_{v_c} n_{σ_c} n_{γ_c}	Wind Axes Load Factors Commands - g's

SYMBOLS	DEFINITION AND UNITS
K_{11}	Yaw Gyro Bias - degrees
K_{12}	Yaw Gyro Drift Rate - degrees/second
K_{13}	Roll Gyro Bias - degrees
K_{14}	Roll Gyro Drift Rate - degrees/second
K_{15}	Tolerance for Assuming β_r is zero - degrees
K_{16}	Tolerance for assuming ϕ is zero - degrees
K_{17}	Error in Initial Yaw Alignment - degrees
K_{18}	One-Half Yaw Dead-Band Width - degrees
K_{19}	Error in Initial Roll Alignment - degrees
K_{20}	One-Half Roll Dead-Band Width - degrees
K_{21}	Error Multiplier for Pitch torque command - dimensionless
K_{22}	Pitch Gyro Bias - degrees
K_{23}	One-Half Pitch Dead-Band Width - degrees
K_{24}	Error in Initial Pitch Alignment - degrees
K_{25}	Pitch Gyro Drift Rate - degrees/second
K_{26}	Error Multiplier for Trim Angle of Attack - dimensionless
RNTP	Moment Due to Misalignment of Thrust and/or Asymmetric Aerodynamics in Pitch - foot-pounds
RNTR	Moment Due to Misalignment of Thrust and/or Asymmetric Aerodynamics in Roll - foot-pounds
RNTY	Moment Due to Misalignment of Thrust and/or Asymmetric Aerodynamics in Yaw - foot-pounds
T_1	Time to Commence Glide Phase - seconds
p_c	Roll Rate Command - degrees/second
P_{2Tc}	Pressure Command - pounds/foot^2
q_{c*}	Dynamic Pressure Command - pounds/foot^2
α_c	Angle of Attack Command - degrees
β_c	Angle of Sideslip Command - degrees
$\dot{\gamma}_c$	Rate Command - degrees/second
γ_c σ_c θ_c ψ_c θ_{c1}	Attitude Commands - degrees
ρ_c	Density Command - slugs/foot^3
ρ_{c1}	Density Command Corrected for Planet Rotation - slugs/foot^3
θ_c'	Pitch-Attitude Command - degrees

SYMBOLS	DEFINITION AND UNITS
$\psi_c{}'$	Yaw-Attitude Command - degrees
$\zeta_1 - \zeta_{20}$	Damping Ratios - dimensionless
Θ_{L_c}	Longitude Command - degrees
ϕ_{L_c}	Latitude Command - degrees
Θ_T ψ_T	Temperature Limiting Attitude Error Signals - degrees
$\tau_A - \tau_Z$ $\tau_1 - \tau_{30}$	Time Constant - seconds
$\omega_1 - \omega_{30}$	Natural Frequency - radians/second

FORCES AND MOMENTS

SYMBOLS	DEFINITION AND UNITS
F	Force - pounds
F_x F_y F_z	Summation of Forces in the Body-Axes System Including the Body Component of Weight - pounds
F_{X_e} F_{Y_e} F_{Z_e}	Summation of Forces in Earth Reference Axes System Including the Body Component of Weight - pounds
F_{x_D} F_{y_D} F_{z_D}	Jet Damping Forces - pounds
H	Angular Momentum (also gravitational potential harmonic constant and enthalpy) - foot-pound-seconds
L M N	Summation of Moments in the Body Axes System (L also lift and N also throttle setting) - foot-pounds
L_D M_D N_D	Jet Damping Moments - foot-pounds
F_{X_A} F_{Y_A} F_{Z_A}	Summation of Forces in the Wind Axes System - pounds
ΔF_x ΔF_y ΔF_z	Generalized Force Input - pounds
ΔL_T ΔM_T ΔN_T	Generalized Moment Input - foot-pounds

GEOPHYSICAL DATA

SYMBOLS	DEFINITION AND UNITS
g_{ref}	Reference Gravitational Acceleration (32.174 feet/second^2) Used to Define Weight
g_x g_y g_z	Components of Gravity in Body-Axes System - feet/second^2
g_X g_Y g_Z	Components of Gravity in Inertial-Axes System - feet/second^2
g_{X_e} g_{Y_e} g_{Z_e}	Components of Gravity in Earth-Reference Axes System - feet/second^2
g_{X_g} g_{Z_g}	Components of Gravity in Geocentric Horizon Coordinates - feet/second^2
J H K	Gravitational Potential Harmonic Constants (H also denotes angular momentum and enthalpy) - dimensionless
k_0-k_3	Constants in the Equation Relating Geodetic and Geocentric Latitude
R_e	Equatorial Radius (reference spheroid) - feet
R_p	Polar Radius (reference spheroid) - feet
U	Gravitational Potential - feet^2/second^2
μ	Gravitational Potential Constant (also coefficient of viscosity) - feet^3/second^2
ω_p	Planet Rotation Rate - radians/second (positive if in same direction as planet Earth)
ω_{X_g} ω_{Z_g}	Components of the Planet's Rotation Rate in the Local-Geocentric Coordinate System - radians/second
ϵ_{25}	Error Multiplier for Atmospheric Density - non-dimensional
ϵ_{26}	Additive Error for Atmospheric Density - slugs/foot^3

xxxvi

Approved for Public Release

LINEAR VELOCITIES

SYMBOLS	DEFINITION AND UNITS
M_N	Mach Number
u v w	Inertial Velocity Components in Body Coordinates - feet/second
u_m v_m w_m	Measured Inertial Velocity Components in Body Coordinates - feet/second
u_w v_w w_w	Inertial Wind Velocity Components in Body Coordinates - feet/second
V	Inertial Speed - feet/second
V_a	Airspeed - feet/second
V_D	Velocity Increment Due to Drag - feet/second
V_{grav}	Velocity Increment Due to Gravity - feet/second
V_g	Ground Referenced Speed - feet/second
V_g'	Check Value of Ground Referenced Velocity V_g - feet/second
V_P	Velocity Increment Due to Rocket Nozzle Back Pressure - feet/second
V_{theo}	Theoretical Velocity Increment Due to T_{VAC} - feet/second
V_w	Wind Speed - feet/second
$\dot{X}_{gw}$ $\dot{Y}_{gw}$ $\dot{Z}_{gw}$	Wind Velocity Components in Local-Geocentric-Horizon Coordinates - feet/second (X_{gw} positive when blowing north, Y_{gw} positive when blowing east, Z_{gw} positive when blowing downward)
$\dot{X}_w$ $\dot{Y}_w$ $\dot{Z}_w$	Wind Velocity Components in Inertial Coordinates - feet/second

POSITION DATA

SYMBOLS	DEFINITION AND UNITS
h	Geodetic Altitude - feet
h'	Geocentric Altitude - feet
R	Distance from Center of Planet to Body - feet
R_D	Total Distance Traveled Over Planet Surface - nautical miles
R_g	Approximate Range of Vehicle from Launch Point Over Great Circle Path - nautical miles
$R\phi_L$	Local Planet Radius - feet
t	Time - seconds
t_s	Stage Time - seconds
Θ_L	Longitude - degrees
ϕ_g	Geodetic Latitude - degrees
ϕ_L	Geocentric Latitude - degrees
K_σ	Constant Used in Equatorial Flight to Specify the Direction of Launch ($K_\sigma = 1$ for easterly launch; $K_\sigma = -1$ for westerly launch) - dimensionless
R_{D_O}	Initial Total Distance Traveled Over Planet Surface - nautical miles
$R\phi_{L_O}$	Initial Local Planet Radius - feet
Θ_{L_O}	Initial Longitude - degrees
ϕ_{g_O}	Initial Geodetic Latitude - degrees
ϕ_{L_O}	Initial Geocentric Latitude - degrees
σ_O	Initial Heading - degrees
X_D	Downrange along Initial Great Circle - nautical miles
Y_D	Crossrange from Initial Great Circle - nautical miles

MISCELLANEOUS

SYMBOLS	DEFINITION AND UNITS
$\overline{1}_x, \overline{1}_y, \overline{1}_z$	Unit Vector - subscript indicates the axes system
c	Subscript c Denotes an Autopilot or Flight-Plan Programmer Command Signal
ref	Subscript ref Indicates Value is a Reference Quantity
$\overline{}$	A Bar Over a Symbol Denotes a Vector
$\dot{}$	A Dot Over a Symbol Denotes Time Derivative
$\ddot{}$	Two Dots Over a Symbol Denotes the Second Derivative with Respect to Time
o	Subscript o Denotes - initial, time zero, origin of axes system, sea level conditions
$\overline{R}$	Radius Vectors
$\overline{\rho}$	
$\overline{r}$	
SL	Subscript Indicates Sea Level Reference Value
ϵ_i $i = 1,2 \ldots n$	Refers to an Error Constant, Either Multiplier or Additive (subscript number defines which one)
r	Subscript r Denotes Rotating Machinery
p	Subscript p Denotes Platform
v	Subscript v Denotes Vertical Axes System

1. INTRODUCTION

In the current wide-spread use of high speed digital computing machines for solving flight path and vehicle motion problems, it is common practice to develop a number of specialized computer programs each applicable to a specific problem. It is usually found desirable, in formulating these programs, to omit many of the terms of a more general formulation which are considered to be of secondary effect to the particular investigation at hand. This limits the range of application of these programs and results in considerable duplication of programming for each new specialized performance analysis. The object of the present study is: (1) the formulation of the generalized equations of motion with six degree of freedom for the flight-path study of any type of vehicle operating in the atmosphere and gravity field of a rotating non-spherical planet, and (2) the design of the digital computer program necessary to solve these equations. A feature of this computer program is the facility by which restricted problems of less than maximum sophistication may also be treated.

The general specifications which were followed in the development of the required Six-Degree-of-Freedom Flight-Path Study computer program are outlined below:

1. Geophysical Characteristics

    Rotating non-spherical earth accounting for oblateness effect on altitude as well as gravity.

    Atmospheric properties consistent with latest information with flexibility to permit use of other atmospheres or atmospheric variations.

    Wind effects.

2. Vehicle Characteristics

    Options to permit various degrees of sophistication in aerodynamic data input or output applicable to boost, interim, or re-entry configurations. Aerodynamic data input as function of multiple variables, such as speed, altitude, and vehicle attitude to be provided. Other options to be of various degrees of refinement.

    No restrictions to small angles of motion or attitude in any degree.

    Vehicle spin effects, including Magnus effects, to be included for n rpm.

    Account for thrust misalignment and transient effects due to stage separation for n stages.

    Include damping derivatives and cross coupling between the various degrees of freedom.

    Include provisions for simulation of vehicle autopilot.

Include provisions for simulation of flight programmer.

Vehicle control to be possible by aerodynamic, main engine and/or vernier thrust vector, retrorocket, and reaction type control.

3. Characteristics of Digital Computer Program

Program to give time history of motion of all six degrees of freedom.

Program utilization of various degrees of complexity from two degrees to six degrees of freedom of motion.

Velocity input and output option relative to the surface of a rotating central body or absolute with respect to axis system.

Provide for performance readout in latitude and longitude according to standard nomenclature, and all pertinent values required in the solution of operational type as well as design problems, e.g., range in both maneuvering and straight-out cases, and energy management parameters.

Coordinate system transformation capability.

Trajectory control during operation by limiting any or all three degrees of rotation, and/or any or all three degrees of translation.

Provision for tying into an aerodynamic heating computer program and an interplanetary trajectory computer program, and provision for handling heating limits.

4. Program Operating Modes

The program should contain a reversible option whereby known trajectory motion becomes the input and aerodynamic data is obtained as a result, as is accomplished in flight test.

The computer program which will handle this degree of problem complexity must, of necessity, be designed on a "unit construction" basis such that the individual building blocks may be readily isolated. In addition, to insure that the program will not become obsolete as requirements develop for the simulation of new vehicle concepts, the basic program must be easily revised. Recognizing that every flight dynamics computer program has certain essential parts which are the same regardless of the characteristics of the specific vehicle involved, the concept of a central program area with interchangeable subprograms has been adopted.

This report presents the analytical and theoretical developments leading to the problem formulation and the computer program design. In the derivations and explanations presented, any simplifying assumptions or approximations which are made are incorporated only after the development of the more general expressions. In this way the degree of approximation involved is made clear, and the form of the terms deleted are specified should they be required at a later time for specific analyses.

2

2. DERIVATION OF EQUATIONS OF MOTION

This section presents the derivation of the equations of motion, of a body in "inertial" space, as required for use in the Six-Degree-of-Freedom Flight-Path Study computer program. One of the features of this program is that problems which require motion analysis in less than six degrees of freedom may also be considered without the penalty of substantial amounts of null arithmetic. Consequently, alternate sets of equations are developed from the original relations by deletion of terms which are not required. The equations of motion will form a portion of the computation loop which is unaffected by the libraries of interchangeable subprograms describing alternate control systems; airframe aerodynamics, atmospheres, and geophysical parameters, or the data-monitoring subprograms to be incorporated. The several coordinate transformations and velocity and angle resolutions, which complete this central portion of the problem, are described in Section 3 of this report.

2.1 **Six-Degree-of-Freedom Analyses**. - Since the equations involving the moments of inertia, aerodynamic forces, and thrust forces are greatly simplified if expressed in body coordinates, this system of body reference will be used. [1] The two basic equations which define the motion of a body are:

$$\overline{F} = \frac{d}{dt} (m\overline{V}) \qquad (2.1) \qquad\qquad \overline{M} = \frac{d}{dt} (\overline{H}) \qquad (2.2)$$

Numerical analyses of these vector equations require their resolution into vector components and definition of the scalar coefficients. These manipulations are discussed in detail in many texts in mechanics (e.g., References (1) through (8)). The essential steps of the derivation are reviewed here, however, for completeness.

To determine the displacement accelerations, consider a point P displaced from the origin or coordinate system x-y-z such that the vector r designates the point. Figure 2.1 illustrates the system.
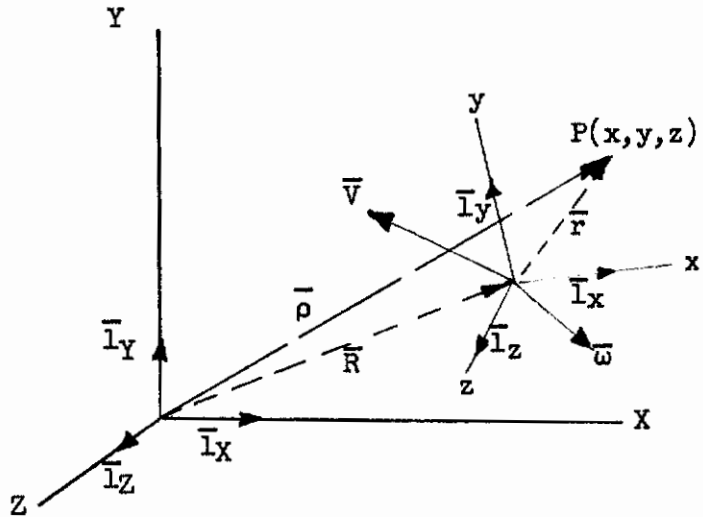
Figure 2.1 Generalized Inertial and Body-Axes Coordinate Systems

---

(1) An exception is made for the three-degree-of-freedom point-mass problem, discussed later, where it is found more convenient to use a wind-axis reference system.

Let the origin of the coordinate system x-y-z be displaced from the origin of a space-fixed coordinate system X-Y-Z by an amount and direction given by $\bar{R}$. Further, let the coordinate system x-y-z rotate in the X-Y-Z space such that the vector, $\bar{\omega}$, defines the rotation.

Then

$$\bar{r} = x\bar{1}_x + y\bar{1}_y + z\bar{1}_z$$

$$\bar{R} = X\bar{1}_X + Y\bar{1}_Y + Z\bar{1}_Z \qquad (2.3)$$

$$\bar{\omega} = \omega_x\bar{1}_x + \omega_y\bar{1}_y + \omega_z\bar{1}_z$$

The coordinate system x-y-z will be recognized as the body axes and the coordinate system X-Y-Z are the non-moving "inertial" or Newtonian axes. The total velocity of the point P is given by

$$\dot{\bar{\rho}} = \dot{\bar{R}} + \dot{\bar{r}} = \dot{X}\bar{1}_X + \dot{Y}\bar{1}_Y + \dot{Z}\bar{1}_Z + (\dot{x} - y\omega_z + z\omega_y)\bar{1}_x$$
$$+ (\dot{y} + x\omega_z - z\omega_x)\bar{1}_y + (\dot{z} - x\omega_y + y\omega_x)\bar{1}_z \qquad (2.4)$$

It is more convenient to express the velocity of the body-axes origin in body-velocity components than in velocity components coincident with the "inertial" reference coordinates. The vector R can be written in any coordinate system, so

$$\dot{\bar{R}} = \bar{V} = \dot{X}\bar{1}_X + \dot{Y}\bar{1}_Y + \dot{Z}\bar{1}_Z = \dot{x}_o\bar{1}_x + \dot{y}_o\bar{1}_y + \dot{z}_o\bar{1}_z$$

and Equation (2.4) may be rewritten as

$$\dot{\bar{\rho}} = \bar{V} + \dot{\bar{r}} = \dot{x}_o\bar{1}_x + \dot{y}_o\bar{1}_y + \dot{z}_o\bar{1}_z + (\dot{x}_p - y_p\omega_z + z_p\omega_y)\bar{1}_x$$
$$+ (\dot{y}_p + x_p\omega_z - z_p\omega_x)\bar{1}_y + (\dot{z}_p - x_p\omega_y + y_p\omega_x)\bar{1}_z \qquad (2.5)$$

where the subscripts o and p have been added to distinguish between the velocity components of the origin and the relative movement of the point P with respect to the origin of the x-y-z coordinate system respectively. Differentiating Equation (2.5) gives the relation for the total acceleration to be

$$\ddot{\bar{\rho}} = [\ddot{x}_o - \dot{y}_o\omega_z + \dot{z}_o\omega_y]\,\bar{1}_x + [\ddot{y}_o + \dot{x}_o\omega_z - \dot{z}_o\omega_x]\,\bar{1}_y + [\ddot{z}_o - \dot{x}_o\omega_y + \dot{y}_o\omega_x]\,\bar{1}_z$$
$$+ [\ddot{x}_p - 2\dot{y}_p\omega_z + 2\dot{z}_p\omega_y - x_p(\omega_z^2 + \omega_y^2) + y_p(\omega_x\omega_y - \dot{\omega}_z) + z_p(\dot{\omega}_y + \omega_x\omega_z)]\,\bar{1}_x$$
$$+ [\ddot{y}_p + 2\dot{x}_p\omega_z - 2\dot{z}_p\omega_x - y_p(\omega_x^2 + \omega_z^2) + z_p(\omega_y\omega_z - \dot{\omega}_x) + x_p(\dot{\omega}_z + \omega_x\omega_y)]\,\bar{1}_y$$
$$+ [\ddot{z}_p - 2\dot{x}_p\omega_y + 2\dot{y}_p\omega_x - z_p(\omega_y^2 + \omega_x^2) + x_p(\omega_z\omega_x - \dot{\omega}_y) + y_p(\dot{\omega}_x + \omega_y\omega_z)]\,\bar{1}_z$$

$$(2.6)$$

This acceleration relation is completely general and applies to any point on the body. In developing the equations of motion, the point of interest, $P(x,y, z)$, is the center of gravity. If the center of gravity is assumed to move, relative to the body, along the x-axis only, the following simplification can be made.

4

$$y_p, \quad z_p, \; = 0 \qquad \dot{y}_p, \; \dot{z}_p, \; \ddot{y}_p, \; \ddot{z}_p = 0$$

The components $\dot{x}_o$, $\dot{y}_o$, $\dot{z}_o$, and ω_x, ω_y, ω_z are more commonly known as u, v, w and p, q, r respectively. The components u, v, and w are the velocities of the reference point on the body. Making the above substitutions gives

$$F_x = m[\dot{u} - vr + wq + \ddot{x}_p - x_p(r^2 + q^2)]$$

$$F_y = m[\dot{v} + ur - wp + 2\dot{x}_p r + x_p(\dot{r} + pq)] \tag{2.7}$$

$$F_z = m[\dot{w} - uq + vp - 2\dot{x}_p q + x_p(rp - \dot{q})]$$

In view of the fact that most vehicles are designed to have small center-of-gravity travel, the acceleration and velocity of the center of gravity are both very small quantities and may be omitted from the problem formulation. If the reference point is further restricted to be the center of gravity, then x_p and its derivatives may be omitted from the equations and the components u, v, and w are the velocities of the center of gravity. In matrix form the equations reduce to the following:

$$
\begin{bmatrix} F_x \\ F_y \\ F_z \end{bmatrix} = m \left\{ \begin{bmatrix} \dot{u} \\ \dot{v} \\ \dot{w} \end{bmatrix} + \begin{bmatrix} 0 & -r & q \\ r & 0 & -p \\ -q & p & 0 \end{bmatrix} \begin{bmatrix} u \\ v \\ w \end{bmatrix} \right\} \tag{2.8}
$$

It may be noted here that in the analysis of flight-test data, where the output of accelerometers, mounted away from the center of gravity, are used to record the motion of the body, the complete form of Equation (2.7) must be used. It will also be noted that, although Equation (2.1) states Newton's Law as the time derivative of the momentum, a formal differentiation of $m\bar{V}$, assuming m to be a function of time, has not been performed in the derivation of Equation (2.8). Such a formal differentiation gives

$$\bar{F} = m\frac{d\bar{V}}{dt} + \frac{dm}{dt}\bar{V}$$

This differentiation leads to erroneous results, however, since the residual momentum of the expelled gases has not been accounted for by this procedure (See Reference 8, page 111). The equation should be

$$\bar{F} = m\frac{d\bar{V}}{dt} + \frac{dm}{dt}\bar{c}$$

5

when the residual momentum of the expelled mass is properly considered. Here, $\bar{c}$ is the velocity of the expelled mass with respect to the continuing body. The contribution $\dot{m}\,\bar{c}$ is the momentum-change portion of the thrust and is included in the summation of external forces.

There are additional accelerations produced which are unique to configurations which have very large fuel-flow rates and which have the thrust nozzle located a considerable distance from the center of gravity. These accelerations, linear and angular, are the so-called jet-damping contributions. The term is a correction to accelerations computed on the basis of only the externally applied forces (or moments) and accounts for the moment of momentum which is imparted to the fuel by the pitching velocity of the body. The derivation of this contribution is considered in greater detail in Appendix One to this report. The principal contribution to the equations for linear acceleration are in the y-and z-direction and have been added to the expressions of (2.8) to give the following result.

$$
\begin{vmatrix} F_x \\ F_y \\ F_z \end{vmatrix} = m \left[\begin{vmatrix} \dot{u} \\ \dot{v} \\ \dot{w} \end{vmatrix} + \begin{vmatrix} 0 & -r & q \\ r & 0 & -p \\ -q & p & 0 \end{vmatrix} \begin{vmatrix} u \\ v \\ w \end{vmatrix} \right] + \begin{vmatrix} 0 \\ -2\dot{m}\,rl_y \\ +2\dot{m}\,ql_z \end{vmatrix} \qquad (2.9)
$$

The relations expressing the rotational motion are obtained in a straightforward manner. The components considered in this analysis come from three basic sources; the time rate of change of the moment of momentum, the gyroscopic moments which arise from the rotating machinery of the vehicle, and the externally applied moments. The moment of momentum of a body (or angular momentum) about its center of gravity, in terms of its components, is given by

$$
\begin{vmatrix} H_x \\ H_y \\ H_z \end{vmatrix} = \begin{vmatrix} I_{xx} & -I_{xy} & -I_{xz} \\ -I_{xy} & I_{yy} & -I_{yz} \\ -I_{xz} & -I_{yz} & I_{zz} \end{vmatrix} \begin{vmatrix} \omega_x \\ \omega_y \\ \omega_z \end{vmatrix}
$$

or, since ω_x, ω_y, and ω_z are p, q, and r, respectively:

$$
\bar{H} = [I_{xx}p - I_{xy}q - I_{xz}r]\,\bar{1}_x + [-I_{xy}p + I_{yy}q - I_{yz}r]\,\bar{1}_y
$$

$$
+ [-I_{xz}p - I_{yz}q + I_{zz}r]\,\bar{1}_y \qquad (2.10)
$$

The required differentiation[*] of the moment of momentum gives

---

*The time rate of change of inertia noted here refers to that change occurring at constant mass only.

$$
\begin{aligned}
\dot{\bar{H}} = &\ [I_{xx}\dot{p} + \dot{I}_{xx}p + (I_{zz} - I_{yy})\,qr - I_{yz}(q^2 - r^2) - I_{xz}(\dot{r} + pq) \\[4pt]
&\ - I_{xy}(\dot{q} - pr) - \dot{I}_{xz}r - \dot{I}_{xy}q]\ \bar{1}_x \\[8pt]
&\ + [I_{yy}\dot{q} + \dot{I}_{yy}q + (I_{xx} - I_{zz})\,pr - I_{xz}(r^2 - p^2) - I_{xy}(\dot{p} + qr) \\[4pt]
&\ - I_{yz}(\dot{r} - pq) - \dot{I}_{xy}p - \dot{I}_{yz}r]\ \bar{1}_y \\[8pt]
&\ + [I_{zz}\dot{r} + \dot{I}_{zz}r + (I_{yy} - I_{xx})pq - I_{xy}(p^2 - q^2) - I_{yz}(\dot{q} + pr) \\[4pt]
&\ - I_{xz}(\dot{p} - qr) - \dot{I}_{xz}p - \dot{I}_{yz}q]\ \bar{1}_z
\end{aligned}
\tag{2.11}
$$

It is the general practice at this point in the derivation of the equations of
motion to assume that the reference axes of the aircraft are principal axes and
that the moments of inertia do not vary with time. This conveniently eliminates
the products of inertia and the time derivatives of the moments and products of
inertia, respectively. However, it is desired to have a more general applicability
than this for the computer program being developed and these terms will be retained.
The inclusion of the time derivatives of the inertia implies that all moment of
momentum has been removed from the mass being lost by the body. This assumes
that the gases have no swirl after they have left the body. Staging and dropping
of discrete masses from the body introduce discontinuities in the mass and inertia
properties of the body. The solution must not proceed across these discontinuities.
Therefore, the integration of the equations of motion will be interrupted when mass
is dropped and automatically re-established immediately thereafter (See Section
4.4 - Stages and Staging).

The jet damping contribution to the expressions for angular acceleration
(from Appendix One) is

$$
\Delta \bar{M}_D = -p\,\dot{m}\,1_1^{\,2}\,\bar{1}_x - q\,\dot{m}\,1_m^{\,2}\,\bar{1}_y - r\,\dot{m}\,1_n^{\,2}\,\bar{1}_z
\tag{2.12}
$$

The expression for the total angular acceleration due to the time rate of change
of the moment of momentum, including jet damping, is conveniently given in matrix
form as shown on the following page:

7

$$
\begin{vmatrix} L \\ M \\ N \end{vmatrix} = \begin{vmatrix} I_{xx} & -I_{xy} & -I_{xz} \\ -I_{xy} & I_{yy} & -I_{yz} \\ -I_{xz} & -I_{yz} & I_{zz} \end{vmatrix} \begin{vmatrix} \dot{p} \\ \dot{q} \\ \dot{r} \end{vmatrix} + \begin{vmatrix} \dot{I}_{xx} - \dot{m} l_1{}^2 & -I_{xy} & -I_{xz} \\ -\dot{I}_{xy} & \dot{I}_{yy} - \dot{m} l_m{}^2 & -\dot{I}_{yz} \\ -\dot{I}_{xz} & -\dot{I}_{yz} & +\dot{I}_{zz} - \dot{m} l_n{}^2 \end{vmatrix} \begin{vmatrix} p \\ q \\ r \end{vmatrix}
$$

$$
+ \begin{vmatrix} 0 & -r & q \\ r & 0 & -p \\ -q & p & 0 \end{vmatrix} \begin{vmatrix} I_{xx} & -I_{xy} & -I_{xz} \\ -I_{xy} & I_{yy} & -I_{yz} \\ -I_{xz} & -I_{yz} & I_{zz} \end{vmatrix} \begin{vmatrix} p \\ q \\ r \end{vmatrix} \qquad (2.13)
$$

The torques due to precession and changes in rotational speed of rotating machinery aboard a vehicle which is free to gyrate in space can contribute significantly to the angular accelerations which the vehicle experiences. Appendix Two of this report derives the torques generated by the precession of rotating machinery in general terms and simplifies these relations as required for the solution of the following problems.

(a) The motion of an aircraft powered by an engine with a rotating mass which is fixed in its orientation with respect to the reference axis of the aircraft.

(b) The motion of an aircraft powered by a rotating-mass engine which can be rotated in a plane parallel to the plane of symmetry (e.g., a convertiplane which is in the transition from vertical flight to forward motion or vice versa).

(c) The motion of a satellite in which motors are being operated (by the proper selection of reference axes).

The gyroscopic moments due to the rotational rates p, q, and r and the angular momentum of the rotating machinery are approximated as follows:

$$
\Delta L_r = -I_{xr}\, \omega_r (q + \dot{\Theta}_r) \sin \Theta_r
$$

$$
\Delta M_r = I_{xr}\, \omega_r (p \sin \Theta_r + r \cos \Theta_r) \qquad (2.14)
$$

$$
\Delta N_r = -I_{xr}\, (q + \dot{\Theta}_r)\, \omega_r \cos \Theta_r
$$

The complete rotational equations of motion are, therefore, from Equations (2.11), (2.12), and (2.13)

$$
\bar{M} = L \bar{1}_x + M \bar{1}_y + N \bar{1}_z
$$

in which

$$
L = I_{xx}\dot{p} + \dot{I}_{xx}p + (I_{zz} - I_{yy})qr - I_{yz}(q^2 - r^2)
$$

$$
- I_{xz}(\dot{r} + pq) - I_{xy}(\dot{q} - pr) - \dot{I}_{xz}r - \dot{I}_{xy}q
$$

$$
- p\,\dot{m}\, l_1{}^2 - I_{xr}\omega_r (q + \dot{\Theta}_r) \sin \Theta_r
$$

$$M = I_{yy}\dot{q} + \dot{I}_{yy}q + (I_{xx} - I_{zz})pr - I_{xz}(r^2 - p^2)$$
$$- I_{xy}(\dot{p} + qr) - I_{yz}(\dot{r} - pq) - \dot{I}_{xy}p - \dot{I}_{yz}r$$
$$- q\dot{m}l_m^2 + I_{xr}\omega_r(p \sin \Theta_r + r \cos \Theta_r)$$

$$N = I_{zz}\dot{r} + \dot{I}_{zz}r + (I_{yy} - I_{xx})pq - I_{xy}(p^2 - q^2)$$
$$- I_{xz}(\dot{p} - qr) - I_{yz}(\dot{q} + pr) - \dot{I}_{xz}p - \dot{I}_{yz}q$$
$$- r\dot{m}l_n^2 - I_{xr}(q + \dot{\Theta}_r) \omega_r\cos \Theta_r$$

These relations, written in matrix form, are:

$$
\begin{vmatrix} L \\ M \\ N \end{vmatrix} =
\begin{vmatrix} I_{xx} & -I_{xy} & -I_{xz} \\ -I_{xy} & I_{yy} & -I_{yz} \\ -I_{xz} & -I_{yz} & I_{zz} \end{vmatrix}
\begin{vmatrix} \dot{p} \\ \dot{q} \\ \dot{r} \end{vmatrix} +
\begin{vmatrix} \dot{I}_{xx}-\dot{m}l_1^2 & -\dot{I}_{xy} & -\dot{I}_{xz} \\ -\dot{I}_{xy} & \dot{I}_{yy}-\dot{m}l_m^2 & -\dot{I}_{yz} \\ -\dot{I}_{xz} & -\dot{I}_{yz} & \dot{I}_{zz}-\dot{m}l_n^2 \end{vmatrix}
\begin{vmatrix} p \\ q \\ r \end{vmatrix}
$$

$$
+ \begin{vmatrix} 0 & -r & q \\ r & 0 & -p \\ -q & p & 0 \end{vmatrix}
\begin{vmatrix} I_{xx} & -I_{xy} & -I_{xz} \\ -I_{xy} & I_{yy} & -I_{yz} \\ -I_{xz} & -I_{yz} & I_{zz} \end{vmatrix}
\begin{vmatrix} p \\ q \\ r \end{vmatrix} +
\begin{vmatrix} -I_{xr}\omega_r(q + \dot{\Theta}_r) \sin \Theta_r \\ I_{xr}\omega_r (p \sin \Theta_r + r \cos \Theta_r) \\ -I_{xr}\omega_r (q + \dot{\Theta}_r) \cos \Theta_r \end{vmatrix} \qquad (2.15)
$$

Equations (2.9) and (2.15) constitute the general six-degree-of-freedom equations of motion which will be used in the computer program. The program instructions will provide for the removal of certain combinations of terms as follows:

(a) All product of inertia terms for the case where the body is inertially symmetrical about the x-axis.

(b) The product of inertia terms I_{xy} and I_{yz} which are zero when the x-z plane is a plane of symmetry.

(c) The terms containing the time rates of change of inertia, products of inertia, and mass.

(d) The gyroscopic contributions of rotating machinery.

(e) The jet damping terms, both forces and moments.

2.2 Three-Degree-of-Freedom Longitudinal Analyses - Three-degree-of-freedom analyses may be used for longitudinal dynamic stability investigations and for simplified performance work where the lateral motion is zero. For the assumed motion the following constraints exist:

$$Fy = 0 \quad L = 0 \quad N = 0 \quad v = 0 \quad p = 0 \quad r = 0$$

9

These restrictions require the motion to be in the equatorial plane when the motion is over a spherical planet. The equations of motion, (2.9) and (2.15), reduce to

$$F_X = m(\dot{u} + wq)$$

$$F_Z = m(\dot{w} - uq) + 2\dot{m}ql_z \qquad (2.16)$$

$$M = I_{yy}\dot{q} + \dot{I}_{yy}q - \dot{m}ql_m^2$$

These equations do not depend on motion in planes other than in the x-z plane and therefore require no additional constraints, except that gyroscopic moments must be assumed to be zero since such moments are not compatible with the assumption of the reduced degrees of freedom.

2.3 <u>Three-Degree-of-Freedom Lateral Analyses</u> - A three-degree-of-freedom problem option is included for analyses of lateral stability problems and preliminary development of the lateral guidance computer loops. In this problem the motion will be computed within the bounds of the following assumptions:

$$F_X = 0 \qquad F_Z = 0 \qquad M = 0$$

The general equations of motion, (2.9) and (2.15), reduce to

$$F_y = m(\dot{v} + ru - wp) - 2\dot{m}rl_y$$

$$L = I_{xx}\dot{p} + \dot{I}_{xx}p - I_{xz}\dot{r} + I_{yz}r^2 + I_{xy}pr$$
$$\qquad - \dot{I}_{xz}r - \dot{m}pl_1^2 \qquad (2.17)$$

$$N = I_{zz}\dot{r} + \dot{I}_{zz}r - I_{xy}p^2 - I_{yz}pr - I_{xz}\dot{p}$$
$$\qquad - \dot{I}_{xz}p - \dot{m}rl_n^2$$

This set of equations is not independent of the motion in the x-y plane due to the velocities u and w appearing in the F_y equation. Hence, it will be necessary to apply an additional constraint that u and w are specified functions of time. Gyroscopic moments must also be omitted from this problem.

2.4 <u>Three-Degree-of-Freedom Trajectory Analyses</u> - A three-degree-of-freedom point-mass problem option is included to permit performance analysis and trajectory computations of aircraft in three-dimensional space. Since the angular rotation relations are omitted in this option, some difficulty is experienced in obtaining the body rates p, q, and r required in Equation (2.9). This difficulty is eliminated, however, if the body axes formulation is abandoned in favor of a planetocentric axis system oriented with the X_e - Y_e axes in the equatorial plane and the Z_e-axis through the South Pole. This coordinate system is selected because of the simplification it affords the six-degree-of-freedom problem for the flat-earth option. The X_e-Y_e-Z_e axis system rotates with the earth, and the X_e-axis designates the longitude of the body at the instant of starting the problem. With this coordinate system, the equations of motion can be obtained directly using Coriolis' Law which states:

$$\bar{F} = m(\bar{a}_r + \bar{a}_m + 2\bar{\omega}_p \times \bar{V}) \qquad (2.18)$$

10

where $\bar{a}_r$ is the acceleration a particle would have if the planet were stationary, and $\bar{a}_m$ is the acceleration a particle would have due to the planet's rotation. $2\bar{\omega}_p \times \bar{V}$ is the Coriolis acceleration, where $\bar{V}$ is the velocity with respect to the planet (i.e., with respect to the rotating coordinate system) and $\bar{\omega}_p$ is the planet's (coordinate system) rotational velocity. It should be noted, however, that because of the manner in which the coordinate system has been established ($+Z_e$ is through the South Pole), the vector $\bar{\omega}_p$ must have a minus sign associated with it in the derivation which follows. Expanding this equation in the Cartesian coordinate system selected, the equations of motion are:

$$F_{X_e} = m\,(\ddot{X}_e - X_e\,\omega_p^2 + 2\,\dot{Y}_e\,\omega_p)$$

$$F_{Y_e} = m\,(\ddot{Y}_e - Y_e\,\omega_p^2 - 2\,\dot{X}_e\,\omega_p) \qquad (2.19)$$

$$F_{Z_e} = m\,(\ddot{Z}_e)$$

Force components in the wind axes are required for use with this coordinate system. The force contributions due to jet damping are omitted in this motion since the rates p, q, and r are undefined.

2.5 <u>Two-Degree-of-Freedom Trajectory Analyses</u> - For a two-degree-of-freedom trajectory analysis, the side-force is zero. This constraint is simply imposed by eliminating the F_{Z_e} equation in (2.19). This requires the trajectory to be in the equatorial plane. The equations of motion are:

$$F_{X_e} = m\,(\ddot{X}_e - X_e\omega_p^2 + 2\,\dot{Y}_e\omega_p)$$

$$F_{Y_e} = m\,(\ddot{Y}_e - Y_e\omega_p^2 - 2\,\dot{X}_e\omega_p) \qquad (2.20)$$

2.6 <u>Flat-Planet Analyses</u> - In certain cases the contributions of a planet's rotational velocity and the centrifugal effects of the body's motion about the planet are truly negligible and only complicate and lengthen the computation (e.g., the dynamic behavior of a missile during the launch phase, or take-off and landing phases of aircraft flight). An additional set of reduced-degree-of-freedom options can be obtained by eliminating the planet's rotational rate and revising the coordinate transformations required to record the motion. The equations of motion are unaffected by this option, however, and a further discussion of flat-planet analyses is more appropriately confined to the descriptions of the coordinate transformations (See Section 3.1).

3. COORDINATE SYSTEMS AND COORDINATE TRANSFORMATIONS

This section presents a description of the reference coordinate systems chosen for the Six-Degree-of-Freedom Flight-Path Study computer program. The coordinate transformations required to relate the various parameters of the computation to the several coordinate systems are also derived. The coordinate transformations required in the program may be categorized as follows:

(1) Transformations inherent in solving the basic equations of motion.

(2) Transformations to provide input data to the guidance, autopilot, and flight-plan programmer simulations.

(3) Transformations to present readout data in the most desirable form and auxiliary transformations which may be required for the definition of certain special parameters. These transformations may be deleted from the program when they are not required.

(4) Transformations to provide input data to connecting interplanetary trajectory programs.

3.1 Coordinate Transformations for Basic Equations of Motion - This section describes the coordinate systems and derives the related transformations under Category (1) above. The coordinate systems and transformations required to describe the rigid airframe motion in six degrees of freedom are modified for use in the optional reduced-degrees-of-freedom problems. The coordinate transformations which relate the aerodynamic angles and velocities to ground-referenced velocities in the presence of winds are also presented.

3.1.1 Body-Axes Coordinates - The equations of motion (Section 2) are solved in a body coordinate system (see Figure 3.1). The origin of this system is at the center of gravity of the aircraft with the x-axis along the geometric longitudinal axis of the body. The positive direction of the x-axis is from the center of gravity to the front of the body. The y-axis is positive to the right extending from the center of gravity in a water-line plane. The
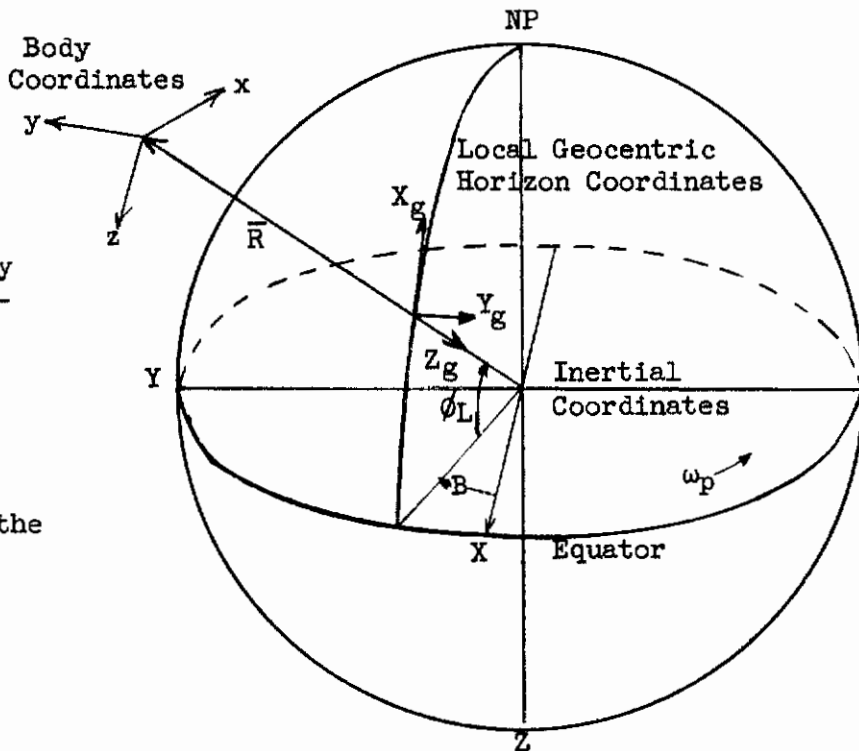
Figure 3.1 Relationship Between Inertial, Geocentric, Local-Geocentric, and Body Coordinates

12

z-axis forms a right-handed orthogonal system. This coordinate system was chosen because inertia characteristics are thus made independent of attitude.

Accelerations and velocities computed in the x-y-z body axis must be related to velocities and accelerations referenced to a fixed point on the surface of the planet to (a) describe the motion which a fixed observer would sense, and (b) to compute the aerodynamic forces on the body immersed in an atmosphere which essentially rotates with the surface of the planet (except for winds which are referenced to a point on the surface of the planet).

3.1.2 <u>Inertial Coordinates</u> - The resolution of the body-axes motion to the motion referred to the surface of the planet will always be made through the intermediate coordinate system assumed to be the "inertial" axes[1]. The assumed "inertial" coordinate system selected has as its origin the center of the planet and is oriented so that the X-and Y-axes are in the equatorial plane with the Z-axis coincident with the polar axis of the planet and positive toward the south pole. The angular orientation of the inertial axes remain fixed (i.e., the axes have no further rotation or linear acceleration) with the X-axis established by the initial instantaneous longitude of the body. The positive direction of the Z-axis was selected so that the inertial coordinate system would coincide with the coordinate system for the flat-planet options discussed in Paragraphs 3.1.8, 3.1.9, and 3.1.10. This will permit the use of the same resolutions for some of the coordinate transformations in both the rotating oblate-planet problems and the flat-planet options[2]. It should be noted that this coordinate system is used only for computational purposes in the program. A resolution, explained in Paragraph 3.1.4, will describe the body position in the customary spherical coordinates. Figure (3.1) aids in the description of the coordinate systems adopted.

3.1.3 <u>Direction Cosines</u> - The direction cosines relating the body x-y-z axes to the inertial coordinate system X-Y-Z are obtained in the following manner. Let $\bar{1}_x$, $\bar{1}_y$, $\bar{1}_z$ be unit vectors along the body axes, x, y, z, respectively, and let $\bar{1}_X$, $\bar{1}_Y$, $\bar{1}_Z$ be unit vectors along the inertial axes, X, Y, Z, respectively. The direction cosine matrix relating these two sets of unit vectors will be of the form:

$$
\begin{vmatrix} \bar{1}_x \\ \bar{1}_y \\ \bar{1}_z \end{vmatrix} = \begin{vmatrix} l_1 & l_2 & l_3 \\ m_1 & m_2 & m_3 \\ n_1 & n_2 & n_3 \end{vmatrix} \begin{vmatrix} \bar{1}_X \\ \bar{1}_Y \\ \bar{1}_Z \end{vmatrix}
\qquad (3.1)
$$

---

[1] An alternate inertial axis system is discussed in Section 3.4 which is normally assumed for certain astronomical work.

[2] This system is most convenient for the six-degree-of-freedom flat-planet option but not necessarily the most convenient for the other reduced-degree-of-freedom options. The complications incurred in the latter case have been accepted, however, as will be explained in Paragraph 3.1.7.

Performing the matrix multiplication indicated gives:

$$\bar{1}_x = l_1\bar{1}_X + l_2\bar{1}_Y + l_3\bar{1}_Z$$

$$\bar{1}_y = m_1\bar{1}_X + m_2\bar{1}_Y + m_3\bar{1}_Z \qquad (3.2)$$

$$\bar{1}_z = n_1\bar{1}_X + n_2\bar{1}_Y + n_3\bar{1}_Z$$

The derivatives of $\bar{1}_x$, $\bar{1}_y$, $\bar{1}_z$ with respect to time in terms of their components in the inertial system are found by differentiating Equation (3.2). These derivatives are:

$$\dot{\bar{1}}_x = \dot{l}_1\bar{1}_X + \dot{l}_2\bar{1}_Y + \dot{l}_3\bar{1}_Z$$

$$\dot{\bar{1}}_y = \dot{m}_1\bar{1}_X + \dot{m}_2\bar{1}_Y + \dot{m}_3\bar{1}_Z \qquad (3.3)$$

$$\dot{\bar{1}}_z = \dot{n}_1\bar{1}_X + \dot{n}_2\bar{1}_Y + \dot{n}_3\bar{1}_Z$$

The derivatives of $\bar{1}_x$, $\bar{1}_y$, $\bar{1}_z$ with respect to time are dependent only on the change in direction of the unit vectors. Therefore,

$$\dot{\bar{1}}_x = \bar{\omega}x\bar{1}_x = r\bar{1}_y - q\bar{1}_z$$

$$\dot{\bar{1}}_y = \bar{\omega}x\bar{1}_y = p\bar{1}_z - r\bar{1}_x \qquad (3.4)$$

$$\dot{\bar{1}}_z = \bar{\omega}x\bar{1}_z = q\bar{1}_x - p\bar{1}_y$$

where

$$\bar{\omega} = p\bar{1}_x + q\bar{1}_y + r\bar{1}_z$$

Equating the relations for $\dot{\bar{1}}_x$ from equations (3.3) and (3.4):

$$\dot{l}_1\bar{1}_X + \dot{l}_2\bar{1}_Y + \dot{l}_3\bar{1}_Z = r\bar{1}_y - q\bar{1}_z$$

Substituting the relationships for $\bar{1}_y$ and $\bar{1}_z$, respectively, gives the relation:

$$\dot{l}_1\bar{1}_X + \dot{l}_2\bar{1}_Y + \dot{l}_3\bar{1}_Z = r(m_1\bar{1}_X + m_2\bar{1}_Y + m_3\bar{1}_Z)$$
$$- q(n_1\bar{1}_X + n_2\bar{1}_Y + n_3\bar{1}_Z) \qquad (3.5)$$

By using the component properties of a vector, the relations

$$\dot{l}_1 = rm_1 - qn_1 \qquad (3.6a)$$

$$\dot{l}_2 = rm_2 - qn_2 \qquad (3.6b)$$

$$\dot{l}_3 = rm_3 - qn_3 \qquad (3.6c)$$

are obtained from Equation (3.5).

Performing the same operation for the $\dot{\bar{1}}_y$ and $\dot{\bar{1}}_z$ components defines the time derivatives of the remaining direction cosines. These are:

14

$$\dot{m}_1 = pn_1 - rl_1 \qquad (3.6d)$$

$$\dot{m}_2 = pn_2 - rl_2 \qquad (3.6e)$$

$$\dot{m}_3 = pn_3 - rl_3 \qquad (3.6f)$$

$$\dot{n}_1 = ql_1 - pm_1 \qquad (3.6g)$$

$$\dot{n}_2 = ql_2 - pm_2 \qquad (3.6h)$$

$$\dot{n}_3 = ql_3 - pm_3 \qquad (3.6i)$$

The nine Equations (3.6a) through (3.6i) are integrated to obtain the instantaneous values of the direction cosines. This method of calculating the direction cosines has been selected instead of the usual evaluation by means of the Euler angles because, regardless of the order of rotation selected, there are points at which certain Euler angles become undefined. The direction cosines evaluated by this method are always defined[3]. The method by which the orthogonality of the direction cosines is maintained is described in Appendix Three. The Euler angles may be calculated from the direction cosines if desired; however, they are not required for component resolution.

The components of inertial velocity in the body coordinate system, u, v, and w, will be resolved into velocity components X, Y, and Z in the inertial coordinates. Since components of inertial velocity are known in body coordinates, a resolution of components using the direction cosines given in Equation (3.6) will give components of inertial velocity in the inertial coordinate system, as follows:

$$\begin{vmatrix} \dot{X} \\ \dot{Y} \\ \dot{Z} \end{vmatrix} = \begin{vmatrix} l_1 & m_1 & n_1 \\ l_2 & m_2 & n_2 \\ l_3 & m_3 & n_3 \end{vmatrix} \begin{vmatrix} u \\ v \\ w \end{vmatrix} \qquad (3.7)$$

3.1.4 <u>Geocentric Coordinates</u> - The components of velocity in inertial coordinates will be integrated and the displacements resolved into the geocentric coordinates of latitude, longitude, and distance from the center of the planet. With the aid of Figure (3.1), several pertinent geometric relationships can be obtained. The angle, B, represents an inertial longitude which differs from the

---

[3] It is recognized that nine integrations are involved in the present method of computation instead of the three that are normally required when the Euler-angle rates are integrated to give the Euler angles. However, a coordinate transformation is required to obtain the rates, and the sines and cosines of the angles must also be computed in the usual direction cosine computation. The machine time required for the two methods of computation is comparable.

15

planet longitude change, $(\Theta_L - \Theta_{L_O})$, by the amount $\omega_p t$. (ω_p is the angular rotational rate of the planet.) The inertial angle is given by:

$$B = \text{Tan}^{-1}\left(\frac{Y}{X}\right) \tag{3.8}$$

and the instantaneous geocentric longitude of the body is:

$$\Theta_L = \Theta_{L_O} - B - \omega_p t \tag{3.9}$$

The geocentric latitude of the vehicle, ϕ_L, can also be expressed in terms of inertial coordinates. Referring to Figure (3.1):

$$\phi_L = \text{Sin}^{-1}\left(\frac{-Z}{\sqrt{X^2 + Y^2 + Z^2}}\right) \tag{3.10}$$

and, the distance from the center of the planet is:

$$R = \sqrt{X^2 + Y^2 + Z^2} \tag{3.11}$$

3.1.5 <u>Local-Geocentric Coordinates</u> - To describe the motion of the body relative to the planet, a local-geocentric-horizon coordinate system is employed. The Z_g-axis of this system is along a radial line which passes through the center of gravity of the body and is positive toward the center of the planet. The X_g-axis of this system is normal to the Z_g-axis, and is positive northward; and Y_g forms a right-handed system. Figure (3.1) shows the relation of this coordinate system to the other systems assumed. The direction cosines relating the orientation of this system in inertial space will now be developed.

To locate the X_g-Y_g-Z_g axes with respect to the X-Y-Z axes, first rotate about Z by an angle $(180° + B)$ and then rotate about Y_g through the angle $(90° - \phi_L)$. The first rotation defines the intermediate coordinate system shown in Figure (3.2). Using the matrix methods of Reference (9) the transformation is given by:
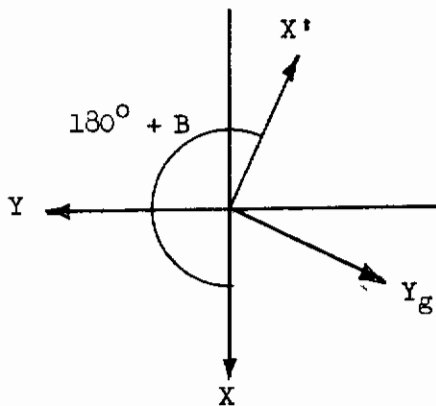
Figure 3.2 - Intermediate Coordinate
System Transformation From
Inertial to Local-Geocentric
Coordinates

$$\begin{vmatrix} \overline{1}_{X'} \\ \overline{1}_{Y_g} \\ \overline{1}_{Z} \end{vmatrix} = \begin{vmatrix} \text{Cos }(180°+B) & \text{Sin }(180°+B) & 0 \\ -\text{Sin }(180°+B) & \text{Cos }(180°+B) & 0 \\ 0 & 0 & 1 \end{vmatrix} \begin{vmatrix} \overline{1}_X \\ \overline{1}_Y \\ \overline{1}_Z \end{vmatrix}$$

or

$$\begin{vmatrix} \overline{1}_{X'} \\ \overline{1}_{Y_g} \\ \overline{1}_{Z} \end{vmatrix} = \begin{vmatrix} -\text{Cos } B & -\text{Sin } B & 0 \\ \text{Sin } B & -\text{Cos } B & 0 \\ 0 & 0 & 1 \end{vmatrix} \begin{vmatrix} \overline{1}_X \\ \overline{1}_Y \\ \overline{1}_Z \end{vmatrix} \tag{3.12}$$

16

The second rotation is shown in Figure (3.3). The transformation matrix for the second rotation is given by:

$$
\begin{vmatrix} \bar{1}_{X_g} \\ \bar{1}_{Y_g} \\ \bar{1}_{Z_g} \end{vmatrix} = \begin{vmatrix} \cos(90° - \phi_L) & 0 & -\sin(90° - \phi_L) \\ 0 & 1 & 0 \\ \sin(90° - \phi_L) & 0 & \cos(90° - \phi_L) \end{vmatrix} \begin{vmatrix} \bar{1}_{X'} \\ \bar{1}_{Y_g} \\ \bar{1}_{Z} \end{vmatrix}
$$

or

$$
\begin{vmatrix} \bar{1}_{X_g} \\ \bar{1}_{Y_g} \\ \bar{1}_{Z_g} \end{vmatrix} = \begin{vmatrix} \sin\phi_L & 0 & -\cos\phi_L \\ 0 & 1 & 0 \\ \cos\phi_L & 0 & \sin\phi_L \end{vmatrix} \begin{vmatrix} \bar{1}_{X'} \\ \bar{1}_{Y_g} \\ \bar{1}_{Z} \end{vmatrix} \qquad (3.13)
$$
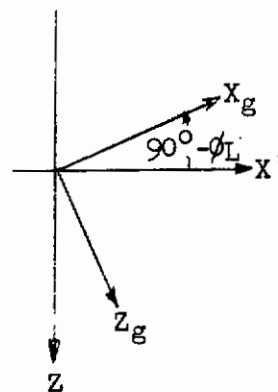
Figure 3.3 - Final Rotation in Transformation From Inertial To Local-Geocentric Coordinates

In this analysis, a positive rotation is defined in the same sense as that adopted for vector cross products in a right-handed system. That is, a positive rotation about the z-axis occurs when the x-axis rotates into the y-axis; positive rotation about the x-axis when the y-axis rotates into the z-axis; and positive rotation about the y-axis when the z-axis rotates into the x-axis. The intermediate coordinate system X', Y_g, Z will be eliminated according to the methods of successive rotation, Reference (9). The complete transformation is given by:

$$
\begin{vmatrix} \bar{1}_{X_g} \\ \bar{1}_{Y_g} \\ \bar{1}_{Z_g} \end{vmatrix} = \begin{vmatrix} \sin\phi_L & 0 & -\cos\phi_L \\ 0 & 1 & 0 \\ \cos\phi_L & 0 & \sin\phi_L \end{vmatrix} \begin{vmatrix} -\cos B & -\sin B & 0 \\ \sin B & -\cos B & 0 \\ 0 & 0 & 1 \end{vmatrix} \begin{vmatrix} \bar{1}_X \\ \bar{1}_Y \\ \bar{1}_Z \end{vmatrix} \qquad (3.14)
$$

which can be reduced to the single transformation matrix.

$$
\begin{vmatrix} \bar{1}_{X_g} \\ \bar{1}_{Y_g} \\ \bar{1}_{Z_g} \end{vmatrix} = \begin{vmatrix} -\sin\phi_L \cos B & -\sin\phi_L \sin B & -\cos\phi_L \\ \sin B & -\cos B & 0 \\ -\cos\phi_L \cos B & -\cos\phi_L \sin B & \sin\phi_L \end{vmatrix} \begin{vmatrix} \bar{1}_X \\ \bar{1}_Y \\ \bar{1}_Z \end{vmatrix} \qquad (3.15)
$$

The direction cosines will be defined as follows:

$$
\begin{vmatrix} \bar{1}_{X_g} \\ \bar{1}_{Y_g} \\ \bar{1}_{Z_g} \end{vmatrix} = \begin{vmatrix} i_1 & j_1 & k_1 \\ i_2 & j_2 & k_2 \\ i_3 & j_3 & k_3 \end{vmatrix} \begin{vmatrix} \bar{1}_X \\ \bar{1}_Y \\ \bar{1}_Z \end{vmatrix} \qquad (3.16)
$$

17

where the i's, j's, and k's are defined in Equation (3.15). For example,

$$j_1 = -\text{Sin } \phi_L \text{ Sin } B$$

The resolution of inertial velocity (in inertial components) to local-geocentric components of surface referenced velocity is obtained by the following manipulation. Let $\bar{R}$ be the displacement of the vehicle in inertial space. Then:

$$\dot{\bar{R}} = \dot{X}\bar{1}_X + \dot{Y}\bar{1}_Y + \dot{Z}\bar{1}_Z \qquad (3.17)$$

and the inertial velocity may also be written with respect to the local-geocentric coordinates as:

$$\dot{\bar{R}} = \frac{\delta\bar{R}}{\delta t} + \bar{\omega}_p \times \bar{R} \qquad (3.18)$$

where $\delta\bar{R}/\delta t$ is the velocity observed in the moving coordinate system X_g-Y_g-Z_g and $\bar{\omega}_p$ is the angular velocity of the planet. The observed surface referenced velocity is:

$$\frac{\delta\bar{R}}{\delta t} = \dot{X}_g\bar{1}_{X_g} + \dot{Y}_g\bar{1}_{Y_g} + \dot{Z}_g\bar{1}_{Z_g} \qquad (3.19)$$

and

$$\bar{\omega}_p = -\omega_p \bar{1}_Z$$

The angular velocity vector will be resolved into components in local-geocentric coordinates as follows:

$$\bar{\omega}_p = \omega_p \text{ Cos } \phi_L \bar{1}_{X_g} - \omega_p \text{ Sin } \phi_L \bar{1}_{Z_g} \qquad (3.20)$$

Writing the displacement vector in local-geocentric coordinates,

$$\bar{R} = -R \bar{1}_{Z_g} \qquad (3.21)$$

The required cross product $\bar{\omega}_p \times \bar{R}$ is:

$$\bar{\omega}_p \times \bar{R} = \omega_p R \text{ Cos } \phi_L \bar{1}_{Y_g} \qquad (3.22)$$

For convenience, the unit vector $\bar{1}_{Y_g}$ will be resolved into components in the inertial coordinates.

$$\begin{aligned}\bar{1}_{Y_g} &= i_2 \bar{1}_X + j_2 \bar{1}_Y + k_2 \bar{1}_Z \\ &= \text{Sin } B \bar{1}_X - \text{Cos } B \bar{1}_Y\end{aligned} \qquad (3.23)$$

From the geometry of Figure (3.1) the relations:

$$R \text{ Cos } \phi_L = \sqrt{X^2 + Y^2} \qquad (3.24)$$

18

$$\sin B = \frac{Y}{\sqrt{X^2 + Y^2}} \tag{3.25}$$

$$\cos B = \frac{X}{\sqrt{X^2 + Y^2}} \tag{3.26}$$

are obtained. Substituting Equations (3.23) through (3.26) into Equation (3.22) gives the inertial components of the required cross product as:

$$\bar{\omega}_p \times \bar{R} = \omega_p Y \bar{1}_X - \omega_p \bar{X} \bar{1}_Y \tag{3.27}$$

Substituting Equations (3.17), (3.19), and (3.27) into equation (3.18) gives:

$$\dot{X}\bar{1}_X + \dot{Y}\bar{1}_Y + \dot{Z}\bar{1}_Z = \dot{X}_g\bar{1}_{X_g} + \dot{Y}_g\bar{1}_{Y_g} + \dot{Z}_g\bar{1}_{Z_g} + \omega_p Y\bar{1}_X - \omega_p X\bar{1}_Y$$

or collecting like terms,

$$(\dot{X} - \omega_p Y)\bar{1}_X + (\dot{Y} + \omega_p X)\bar{1}_Y + \dot{Z}\bar{1}_Z = \dot{X}_g\bar{1}_{X_g} + \dot{Y}_g\bar{1}_{Y_g} + \dot{Z}_g\bar{1}_{Z_g} \tag{3.28}$$

Converting the unit vectors $\bar{1}_X$, $\bar{1}_Y$, $\bar{1}_Z$ to components in the moving system by using the direction cosines determined in Equation (3.15), and equating components in the moving coordinate system, gives the following relationship.

$$
\begin{vmatrix} \dot{X}_g \\ \dot{Y}_g \\ \dot{Z}_g \end{vmatrix} =
\begin{vmatrix} i_1 & j_1 & k_1 \\ i_2 & j_2 & k_2 \\ i_3 & j_3 & k_3 \end{vmatrix}
\begin{vmatrix} \dot{X} - \omega_p Y \\ \dot{Y} + \omega_p X \\ \dot{Z} \end{vmatrix} \tag{3.29}
$$

One other coordinate system is used in the point-mass reduced-degree-of-freedom operation of the program. This system will be discussed and the transformation derived in Paragraph 3.1.10.

3.1.6 <u>Inverse Transformations</u> - The preceding development completes the calculation of planet-referenced velocities and displacements. Several resolutions are necessary, however, to transform information in planet-referenced coordinates back to body coordinates. These transformations will use the inverse of the direction cosine matrices previously derived.

Gravity components, calculated in the geophysical data subprograms, are considered inputs to the central program. These components are normally specified in local-geocentric coordinates and must be resolved into components in body coordinates. The first transformation will use the inverse of the transformation in Equation (3.15) to resolve local-geocentric gravity components into inertial gravity components.

$$
\begin{vmatrix} g_X \\ g_Y \\ g_Z \end{vmatrix} =
\begin{vmatrix} i_1 & i_2 & i_3 \\ j_1 & j_2 & j_3 \\ k_1 & k_2 & k_3 \end{vmatrix}
\begin{vmatrix} g_{X_g} \\ 0 \\ g_{Z_g} \end{vmatrix} \tag{3.30}
$$

The second step will resolve the inertial components of gravity into the required body components g_x, g_y, g_z. The direction-cosine matrix relating inertial coordinates with body coordinates was derived previously and is given in Equation (3.1). The required transformation is, therefore:

$$\begin{vmatrix} g_x \\ g_y \\ g_z \end{vmatrix} = \begin{vmatrix} l_1 & l_2 & l_3 \\ m_1 & m_2 & m_3 \\ n_1 & n_2 & n_3 \end{vmatrix} \begin{vmatrix} g_X \\ g_Y \\ g_Z \end{vmatrix} \tag{3.31}$$

The direction cosines are defined by the relations of Equation (3.6). A sequence of resolutions similar to those leading to Equation (3.31) is required to resolve local-geocentric components of winds into body-axes components. To obtain inertial components of wind the inverse of Equation (3.29) applies.

$$\begin{vmatrix} \dot{X}_w - \omega_p Y \\ \dot{Y}_w + \omega_p X \\ \dot{Z}_w \end{vmatrix} = \begin{vmatrix} i_1 & i_2 & i_3 \\ j_1 & j_2 & j_3 \\ k_1 & k_2 & k_3 \end{vmatrix} \begin{vmatrix} \dot{X}_{g_w} \\ \dot{Y}_{g_w} \\ \dot{Z}_{g_w} \end{vmatrix} \tag{3.32}$$

The components $\omega_p Y$ and $-\omega_p X$ must be added to the result to obtain inertial components of winds. Resolving inertial wind components to body-axis components requires the same direction-cosine matrix used in Equation (3.31), and the body components of winds are:

$$\begin{vmatrix} u_w \\ v_w \\ w_w \end{vmatrix} = \begin{vmatrix} l_1 & l_2 & l_3 \\ m_1 & m_2 & m_3 \\ n_1 & n_2 & n_3 \end{vmatrix} \begin{vmatrix} \dot{X}_w \\ \dot{Y}_w \\ \dot{Z}_w \end{vmatrix} \tag{3.33}$$

The body components of airspeed are determined by subtracting the body components of wind from the body components of velocity.

The body components of airspeed will be used to compute the angle of attack and sideslip.

$$\alpha = \operatorname{Tan}^{-1}\left(\frac{w - w_w}{u - u_w}\right) \tag{3.34}$$

$$\beta = \operatorname{Tan}^{-1}\left(\frac{v - v_w}{u - u_w}\right) \tag{3.35}$$

The definitions of angle of attack and sideslip are consistent with the aerodynamic data normally obtained from wind tunnel tests of sting-mounted models because of the manner in which the sting may be moved. The corresponding transformations from wind axes to body axes are given as Section 3.1.11. If aerodynamic data as obtained from turntable-and-strut mounted models are used, an alternate definition may be required depending upon the procedure used in data reduction.

3.1.7 <u>Reduced-Degree-of-Freedom Analyses Options</u> - The following para-
graphs describe the coordinate transformations required to account for the
motion of the body when the program is operating in several reduced-degree-of-
freedom modes. From a program economics standpoint, it is more convenient to
solve the equations of motion in vehicle body axis (with the exception of the
point-mass option) and revise the coordinate transformations than to rewrite
the equations of motion because the limited-motion transformations are quite
simple. In general, however these transformations can not be obtained simply
by deleting terms from the unrestricted-motion transformations because the
constraints imposed by limiting the motion imply certain planes of operation.
For example, the three-degree-of-freedom longitudinal analysis is obtained by
excluding, among other things, the side force, which includes side-force
components of Coriolis acceleration. This restriction can be fulfilled only
when the motion is in the equatorial plane. When the restricted plane of motion
is recognized, some of the required transformations can be calculated from the
general transformations by suitable substitutions.

3.1.8 <u>Three-Degree-of-Freedom Longitudinal Analyses</u> - The three equations
of motion involving the summation of forces along the x- and z-body axes and
the summation of moments about the y-axis are solved for the translational
accelerations $\dot{u}$ and $\dot{w}$ and the angular acceleration $\dot{q}$. Integration of these
quantities yields the components of inertial velocity u and w and the pitch
rate q. Integration of q gives the pitch attitude with respect to the inertial
X - Z-axes.

<u>Flat-Planet Problem</u> - The inertial coordinates in the flat-planet problem
are the X_g-Z_g elevation-plane coordinates. Velocity components in the X_g-Z_g
coordinate system may be found by direct resolution through the angle Θ which
is obtained by integrating q. The direction cosines relating the body and X_g-Z_g
coordinates are:

$$\begin{vmatrix} X_g \\ Z_g \end{vmatrix} = \begin{vmatrix} \cos\Theta & \sin\Theta \\ -\sin\Theta & \cos\Theta \end{vmatrix} \begin{vmatrix} x \\ z \end{vmatrix} \qquad (3.36)$$
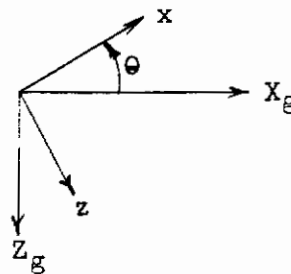
The velocity may be resolved using the same transformation, so that

$$\begin{vmatrix} \dot{X}_g \\ \dot{Z}_g \end{vmatrix} = \begin{vmatrix} \cos\Theta & \sin\Theta \\ -\sin\Theta & \cos\Theta \end{vmatrix} \begin{vmatrix} u \\ w \end{vmatrix} \qquad (3.37)$$

Positions in the X_g-Z_g system are then determined by integration. Components
of wind and gravity along the body axes are resolved using the inverse of
Equation (3.36). For winds:

$$\begin{vmatrix} u_W \\ w_W \end{vmatrix} = \begin{vmatrix} \cos\Theta & -\sin\Theta \\ \sin\Theta & \cos\Theta \end{vmatrix} \begin{vmatrix} \dot{X}_{gW} \\ \dot{Z}_{gW} \end{vmatrix} \qquad (3.38)$$

21

The body components of airspeed may be calculated and the angle of attack computed as in Equation (3.34).

In the flat-planet problem, g_{X_g} = zero and $g_{Z_g} = g_{ref}$. Therefore, the body components of gravity are:

$$g_z = g_{ref} \, \text{Cos} \, \Theta$$

$$g_x = -g_{ref} \, \text{Sin} \, \Theta \tag{3.39}$$

Rotating-Planet Problem - A three-degree-of-freedom longitudinal problem with a rotating planet must be confined to the equatorial plane in order that all components of Coriolis acceleration are included in the equations of motion. This means that the coordinate system used in this problem is the X-Y inertial axes in the equatorial plane. At time equal zero, the vehicle lies on the X-inertial axis. The inertial angle B is equal to $\Theta_{L_0} - \Theta_L - \omega_p t$, as in the six-degree problem, and may be expressed as a function of inertial displacement:

$$B = \text{Tan}^{-1} \left(\frac{Y}{X} \right) \tag{3.40}$$

The angle B locates the local-geocentric-horizon coordinates which will be referred to as the Y_g-Z_g coordinates since X_g is not necessary in this problem (see Figure (3.4):
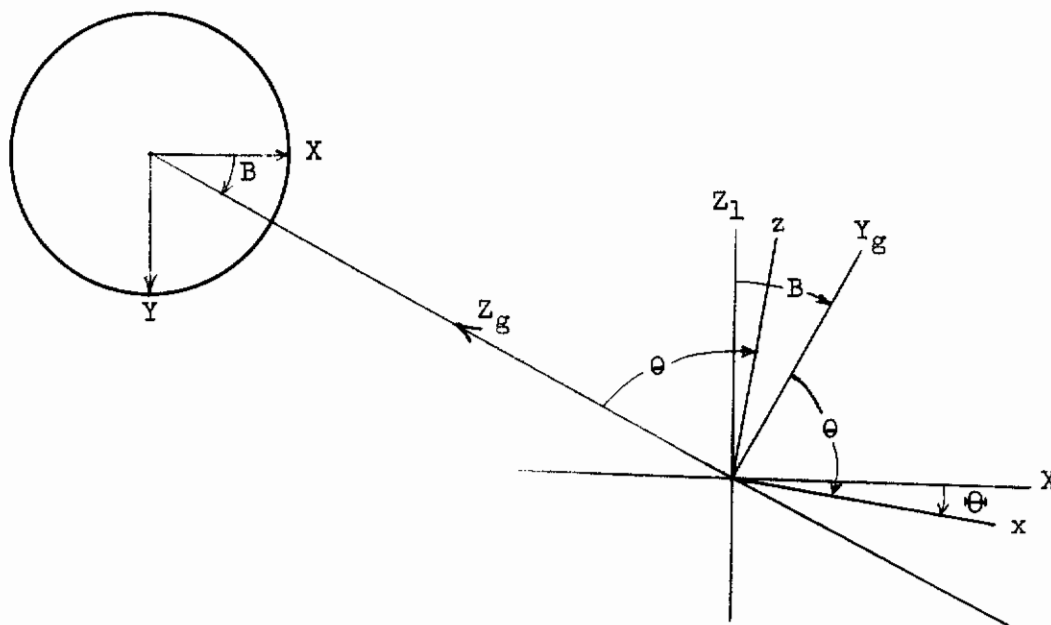
Figure 3.4 - Relation Between Body Axes, Local-Geocentric, and Inertial Coordinates for Motion in Equatorial Plane

22

The direction cosines relating the inertial axes X - Y and the body axes x-z may be determined by rotating the X-Y-Z system about X through $90°$ to define the coordinates, $X-Y_1-Z_1$, and then rotating this system through Θ to reach body coordinates. The transformation is defined by:

$$
\begin{vmatrix} x \\ y \\ z \end{vmatrix} = \begin{vmatrix} \Theta \\ Y_1 \end{vmatrix} \begin{vmatrix} 90° \\ X \end{vmatrix} \begin{vmatrix} X \\ Y \\ Z \end{vmatrix}
$$

(3.41)

or, substituting the individual rotation matrices,

$$
\begin{vmatrix} x \\ y \\ z \end{vmatrix} = \begin{vmatrix} \cos\Theta & 0 & -\sin\Theta \\ 0 & 1 & 0 \\ \sin\Theta & 0 & \cos\Theta \end{vmatrix} \begin{vmatrix} 1 & 0 & 0 \\ 0 & \cos 90° & \sin 90° \\ 0 & -\sin 90° & \cos 90° \end{vmatrix} \begin{vmatrix} X \\ Y \\ Z \end{vmatrix}
$$

The inertial angle Θ is $\int_0^t q\, dt + \Theta_0 - 90°$. The direction cosines relating body and inertial coordinates are given by the elements of the resulting matrix.

$$
\begin{vmatrix} x \\ y \\ z \end{vmatrix} = \begin{vmatrix} \cos\Theta & \sin\Theta & 0 \\ 0 & 0 & 1 \\ \sin\Theta & -\cos\Theta & 0 \end{vmatrix} \begin{vmatrix} X \\ Y \\ Z \end{vmatrix}
$$

(3.42)

Expanding the transformation

$$x = X \cos\Theta + Y \sin\Theta$$

$$y = Z$$

$$z = X \sin\Theta - Y \cos\Theta$$

But $Z = 0$ since the motion is restricted to the X-Y plane and the required transformation reduces to:

$$
\begin{vmatrix} x \\ z \end{vmatrix} = \begin{vmatrix} \cos\Theta & \sin\Theta \\ \sin\Theta & -\cos\Theta \end{vmatrix} \begin{vmatrix} X \\ Y \end{vmatrix}
$$

(3.43)

Inertial components of inertial velocity may be found by using the transpose of the transformation matrix Equation (3.43)

$$
\begin{vmatrix} \dot{X} \\ \dot{Y} \end{vmatrix} = \begin{vmatrix} \cos\Theta & \sin\Theta \\ \sin\Theta & -\cos\Theta \end{vmatrix} \begin{vmatrix} u \\ w \end{vmatrix}
$$

(3.44)

Because positive rotations were used in Equation (3.41), the resulting body-axis orientation is for a normal upright easterly flight. To obtain the proper orientation for a westerly flight, the rotation about the X-axis is negative and Equation

23

(3.41) becomes

$$
\begin{vmatrix} x \\ y \\ z \end{vmatrix} = \begin{vmatrix} -\Theta \\ & Y_1 \end{vmatrix} \begin{vmatrix} -90° \\ & X \end{vmatrix} \begin{vmatrix} X \\ Y \\ Z \end{vmatrix}
\tag{3.45}
$$

Equations (3.43) and (3.44) then become

$$
\begin{vmatrix} x \\ z \end{vmatrix} = \begin{vmatrix} \text{Cos } \Theta & \text{Sin } \Theta \\ -\text{Sin } \Theta & +\text{Cos } \Theta \end{vmatrix} \begin{vmatrix} X \\ Y \end{vmatrix}
\tag{3.46}
$$

and

$$
\begin{vmatrix} \dot{X} \\ \dot{Y} \end{vmatrix} = \begin{vmatrix} \text{Cos } \Theta & -\text{Sin } \Theta \\ \text{Sin } \Theta & \text{Cos } \Theta \end{vmatrix} \begin{vmatrix} u \\ w \end{vmatrix}
\tag{3.47}
$$

A single equation for each transformation may be obtained for both easterly and westerly flight by incorporating the constant K_σ, as follows

$$
\begin{vmatrix} x \\ z \end{vmatrix} = \begin{vmatrix} \text{Cos } \Theta & \text{Sin } \Theta \\ K_\sigma\text{Sin } \Theta & -K_\sigma\text{Cos } \Theta \end{vmatrix} \begin{vmatrix} X \\ Y \end{vmatrix}
\tag{3.48}
$$

and

$$
\begin{vmatrix} \dot{X} \\ \dot{Y} \end{vmatrix} = \begin{vmatrix} \text{Cos } \Theta & K_\sigma\text{Sin } \Theta \\ \text{Sin } \Theta & -K_\sigma\text{Cos } \Theta \end{vmatrix} \begin{vmatrix} u \\ w \end{vmatrix}
\tag{3.49}
$$

where

$$K_\sigma = +1 \text{ for easterly flight}$$

$$K_\sigma = -1 \text{ for westerly flight}$$

The resolution of inertial components of inertial velocity to local-geocentric components of planet-referenced velocity is obtained by setting $\phi_L = 0$ in Equation (3.29). The transformation becomes:

$$
\begin{vmatrix} \dot{X}_g \\ \dot{Y}_g \\ \dot{Z}_g \end{vmatrix} = \begin{vmatrix} 0 & 0 & -1 \\ \text{Sin } B & -\text{Cos } B & 0 \\ -\text{Cos } B & -\text{Sin } B & 0 \end{vmatrix} \begin{vmatrix} \dot{X} - \omega_p Y \\ \dot{Y} + \omega_p X \\ \dot{Z} \end{vmatrix}
$$

This may be simplified to a single-plane transformation by deleting $\dot{X}_g$ and $\dot{Z}$ in a manner similar to that used to derive Equation (3.48).

$$\begin{vmatrix} \dot{Y}_g \\ \dot{Z}_g \end{vmatrix} = \begin{vmatrix} \text{Sin } B & -\text{Cos } B \\ -\text{Cos } B & -\text{Sin } B \end{vmatrix} \begin{vmatrix} \dot{X} - \omega_p Y \\ \dot{Y} + \omega_p X \end{vmatrix} \qquad (3.50)$$

The inertial components of winds are determined by using the transpose of the transformation matrix of Equation (3.50), and are

$$\begin{vmatrix} \dot{X}_W - \omega_p Y \\ \dot{Y}_W + \omega_p X \end{vmatrix} = \begin{vmatrix} \text{Sin } B & -\text{Cos } B \\ -\text{Cos } B & -\text{Sin } B \end{vmatrix} \begin{vmatrix} \dot{Y}_{g_W} \\ \dot{Z}_{g_W} \end{vmatrix} \qquad (3.51)$$

The terms $\omega_p Y$ and $\omega_p X$ are inertial components of the velocity due to the planet's rotation. It will be convenient to resolve this rotational velocity component to local-geocentric components. This operation may be verified by substituting Equations (3.17), (3.19), and (3.22) into (3.18) and comparing components.

$$\begin{vmatrix} \dot{X}_W \\ \dot{Y}_W \end{vmatrix} = \begin{vmatrix} \text{Sin } B & -\text{Cos } B \\ -\text{Cos } B & -\text{Sin } B \end{vmatrix} \begin{vmatrix} \dot{Y}_{g_W} + \omega_p R \\ \dot{Z}_{g_W} \end{vmatrix} \qquad (3.52)$$

The body components of winds are required and may be determined from the inverse of the transformation matrix of Equation (3.49).

$$\begin{vmatrix} u_W \\ w_W \end{vmatrix} = \begin{vmatrix} \text{Cos } \theta & \text{Sin } \theta \\ K_\sigma \text{Sin } \theta & -K_\sigma \text{Cos } \theta \end{vmatrix} \begin{vmatrix} \dot{X}_W \\ \dot{Y}_W \end{vmatrix} \qquad (3.53)$$

The resolution of wind components from local-geocentric to body coordinates may be accomplished by combining Equations (3.52) and (3.53) according to the method of Reference (9).

The transformation is:

$$\begin{vmatrix} u_W \\ w_W \end{vmatrix} = \begin{vmatrix} \text{Cos } \theta & \text{Sin } \theta \\ \text{Sin } \theta & -\text{Cos } \theta \end{vmatrix} \begin{vmatrix} \text{Sin } B & -\text{Cos } B \\ -\text{Cos } B & -\text{Sin } B \end{vmatrix} \begin{vmatrix} \dot{Y}_{g_W} + \omega_p R \\ \dot{Z}_{g_W} \end{vmatrix}$$

or

$$\begin{vmatrix} u_W \\ w_W \end{vmatrix} = \begin{vmatrix} (\text{Cos } \theta \text{ Sin } B - \text{Sin } \theta \text{ Cos } B) & (-\text{Cos } B \text{ Cos } \theta - \text{Sin } B \text{ Sin } \theta) \\ (\text{Sin } \theta \text{ Sin } B + \text{Cos } \theta \text{ Cos } B) & (-\text{Sin } \theta \text{ Cos } B + \text{Cos } \theta \text{ Sin } B) \end{vmatrix} \begin{vmatrix} \dot{Y}_{g_W} + \omega_p R \\ \dot{Z}_{g_W} \end{vmatrix}$$

which simplifies to

$$\begin{vmatrix} u_W \\ w_W \end{vmatrix} = \begin{vmatrix} \text{Sin } (B - \theta) & -\text{Cos } (B - \theta) \\ \text{Cos } (B - \theta) & \text{Sin } (B - \theta) \end{vmatrix} \begin{vmatrix} \dot{Y}_{g_W} + \omega_p R \\ \dot{Z}_{g_W} \end{vmatrix} \qquad (3.54)$$

25

From Figure (3.4) the following relationship between Θ, $\dot{\Theta}$, and B may be written:

$$90° = K_\sigma B + \Theta - K_\sigma \dot{\Theta}$$

$$\Theta = 90° - K_\sigma (B - \dot{\Theta}) \tag{3.55}$$

Therefore:

$$\text{Sin } \Theta = \text{Cos } (B - \dot{\Theta})$$

$$K_\sigma \text{ Cos } \Theta = \text{Sin } (B - \dot{\Theta}) \tag{3.56}$$

Substituting Equation (3.56) into Equation (3.54) and incorporating the factor K_σ as defined for Equations (3.48) and (3.49)

$$\begin{vmatrix} u_W \\ w_W \end{vmatrix} = \begin{vmatrix} K_\sigma \text{Cos } \Theta - \text{Sin } \Theta \\ K_\sigma \text{Sin } \Theta \quad \text{Cos } \Theta \end{vmatrix} \begin{vmatrix} \dot{Y}_{g_W} + \omega_p R \\ \dot{Z}_{g_W} \end{vmatrix} \tag{3.57}$$

Comparison of this equation with Equation (3.38) suggests that the same wind transformation matrix may be used for both rotating and flat-planet three-degree-of-freedom longitudinal problems. The component $\omega_p R$ must be included in the case of the rotating planet, however, to ensure that the vector defined by the transformed components is the same vector as described by the original components. The local Euler angle Θ then is the only attitude angle required for resolutions in the three-degree-of-freedom longitudinal analysis problem. The angle of attack is computed as in Equation (3.34). The component resolution of gravity for the rotating-planet mode of operation of this problem is given by Equation (3.39) since gX_g is also zero in the equatorial plane.

3.1.9 <u>Three-Degree-of-Freedom Lateral Analyses</u> - Three-degree-of-freedom lateral analyses are often performed in the design of aircraft, autopilots, and guidance computers on the basis that the lateral and longitudinal motions are independent of each other. Although the information obtained from such an analysis is considered quite valuable, certain inconsistencies are created in the mechanics of solving the problem. The three-degree-of-freedom lateral motion is not defined completely by the three accelerations considered, as noted in Paragraph 2.3. Therefore, the motion calculated is treated as a perturbation motion. The assumptions made concerning this motion are:

(a) The lateral displacement from a given straight-line track is due only to the velocity imparted by body side-force accelerations. The displacements from the reference line due to the axial velocity and yaw angle are neglected.

(b) The center-of-gravity of the body is assumed to travel in the plane established by the motion described above. The vertical and lateral displacements due to the sinking velocity and the roll attitude of the body are neglected.

The coordinate systems and transformations which retain these assumptions and constraints are described and derived in the following paragraphs. The intent of this option is to provide a digital simulation of the normal lateral-dynamics problem assumed for control-system analysis, and further, to provide this problem option in such a form that the validity of the assumption of decoupled motion may be easily verified. The inconsistencies of the usual dynamic analysis will be

26

observed as the discussion proceeds. For operation of the program in the three-degree-of-freedom lateral mode, the equations of motion describing translation in the y direction and the two moment equations for yaw and roll are solved for $\dot{p}$, $\dot{r}$, and $\dot{v}$. The velocity components u and w appearing in the y-acceleration equation are programmed input functions, as noted in Paragraph 2.3. The computed accelerations are integrated to obtain the body angular velocities p and r, and the body component of velocity v. Body angular velocities will be resolved into inertial components. The required rotations are conveniently represented on a unit sphere, Figure (3.5). The labelled points represent the intersection of a particular coordinate axis with the surface of the unit sphere. Since only a flat planet is considered in this optional mode, the X_g-Y_g-Z_g coordinates are the inertial coordinates. Only two rotations are required to orient the body axis, x-y-z, with respect to the inertial axes since the Euler angle Θ is arbitrarily set to zero[4]. The first rotation is about the Z_g-axis through the angle ψ and the final rotation is about the x-axis through the roll angle ϕ. The angular rotation rate of the body axes may be written as the vector $\overline{\omega}$.
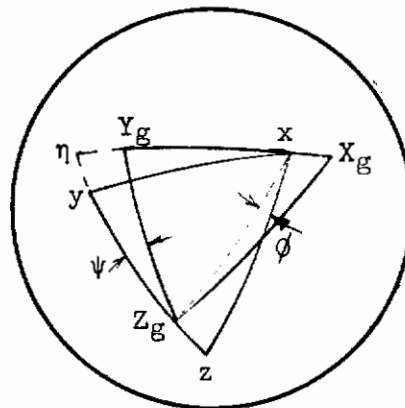
Figure 3.5 – Unit Sphere Diagram For Lateral Motion Coordinate Transformations

$$\overline{\omega} = p\,\overline{1}_x + r\,\overline{1}_z \qquad (3.58)$$

which may be expressed in the x-η-Z_g system (since these are the axes about which the rotations occur) as:

$$\overline{\omega} = \dot{\phi}\,\overline{1}_x + \dot{\Theta}\,\overline{1}_\eta + \dot{\psi}\,\overline{1}_{Z_g} \qquad (3.59)$$

The unit vector $\overline{1}_z$ has components in the x-η-Z_g coordinate system which are:

$$\overline{1}_z = \text{Cos } \phi\,\overline{1}_{Z_g} - \text{Sin } \phi\,\overline{1}_\eta$$

---

(4)   This assumption is normally made in the three-degree-of-freedom lateral dynamic analysis, but is inconsistent with the assumptions regarding the velocity components u and w which define the body angle of attack ($\alpha = \text{Tan}^{-1}(w/u)$). Since the Euler angle Θ is the angle between the horizontal plane, in which the lateral motion is assumed to occur, and the body axis, x, the Euler angle should be $\Theta = \alpha$. This discrepancy is normally disregarded in the perturbation analyses conducted in lateral dynamics investigations and will also be neglected here. This is done so that an evaluation may be obtained of the errors incurred by assuming the motions in the longitudinal and lateral planes to be decoupled.

Substituting this expression for the body unit vector in the z-direction into Equation (3.58) resolves the expression for $\bar{\omega}$ into components in the x-η-Z_g system as follows:

$$\bar{\omega} = p\,\bar{1}_x - r\,\text{Sin}\,\phi\,\bar{1}_\eta + r\,\text{Cos}\,\phi\,\bar{1}_{Z_g} \qquad (3.60)$$

Comparing the scalar coefficients of similar unit vectors in Equations (3.59) and (3.60) provides the required relations for resolving the body angular rates into Euler angle rates.

$$\begin{aligned} \dot{\phi} &= p \\ \dot{\Theta} &= -r\,\text{Sin}\,\phi \\ \dot{\psi} &= r\,\text{Cos}\,\phi \end{aligned} \qquad (3.61)$$

However, the perturbation displacements in the pitch plane are not permitted in the analysis, as noted in the introductory paragraph to this section. Therefore, the velocity

$$\dot{\Theta} = -r\,\text{Sin}\,\phi$$

must be disregarded, since it rotates the plane in which the lateral perturbation motion is assumed to occur. This is the second major inconsistency of the normal lateral analysis. The resolution which will be used is:

$$\begin{aligned} \dot{\phi} &= p \\ \dot{\psi} &= r\,\text{Cos}\,\phi \end{aligned}$$

These relations point up a third inconsistency of the normal lateral dynamic analysis, which is that the roll and yaw rates above are integrated to define the perturbed attitudes of the body. However, these are not the total motion of the body and the displacements which actually occur due to the combinations of u and w velocities in the ψ and ϕ directions, respectively are ignored. The gravitational component resolution required is:

$$g_y = g_{Z_g}\,\text{Sin}\,\phi \qquad (3.62)$$

since the pitch angle Θ is arbitrarily set to zero and angle of attack is ignored.

The component of wind in the y-direction may be calculated by resolving the Y_g component of wind to the body axes.

$$v_w = \dot{Y}_{g_w}\,\text{Cos}\,\widehat{Y_g\,y}$$

From the spherical trigonometry of the triangle of reference, Figure (3.5),

$$\text{Cos}\,\widehat{Y_g\,y} = \text{Cos}\,\phi\,\text{Cos}\,\psi$$

Therefore,

$$v_w = \dot{Y}_{g_w}\,\text{Cos}\,\phi\,\text{Cos}\,\psi \qquad (3.63)$$

28

The body component of translational velocity will be resolved to a component of velocity along the Y_g-axis only, as velocities in the elevation plane are not computed in this option. This resolution may be written:

$$\dot{Y}_g \ = \ v \ \text{Cos} \ \widehat{Y_g y} = v \ \text{Cos} \ \phi \ \text{Cos} \ \psi \qquad (3.64)$$

    3.1.10 **Point Mass Analyses** - For this option the rotational body rates p, q, and r are undefined. It is, therefore, necessary to rederive the equations of motion in such a manner as to avoid this complication. The most convenient coordinate system is considered to be a Cartesian planetocentric coordinate system designated X_e-Y_e-Z_e. The origin of this system lies on the polar axis of the planet and in the equatorial plane. The Z_e-axis is collinear with the polar axes and positive toward the south pole. The X_e-axis is in the equatorial plane and is fixed at the longitude of the vehicle at time equal zero; (i.e., the coordinate system rotates with the planet) the Y_e-axis is positioned to form a right-handed system. The inertial coordinates X-Y-Z and the coordinates X_e-Y_e-Z_e coincide at time zero.

    The components of the planet-referenced acceleration are integrated to obtain the planet-referenced velocity components $\dot{X}_e$-$\dot{Y}_e$-$\dot{Z}_e$. Vehicle positions in this coordinate system are determined by integration of these velocities. The position of the missile in a planet-referenced spherical coordinate system will be determined. The spherical coordinates are longitude, geocentric latitude, and distance from the center of the planet. The angle "C" (see Figure (3.6)) represents the change in longitude of the vehicle and may be written:

$$C \ = \ \Theta_{L_o} - \Theta_L \qquad (3.65)$$

Thus the angle C differs from the angle B of the six-degree-of-freedom program by the planet's rotation, $\omega_p t$. The angle C is related to the vehicle displacement by the expression:

$$C \ = \ \text{Tan}^{-1} \left(\frac{Y_e}{X_e} \right) \qquad (3.66)$$

    The geocentric latitude, altitude, distance from the planet's center, and geodetic latitude are computed as in the six-degree-of-freedom program, (see Paragraph 3.1.4). Components of planet-referenced velocity $\dot{X}_e$-$\dot{Y}_e$-$\dot{Z}_e$ will be resolved into velocity components in local-geocentric-horizon coordinates X_g-Y_g-Z_g. The direction cosines describing the orientation of the local-geocentric horizon relative to X_e-Y_e-Z_e coordinates may be derived in a manner similar to that of the six-degree-of-freedom problem, (see Equation (3.15). The only difference is that the angle C must be used in place of B and X_e-Y_e-Z_e used in place of X-Y-Z respectively. Since B = Θ_{L_o} - Θ_L - $\omega_p t$, the angle C may be calculated by setting ω_p equal to zero in B. Therefore, the direction cosines required to orient the local-geocentric coordinates may be calculated as in the six-degree-of-freedom problem if ω_p is set equal to zero, since both local-geocentric and X_e-Y_e-Z_e are planet-fixed coordinates. The required resolution is obtained from Equation (3.15). The subscript zero indicates that the direction cosines are evaluated with ω_p = 0.

29

$$
\begin{vmatrix} \dot{X}_g \\ \dot{Y}_g \\ \dot{Z}_g \end{vmatrix} = \begin{vmatrix} i_{10} & j_{10} & k_{10} \\ i_{20} & j_{20} & k_{20} \\ i_{30} & j_{30} & k_{30} \end{vmatrix} \begin{vmatrix} \dot{X}_e \\ \dot{Y}_e \\ \dot{Z}_e \end{vmatrix}
\qquad (3.67)
$$

The planet-referenced velocity may be calculated from its components:

$$
V_g = \sqrt{\dot{X}_g{}^2 + \dot{Y}_g{}^2 + \dot{Z}_g{}^2}
\qquad (3.68)
$$
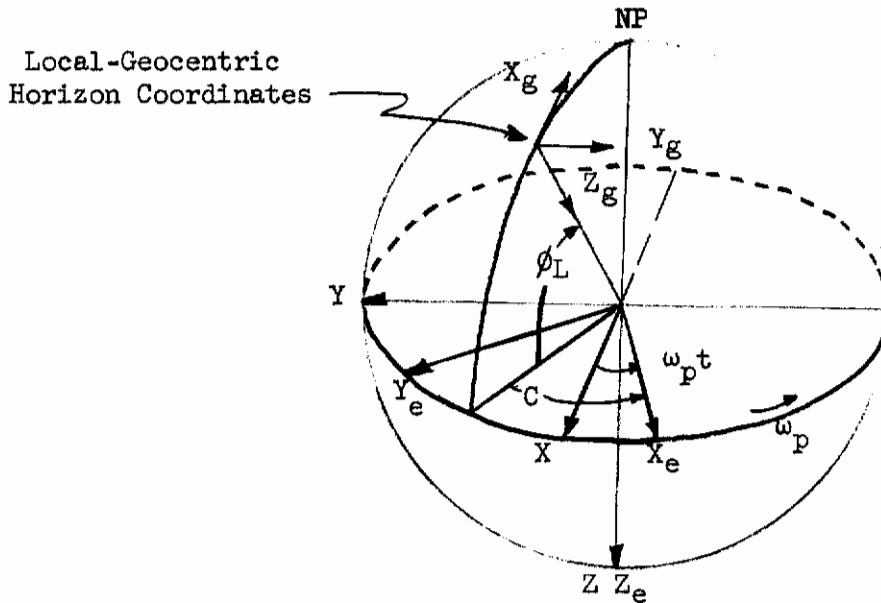
Figure 3.6 Relation Between Local-Geocentric,
Inertial, and Earth-Referenced Coordinates for Point-Mass Problems

The flight-path angles[5] are computed as in the six-degree-of-freedom problem:

$$
\sigma = \text{Sin}^{-1}\left(\frac{\dot{Y}_g}{\sqrt{\dot{X}_g{}^2 + \dot{Y}_g{}^2}} \right)
\qquad (3.69)
$$

$$
\gamma = \text{Sin}^{-1}\left(\frac{-\dot{Z}_g}{V_g} \right)
\qquad (3.70)
$$

Equations (3.68), (3.69), and (3.70) are applicable to both the oblate- and flat-planet options.

––––––––––––––

(5) The flight-path angles are defined by surface-referenced velocities with respect to the local horizon and longitude lines.

The aerodynamic and thrust forces for the point-mass problem will normally be summed in a wind-axis coordinate system, X_A-Y_A-Z_A. Since the equations of motion are solved in the X_e-Y_e-Z_e coordinates, the wind-axis components of forces must be revolved into the components of this system.

The forces will first be resolved from the wind axes to the local-geocentric coordinates. The wind axes are defined relative to the local geocentric axes by three angles: heading, σ; flight path attitude, γ; and bank, B_A.
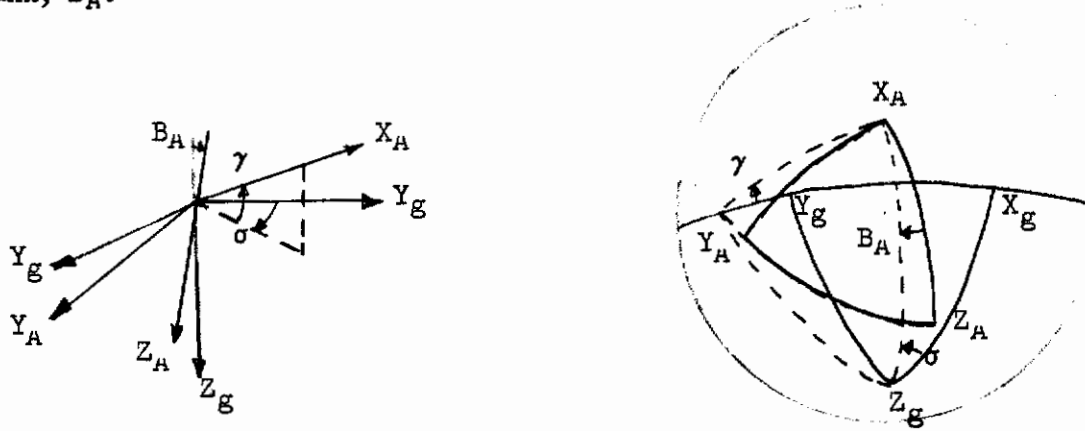
Figure 3.7 - Relationship Between Local-Geocentric Axes and Wind Axes

The transformations are:

$$
\begin{vmatrix} X' \\ Y' \\ Z_g \end{vmatrix} = \begin{vmatrix} \cos \sigma & \sin \sigma & 0 \\ -\sin \sigma & \cos \sigma & 0 \\ 0 & 0 & 1 \end{vmatrix} \begin{vmatrix} X_g \\ Y_g \\ Z_g \end{vmatrix}
$$
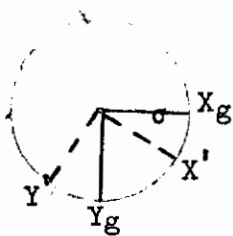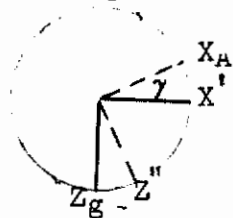
$$
\begin{vmatrix} X_A \\ Y' \\ Z'' \end{vmatrix} = \begin{vmatrix} \cos \gamma & 0 & -\sin \gamma \\ 0 & 1 & 0 \\ \sin \gamma & 0 & \cos \gamma \end{vmatrix} \begin{vmatrix} X' \\ Y' \\ Z_g \end{vmatrix}
$$
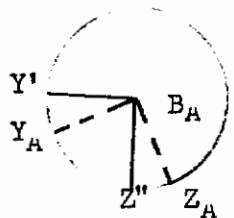
$$
\begin{vmatrix} X_A \\ Y_A \\ Z_A \end{vmatrix} = \begin{vmatrix} 1 & 0 & 0 \\ 0 & \cos B_A & \sin B_A \\ 0 & -\sin B_A & \cos B_A \end{vmatrix} \begin{vmatrix} X_A \\ Y' \\ Z'' \end{vmatrix}
$$

31

The complete transformation then is:

$$
\begin{vmatrix} X_A \\ Y_A \\ Z_A \end{vmatrix} = \begin{vmatrix} \cos\gamma\cos\sigma & \cos\gamma\sin\sigma & -\sin\gamma \\ -\sin\sigma\cos B_A + \sin\gamma\cos\sigma\sin B_A & \cos\sigma\cos B_A + \sin\gamma\sin\sigma\sin B_A & \cos\gamma\sin B_A \\ \sin\sigma\sin B_A + \sin\gamma\cos\sigma\cos B_A & -\cos\sigma\sin B_A + \sin\gamma\sin\sigma\cos B_A & \cos\gamma\cos B_A \end{vmatrix} \begin{vmatrix} X_g \\ Y_g \\ Z_g \end{vmatrix} \quad (3.71)
$$

which will be defined as

$$
= \begin{vmatrix} r_1 & s_1 & t_1 \\ r_2 & s_2 & t_2 \\ r_3 & s_3 & t_3 \end{vmatrix} \begin{vmatrix} X_g \\ Y_g \\ Z_g \end{vmatrix} \quad (3.72)
$$

The resolution of forces from wind axes to local geocentric becomes:

$$
\begin{vmatrix} FX_g \\ FY_g \\ FZ_g \end{vmatrix} = \begin{vmatrix} r_1 & r_2 & r_3 \\ s_1 & s_2 & s_3 \\ t_1 & t_2 & t_3 \end{vmatrix} \begin{vmatrix} FX_A \\ FY_A \\ FZ_A \end{vmatrix} \quad (3.73)
$$

For the rotating-planet, the local geocentric components must be resolved to components in the X_e-Y_e-Z_e system. The required direction cosines are given by Equation (3.67) evaluated using the angle C in place of angle B.

$$
\begin{vmatrix} FX_e \\ FY_e \\ FZ_e \end{vmatrix} = \begin{vmatrix} i_{10} & i_{20} & i_{30} \\ j_{10} & j_{20} & j_{30} \\ j_{10} & j_{20} & j_{30} \end{vmatrix} \begin{vmatrix} FX_g \\ FY_g \\ FZ_g \end{vmatrix} \quad (3.74)
$$

The combined transformation from wind axes to local geocentric will be defined as a single matrix.

$$
\begin{vmatrix} FX_e \\ FY_e \\ FZ_e \end{vmatrix} = \begin{vmatrix} o_1 & o_2 & o_3 \\ p_1 & p_2 & p_3 \\ q_1 & q_2 & q_3 \end{vmatrix} \begin{vmatrix} FX_A \\ FY_A \\ FZ_A \end{vmatrix} + \begin{vmatrix} mgX_e \\ mgY_e \\ mgZ_e \end{vmatrix} \quad (3.75)
$$

3.1.11 <u>Body-Axes to Wind-Axes Transformation</u> - To permit the use of body (x, y, z) axes aerodynamic data and to convert the body axes components of thrust to the wind axes system, a coordinate transformation must be made. The coordinate transformation below is first through the angle of attack, α, and then through an auxiliary angle, β'.

$$\tan \beta' = \frac{v}{u} \cos \alpha$$

$$= \tan \beta \cos \alpha$$
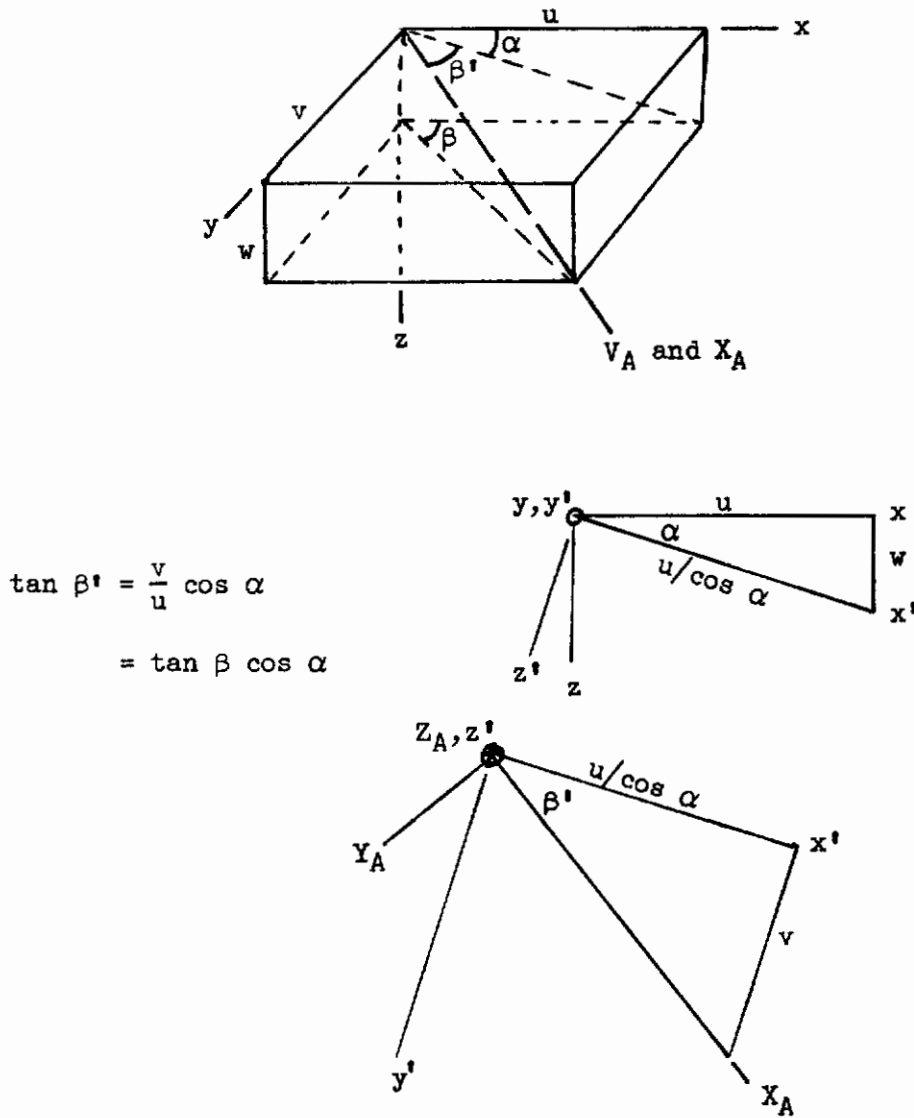
Figure 3.8   Relationship Between Body Axes
and Wind Axes

33

$$
\begin{vmatrix} x' \\ y' \\ z' \end{vmatrix} = \begin{vmatrix} \cos\alpha & 0 & \sin\alpha \\ 0 & 1 & 0 \\ -\sin\alpha & 0 & \cos\alpha \end{vmatrix} \begin{vmatrix} x \\ y \\ z \end{vmatrix}
$$

$$
\begin{vmatrix} X_A \\ Y_A \\ Z_A \end{vmatrix} = \begin{vmatrix} \cos\beta' & \sin\beta' & 0 \\ -\sin\beta' & \cos\beta' & 0 \\ 0 & 0 & 1 \end{vmatrix} \begin{vmatrix} x' \\ y' \\ z' \end{vmatrix}
$$

$$
= \begin{vmatrix} \cos\beta'\cos\alpha & \sin\beta' & \cos\beta'\sin\alpha \\ -\sin\beta'\cos\alpha & \cos\beta' & -\sin\beta'\sin\alpha \\ -\sin\alpha & 0 & \cos\alpha \end{vmatrix} \begin{vmatrix} x \\ y \\ z \end{vmatrix} \qquad (3.76)
$$

which is defined as the u-v-w direction cosines.

$$
\begin{vmatrix} X_A \\ Y_A \\ Z_A \end{vmatrix} = \begin{vmatrix} u_1 & u_2 & u_3 \\ v_1 & v_2 & v_3 \\ w_1 & w_2 & w_3 \end{vmatrix} \begin{vmatrix} x \\ y \\ z \end{vmatrix} \qquad (3.77)
$$

$$
\begin{vmatrix} -C_D \\ C_Y \\ -C_L \end{vmatrix} = \begin{vmatrix} u_1 & u_2 & u_3 \\ v_1 & v_2 & v_3 \\ w_1 & w_2 & w_3 \end{vmatrix} \begin{vmatrix} -C_A \\ C_y \\ -C_N \end{vmatrix} \qquad (3.77a)
$$

The relationship between body and wind-axes aerodynamic coefficients is then established, noting the negative directions of the coefficients relative to the axes system.

If the assumption is made that the body xy plane lies in the vertical, $\phi = 0$, an alternate transformation can be made (Figure 3.9) using the pitch angle Θ, the difference between the azimuth heading and the yaw angle, $\sigma - \psi$, and the flight path angle, γ.

The direction cosines required for this transformation from body to the <u>vertical</u> wind axes system are:

$$
\begin{vmatrix} X_{A_V} \\ Y_{A_V} \\ Z_{A_V} \end{vmatrix} = \begin{vmatrix} \cos\gamma & 0 & -\sin\gamma \\ 0 & 1 & 0 \\ \sin\gamma & 0 & \cos\gamma \end{vmatrix} \begin{vmatrix} \cos(\sigma-\psi) & \sin(\sigma-\psi) & 0 \\ -\sin(\sigma-\psi) & \cos(\sigma-\psi) & 0 \\ 0 & 0 & 1 \end{vmatrix} \begin{vmatrix} \cos\Theta & 0 & \sin\Theta \\ 0 & 1 & 0 \\ -\sin\Theta & 0 & \cos\Theta \end{vmatrix} \begin{vmatrix} x \\ y \\ z \end{vmatrix}
$$

$$(3.78)$$

34
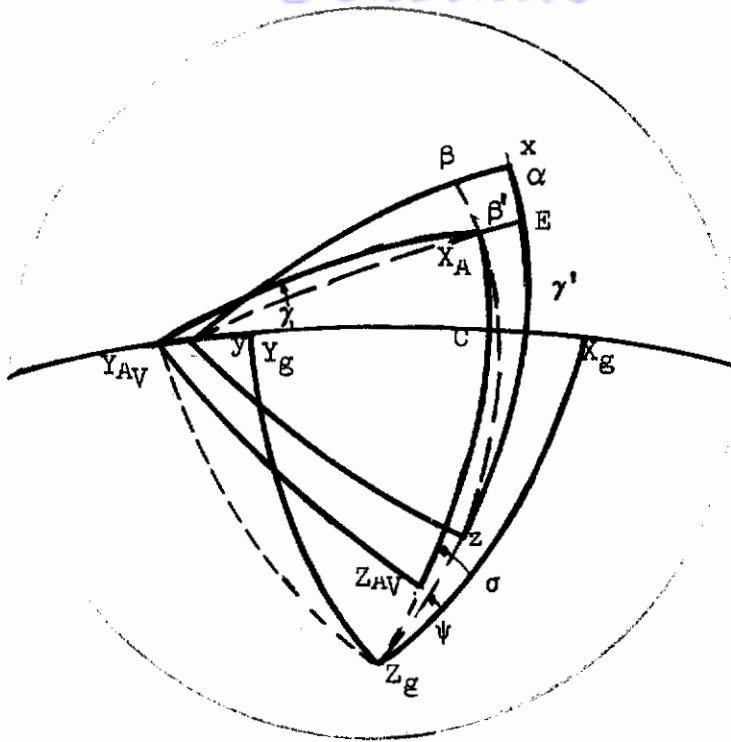
Figure 3.9 - Relationship Between Body Axes and Vertical
Wind Axes With Zero Body Roll Angle

The angles γ and σ are computed in the point mass options; Θ and ψ are not.
Applying the law of sines to the spherical triangle X_A-Z_g-E:

$$\sin(\sigma - \psi) = \frac{\sin\beta'}{\cos\gamma} \tag{3.79}$$

The sine of β' may be expressed in terms of the body coordinate components of
velocity as:

$$\sin\beta' = \frac{v}{V} = \frac{v}{\sqrt{u^2 + v^2 + w^2}} \tag{3.80}$$

Dividing numerator and denominator by u and expressing in terms of α and β

$$\sin\beta' = \frac{\tan\beta}{\sqrt{1 + \tan^2\alpha + \tan^2\beta}} \tag{3.81}$$

Substituting Equation (3.81) into Equation (3.79)

$$\sigma - \psi = \sin^{-1}\left(\frac{\tan\beta}{\cos\gamma\sqrt{1 + \tan^2\alpha + \tan^2\beta}}\right) \tag{3.82}$$

35

Since the body roll angle is zero:

$$\Theta = \alpha + \gamma' \tag{3.83}$$

Applying the law of sines to triangle X_A-y-C:

$$\sin \gamma' = \left(\frac{\sin \gamma}{\cos \beta'}\right) = \left(\frac{\sin \gamma}{\sqrt{1 - \sin^2 \beta'}}\right) \tag{3.84}$$

The angles Θ and σ-ψ can now be evaluated in terms of α and β for use in the vertical wind transformation, Equation (3.78).

This transformation from body axes to a vertical wind axes, with the assumption of zero roll, is the transformation used in the computer program. Thus, the load factors computed are also in the vertical wind axes system. The transformation from the vertical wind coordinates to the local geocentric is given by Equation (3.71), noting that the bank angle is zero for the vertical wind axes system.

3.1.12 **Winds in a Point Mass Analysis** - The effect of wind can be introduced in a point mass problem when the vehicle's angular position is dictated by an assumed perfect control system. The wind computations in this section are specifically designed for a control system using three rate-integrating gyros. The wind components will produce an angle of attack and an angle of sideslip which are not removed by the assumed aerodynamic stability of the vehicle, since the vehicle's angular position is fixed by other means, e.g., reaction control. The above conditions must be realized before the optional computations presented in this section can provide meaningful results. Only Flight Plan Programmer 10 meets these requisites.

The change in α and β due to the three components of wind is to be determined assuming that no instrument errors are present. Figure (3.10) contains the geometry necessary to consider winds. X_A'-Y_A'-Z_A' is the location of the wind coordinate system before the perturbing wind components are introduced. X_A-Y_A-Z_A is the new location of the wind coordinates after the perturbation occurs. X_A is coincident with the airspeed vector, Z_A is coincident with the lift but is positive in the opposite direction, Y_A defines the side force.

The three local geocentric components of winds will be introduced in a tabular listing with altitude as the independent variable. Let the three components of wind be written as follows:

$$\overline{V}_w = \dot{X}_{g_w} \overline{1}_{x_g} + \dot{Y}_{g_w} \overline{1}_{y_g} + \dot{Z}_{g_w} \overline{1}_{z_g} \tag{3.85}$$

$$\dot{X}_g \quad \text{North}$$
$$\dot{Y}_g \quad \text{East}$$
$$\dot{Z}_g \quad \text{Directed toward center of earth}$$

The airspeed vector is given by:

$$\overline{V}_a = \overline{V}_g - \overline{V}_w \tag{3.86}$$

36

WIND COMPONENTS FOR A POINT MASS ANALYSIS

$X_A Y_A Z_A$ IS A WIND COORDINATE SYSTEM $\overline{C}_D = -C_D \overline{1}_{X_A}$ $\overline{C}_y = C_y \overline{1}_{Y_A}$ $\overline{C}_L = -C_L \overline{1}_{Z_A}$

x y z BODY COORDINATES $\quad$ $X_g Y_g Z_g$ LOCAL GEOCENTRIC COORDINATES
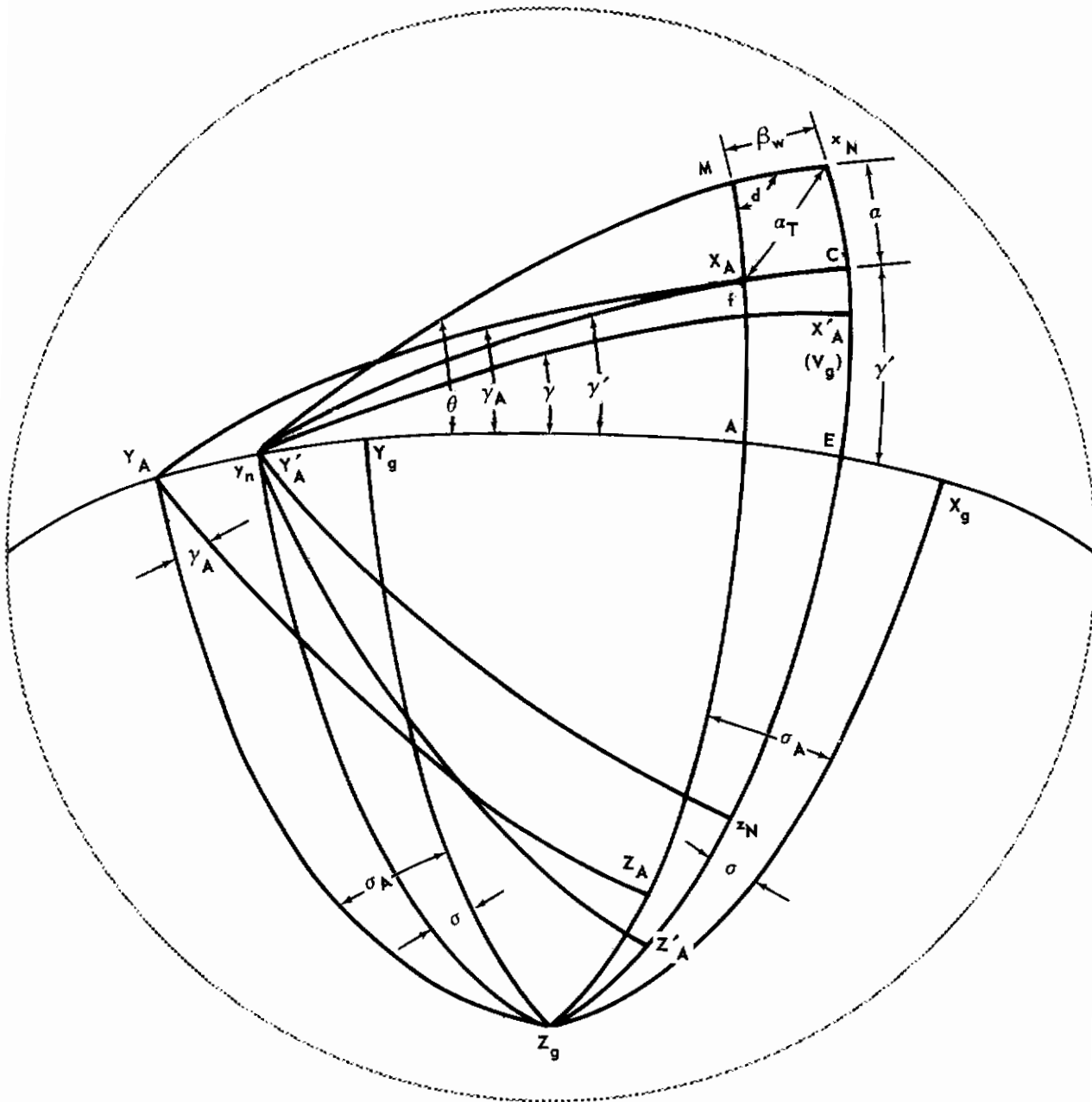
FIGURE 3.10

where V_g is the velocity relative to an atmosphere which has the same angular velocity as the earth. The three local geocentric components of airspeed are:

$$\overline{V}_a = (\dot{X}_g - \dot{X}_{g_w})\, \overline{I}_{x_g} + (\dot{Y}_g - \dot{Y}_{g_w})\, \overline{I}_{y_g} + (\dot{Z}_g - \dot{Z}_{g_w})\, \overline{I}_{z_g} \tag{3.87}$$

The elevation and azimuthal flight path angles of the airspeed vector are:

$$\gamma_a = \sin^{-1}\left(\frac{-(\dot{Z}_g - \dot{Z}_{g_w})}{V_a}\right) \tag{3.88}$$

$$\sigma_a = \tan^{-1}\left(\frac{\dot{Y}_g - \dot{Y}_{g_w}}{\dot{X}_g + \dot{X}_{g_w}}\right) \tag{3.89}$$

The summation of the external forces in Option Six is performed in the wind coordinate system ($X_A Y_A Z_A$), and the resulting components are resolved to the local geocentric system through the r-s-t direction cosines. The r-s-t direction cosines are derived with the lift vector restricted to the vertical plane. This derivation is unsuitable when the direction of the lift is dependent on the vehicle's roll angle. The additional angle required to define the direction of the lift (negative Z_A axis) is the bank angle, B_A. The bank angle is measured in a plane perpendicular to the airspeed vector ($\overline{V}_a$) and is referenced to the vertical plane containing X_A. The resulting r-s-t direction cosines will be altered by adding the rotation about the X_A axis through the bank angle to the sequence of rotations, thus leading to Equation (3.71) transposed.

$$
\begin{vmatrix} F_{X_g} \\ F_{Y_g} \\ F_{Z_g} \end{vmatrix}
=
\begin{vmatrix}
\cos\gamma_A \cos\sigma_A & -\sin\sigma_A & \sin\gamma_A \cos\sigma_A \\
\cos\gamma_A \sin\sigma_A & \cos\sigma_A & \sin\gamma_A \sin\sigma_A \\
-\sin\gamma_A & 0 & \cos\gamma_A
\end{vmatrix}
\begin{vmatrix}
1 & 0 & 0 \\
0 & \cos B_A & -\sin B_A \\
0 & \sin B_A & \cos B_A
\end{vmatrix}
\begin{vmatrix} F_{X_a} \\ F_{Y_a} \\ F_{Z_a} \end{vmatrix}
$$

where F_{X_a}, F_{Y_a}, and F_{Z_a} are the components of aerodynamic and thrust forces in the wind coordinate system. Performing the indicated matrix multiplication gives:

$$
\begin{vmatrix} F_{X_g} \\ F_{Y_g} \\ F_{Z_g} \end{vmatrix}
=
\begin{vmatrix}
\cos\gamma_A \cos\sigma_A & \begin{array}{l}-\sin\sigma_A \cos B_A \\ +\sin\gamma_A \cos\sigma_A \sin B_A\end{array} & \begin{array}{l}\sin\sigma_A \sin B_A \\ +\sin\gamma_A \cos\sigma_A \cos B_A\end{array} \\
\cos\gamma_A \sin\sigma_A & \begin{array}{l}\cos\sigma_A \cos B_A \\ +\sin\gamma_A \sin\sigma_A \sin B_A\end{array} & \begin{array}{l}-\cos\sigma_A \sin B_A \\ +\sin\gamma_A \sin\sigma_A \cos B_A\end{array} \\
-\sin\gamma_A & \cos\gamma_A \sin B_A & \cos\gamma_A \cos B_A
\end{vmatrix}
\begin{vmatrix} F_{X_a} \\ F_{Y_a} \\ F_{Z_a} \end{vmatrix}
\tag{3.90}
$$

The r-s-t direction cosines are to be defined by corresponding positions in equation (3.90) and (3.91).

$$
\begin{vmatrix} F_{X_g} \\ F_{Y_g} \\ F_{Z_g} \end{vmatrix} = \begin{vmatrix} r_1 & r_2 & r_3 \\ s_1 & s_2 & s_3 \\ t_1 & t_2 & t_3 \end{vmatrix} \begin{vmatrix} F_{X_a} \\ F_{Y_a} \\ F_{Z_a} \end{vmatrix} \tag{3.91}
$$

The development of the direction cosines relating the wind and body systems presented in Section 3.1.11 is also performed with the restriction that the lift is in the vertical plane. This restriction will be removed by permitting an additional rotation of the existing wind coordinate about the velocity (V_A) through the bank angle, B_A. This change is required to permit the correct summation of aerodynamic and thrust forces. The additional rotation matrix is made to Equation (3.78).

$$
\begin{vmatrix} X_A \\ Y_A \\ Z_A \end{vmatrix} = \begin{vmatrix} 1 & 0 & 0 \\ 0 & \cos B_A & \sin B_A \\ 0 & -\sin B_A & \cos B_A \end{vmatrix} \begin{vmatrix} \cos\gamma_A & 0 & -\sin\gamma_A \\ 0 & 1 & 0 \\ \sin\gamma_A & 0 & \cos\gamma_A \end{vmatrix} \begin{vmatrix} \cos(\sigma-\psi) & \sin(\sigma-\psi) & 0 \\ -\sin(\sigma-\psi) & \cos(\sigma-\psi) & 0 \\ 0 & 0 & 1 \end{vmatrix} \begin{vmatrix} \cos\theta & 0 & \sin\theta \\ 0 & 1 & 0 \\ -\sin\theta & 0 & \cos\theta \end{vmatrix} \begin{vmatrix} x \\ y \\ z \end{vmatrix}
$$
$$\tag{3.92}$$

3.2 <u>Guidance and Autopilot Coordinate Transformations</u> - The vehicle attitude information taken from the gimbals of a stabilized platform and the outputs of platform-mounted accelerometers may be required in certain autopilot and guidance-system computations in the Six-Degree-of-Freedom Flight-Path Study computer program. This section presents the derivation of the equations relating accelerometer and attitude information to data computed in the central program. The method for deriving coordinate transformations for any gimbal arrangement is presented for reference.

3.2.1 <u>Gimbal Arrangements and Rotation Sequences</u> - Three frequently used gimbal arrangements will be considered in this section. Each gimbal is equivalent to an intermediate coordinate system in a series of Euler-angle rotations. Reading from the inner gimbal to the outer gimbal (and neglecting redundant gimbals) the arrangements considered are:

(1) Yaw-Pitch-Roll

(2) Pitch-Yaw-Roll

(3) Pitch-Roll-Yaw

where the analogy between coordinate system rotations and gimbal movement is used. Other gimbal arrangements are possible; however, the three discussed in this section are the ones most frequently utilized. The transformations for the alternate arrangements can be obtained using these same techniques.

3.2.2 <u>Euler Angles</u> - In the central program, the direction cosines relating the vehicle body-coordinate system to a fixed inertial system are calculated by integrating functions of the body angular velocities, p, q, and

39

r. The direction cosines relating the body and inertial systems are determined by the cosines of the angles between the various axes of the coordinate systems and are dependent only upon the position of the body coordinates referenced to inertial coordinates. That is, the order of rotation selected to arrive at a certain orientation does not alter the numerical values of the direction cosines for that orientation.

Each individual direction cosine may, therefore, be defined in terms of the Euler angles from a given sequence of rotations. These definitions will provide the Euler angles of the body with respect to the platform coordinate system for the three rotational sequences selected.

The direction cosines, in terms of the three sets of Euler angles, will be derived using the method of Reference (9). The technique used is to find the direction cosines for each individual rotation in a sequence and determine the complete transformation by multiplying the individual direction cosine matrices. The overall picture of the rotations is best observed on a unit-sphere diagram. The points on the unit sphere represent the intersections of the coordinate axes with the surface of the sphere.

The order of rotation and the axis about which rotation occurs can be described using the following diagram.

AXIS AND ROTATION   ORDER

X	Y	Z		
		$\uparrow\downarrow \psi$	1.	
ξ	η	Z		
	$\uparrow\downarrow \theta$		2.	
x	η	ζ		
$\uparrow\downarrow \phi$			3.	
x	y	z		

This diagram indicates that the first rotation is about the inertial Z-axis through the Euler angle ψ. The second rotation is about the intermediate axis η through the angle θ. The final rotation is about the body x-axis through the angle ϕ.
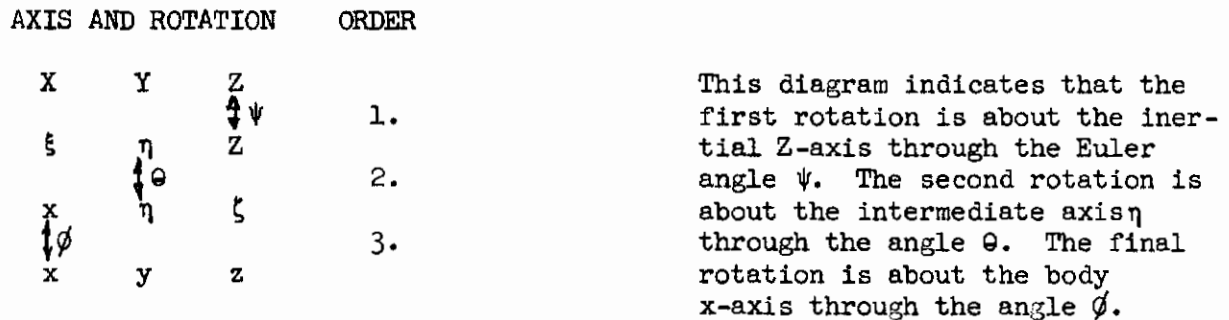
The derivation of each sequence of rotations will proceed in the following manner:

(a) The order of rotation will be defined.

(b) The unit sphere showing all three rotations will be presented.

(c) The individual rotations will be shown in three separate diagrams that contain the plane perpendicular to the appropriate axis of rotation.

(d) The direction cosines for each individual rotation will be written in this manner:

$$\begin{vmatrix} \xi \\ \eta \\ x \end{vmatrix} = \begin{vmatrix} c_{\xi X} & c_{\xi Y} & c_{\xi Z} \\ c_{\eta X} & c_{\eta Y} & c_{\eta Z} \\ c_{xX} & c_{xY} & c_{xZ} \end{vmatrix} \begin{vmatrix} X \\ Y \\ Z \end{vmatrix}$$

40

where C_{1j} is the cosine of the angle between the i and j axes.

(e) The matrix of direction cosines relating the inertial and body coordinates will be determined by matrix multiplication.

The computation sequences required for these computations are outlined by the functional flow diagram, Figure (3.11).

YAW-PITCH-ROLL ROTATION
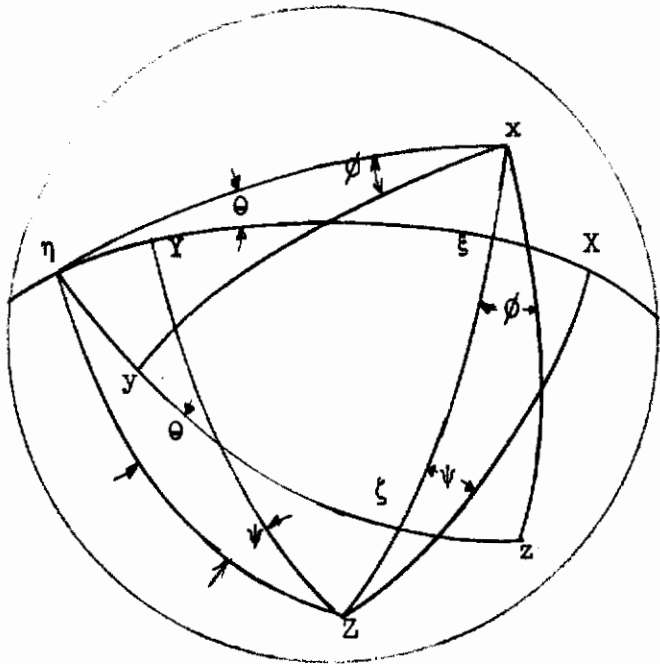
AXIS AND ROTATION			ORDER
X	Y	Z	1.
ξ	η	Z	2.
x	η	ζ	3.
x	y	z	

Figure 3.12 Unit Sphere For
Yaw-Pitch-Roll Sequence of Rotation

FIRST ROTATION

$$\begin{vmatrix} \xi \\ \eta \\ Z \end{vmatrix} = \begin{vmatrix} \cos \psi & \sin \psi & 0 \\ -\sin \psi & \cos \psi & 0 \\ 0 & 0 & 1 \end{vmatrix} \begin{vmatrix} X \\ Y \\ Z \end{vmatrix}$$

SECOND ROTATION

$$\begin{vmatrix} x \\ \eta \\ \zeta \end{vmatrix} = \begin{vmatrix} \cos \Theta & 0 & -\sin \Theta \\ 0 & 1 & 0 \\ \sin \Theta & 0 & \cos \Theta \end{vmatrix} \begin{vmatrix} \xi \\ \eta \\ Z \end{vmatrix}$$

41

HOW IS PLATFORM ALIGNED?

INERTIALLY FIXED	TORQUED ABOUT POLAR AXIS	TORQUED TO LOCAL GEOCENTRIC

$$B_p = 0$$
$$\phi_{L_p} = \phi_{g_0}$$
$$A = A_0$$

$$B_p = -\omega_p t$$
$$\phi_{L_p} = \phi_{L_0}$$
$$A = A_0$$

$$a_1 = -\cos B_p \sin \phi_{L_p} \cos A + \sin B_p \sin A$$

$$a_2 = -\sin B_p \sin \phi_{L_p} \cos A - \sin A \cos B_p$$

$$a_3 = -\cos \phi_{L_p} \cos A$$

$$b_1 = \cos B_p \sin \phi_{L_p} \sin A + \sin B_p \cos A$$

$$b_2 = \sin B_p \sin \phi_{L_p} \sin A - \cos B_p \cos A$$

$$b_3 = \cos \phi_{L_p} \sin A$$

$$c_1 = -\cos B_p \cos \phi_{L_p}$$

$$c_2 = -\sin B_p \cos \phi_{L_p}$$

$$c_3 = \sin \phi_{L_p}$$

$$\begin{vmatrix} a_1 & a_2 & a_3 \\ b_1 & b_2 & b_3 \\ c_1 & c_2 & c_3 \end{vmatrix} = \begin{vmatrix} i_1 & j_1 & k_1 \\ i_2 & j_2 & k_2 \\ i_3 & j_3 & k_3 \end{vmatrix}$$

TYPE OF GIMBAL SYSTEM

$\theta - \psi - \phi$	$\psi - \theta - \phi$	$\theta - \phi - \psi$

$$\theta_p' = \tan^{-1}\left[\frac{-(c_1 \ell_1 + c_2 \ell_2 + c_3 \ell_3)}{a_1 \ell_1 + a_2 \ell_2 + a_3 \ell_3}\right]$$

$$\psi_p' = \sin^{-1}(b_1 \ell_1 + b_2 \ell_2 + b_3 \ell_3)$$

$$\phi_p' = \tan^{-1}\left[\frac{-(b_1 n_1 + b_2 n_2 + b_3 n_3)}{b_1 m_1 + b_2 m_2 + b_3 m_3}\right]$$

$$\theta_p = -\sin^{-1}(c_1 \ell_1 + c_2 \ell_2 + c_3 \ell_3)$$

$$\psi_p = \tan^{-1}\left[\frac{b_1 \ell_1 + b_2 \ell_2 + b_3 \ell_3}{a_1 \ell_1 + a_2 \ell_2 + a_3 \ell_3}\right]$$

$$\phi_p = \tan^{-1}\left[\frac{c_1 m_1 + c_2 m_2 + c_3 m_3}{c_1 n_1 + c_2 n_2 + c_3 n_3}\right]$$

$$\theta_p'' = \tan^{-1}\left[\frac{a_1 n_1 + a_2 n_2 + a_3 n_3}{c_1 n_1 + c_2 n_2 + c_3 n_3}\right]$$

$$\psi_p'' = \tan^{-1}\left[\frac{b_1 \ell_1 + b_2 \ell_2 + b_3 \ell_3}{b_1 m_1 + b_2 m_2 + b_3 m_3}\right]$$

$$\phi_p'' = \sin^{-1}\left[-(b_1 n_1 + b_2 n_2 + b_3 n_3)\right]$$

HOW ARE THE ACCELEROMETERS MOUNTED

PLATFORM MOUNTED   BODY MOUNTED

NO ACCELEROMETERS

$$\begin{vmatrix} A_{x_p} \\ A_{y_p} \\ A_{z_p} \end{vmatrix} = \begin{vmatrix} a_1 & a_2 & a_3 \\ b_1 & b_2 & b_3 \\ c_1 & c_2 & c_3 \end{vmatrix} \begin{vmatrix} \ell_1 & m_1 & n_1 \\ \ell_2 & m_2 & n_2 \\ \ell_3 & m_3 & n_3 \end{vmatrix} \begin{vmatrix} \frac{F_x}{m} - g_x \\ \frac{F_y}{m} - g_y \\ \frac{F_z}{m} - g_z \end{vmatrix}$$

$$a_x = \frac{F_x}{m} - g_x$$
$$a_y = \frac{F_y}{m} - g_y$$
$$a_z = \frac{F_z}{m} - g_z$$

CONTINUE PROBLEM

FIGURE 3.11, FUNCTIONAL FLOW DIAGRAM —
PLATFORM ANGLES FOR SIX-DEGREE-OF-FREEDOM OBLATE ROTATING PLANET OPTION

42

THIRD ROTATION

$$
\begin{vmatrix} x \\ y \\ z \end{vmatrix} = \begin{vmatrix} 1 & 0 & 0 \\ 0 & \cos\phi & \sin\phi \\ 0 & -\sin\phi & \cos\phi \end{vmatrix} \begin{vmatrix} x \\ \eta \\ \zeta \end{vmatrix}
$$

The transformation matrix is given by

$$
\begin{vmatrix} x \\ y \\ z \end{vmatrix} = \begin{vmatrix} \phi \end{vmatrix} \begin{vmatrix} \Theta \end{vmatrix} \begin{vmatrix} \psi \end{vmatrix} \begin{vmatrix} X \\ Y \\ Z \end{vmatrix}
$$

or, in terms of the planar rotation matrices, the intermediate axes are elim-inated by

$$
\begin{vmatrix} x \\ y \\ z \end{vmatrix} = \begin{vmatrix} 1 & 0 & 0 \\ 0 & \cos\phi & \sin\phi \\ 0 & -\sin\phi & \cos\phi \end{vmatrix} \begin{vmatrix} \cos\Theta & 0 & -\sin\Theta \\ 0 & 1 & 0 \\ \sin\Theta & 0 & \cos\Theta \end{vmatrix} \begin{vmatrix} \cos\psi & \sin\psi & 0 \\ -\sin\psi & \cos\psi & 0 \\ 0 & 0 & 1 \end{vmatrix} \begin{vmatrix} X \\ Y \\ Z \end{vmatrix}
$$

The direction cosine elements of the transformation matrix are obtained by per-forming the indicated multiplication. For the yaw-pitch-roll rotational sequence

$$
\begin{vmatrix} x \\ y \\ z \end{vmatrix} = \begin{vmatrix} (\cos\Theta\cos\psi) & (\cos\Theta\sin\psi) & (-\sin\Theta) \\ (-\cos\phi\sin\psi + \sin\phi\sin\Theta\cos\psi) & (\cos\phi\cos\psi + \sin\phi\sin\Theta\sin\psi) & (\sin\phi\cos\Theta) \\ (\sin\phi\sin\psi + \cos\phi\sin\Theta\cos\psi) & (-\sin\phi\cos\psi + \cos\phi\sin\Theta\sin\psi) & (\cos\phi\cos\Theta) \end{vmatrix} \begin{vmatrix} X \\ Y \\ Z \end{vmatrix}
$$

(3.93)
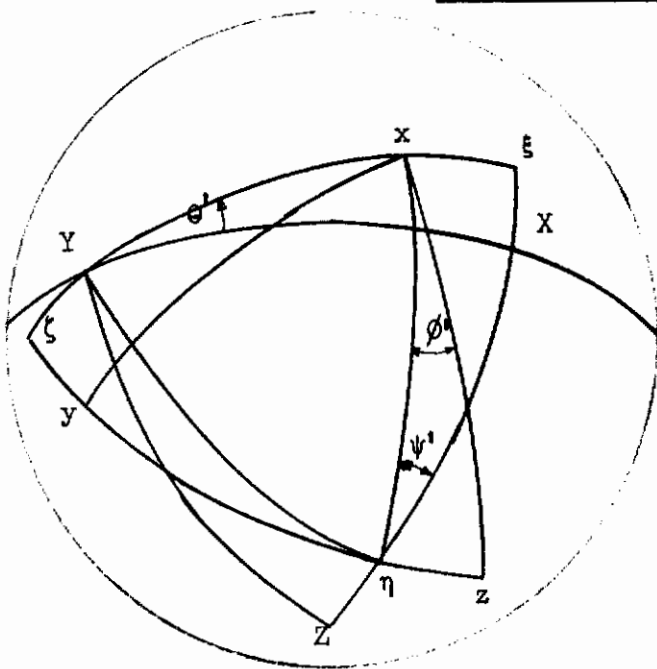
43

Figure 3.13 Unit Sphere For
Pitch-Yaw-Roll Sequence of Rotation

AXIS AND ROTATION   ORDER

X	Y	Z	
	Θ'		1.
ξ	Y	η	
		ψ'	2.
x	ζ	η	
ϕ'			3.
x	y	z	

FIRST ROTATION

$$\begin{vmatrix} \xi \\ Y \\ \eta \end{vmatrix} = \begin{vmatrix} \cos\Theta' & 0 & -\sin\Theta' \\ 0 & 1 & 0 \\ \sin\Theta' & 0 & \cos\Theta' \end{vmatrix} \begin{vmatrix} X \\ Y \\ Z \end{vmatrix}$$

SECOND ROTATION

$$\begin{vmatrix} x \\ \zeta \\ \eta \end{vmatrix} = \begin{vmatrix} \cos\psi' & \sin\psi' & 0 \\ -\sin\psi' & \cos\psi' & 0 \\ 0 & 0 & 1 \end{vmatrix} \begin{vmatrix} \xi \\ Y \\ \eta \end{vmatrix}$$

44

THIRD ROTATION

$$
\begin{vmatrix} x \\ y \\ z \end{vmatrix} = \begin{vmatrix} 1 & 0 & 0 \\ 0 & \text{Cos } \phi' & \text{Sin } \phi' \\ 0 & -\text{Sin } \phi' & \text{Cos } \phi' \end{vmatrix} \begin{vmatrix} x \\ \zeta \\ \eta \end{vmatrix}
$$

The transformation matrix is given by

$$
\begin{vmatrix} x \\ y \\ z \end{vmatrix} = \begin{vmatrix} \phi' \end{vmatrix} \begin{vmatrix} \psi' \end{vmatrix} \begin{vmatrix} \Theta' \end{vmatrix} \begin{vmatrix} X \\ Y \\ Z \end{vmatrix}
$$

or, in terms of the planar rotation matrices, the intermediate axes are elim-inated by

$$
\begin{vmatrix} x \\ y \\ z \end{vmatrix} = \begin{vmatrix} 1 & 0 & 0 \\ 0 & \text{Cos } \phi' & \text{Sin } \phi' \\ 0 & -\text{Sin } \phi' & \text{Cos } \phi' \end{vmatrix} \begin{vmatrix} \text{Cos } \psi' & \text{Sin } \psi' & 0 \\ -\text{Sin } \psi' & \text{Cos } \psi' & 0 \\ 0 & 0 & 1 \end{vmatrix} \begin{vmatrix} \text{Cos } \Theta' & 0 & -\text{Sin } \Theta' \\ 0 & 1 & 0 \\ \text{Sin } \Theta' & 0 & \text{Cos } \Theta' \end{vmatrix} \begin{vmatrix} X \\ Y \\ Z \end{vmatrix}
$$

The direction cosine elements of the transformation matrix are obtained by performing the indicated multiplication. For the pitch-yaw-roll rotational sequence

$$
\begin{vmatrix} x \\ y \\ z \end{vmatrix} = \begin{vmatrix} (\text{Cos } \psi' \text{ Cos } \Theta') & (\text{Sin } \psi') & (-\text{Cos } \psi' \text{ Sin } \Theta) \\ (\text{Sin } \phi' \text{ Sin } \Theta' \\ -\text{Cos } \phi' \text{ Sin } \psi' \text{ Cos } \Theta') & (\text{Cos } \phi' \text{ Cos } \psi') & (\text{Sin } \phi' \text{ Cos } \Theta' + \text{Cos } \phi' \text{ Sin } \Theta' \text{ Sin } \psi') \\ (\text{Cos } \phi' \text{ Sin } \Theta' + \text{Cos } \Theta' \text{ Sin } \psi' \text{ Sin } \phi') & (-\text{Sin } \phi' \text{ Cos } \psi') & (\text{Cos } \phi' \text{ Cos } \Theta' - \text{Sin } \phi' \text{ Sin } \Theta' \text{ Sin } \psi') \end{vmatrix} \begin{vmatrix} X \\ Y \\ Z \end{vmatrix}
$$

(3.94)

PITCH-ROLL-YAW ROTATION
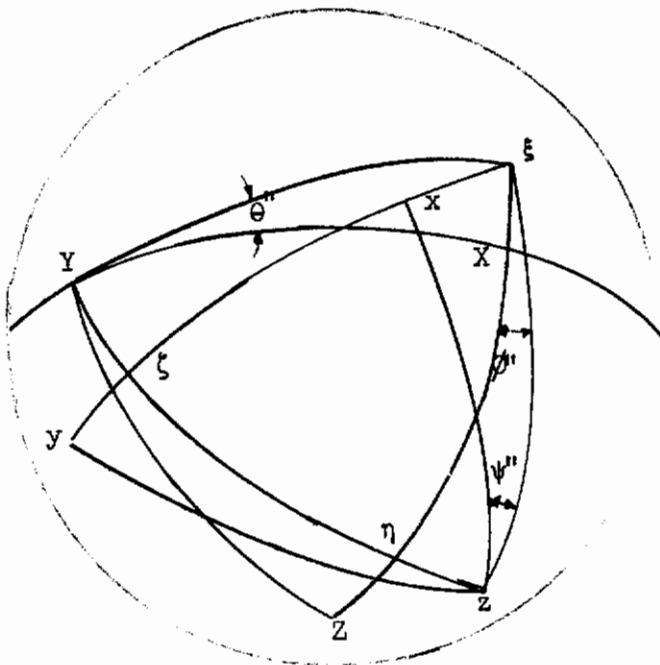
Figure 3.14 Unit Sphere For
Pitch-Roll-Yaw Sequence of Rotation

AXIS AND ROTATION   ORDER

X	Y	Z	
	θ''		1.
ξ ϕ''	Y	η	2.
ξ	ζ	z ψ''	3.
x	y	z	

FIRST ROTATION

$$\begin{vmatrix} \xi \\ Y \\ \eta \end{vmatrix} = \begin{vmatrix} \cos\theta'' & 0 & -\sin\theta'' \\ 0 & 1 & 0 \\ \sin\theta'' & 0 & \cos\theta'' \end{vmatrix} \begin{vmatrix} X \\ Y \\ Z \end{vmatrix}$$
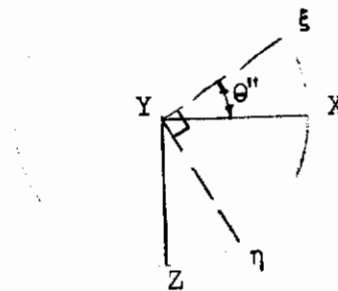
SECOND ROTATION

$$\begin{vmatrix} \xi \\ \zeta \\ Z \end{vmatrix} = \begin{vmatrix} 1 & 0 & 0 \\ 0 & \cos\phi'' & \sin\phi'' \\ 0 & -\sin\phi'' & \cos\phi'' \end{vmatrix} \begin{vmatrix} \xi \\ Y \\ \eta \end{vmatrix}$$

46
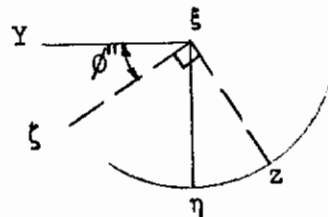
THIRD ROTATION

$$
\begin{vmatrix} x \\ y \\ z \end{vmatrix} =
\begin{vmatrix} \cos\psi'' & \sin\psi'' & 0 \\ -\sin\psi'' & \cos\psi'' & 0 \\ 0 & 0 & 1 \end{vmatrix}
\begin{vmatrix} \xi \\ \zeta \\ z \end{vmatrix}
$$

The transformation matrix is given by

$$
\begin{vmatrix} x \\ y \\ z \end{vmatrix} =
\begin{vmatrix} \psi'' \end{vmatrix}
\begin{vmatrix} \phi'' \end{vmatrix}
\begin{vmatrix} \Theta'' \end{vmatrix}
\begin{vmatrix} X \\ Y \\ Z \end{vmatrix}
$$

or, in terms of the planar rotation matrices, the intermediate axes are elim-
inated by

$$
\begin{vmatrix} x \\ y \\ z \end{vmatrix} =
\begin{vmatrix} \cos\psi'' & \sin\psi'' & 0 \\ -\sin\psi'' & \cos\psi'' & 0 \\ 0 & 0 & 1 \end{vmatrix}
\begin{vmatrix} 1 & 0 & 0 \\ 0 & \cos\phi'' & \sin\phi'' \\ 0 & -\sin\phi'' & \cos\phi' \end{vmatrix}
\begin{vmatrix} \cos\Theta'' & 0 & -\sin\Theta'' \\ 0 & 1 & 0 \\ \sin\Theta'' & 0 & \cos\Theta'' \end{vmatrix}
\begin{vmatrix} X \\ Y \\ Z \end{vmatrix}
$$

The direction cosine elements of the transformation matrix are obtained by
performing the indicated multiplication. For the pitch-roll-yaw rotational
sequence

$$
\begin{vmatrix} x \\ y \\ z \end{vmatrix} =
\begin{vmatrix}
(\cos\psi''\cos\Theta'' + \sin\psi''\sin\phi''\sin\Theta'') & (\sin\psi''\cos\phi'') & (-\cos\psi''\sin\Theta'' + \sin\psi''\sin\phi''\cos\Theta'') \\
(-\sin\psi''\cos\Theta'' + \cos\psi''\sin\phi''\sin\Theta'') & (\cos\psi''\cos\phi'') & (\sin\Theta''\sin\psi'' + \cos\psi''\sin\phi''\cos\Theta'') \\
(\cos\phi''\sin\Theta'') & (-\sin\phi'') & (\cos\phi''\cos\Theta'')
\end{vmatrix}
\begin{vmatrix} X \\ Y \\ Z \end{vmatrix}
$$

$$(3.95)$$

The direction cosines relating body and inertial coordinates are assigned the following symbols in the central program (see Equation (3.1)).

$$
\begin{vmatrix} x \\ y \\ z \end{vmatrix} = \begin{vmatrix} l_1 & l_2 & l_3 \\ m_1 & m_2 & m_3 \\ n_1 & n_2 & n_3 \end{vmatrix} \begin{vmatrix} X \\ Y \\ Z \end{vmatrix}
\qquad (3.96)
$$

By comparing identical positions in the matrix of Equation (3.96) with the matrices in Equations (3.93), (3.94), or (3.95), the direction cosines above are defined in terms of the appropriate sequence of Euler angles.

   3.2.3   Platform Coordinates - An orthogonal platform coordinate system, X_p-Y_p-Z_p is defined by the sensitive axes of three mutually perpendicular accelerometers. The direction cosines describing the inertial orientation of platform coordinates will not be derived. The angles used to orient the platform are the inertial angle, B_p, geocentric latitude ϕ_{L_p}, and azimuth A. The sequence of rotation is given in the following diagram:

AXIS AND ROTATION   ORDER

X   Y   Z
     $(180°+B_p)$ 1.
   ζ Y_g Z
$(90°-\phi_{L_p})$ 2.
   X_g Y_g Z_g
              A   3.
   X_p Y_p Z_p
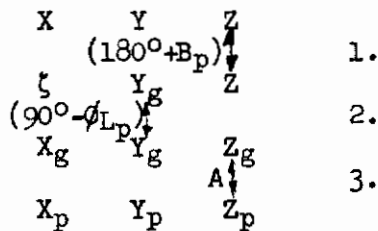
The first two rotations coincide with the sequence used in Equation (3.15) to define the local-geocentric-horizon coordinates. The direction cosines which relate the local-geocentric coordinate system to the inertial coordinates will be used for the first two rotations.

$$
\begin{vmatrix} X_g \\ Y_g \\ Z_g \end{vmatrix} = \begin{vmatrix} -\cos B_p \sin \phi_{L_p} & -\sin B_p \sin \phi_{L_p} & -\cos \phi_{L_p} \\ \sin B_p & -\cos B_p & 0 \\ -\cos B_p \cos \phi_{L_p} & -\sin B_p \cos \phi_{L_p} & \sin \phi_{L_p} \end{vmatrix} \begin{vmatrix} X \\ Y \\ Z \end{vmatrix}
\qquad (3.97)
$$

The direction cosines defining the platform coordinates with reference to local-geocentric horizon coordinates may be obtained by rotating about the Z_g-axis through the azimuth angle A, as shown in Figure (3.15).
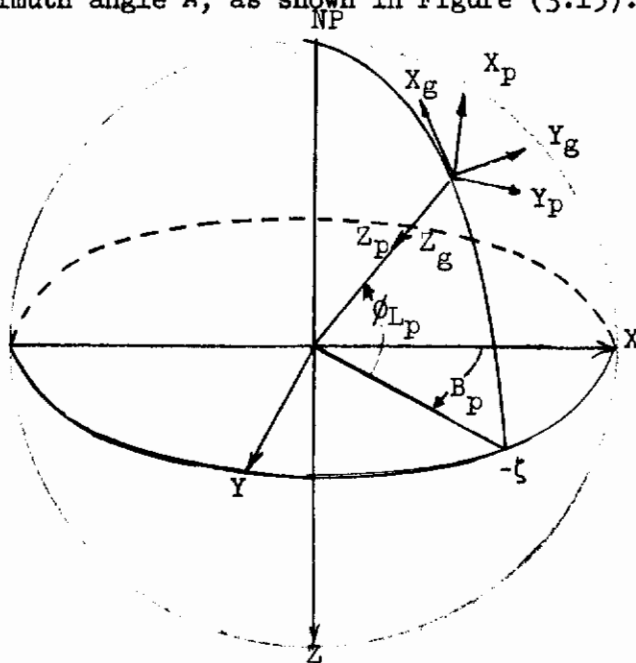
Figure 3.15 Relation of Platform and
Local-Geocentric Horizon Coordinates

The transformation matrix for this rotation is:

$$
\begin{vmatrix} X_p \\ Y_p \\ Z_p \end{vmatrix} = \begin{vmatrix} \text{Cos } A & \text{Sin } A & 0 \\ -\text{Sin } A & \text{Cos } A & 0 \\ 0 & 0 & 1 \end{vmatrix} \begin{vmatrix} X_g \\ Y_g \\ Z_g \end{vmatrix} \tag{3.98}
$$

The direction cosines defining the X_p, Y_p, and Z_p platform coordinates may then be determined by substituting Equation (3.98) into Equation (3.97).

The direction cosines defining the transformation from the inertial coordinate system to the platform coordinate system, in terms of the orientation angles, are:

$$
\begin{vmatrix} X_p \\ Y_p \\ Z_p \end{vmatrix} = \begin{vmatrix} (-\text{Cos } B_p \text{ Sin } \phi_{L_p} \text{ Cos } A & (-\text{Sin } B \text{ Sin } \phi_{L_p} \text{ Cos } A & (-\text{Cos } \phi_{L_p} \text{ Cos } A) \\ \quad + \text{Sin } B_p \text{ Sin } A) & \quad -\text{Sin } A \text{ Cos } B_p) & \\ (\text{Cos } B_p \text{ Sin } \phi_{L_p} \text{ Sin } A & (\text{Sin } B_p \text{ Sin } \phi_{L_p} \text{ Sin } A & (\text{Cos } \phi_{L_p} \text{ Sin } A) \\ \quad + \text{Sin } B_p \text{ Cos } A & \quad - \text{Cos } B_p \text{ Cos } A) & \\ (-\text{Cos } B_p \text{ Cos } \phi_{L_p}) & (-\text{Sin } B_p \text{ Cos } \phi_{L_p}) & (\text{Sin } \phi_{L_p}) \end{vmatrix} \begin{vmatrix} X \\ Y \\ Z \end{vmatrix}
$$

$$\tag{3.99}$$

For convenience, the direction cosines in the matrix will be defined by the notation,

$$
\begin{vmatrix} X_p \\ Y_p \\ Z_p \end{vmatrix} = \begin{vmatrix} a_1 & a_2 & a_3 \\ b_1 & b_2 & b_3 \\ c_1 & c_2 & c_3 \end{vmatrix} \begin{vmatrix} X \\ Y \\ Z \end{vmatrix}
\tag{3.100}
$$

3.2.4 <u>Platform Angles for a Flat-Planet Problem</u> - For a flat-planet problem, the orientation of the platform coordinate system will be assumed to coincide with the flat-planet coordinates. Therefore, the angles measured on the gimbals of this platform may be determined for the three gimbal arrangements considered. For the yaw-pitch-roll gimbal system, the following direction cosine relationships are obtained by comparing corresponding positions in the matrices used in Equations (3.93) and (3.96). Five elements are sufficient to define these angles.

$$l_3 = -\text{Sin } \Theta$$

$$l_2 = \text{Cos } \Theta \ \text{Sin } \Psi$$

$$l_1 = \text{Cos } \Theta \ \text{Cos } \Psi \tag{3.101}$$

$$m_3 = \text{Sin } \phi \ \text{Cos } \Theta$$

$$n_3 = \text{Cos } \phi \ \text{Cos } \Theta$$

The first equation defines the angle Θ. The angles Ψ and ϕ may be defined explicitly by combining the second and third equation and the fourth and fifth equation, thus,

$$\text{Sin } \Theta = -l_3$$

$$\text{Tan } \Psi = l_2/l_1$$

and $$\text{Tan } \phi = m_3/n_3$$

For the flat-planet problem with the platform stabilized to coincide with the X_g-Y_g-Z_g coordinates, these angles represent the angles measured on the gimbals and will be designated with a subscript p.

$$\Theta_p = -\text{Sin}^{-1} l_3$$

$$\Psi_p = \text{Tan}^{-1} l_2/l_1 \tag{3.102}$$

$$\phi_p = \text{Tan}^{-1} m_3/n_3$$

Similarly, the angles measured on a pitch-yaw-roll gimbal arrangement may be computed by comparing identical positions in the matrices used in Equations (3.94) and (3.96).

$$l_2 = Sin \, \psi_p'$$

$$l_1 = Cos \, \psi_p' \, Cos \, \Theta_p'$$

$$l_3 = -Cos \, \psi_p' \, Sin \, \Theta_p'$$

$$m_2 = Cos \, \phi_p' \, Cos \, \psi_p'$$

$$n_2 = -Sin \, \phi_p' \, Cos \, \psi_p' \qquad (3.103)$$

Then

$$Sin \, \psi_p' = l_2$$

$$Tan \, \Theta_p' = -l_3/l_1$$

$$Tan \, \phi_p' = -n_2/m_2$$

Again for the flat-planet problem, the gimbal angles for this arrangement are:

$$\psi_p' = Sin^{-1} \, l_2$$

$$\Theta_p' = Tan^{-1} \, -l_3/l_1$$

$$\phi_p' = Tan^{-1} \, -n_2/m_2 \qquad (3.104)$$

The appropriate direction cosines for the computation of the angles for a pitch-roll-yaw system are:

$$n_2 = -Sin \, \phi_p''$$

$$m_2 = Cos \, \psi_p'' \, Cos \, \phi_p''$$

$$l_2 = Sin \, \psi_p'' \, Cos \, \phi_p''$$

$$n_1 = Cos \, \phi_p'' \, Sin \, \Theta_p'' \qquad (3.105)$$

$$n_3 = Cos \, \phi_p'' \, Cos \, \Theta_p''$$

The platform angles are found from these direction cosines to be:

$$\phi_p'' = -Sin^{-1} \, n_2$$

$$\Theta_p'' = Tan^{-1} \, n_1/n_3 \qquad (3.106)$$

$$\psi_p'' = Tan^{-1} \, l_2/m_2$$

51

For the flat-planet problem, the angles derived in Equations (3.101) through (3.106) represent the attitudes of the vehicle with respect to the X_g-Y_g-Z_g flat-planet coordinates and also with respect to a platform coordinate system whose respective X_p-Y_p-Z_p axes are parallel to X_g-Y_g-Z_g. Since the orientation of the platform in this problem also corresponds to the orientation of the inertial coordinates X-Y-Z of the rotating-planet problem in the equatorial plane, these angles are also the inertial attitudes (Ψ, Θ, Φ) of the vehicle with respect to X-Y-Z coordinates of the rotating-planet problem. The computation of these platform relations are summarized, along with the accelerometer indication in Figure (3.16).

3.2.5 <u>Platform Angles for Rotating-Planet Problem</u> - The attitude angles available from the orientation of the platform gimbals will also be required in the guidance and control subprograms for the rotating-planet problem. In Paragraph 3.2.4, the direction cosines relating the platform coordinates and the body coordinates were known, and it was relatively simple to obtain functions of the platform angles. For the rotating-planet problem, it will be necessary to express the direction cosines relating the body and platform coordinates in terms of the l-m-n and a-b-c direction cosines. When this is accomplished, the procedure developed in Section 3.2.4 will be used to obtain the platform angles. Let this required set of direction cosines be defined in general form as:

$$
\begin{vmatrix} X_p \\ Y_p \\ Z_p \end{vmatrix} = \begin{vmatrix} d_1 & e_1 & f_1 \\ d_2 & e_2 & f_2 \\ d_3 & e_3 & f_3 \end{vmatrix} \begin{vmatrix} x \\ y \\ z \end{vmatrix} \tag{3.107}
$$

The direction cosines in this 3-by-3 matrix may be defined in terms of any one of the three sequences of rotations derived in Equations (3.93), (3.94), and (3.95). For the yaw-pitch-roll sequence, this matrix is obtained by using platform Euler angles in Equation (3.93).

$$
\begin{vmatrix} X_p \\ Y_p \\ Z_p \end{vmatrix} = \begin{vmatrix} (\cos \Theta_p \cos \Psi_p) & (\sin \phi_p \sin \Theta_p \cos \Psi_p - \cos \phi_p \sin \Psi_p) & (\cos \phi_p \sin \Theta_p \cos \Psi_p + \sin \Psi_p \sin \phi_p) \\ (\cos \Theta_p \sin \Psi_p) & (\sin \phi_p \sin \Theta_p \sin \Psi_p + \cos \phi_p \cos \Psi_p) & (\cos \phi_p \sin \Theta_p \sin \Psi_p - \sin \phi_p \cos \Psi_p) \\ (-\sin \Theta_p) & (\sin \phi_p \cos \Theta_p) & (\cos \phi_p \cos \Theta_p) \end{vmatrix} \begin{vmatrix} x \\ y \\ z \end{vmatrix}
$$

$$(3.108)$$

The d-e-f set of direction cosines will be expressed in terms of the a-b-c and l-m-n direction cosines. The a-b-c direction cosines relating platform and inertial coordinates were derived in Equations (3.96) through (3.100); these a-b-c direction cosines may be evaluated from input data and/or from central program information according to the platform orientation scheme selected (see Paragraph 3.2.6). Equation (3.100) is repeated here for convenience.

TYPE OF GIMBAL SYSTEM

θ-ψ-ϕ	ψ-θ-ϕ	θ-ϕ-ψ

$$\theta_p' = TAN^{-1}\left(\frac{-\ell_3}{\ell_1}\right)$$
$$\psi_p' = SIN^{-1}\ell_2$$
$$\phi_p' = TAN^{-1}\left(\frac{-n_2}{m_2}\right)$$

$$\theta_p = SIN^{-1} -\ell_3$$
$$\psi_p = TAN^{-1}\left(\frac{\ell_2}{\ell_1}\right)$$
$$\phi_p = TAN^{-1}\left(\frac{m_3}{n_3}\right)$$

$$\theta_p'' = TAN^{-1}\left(\frac{n_1}{n_3}\right)$$
$$\psi_p'' = TAN^{-1}\left(\frac{\ell_2}{m_2}\right)$$
$$\phi_p'' = -SIN^{-1} n_2$$

HOW ARE THE ACCELEROMETERS MOUNTED

PLATFORM MOUNTED

BODY MOUNTED

No ACCELEROMETERS

$$\begin{vmatrix} A_{X_p} \\ A_{Y_p} \\ A_{z_p} \end{vmatrix} = \begin{vmatrix} \ell_1 & m_1 & n_1 \\ \ell_2 & m_2 & n_2 \\ \ell_3 & m_3 & n_3 \end{vmatrix} \begin{vmatrix} \frac{F_x}{m} - g_x \\ \frac{F_y}{m} - g_y \\ \frac{F_z}{m} - g_z \end{vmatrix}$$

$$a_x = \frac{F_x}{m} - g_x$$
$$a_y = \frac{F_y}{m} - g_y$$
$$a_z = \frac{F_z}{m} - g_z$$

CONTINUE PROBLEM
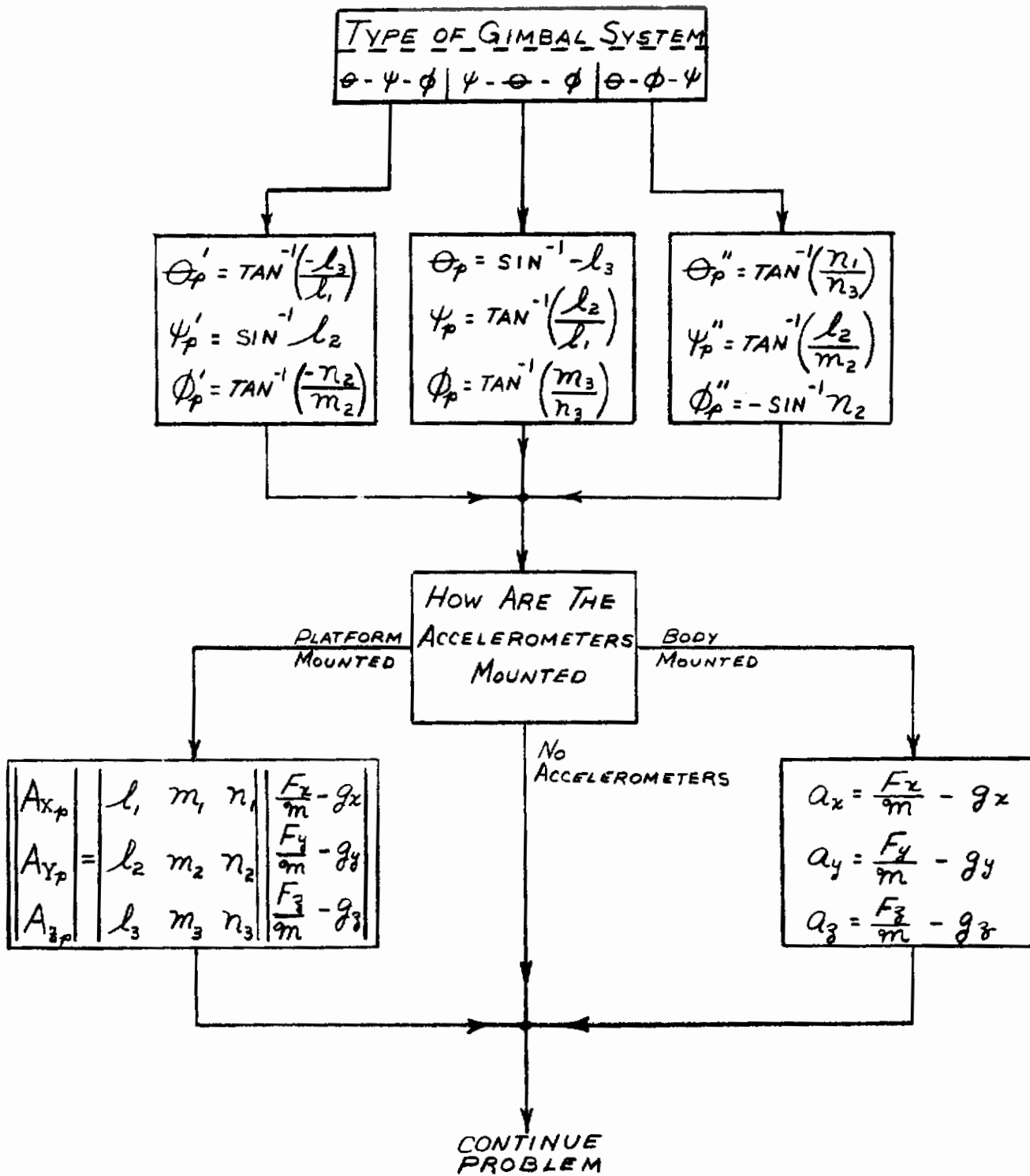
FIGURE 3.16, FUNCTIONAL FLOW DIAGRAM –
PLATFORM ANGLES FOR SIX-DEGREE-OF-FREEDOM FLAT-PLANET OPTION

53

$$\begin{vmatrix} X_p \\ Y_p \\ Z_p \end{vmatrix} = \begin{vmatrix} a_1 & a_2 & a_3 \\ b_1 & b_2 & b_3 \\ c_1 & c_2 & c_3 \end{vmatrix} \begin{vmatrix} X \\ Y \\ Z \end{vmatrix} \qquad (3.100)$$

The transformation from inertial coordinates to body coordinates was derived in Paragraph 3.1.3 and the direction cosines in this transformation are calculated in the central program as follows:

$$\begin{vmatrix} X \\ Y \\ Z \end{vmatrix} = \begin{vmatrix} l_1 & m_1 & n_1 \\ l_2 & m_2 & n_2 \\ l_3 & m_3 & n_3 \end{vmatrix} \begin{vmatrix} x \\ y \\ z \end{vmatrix} \qquad (3.109)$$

Equations (3.100) and (3.109) may be combined according to the laws of matrix multiplication to give

$$\begin{vmatrix} X_p \\ Y_p \\ Z_p \end{vmatrix} = \begin{vmatrix} a_1 & a_2 & a_3 \\ b_1 & b_2 & b_3 \\ c_1 & c_2 & c_3 \end{vmatrix} \begin{vmatrix} l_1 & m_1 & n_1 \\ l_2 & m_2 & n_2 \\ l_3 & m_3 & n_3 \end{vmatrix} \begin{vmatrix} x \\ y \\ z \end{vmatrix} \qquad (3.110)$$

Since the product of the matrices in Equation (3.110) are the direction cosines relating platform and body coordinates, this product is the required set of d-e-f direction cosines, and

$$\begin{vmatrix} d_1 & e_1 & f_1 \\ d_2 & e_2 & f_2 \\ d_3 & e_3 & f_3 \end{vmatrix} = \begin{vmatrix} (a_1 l_1 + a_2 l_2 + a_3 l_3) & (a_1 m_1 + a_2 m_2 + a_3 m_3) & (a_1 n_1 + a_2 n_2 + a_3 n_3) \\ (b_1 l_1 + b_2 l_2 + b_3 l_3) & (b_1 m_1 + b_2 m_2 + b_3 m_3) & (b_1 n_1 + b_2 n_2 + b_3 n_3) \\ (c_1 l_1 + c_2 l_2 + c_3 l_3) & (c_1 m_1 + c_2 m_2 + c_3 m_3) & (c_1 n_1 + c_2 n_2 + c_3 n_3) \end{vmatrix}$$

$$(3.111)$$

Functions of the three angles of the yaw-pitch-roll sequence may be determined by equating corresponding positions in the matrix on the right of Equation (3.111) with the matrix of Equation (3.100). First equate the terms in the 31 position (third row, first column).

$$- \operatorname{Sin} \Theta_p = c_1 l_1 + c_2 l_2 + c_3 l_3$$

The pitch attitude of the missile with respect to the platform is then given by:

$$\Theta_p = - \operatorname{Sin}^{-1} (c_1 l_1 + c_2 l_2 + c_3 l_3) \qquad (3.112)$$

Equating the 11 and 21 positions in each matrix gives the following relationships:

$$\operatorname{Cos} \Theta_p \operatorname{Sin} \psi_p = b_1 l_1 + b_2 l_2 + b_3 l_3 \qquad (3.113)$$

$$\operatorname{Cos} \Theta_p \operatorname{Cos} \psi_p = a_1 l_1 + a_2 l_2 + a_3 l_3 \qquad (3.114)$$

54

Dividing Equation (3.113) by (3.114) gives an expression for the angle ψ_p;

$$\psi_p = \text{Tan}^{-1} \left(\frac{b_1 l_1 + b_2 l_2 + b_3 l_3}{a_1 l_1 + a_2 l_2 + a_3 l_3} \right) \qquad (3.115)$$

Finally, the roll angle ϕ_p will be found from the 32 and 33 positions

$$\text{Cos } \theta_p \text{ Sin } \phi_p = c_1 m_1 + c_2 m_2 + c_3 m_3 \qquad (3.116)$$

$$\text{Cos } \theta_p \text{ Cos } \phi_p = c_1 n_1 + c_2 n_2 + c_3 n_3 \qquad (3.117)$$

Dividing Equation (3.116) by (3.117) provides an expression for the roll angle:

$$\phi_p = \text{Tan}^{-1} \left(\frac{c_1 m_1 + c_2 m_2 + c_3 m_3}{c_1 n_1 + c_2 n_2 + c_3 n_3} \right) \qquad (3.118)$$

This completes the solution for the three angles for the yaw-pitch-roll sequence for a rotating-planet problem. The platform angles for the other two sequences are found in a similar fashion and are given as follows:

Pitch-Yaw-Roll Sequence

$$\psi'_p = \text{Sin}^{-1} (b_1 l_1 + b_2 l_2 + b_3 l_3) \qquad (3.119)$$

$$\theta'_p = \text{Tan}^{-1} \left(\frac{-(c_1 l_1 + c_2 l_2 + c_3 l_3)}{a_1 l_1 + a_2 l_2 + a_3 l_3} \right) \qquad (3.120)$$

$$\phi'_p = \text{Tan}^{-1} \left(\frac{-(b_1 n_1 + b_2 n_2 + b_3 n_3)}{b_1 m_1 + b_2 m_2 + b_3 m_3} \right) \qquad (3.121)$$

Pitch-Roll-Yaw Sequence

$$\phi''_p = \text{Sin}^{-1} \left(-(b_1 n_1 + b_2 n_2 + b_3 n_3) \right) \qquad (3.122)$$

$$\theta''_p = \text{Tan}^{-1} \left(\frac{a_1 n_1 + a_2 n_2 + a_3 n_3}{c_1 n_1 + c_2 n_2 + c_3 n_3} \right) \qquad (3.123)$$

$$\psi''_p = \text{Tan}^{-1} \left(\frac{b_1 l_1 + b_2 l_2 + b_3 l_3}{b_1 m_1 + b_2 m_2 + b_3 m_3} \right) \qquad (3.124)$$

3.2.6 Platform Orientation - For many problems, it is convenient to torque the platform in some prescribed manner. The actual dynamics of platform stabilization will not be considered in this problem, however, the platform can be oriented in any prescribed fashion by adjusting the direction cosines relating

the platform and inertial coordinates. These direction cosines are functions of the inertial angle $B_p = \Theta_{L_0} - \Theta_L - \omega_p t$, the platform geocentric latitude, ϕ_{L_p}, and the aximuth of the platform. Three cases of platform orientation will now be considered.

Case I Platform Inertially Fixed - The platform may be fixed inertially at any desired orientation by using the appropriate angles, B_p, ϕ_{L_p}, and A in the evaluation of the a-b-c direction cosines relating platform and inertial coordinates. The usual procedure could also be aligned by a stellar fix. In this instance, $B_p = 0$, ϕ_{L_p} = geodetic latitude of the launch site, and A is the desired azimuth. These values are constants during the flight since the platform is fixed inertially.

Case II Platform Torqued at Constant Rate About the Polar Axis - The constant angular rate selected for this application is usually the angular rotational rate of the planet in question. The platform coordinates now become a tangent plane fixed to the planet at a point which is usually the launch site. Then the angle $B_p = -\omega_p t$, ϕ_{L_p} is the geodetic latitude of the launch site and A is the desired azimuth.

Case III Platform Aligned With the Local-Geocentric-Horizon Coordinates - The platform is rotated so that Z_p is aligned geocentrically downward and the X_p-axis is pointing northward in a meridian plane. This orientation of the platform coincides with the orientation of local-geocentric-horizon coordinates. The direction cosines relating the local-geocentric-horizon coordinates and inertial coordinates are continuously evaluated in the central program and may be used as the direction cosines relating the platform and inertial coordinates for this case only; thus

$$
\begin{vmatrix} a_1 & a_2 & a_3 \\ b_1 & b_2 & b_3 \\ c_1 & c_2 & c_3 \end{vmatrix} = \begin{vmatrix} i_1 & j_1 & k_1 \\ i_2 & j_2 & k_2 \\ i_3 & j_3 & k_3 \end{vmatrix}
\tag{3.125}
$$

These three cases are among the ones most frequently used. Additional methods of platform orientation may be simulated by following the procedures used in developing these three cases.

3.2.7 Platform Coordinate Transformations - Reduced Degrees of Freedom - When an autopilot is used to control the flight of a vehicle which is constrained to motion in reduced degrees of freedom, the platform motion has a similar constraint applied to it. The coordinate transformations required to relate the platform to the body axes are simplified for the same reasons the transformations of Paragraph 3.1.7 are reduced. Of the reduced-degree-of-freedom options available, the three-degree-of-freedom longitudinal option is best suited to the use of a platform in conjunction with the autopilot. The platform transformations which follow are applicable to this option. The platform coordinate system will be defined as the X_p-Z_p axis for the three-degree longitudinal problem; three possibilities are considered for the rotating-planet problem in the equatorial plane.

1. **Platform inertially fixed at launch site.**
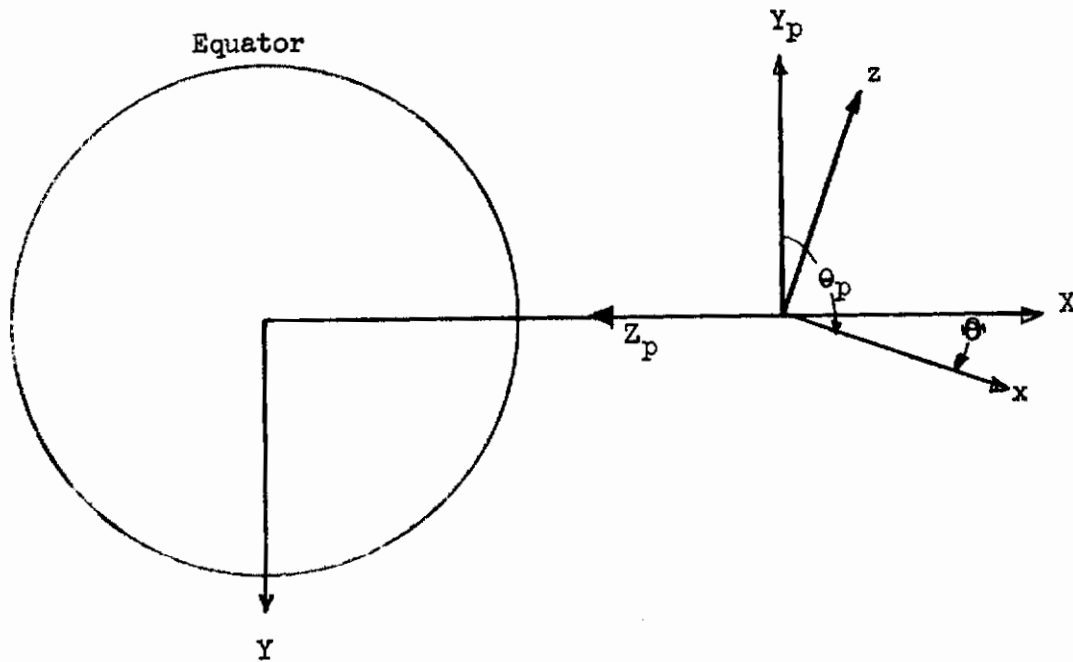
Figure 3.17 Platform Coordinate
System Inertially Fixed at Launch Site

The platform axes are situated in the position of the Y_g-Z_g coordinate system at t = 0. (See Figure (3.4), Paragraph (3.1.8)). The angle of the body axes with the platform axes is 90° + Θ, therefore:

$$\Theta_p = \Theta + 90^\circ \qquad\qquad (3.126)$$

2. **Platform torqued at the planet rotational rate.**
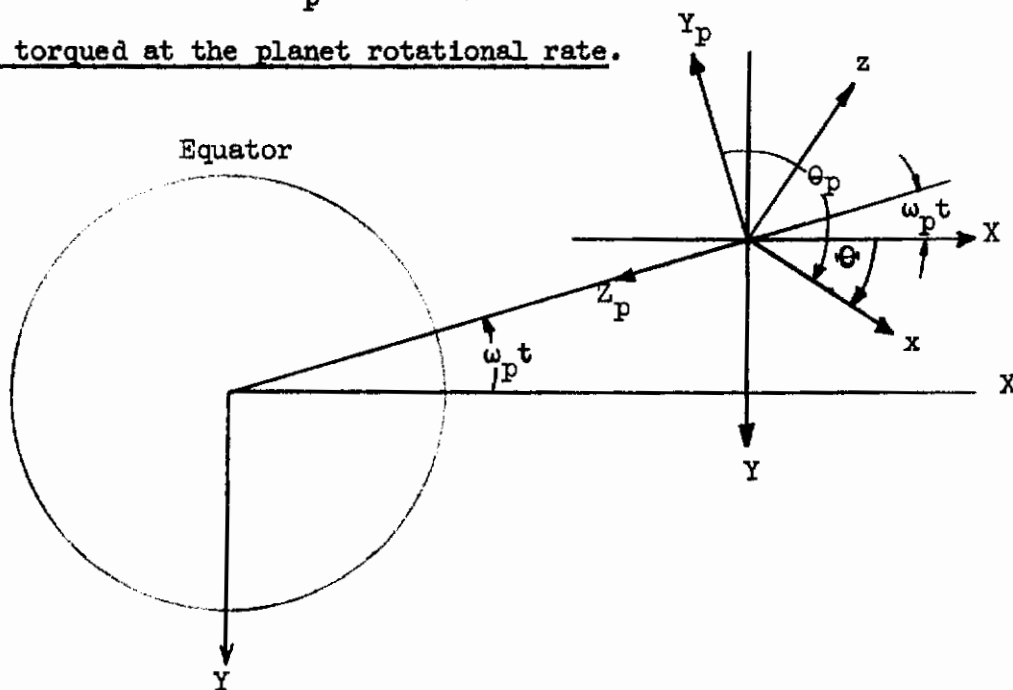
Figure 3.18 Platform Coordinate
System Torqued at a Constant Rate

57

From Figure (3.17) for eastward flight $\Theta_p = 90^\circ + \omega_p t + \Theta$. Similarly, for westward flight $\Theta_p = 90^\circ - \omega_p t + \Theta$.

The appropriate sign is inserted by using the factor K_σ:

$$\Theta_p = 90^\circ + K_\sigma \, \omega_p t + \Theta \qquad (3.127)$$

3. <u>Platform torqued to local-geocentric</u> - In this case local-geocentric coordinates Y_g-Z_g are identical to platform coordinates Y_p-Z_p so the platform angle is the angle with the local-geocentric horizon, Θ, given by Equation (3.55), Paragraph (3.1.8),

$$\Theta = \Theta_p = 90^\circ - K_\sigma \, \beta + \Theta \qquad (3.128)$$

For a three-degree longitudinal flat-planet problem with the platform coordinates coinciding with the flat-planet coordinates, the platform angle is the same as the pitch attitude, Θ, with the flat-planet (inertial) coordinates, so that:

$$\Theta_p = \Theta \qquad (3.129)$$

The computations required to determine the platform angle for the three-degree-of-freedom, longitudinal, equatorial-plane option are summarized in Figure (3.19).

(a) EQUATORIAL PLANE
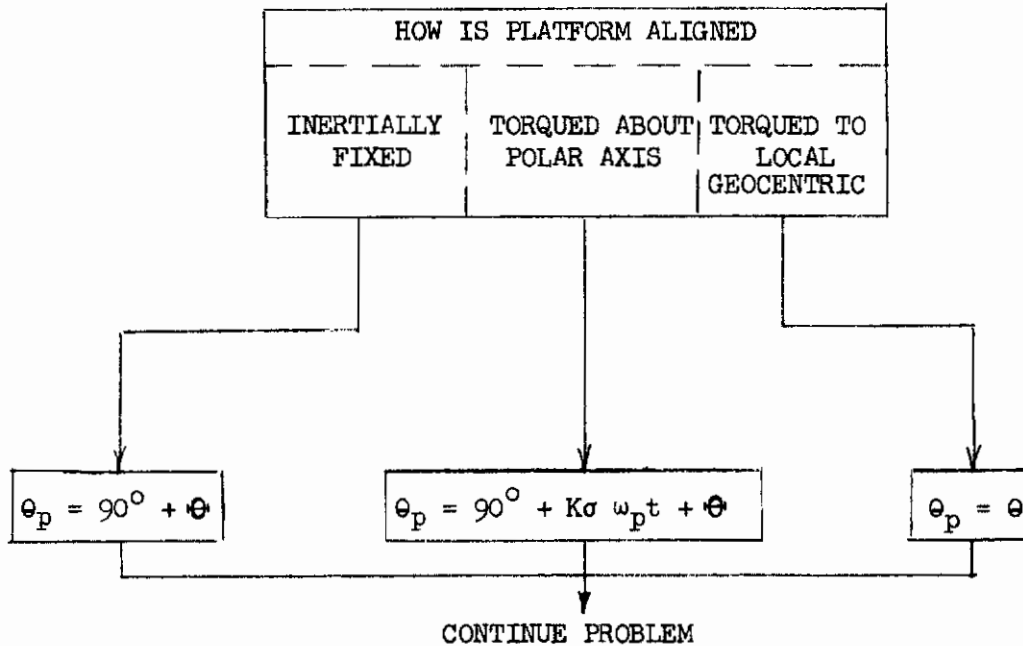
(b) FLAT PLANET
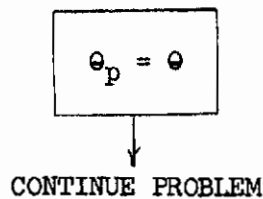
Figure 3.19 Functional Flow Diagram—Platform
Angle for Three-Degree-of-Freedom Longitudinal Computation

58

3.2.8 <u>Accelerometer Indications</u> - Let $\overline{A}$ be the vector sum of the platform accelerometer outputs and $\overline{g}$ be the mass attractive acceleration of the planet. The accelerometers are calibrated to read zero when they are unaccelerated and aligned such that the sensitive axis is perpendicular to $\overline{g}$. The vector $\overline{R}$ will represent the displacement of the platform with respect to the center of the planet. It will be shown that $\overline{A} = \overline{R} - \overline{g}$ where $\overline{R}$ is the inertial acceleration of the platform. Consider the vehicle accelerating vertically at 1g with respect to a spherical body. In local-geocentric-horizon components then

$$\ddot{\overline{R}} = -g \, \overline{1}_{Z_g} \qquad (3.130)$$

In the absence of a gravitational field, the accelerometer should read -1g. Positive motion of the accelerometer mass along the Z_g axis represents a negative acceleration in this case, and the vector $\overline{g}$ is equal to $g \, \overline{1}_{Z_g}$. Consideration of the gravitational field will cause an additional displacement of the accelerometer mass in the positive Z_g direction giving a total indication of -2g. The equation

$$\overline{A} = \ddot{\overline{R}} - \overline{g} \qquad (3.131)$$

will be evaluated from the data

$$\ddot{\overline{R}} = - 1g \, \overline{1}_{Z_g}$$

so that

$$\overline{A} = - 2g \, \overline{1}_{Z_g} \qquad (3.132)$$

Figure 3.20 Accelerometer With Sensitive Axis Aligned With Local-Geocentric Vertical

This result is shown schematically in Figure (3.20).

The vector $\overline{A}$ is equal to the vector sum of the accelerations produced by the externally applied forces. The body components of the externally applied forces may be taken from the separate subprogram which gives the summation of forces and moments. F_x, F_y, and F_z are the body components of the external forces plus the weight. The weight must then be subtracted to determine the body components of $\overline{A}$:

$$\overline{A} = \ddot{\overline{R}} - \overline{g} = \left(\frac{F_x - m g_x}{m} \right) \overline{1}_x + \left(\frac{F_y - m g_y}{m} \right) \overline{1}_y + \left(\frac{F_z - m g_z}{m} \right) \overline{1}_z \qquad (3.133)$$

The body components of the vector $\overline{A}$ will now be resolved to platform coordinate components; these platform components will then represent the accelerometer outputs. This resolution utilizes the direction cosine matrix of Equation (3.110) which relates these two coordinate systems, thus

59

$$
\begin{vmatrix} A_{X_p} \\ A_{Y_p} \\ A_{Z_p} \end{vmatrix} = \begin{vmatrix} a_1 & a_2 & a_3 \\ b_1 & b_2 & b_3 \\ c_1 & c_2 & c_3 \end{vmatrix} \begin{vmatrix} l_1 & m_1 & n_1 \\ l_2 & m_2 & n_2 \\ l_3 & m_3 & n_3 \end{vmatrix} \begin{vmatrix} \frac{F_x}{m} - g_x \\ \frac{F_y}{m} - g_y \\ \frac{F_z}{m} - g_z \end{vmatrix} \qquad (3.134)
$$

where A_{X_p}, A_{Y_p}, and A_{Z_p} represent the output of accelerometers whose sensitive axes are aligned along the three platform coordinate axes.

3.3 <u>Auxiliary Transformations</u> - The computer program developed in the Six-Degree-of-Freedom Flight-Path Study is a generalized program capable of calculating the motion of various types of flight vehicles. To define completely the various trajectories which may be analyzed requires the computation of a wide variety of flight parameters. It is evident, however, that for many analyses the computation of the entire library of these parameters is unnecessary. It is the purpose of the present discussion to specify and derive the special relations and transformations for those auxiliary parameters which, in the interest of program simplification, may be deleted from the computation if the parameter is not required. The coordinate transformations and auxiliary parameters discussed in the present analysis may be generally considered as Category (3) transformations, as defined at the beginning of Section 3. Under certain conditions, however, the transformations may be equally pertinent to other categories. (For example, α and β may be required to compute aerodynamic forces related to Category (1) as well as being used for the convenience of the analysts in readout, Category (3)).

3.3.1 <u>Angular Rates</u> - In most cases, machine differentiation is accurate enough to determine the time derivative of a function. For this reason, the angular rates of angle of attack, side slip, elevation flight-path and azimuth angle are obtained by this manner in the present formulation of the Six-Degree-of-Freedom Flight-Path Study computer program. In some cases, however, it may be desirable to have analytical expressions for these angular rates. For this reason, the following paragraphs will present a derivation of expressions for the time rates of change of the vertical and horizontal flight-path angles, γ and σ, and of the aerodynamic angle of attack and sideslip. The basic definitions of these parameters are given in Section 3.1.

(a) <u>Derivation of time rate of change of flight-path angle, $\dot{\gamma}$</u>

The elevation flight-path angle is defined as

$$
\gamma = \sin^{-1}\left(\frac{-\dot{Z}_g}{V_g}\right) \qquad (3.135)
$$

Differentiating

$$
\dot{\gamma} = \left[\frac{1}{\sqrt{1 - \left(\frac{-\dot{Z}_g}{V_g}\right)^2}}\right]\left[\frac{V_g(-\ddot{Z}_g) - (-\dot{Z}_g)(\dot{V}_g)}{V_g^2}\right] \qquad (3.136)
$$

60

The surface-referenced speed is

$$V_g = \sqrt{\dot{X}_g{}^2 + \dot{Y}_g{}^2 + \dot{Z}_g{}^2} \tag{3.137}$$

from which is obtained the derivative

$$\dot{V}_g = \frac{\dot{X}_g\ddot{X}_g + \dot{Y}_g\ddot{Y}_g + \dot{Z}_g\ddot{Z}_g}{\sqrt{\dot{X}_g^2 + \dot{Y}_g^2 + \dot{Z}_g^2}} = \frac{\dot{X}_g\ddot{X}_g + \dot{Y}_g\ddot{Y}_g + \dot{Z}_g\ddot{Z}_g}{V_g} \tag{3.138}$$

Substituting Equation (3.138) into Equation (3.136) gives

$$\dot{\gamma} = \frac{\dot{Z}_g(\dot{X}_g\ddot{X}_g + \dot{Y}_g\ddot{Y}_g + \dot{Z}_g\ddot{Z}_g) - V_g^2\ddot{Z}_g}{V_g^2 \sqrt{V_g^2 - \dot{Z}_g^2}} \tag{3.139}$$

(b) <u>Derivation of time rate of change of heading angle, $\dot{\sigma}$</u>

The horizontal flight-path angle is defined by

$$\sigma = \text{Sin}^{-1}\left(\frac{\dot{Y}_g}{\sqrt{\dot{X}_g{}^2 + \dot{Y}_g{}^2}}\right) \tag{3.140}$$

Differentiating with respect, to time, and rearranging the product of fractions which is obtained, results in

$$\dot{\sigma} = \frac{\ddot{Y}_g(\dot{X}_g{}^2 + \dot{Y}_g{}^2) - \dot{Y}_g(\dot{X}_g\ddot{X}_g + \dot{Y}_g\ddot{Y}_g)}{\dot{X}_g(\dot{X}_g{}^2 + \dot{Y}_g{}^2)} \tag{3.141}$$

Relations for the quantities $\dot{X}_g$, $\dot{Y}_g$, $\dot{Z}_g$, and V_g, which appear in the $\dot{\gamma}$- and $\dot{\sigma}$- equations, are derived in Section 3.1, Equation (3.29). Also appearing in the $\dot{\gamma}$- and $\dot{\sigma}$-equations are the quantities $\ddot{X}_g$, $\ddot{Y}_g$, and $\ddot{Z}_g$, for which expressions are derived as follows:

Let $\bar{R}$ be the displacement vector of the vehicle from the center of the planet, see Figure (3.1). In inertial coordinates

$$\bar{R} = X\bar{1}_X + Y\bar{1}_Y + Z\bar{1}_Z \tag{3.142}$$

61

and in local-geocentric coordinates

$$\overline{R} = -R\overline{1}_{Z_g} \tag{3.143}$$

The velocity of the body is

$$\overline{V} = \frac{d}{dt}(\overline{R}) = \frac{\delta\overline{R}}{\delta t} + \overline{\omega}_p \times \overline{R} \tag{3.144}$$

where $\delta\overline{R}/\delta t$ is the derivative of $\overline{R}$ with respect to the moving coordinate system X_g-Y_g-Z_g. The acceleration, which is ultimately required, is

$$\overline{a} = \frac{d}{dt}\left(\frac{\delta\overline{R}}{\delta t} + \overline{\omega}_p \times \overline{R}\right) = \frac{\delta^2\overline{R}}{\delta t^2} + \overline{\omega}_p \times \frac{\delta\overline{R}}{\delta t} + \overline{\omega}_p \times \frac{d\overline{R}}{dt} + \frac{d\overline{\omega}_p}{dt} \times \overline{R} \tag{3.145}$$

In terms of the local-geocentric coordinate system, the velocity and acceleration contributions are

$$\frac{\delta\overline{R}}{\delta t} = \dot{X}_g\overline{1}_{X_g} + \dot{Y}_g\overline{1}_{Y_g} + \dot{Z}_g\overline{1}_{Z_g} \tag{3.146}$$

and

$$\frac{\delta^2\overline{R}}{\delta t^2} = \ddot{X}_g\overline{1}_{X_g} + \ddot{Y}_g\overline{1}_{Y_g} + \ddot{Z}_g\overline{1}_{Z_g} \tag{3.147}$$

The cross products require several vector manipulations to obtain expressions in a usable form. The acceleration of Equation (3.145) is more conventionally written

$$\overline{a} = \frac{\delta^2\overline{R}}{\delta t^2} + 2\overline{\omega}_p \times \frac{\delta\overline{R}}{\delta t} + \overline{\omega}_p \times (\overline{\omega}_p \times \overline{R}) \tag{3.148}$$

since the time rate of change of the planet's rotational velocity may be taken as zero.

The rotational rate of the planet is

$$\overline{\omega}_p = -\omega_p \overline{1}_Z$$

in inertial coordinates but may be expressed more conveniently in terms of the local-geocentric coordinates for the present derivation by

$$\overline{\omega}_p = \omega_{X_g}\overline{1}_{X_g} + \omega_{Z_g}\overline{1}_{Z_g} \tag{3.149}$$

where, from Figure (3.1)

$$\omega_{X_g} = \omega_p \cos \phi_L$$

$$\omega_{Z_g} = \omega_p \sin \phi_L$$

None of the planet's rotational rate appears in the Y_g axis since $\bar{\omega}_p$ and $\bar{1}_{Y_g}$ are perpendicular vectors. The Coriolis acceleration, $2\bar{\omega}_p \times \delta\bar{R}/\delta t$ is

$$2\bar{\omega}_p \times \frac{\delta\bar{R}}{\delta t} = 2 \begin{vmatrix} \bar{1}_{X_g} & \bar{1}_{Y_g} & \bar{1}_{Z_g} \\ \omega_{X_g} & 0 & \omega_{Z_g} \\ \dot{X}_g & \dot{Y}_g & \dot{Z}_g \end{vmatrix} = 2\left[-(\dot{Y}_g\omega_{Z_g})\bar{1}_{X_g} + (\omega_{Z_g}\dot{X}_g - \omega_{X_g}\dot{Z}_g)\bar{1}_{Y_g} \right. $$
$$\left. + (\omega_{X_g}\dot{Y}_g)\bar{1}_{Z_g}\right] \qquad (3.150)$$

The centripetal acceleration, $\bar{\omega}_p \times (\bar{\omega}_p \times \bar{R})$, is similarly obtained using Equations (3.143) and (3.149), to be

$$\bar{\omega}_p \times (\bar{\omega}_p \times \bar{R}) = -(\omega_{X_g}\omega_{Z_g}R)\bar{1}_{X_g} + (\omega_{X_g}^2 R)\bar{1}_{Z_g} \qquad (3.151)$$

Substituting Equations (3.147), (3.150), and (3.151) into Equation (3.148) and collecting like terms gives

$$\bar{a} = \left[\ddot{X}_g - 2\dot{Y}_g\omega_{Z_g} - \omega_{Z_g}\omega_{X_g}R\right]\bar{1}_{X_g} + \left[\ddot{Y}_g + 2(\dot{X}_g\omega_{Z_g} - \dot{Z}_g\omega_{X_g})\right]\bar{1}_{Y_g}$$
$$+ \left[\ddot{Z}_g + 2\dot{Y}_g\omega_{X_g} + \omega_{X_g}^2\omega R\right]\bar{1}_{Z_g} \qquad (3.152)$$

The acceleration, in inertial coordinates, is

$$\bar{a} = \ddot{X}\bar{1}_X + \ddot{Y}\bar{1}_Y + \ddot{Z}\bar{1}_Z \qquad (3.153)$$

Equations (3.152) and (3.153) are equal, and by means of the direction-cosine matrix relating inertial unit vectors to local-geocentric unit vectors, Equation (3.15), Section (3.1), the conversion is

$$\begin{vmatrix} \ddot{X}_g - 2\dot{Y}_g\omega_{Z_g} - \omega_{Z_g}\omega_{X_g}R \\ \ddot{Y}_g + 2(\dot{X}_g\omega_{Z_g} - \dot{Z}_g\omega_{X_g}) \\ \ddot{Z}_g + 2\dot{Y}_g\omega_{X_g} + \omega_{X_g}^2 R \end{vmatrix} = \begin{vmatrix} i_1 & j_1 & k_1 \\ i_2 & j_2 & k_2 \\ i_3 & j_3 & k_3 \end{vmatrix} \begin{vmatrix} \ddot{X} \\ \ddot{Y} \\ \ddot{Z} \end{vmatrix} \qquad (3.154)$$

Since $\ddot{X}_g$, $\ddot{Y}_g$, and $\ddot{Z}_g$ are the required quantities, the components of Coriolis and centripetal accelerations must be subtracted. The inertial components of acceleration may be calculated by the direction-cosine matrix relating body-coordinate unit vectors to inertial-coordinate unit vectors, Equation (3.1), Section (3.1): [6]

$$\begin{vmatrix} \ddot{X} \\ \ddot{Y} \\ \ddot{Z} \end{vmatrix} = \begin{vmatrix} l_1 & m_1 & n_1 \\ l_2 & m_2 & n_2 \\ l_3 & m_3 & n_3 \end{vmatrix} \begin{vmatrix} \dfrac{F_x}{m} \\ \dfrac{F_y}{m} \\ \dfrac{F_z}{m} \end{vmatrix} \qquad (3.155)$$

---

(6) Note that F_x, F_y, and F_z include the weight components of the vehicle.

(c) <u>Derivation of the time rate of change of angle of attack, $\dot{\alpha}$</u>

The angle of attack is defined by

$$\alpha = \text{Tan}^{-1}\left(\frac{w - w_w}{u - u_w}\right) \tag{3.156}$$

Taking the derivative of Equation (3.156) gives the required solution for $\dot{\alpha}$;

$$\dot{\alpha} = \frac{(u - u_w)(\dot{w} - \dot{w}_w) - (w - w_w)(\dot{u} - \dot{u}_w)}{(u - u_w)^2 + (w - w_w)^2} \tag{3.157}$$

(d) <u>Derivation of the time rate of change of sideslip angle, $\dot{\beta}$</u>

The angle of sideslip is defined by

$$\beta = \text{Tan}^{-1}\left(\frac{v - v_w}{u - u_w}\right) \tag{3.158}$$

Taking the derivative of Equation (3.158) gives the required solution for $\dot{\beta}$;

$$\dot{\beta} = \frac{(u - u_w)(\dot{v} - \dot{v}_w) - (v - v_w)(\dot{u} - \dot{u}_w)}{(u - u_w)^2 + (v - v_w)^2} \tag{3.159}$$

The quantities u_w, v_w, w_w, which appear in the $\dot{\alpha}$ and $\dot{\beta}$ equations, have been defined by Equation (3.33) of Section (3.1). The quantities, $\dot{u}$, $\dot{v}$, $\dot{w}$, u, v and w are obtained by the solution of the equations of motion. Relations for the quantities $\dot{u}_w$, $\dot{v}_w$, and $\dot{w}_w$ are obtained as follows:

Wind velocities are normally given in local-geocentric coordinates. The transformation of these data to body coordinates is made through the inertial coordinate system. The required direction cosine matrices are

$$\begin{vmatrix} \overline{1}_X \\ \overline{1}_Y \\ \overline{1}_Z \end{vmatrix} = \begin{vmatrix} i_1 & i_2 & i_3 \\ j_1 & j_2 & j_3 \\ k_1 & k_2 & k_3 \end{vmatrix} \begin{vmatrix} \overline{1}_{X_g} \\ \overline{1}_{Y_g} \\ \overline{1}_{Z_g} \end{vmatrix}$$

and

$$\begin{vmatrix} \overline{1}_x \\ \overline{1}_y \\ \overline{1}_z \end{vmatrix} = \begin{vmatrix} l_1 & l_2 & l_3 \\ m_1 & m_2 & m_3 \\ n_1 & n_2 & n_3 \end{vmatrix} \begin{vmatrix} \overline{1}_X \\ \overline{1}_Y \\ \overline{1}_Z \end{vmatrix}$$

64

as defined by Equations (3.15) and (3.1). These transformation matrices are the inverse of those used in Equations (3.154) and (3.155), above. The time rates of change of vehicle velocity due to change in wind velocity are:

$$
\begin{vmatrix} \dot{u}_w \\ \dot{v}_w \\ \dot{w}_w \end{vmatrix} = \begin{vmatrix} l_1 & l_2 & l_3 \\ m_1 & m_2 & m_3 \\ n_1 & n_2 & n_3 \end{vmatrix} \begin{vmatrix} i_1 & i_2 & i_3 \\ j_1 & j_2 & j_3 \\ k_1 & k_2 & k_3 \end{vmatrix} \begin{vmatrix} \ddot{X}_{g_w} - 2\dot{Y}_{g_w}\,\omega Z_g - \omega_{X_g}\omega Z_g\,R \\ \ddot{Y}_{g_w} + 2(\omega Z_g \dot{X}_{g_w} - \omega_{X_g}\dot{Z}_{g_w}) \\ \ddot{Z}_{g_w} + 2\omega_{X_g}\dot{Y}_{g_w} + \omega_{X_g}^2\,R \end{vmatrix}
\tag{3.160}
$$

The methods by which the acceleration components of the wind velocity are obtained depends upon the manner in which wind data have been incorporated into the problem. In general form, the derivatives are:

$$
\ddot{X}_{g_w} = \frac{d}{dt}(\dot{X}_{g_w}) = \frac{\partial \dot{X}_{g_w}}{\partial t} + \frac{\partial \dot{X}_{g_w}}{\partial h}\frac{dh}{dt} + \frac{\partial \dot{X}_{g_w}}{\partial \phi_L}\frac{d\phi_L}{dt} + \frac{\partial \dot{X}_{g_w}}{\partial \Theta_L}\frac{d\Theta_L}{dt}
$$

$$
\ddot{Y}_{g_w} = \frac{d}{dt}(\dot{Y}_{g_w}) = \frac{\partial \dot{Y}_{g_w}}{\partial t} + \frac{\partial \dot{Y}_{g_w}}{\partial h}\frac{dh}{dt} + \frac{\partial \dot{Y}_{g_w}}{\partial \phi_L}\frac{d\phi_L}{dt} + \frac{\partial \dot{Y}_{g_w}}{\partial \Theta_L}\frac{d\Theta_L}{dt} \tag{3.161}
$$

$$
\ddot{Z}_{g_w} = \frac{d}{dt}(\dot{Z}_{g_w}) = \frac{\partial \dot{Z}_{g_w}}{\partial t} + \frac{\partial \dot{Z}_{g_w}}{\partial h}\frac{dh}{dt} + \frac{\partial \dot{Z}_{g_w}}{\partial \phi_L}\frac{d\phi_L}{dt} + \frac{\partial \dot{Z}_{g_w}}{\partial \Theta_L}\frac{d\Theta_L}{dt}
$$

When the wind data are incorporated into the problem by curve-read techniques, the total derivative is obtained by machine differentiation.

    3.3.2 <u>Inertial Components of Planet Referenced Velocity (Point-Mass Problem)</u> - In the point-mass problem, the planet-referenced velocities $\dot{X}_e$, $\dot{Y}_e$, and $\dot{Z}_e$ are normally calculated. However, the inertial velocities $\dot{X}$, $\dot{Y}$, and $\dot{Z}$ may be required for reference purposes or to provide initial conditions for interplanetary trajectory computations. The transformation between inertial velocities and planet-referenced velocities is derived as follows:
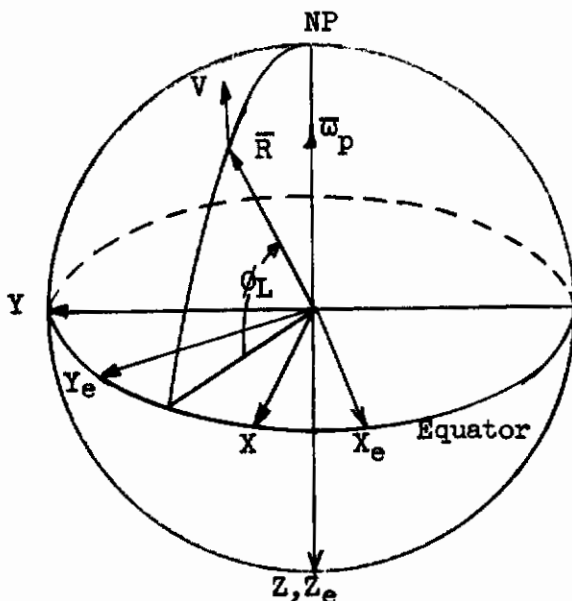
Figure 3.21 Inertial and Earth-
Referenced Coordinate Systems

65

Let $\bar{R}$ be the displacement of the point-mass, (see Figure (3.21)).

In inertial coordinates

$$\bar{R} = X\bar{1}_X + Y\bar{1}_Y + Z\bar{1}_Z \tag{3.162}$$

and

$$\bar{V} = \dot{\bar{R}} = \dot{X}\bar{1}_X + \dot{Y}\bar{1}_Y + \dot{Z}\bar{1}_Z \tag{3.163}$$

In planet-referenced coordinates

$$\bar{R} = X_e\bar{1}_{X_e} + Y_e\bar{1}_{Y_e} + Z_e\bar{1}_{Z_e}$$

However, due to the rotation of the X_e, Y_e, Z_e coordinate system, the velocity is

$$\bar{V} = \dot{\bar{R}} = \frac{\delta\bar{R}}{\delta t} + \bar{\omega}_p \times \bar{R} \tag{3.164}$$

where

$$\frac{\delta\bar{R}}{\delta t} = \dot{X}_e\bar{1}_{X_e} + \dot{Y}_e\bar{1}_{Y_e} + \dot{Z}_e\bar{1}_{Z_e} \tag{3.165}$$

The planet's rotation is about the Z-axis which is also the Z_e-axis. Therefore

$$\bar{\omega}_p = -\omega_p\bar{1}_Z = -\omega_p\bar{1}_{Z_e}$$

and the required cross product is:

$$\bar{\omega}_p \times \bar{R} = \begin{vmatrix} \bar{1}_{X_e} & \bar{1}_{Y_e} & \bar{1}_{Z_e} \\ 0 & 0 & -\omega_p \\ X_e & Y_e & Z_e \end{vmatrix} = (Y_e\omega_p)\bar{1}_{X_e} - (X_e\omega_p)\bar{1}_{Y_e} \tag{3.166}$$

Substituting Equations (3.163), (3.165), and (3.166) into Equation (3.164)

$$\dot{X}\bar{1}_X + \dot{Y}\bar{1}_Y + \dot{Z}\bar{1}_Z = (\dot{X}_e + \omega_p Y_e)\bar{1}_{X_e} + (\dot{Y}_e - \omega_p X_e)\bar{1}_{Y_e} + (\dot{Z}_e)\bar{1}_{Z_e} \tag{3.167}$$

The relation between the unit vectors in the inertial system and unit vectors in the planet referenced system are obtained by a single rotation about the Z-axis.

The transformation matrix is:

$$\begin{vmatrix} \bar{1}_{X_e} \\ \bar{1}_{Y_e} \\ \bar{1}_{Z_e} \end{vmatrix} = \begin{vmatrix} \cos\omega_p t & -\sin\omega_p t & 0 \\ \sin\omega_p t & \cos\omega_p t & 0 \\ 0 & 0 & 1 \end{vmatrix} \begin{vmatrix} \bar{1}_X \\ \bar{1}_Y \\ \bar{1}_Z \end{vmatrix} \tag{3.168}$$

66

The transformation from planet-referenced velocities to inertial velocities is made with the inverse of the matrix of Equation (3.168) and the component relations derived in Equation (3.167).

$$
\begin{vmatrix} \dot{X} \\ \dot{Y} \\ \dot{Z} \end{vmatrix} = \begin{vmatrix} \text{Cos } \omega_p t & \text{Sin } \omega_p t & 0 \\ -\text{Sin } \omega_p t & \text{Cos } \omega_p t & 0 \\ 0 & 0 & 1 \end{vmatrix} \begin{vmatrix} \dot{X}_e + \omega_p Y_e \\ \dot{Y}_e - \omega_p X_e \\ \dot{Z}_e \end{vmatrix} \tag{3.169}
$$

The components of inertial velocities are used to calculate the speed of the body as:

$$
V = \sqrt{\dot{X}^2 + \dot{Y}^2 + \dot{Z}^2} \tag{3.170}
$$

Equation (3.170) is valid regardless of the initial coordinate system involved.

3.4 Interplanetary Trajectory Problem Coordinate Transformations - The Six-Degree-of-Freedom Flight-Path Study computer program may be used to compute the injection conditions for vehicles embarking on deep-space journeys from a planet; and may also be used to compute the terminal trajectory of vehicles approaching a planet from such journeys. Since the Six-Degree-of-Freedom Flight-Path Study computer program considers the actual volume and gravitational effects of a planet's oblateness, as well as the atmosphere, this program is suited to the detailed computation of the motion of a space vehicle in the proximity of a planet. Use of this program would be costly from the standpoint of machine and analyst time, however, and a reduced-degrees-of-freedom point-mass problem formulation which accounts for the position of the planets and the resulting strength and direction of the gravitational field at the location of the vehicle would be more useful. The following paragraphs explain the coordinate systems convenient to such a problem and derive the coordinate transformations required for the transition. It should be noted that the coordinate transformations presented in the following paragraphs are performed only once in the computation of a trajectory using the Six-Degree-of-Freedom Flight-Path Study computer program, whereas the transformations presented in the preceding paragraphs of Section 3 are required at every time step.

3.4.1 The Coordinates of the Interplanetary Trajectory Problem - The coordinate system normally adopted for the interplanetary trajectory problem is a heliocentric, equatorial, Cartesian axis system based upon the Earth's equatorial plane and the mean vernal equinox of reference date in ephemeris time. This system will be called the ϒ-Λ-Γ coordinate system for the Six-Degree-of-Freedom Flight-Path Study. The ϒ- and Λ-axis are in the equatorial plane of reference date, ephemeris time, with ϒ pointing to the mean vernal equinox of this date. The Γ axis is perpendicular to the plane of the ϒ-Λ and is positive toward the north pole of the Earth. The position of the planets is normally given in this coordinate system, and the position and velocity of the vehicle will be conveniently calculated in this coordinate system by an interplanetary trajectory computer program. The vehicle position and velocity will be computed relative to the center of the sun. It is assumed that the interplanetary program also has the capability of translating the origin of the coordinate system from the center of the sun to the center of a planet without disturbing the angular orientation of the axes in space. The

planetocentric-equatorial components of the planet-reference position and velocity may then be computed in the interplanetary trajectory problem.

3.4.2 <u>The Inertial Coordinates of the Six-Degree-of-Freedom Problem</u> - The X-Y-Z "inertial" coordinates of the six-degree-of-freedom problem have been defined in Section 3.1. The X-and Y-axis of this system are in the equatorial plane of the planet with X inertially fixed to the meridian of the vehicle at the time of problem initiation. When transferring from the interplanetary trajectory problem to the six-degree problem, the X-axis will be determined by the planet meridian of the vehicle at the time of transfer. The Z-axis is aligned with the polar axis of the planet and is positive towards the south pole.

3.4.3 <u>Astronomical Angles Required for the Coordinate Transformation</u> - A convenient derivation of the direction cosines relating the X-Y-Z and Υ-Λ-Γ coordinate systems may be made using the right ascension (α_N) and declination (δ_N) of the planet's north polar axis with respect to the Υ-Λ-Γ coordinate system of the reference date. The right ascension and declination of the north pole of several of the planets may be found on Pages 521 and 522 of the 1960 American Ephermeris and Nautical Almanac (Reference (10)). The two rotations through α_N and δ_N define the equatorial plane of the planet; one more rotation, the hour angle, is necessary to orient the X-axis of the Six-Degree-of-Freedom problem. This procedure may be used for transferring either to or from the Six-Degree-of-Freedom Flight-Path Study computer program.

3.4.4 <u>Transformation From Interplanetary to the Six-Degree-of-Freedom</u> <u>Inertial Coordinate System</u> - The information required to evaluate the direction cosines in this coordinate transformation are:

1. The right ascension and declination of the north polar axis of the planet in question.

2. Position components in the mean-equinox-of-reference-date coordinate system with the origin at the center of the subject planet.

The required direction cosines will be determined by the multiplication of the transformation matrices of each individual rotation required to align the two coordinate systems according to the methods of Reference (9). The sequence of rotations is given by: (See Figure (3.22)).

$$\begin{vmatrix} \bar{1}_X \\ \bar{1}_Y \\ \bar{1}_Z \end{vmatrix} = \begin{vmatrix} 180° \\ \\ X \end{vmatrix} \begin{vmatrix} \lambda_N \\ \\ -Z \end{vmatrix} \begin{vmatrix} 90°-\delta_N \\ \\ A \end{vmatrix} \begin{vmatrix} \alpha_N \\ \\ \Gamma \end{vmatrix} \begin{vmatrix} \bar{1}_\Upsilon \\ \bar{1}_\Lambda \\ \bar{1}_\Gamma \end{vmatrix} \qquad (3.171)$$

The equatorial plane of the planet is defined by the coordinate system A-B-(-Z) which is obtained by rotating through α_N and ($90°-\delta_N$). The X-axis will be located in this plane by the meridian of the vehicle at the time of transfer. The angle λ_N specifies the hour angle of the meridian of the vehicle with reference to A and may be determined from vehicle position components, as noted in the next paragraph.

68
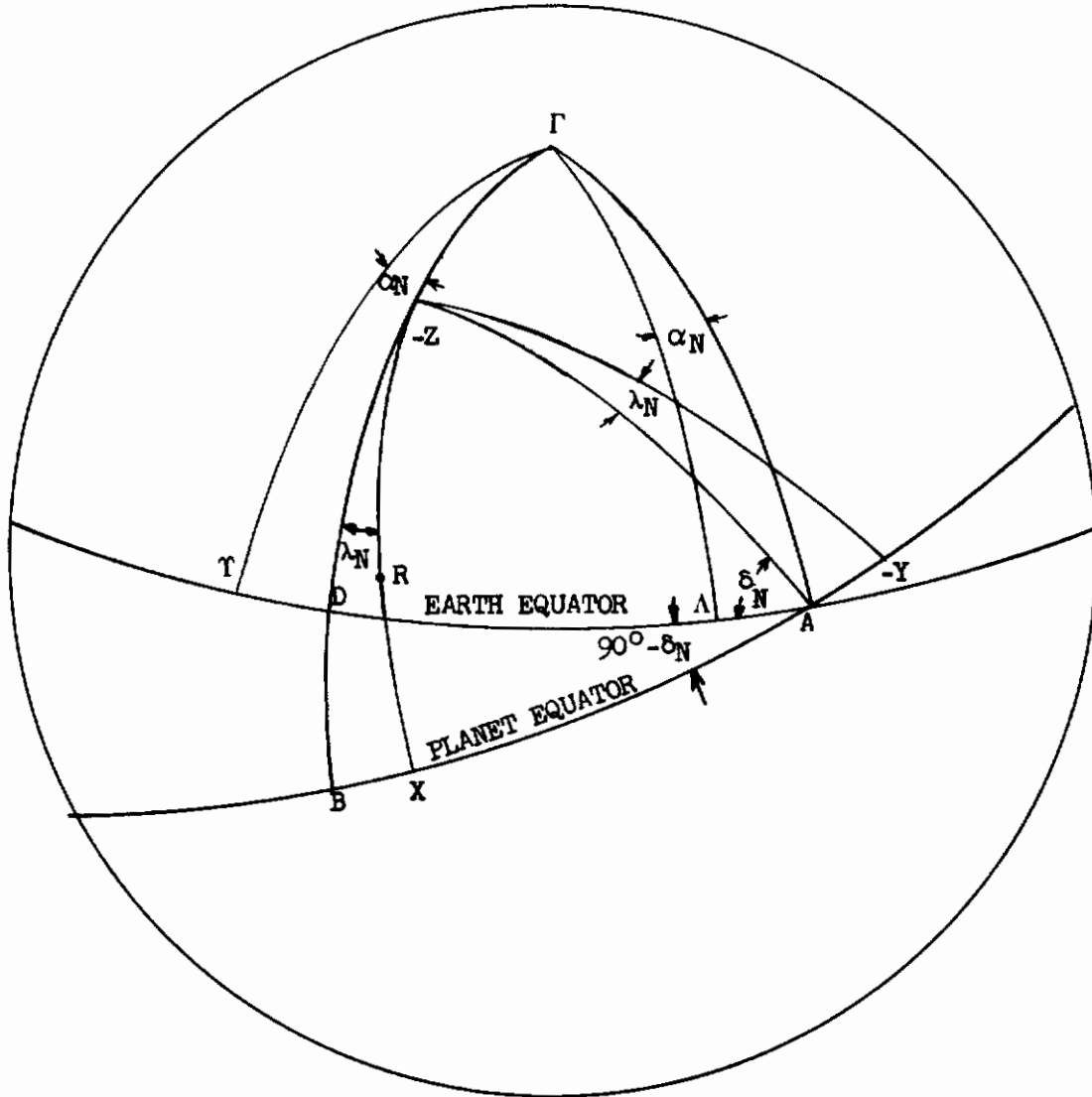
FIGURE 3.22 A UNIT SPHERE SHOWING TRANSFORMATION
FROM AN INTERPLANETARY TRAJECTORY PROBLEM TO THE
SIX-DEGREE-OF-FREEDOM PROBLEM INERTIAL COORDINATES

69

The direction cosines of the transformation will be obtained by writing Equation (3.171) in terms of the individual transformations as follows:

$$
\begin{vmatrix} \bar{1}_X \\ \bar{1}_Y \\ \bar{1}_Z \end{vmatrix} = \begin{vmatrix} 1 & 0 & 0 \\ 0 & -1 & 0 \\ 0 & 0 & -1 \end{vmatrix} \begin{vmatrix} \cos \lambda_N & \sin \lambda_N & 0 \\ -\sin \lambda_N & \cos \lambda_N & 0 \\ 0 & 0 & 1 \end{vmatrix} \begin{vmatrix} \sin \delta_N & 0 & -\cos \delta_N \\ 0 & 1 & 0 \\ \cos \delta_N & 0 & \sin \delta_N \end{vmatrix} \begin{vmatrix} \cos \alpha_N & \sin \alpha_N & 0 \\ -\sin \alpha_N & \cos \alpha_N & 0 \\ 0 & 0 & 1 \end{vmatrix} \begin{vmatrix} \bar{1}_\Upsilon \\ \bar{1}_\Lambda \\ \bar{1}_\Gamma \end{vmatrix}
$$

Carrying out the indicated multiplication gives the required transformation,

$$
\begin{vmatrix} \bar{1}_X \\ \bar{1}_Y \\ \bar{1}_Z \end{vmatrix} = \begin{vmatrix} (\cos \lambda_N \sin \delta_N \cos \alpha_N - \sin \lambda_N \sin \alpha_N) & (\cos \lambda_N \sin \delta_N \sin \alpha_N + \sin \lambda_N \cos \alpha_N) & (-\cos \lambda_N \cos \delta_N) \\ (\sin \lambda_N \sin \delta_N \cos \alpha_N + \cos \lambda_N \sin \alpha_N) & (\sin \lambda_N \sin \delta_N \sin \alpha_N - \cos \lambda_N \cos \alpha_N) & (-\cos \delta_N \sin \lambda_N) \\ (-\cos \delta_N \cos \alpha_N) & (-\cos \delta_N \sin \alpha_N) & (-\sin \delta_N) \end{vmatrix} \begin{vmatrix} \bar{1}_\Upsilon \\ \bar{1}_\Lambda \\ \bar{1}_\Gamma \end{vmatrix}
$$

$$(3.172)$$

Since the X-axis is established by the position of the vehicle at zero-time, when the transfer is made to the Six-Degrees-of-Freedom Flight-Path Study, the Y component of the transformation of Equation (3.172) must be

$$(\sin \lambda_N \sin \delta_N \cos \alpha_N + \cos \lambda_N \sin \alpha_N)\Upsilon + (\sin \lambda_N \sin \delta_N \sin \alpha_N - \cos \lambda_N \cos \alpha_N)\Lambda$$

$$- (\cos \delta_N \sin \lambda_N)\Gamma \equiv 0$$

which, solved for λ_N, gives

$$\lambda_N = \tan^{-1} \left[\frac{\Lambda \cos \alpha_N - \Upsilon \sin \alpha_N}{\Upsilon \cos \alpha_N \sin \delta_N + \Lambda \sin \alpha_N \sin \delta_N - \Gamma \cos \delta_N} \right] \qquad (3.173)$$

3.4.5 **Transformation From the Six-Degree-of-Freedom to Interplanetary Coordinates** - The direction cosines derived in this section are applicable when transferring the computations from the six-degree-of-freedom problem to an interplanetary trajectory problem. The final angle (λ_N) in the sequence of rotations discussed in Section 3.4.4 was determined from knowledge of the vehicle position in the mean-equinox-of-reference-date coordinate system. Since these position components are not known when transferring from the six-degree-of-freedom problem to an interplanetary problem, another method of determining λ_N must be used. Since the right ascension of the north-polar axis of the planet establishes the line of intersection of the planet's equatorial plane and the Earth equatorial plane of date, the hour angle of the launch site at the time of launch with this datum is required. Unfortunately, planet hour angles are not usually referenced to this point; however, the angle λ_N may be evaluated from the planet hour angle of the vernal equinox with the planet meridian of the launch point at the time of launch. From Figure (3.23), the required relationship is:

70
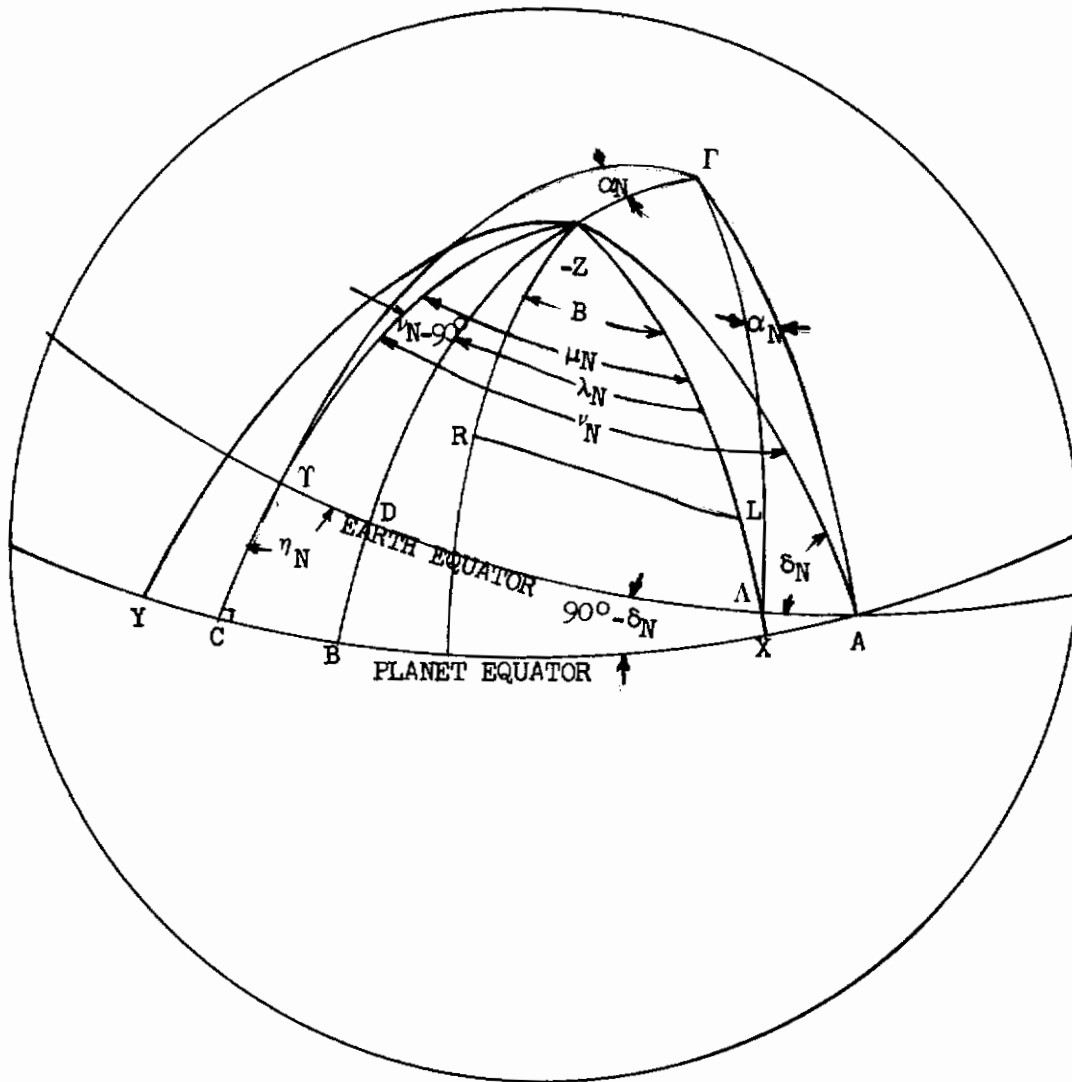
L = Launch Point

R = Vehicle Position at
    Time of Transfer

FIGURE 3.23   UNIT SPHERE DIAGRAM
SHOWING THE TRANSFORMATION FROM THE SIX-DEGREE-OF-FREEDOM
PROBLEM TO AN INTERPLANETARY TRAJECTORY PROBLEM

71

$$\lambda_N = \mu_N - \nu_N + 90^\circ \tag{3.174}$$

where μ_N is the hour angle of the vernal equinox of date with the launch point at the time of launch, and ν_N is the angle of the vernal equinox of date with the intersection of planet's equatorial plane and the Earth equatorial plane of the reference date.

The angle ν_N will be determined from the spherical triangle ΥCA (Figure (3.23)). By the law of cosines for sides:

$$\text{Cos } \nu_N = \text{Cos } \widehat{\Upsilon C} \text{ Cos } (90 + \alpha_N) + \text{Sin } \widehat{\Upsilon C} \text{ Sin } (90 + \alpha_N) \text{ Cos } \eta_N \tag{3.175}$$

Several terms in the equation must be related to the known parameters α_N and δ_N. The cosine of η_N may be found from the law of cosines for angles:

$$\text{Cos } \eta_N = \text{Cos } \delta_N \text{ Cos } \nu_N \tag{3.176}$$

From the law of sines:

$$\text{Sin } \widehat{\Upsilon C} = \text{Cos } \delta_N \text{ Cos } \alpha_N \tag{3.177}$$

The cosine of the arc $\widehat{\Upsilon C}$ is also required in Equation (3.175) and is easily obtained by the trigomometric identity:

$$\text{Cos } \widehat{\Upsilon C} = \sqrt{1 - \text{Cos}^2 \delta_N \text{ Cos}^2 \alpha_N} \tag{3.178}$$

Substituting Equations (3.176), (3.177), and (3.178) into Equation (3.175) and solving for Cos ν_N gives the relation:

$$\text{Cos } \nu_N = \left(\frac{-\text{Sin } \alpha_N}{\sqrt{1 - \text{Cos}^2 \delta_N \text{ Cos}^2 \alpha_N}} \right) \tag{3.179}$$

The angle λ_N is then obtained from Equation (3.174):

$$\lambda_N = \mu_N - \text{Cos}^{-1} \left(\frac{-\text{Sin } \alpha_N}{\sqrt{1 - \text{Cos}^2 \delta_N \text{ Cos}^2 \alpha_N}} \right) + 90^\circ \tag{3.180}$$

The angle λ_N completes the set of angles that will be used to rotate the $\Upsilon - \Lambda - \Gamma$ coordinates into congruence with the X-Y-Z system. The transformation matrix for each individual rotation will be determined and the required direction cosines will be obtained by multiplying these matrices.

$$\begin{vmatrix} \bar{1}_X \\ \bar{1}_Y \\ \bar{1}_Z \end{vmatrix} = \begin{vmatrix} 180^\circ \\ \\ X \end{vmatrix} \begin{vmatrix} \lambda_N \\ \\ -Z \end{vmatrix} \begin{vmatrix} 90 - \delta_N \\ \\ A \end{vmatrix} \begin{vmatrix} \alpha_N \\ \\ \Gamma \end{vmatrix} \begin{vmatrix} \bar{1}_\Upsilon \\ \bar{1}_\Lambda \\ \bar{1}_\Gamma \end{vmatrix} \tag{3.181}$$

This sequence of rotations is identical to the sequence in Section (3.4.4). Therefore, the definitions of the direction cosines used in Section (3.4.4) also

may be used when transferring from the six-degree-of-freedom problem to an interplanetary trajectory problem. The angle λ_N is computed in a different manner in each case, but this will not affect the definitions of the direction cosines. The transformation from X-Y-Z to Υ - Λ - Γ coordinates is therefore given by the inverse of Equation (3.172).

$$
\begin{vmatrix} \bar{1}_\Upsilon \\ \bar{1}_\Lambda \\ \bar{1}_\Gamma \end{vmatrix} = \begin{vmatrix} (\cos \lambda_N \sin \delta_N \cos \alpha_N & (\sin \lambda_N \sin \delta_N \cos \alpha_N & -\cos \delta_N \cos \alpha_N \\ \quad -\sin \lambda_N \sin \alpha_N) & \quad +\cos \lambda_N \sin \alpha_N) & \\ (\cos \lambda_N \sin \delta_N \sin \alpha_N & (\sin \lambda_N \sin \delta_N \sin \alpha_N & -\cos \delta_N \sin \alpha_N \\ \quad +\sin \lambda_N \cos \alpha_N) & \quad -\cos \lambda_N \cos \alpha_N) & \\ (-\cos \lambda_N \cos \delta_N) & (-\cos \delta_N \sin \lambda_N) & -\sin \delta_N \end{vmatrix} \begin{vmatrix} \bar{1}_X \\ \bar{1}_Y \\ \bar{1}_Z \end{vmatrix}
$$

$$(3.182)$$

4. VEHICLE CHARACTERISTICS

The methods by which the aerodynamic, propulsive, and physical characteristics of a vehicle are introduced into the Six-Degree-of-Freedom Flight-Path Study computer program are presented in this section. The form and preparation of these input data are discussed together with methods by which stages and staging may be used to increase the effective data storage area allotted to a description of the vehicle's properties.

4.1 Aerodynamic Coefficients

4.1.1 Form of Data Input - The primary objective of the aerodynamic data input subprogram is to provide for a complete accounting of the various contributions to the aerodynamic forces and moments regardless of the flight conditions or the vehicle being considered. Two powerful techniques are available for use in digital computer programs; (a) an n-dimensional table look-up and interpolation and (b) an m-order polynomial function of n variables prepared by "curve fit" techniques. In the first method, the proper value for each term is obtained by an interpolation in "n" dimensions where the number of dimensions is taken to be the number of parameters to be varied independently plus the dependent variable. This method has the advantage of accurately describing even the most non-linear variations with a minimum of preparation effort. The amount of storage space which must be allocated to such a method, however, can achieve completely unreasonable proportions and may require substantial computing time for the interpolation as the number of dimensions is increased. The second method has essentially the opposite characteristics; that is, a large amount of data may be represented with a minimum amount of storage space and the computation time is held to reasonable limits but the data variations which may be represented must be regular. A substantial amount of effort is usually required for the preparation of data by a curve-fit technique. Both of these methods are very convenient when the amount of data to be handled is moderate, but tend to become unmanageable when large amounts of data are required. This usually occurs when the program, having several degrees of freedom, is committed to one or the other of these two techniques. Therefore, the Six-Degree-of-Freedom Flight-Path Study computer program will incorporate both of the techniques discussed as a compromise to take advantage of the more desirable features of both. To do this, a general set of data equations will be programmed which define each of the aerodynamic forces or moments. In general, the coefficients for these equations will be obtained from a curve-read interpolation. Several simplifications may be made to the equations depending on the flight condition and vehicle to be considered.

The effects of the following parameters will be considered:

(a) Angle of attack and its time derivative $(\alpha, \dot{\alpha})$

(b) Angle of sideslip and its time derivative $(\beta, \dot{\beta})$

(c) Roll, pitch, and yaw control deflections $(\delta_p, \delta_q, \delta_r)$

(d) Roll, pitch, and yaw angular rates (p, q, r)

(e) Mach number (M_N)

(f) Center-of-gravity position $(x_{C.G.})$

(g) Reference structural temperature $(T_{s_{ref}})$

The aerodynamic forces and moments considered with respect to each coordinate axis include the effects of angle of attack and sideslip, primary control deflection with respect to each axis, lag of downwash, and primary damping effects. In addition, the rolling moment due to yaw rate is included, and Magnus forces and moments are accounted for in one of the airframe options. Complete generality in the aerodynamic coupling effects has not been included in the present subprogram options since the descriptive terms required depend upon the particular problem considered. However, the storage space provided for the several existing options is considered to be adequate to accommodate other special problem formulations through substitution of terms.

Quite often the particular application will not require some of the terms listed in order to describe completely the flight path and vehicle under consideration. The subprogram will be arranged so that the computer will assign a constant value to any curve for which the data has not been supplied. For most curves, the constant value will be zero. This technique will reduce substantially the time required for the preparation of data. Values intermediate to those introduced in a tabular listing will be obtained by linear interpolation. The method of incorporating data for staged vehicles is discussed in Paragraph 4.4. The method of introducing the effects of static aerothermoelasticity is outlined in Appendix Four.

4.1.2 Flight Path and Vehicle Types - In most of the cases discussed below, a "curve-fit" technique will be used to obtain all or a portion of the aerodynamic terms. For the purposes of this subprogram, it will be assumed that the curve fit has been selected to represent the variation of the coefficient about the trim conditions. This may have the effect of removing physical significance from some of the individual terms, and only the sum of the terms will represent the data. A typical example is indicated below.
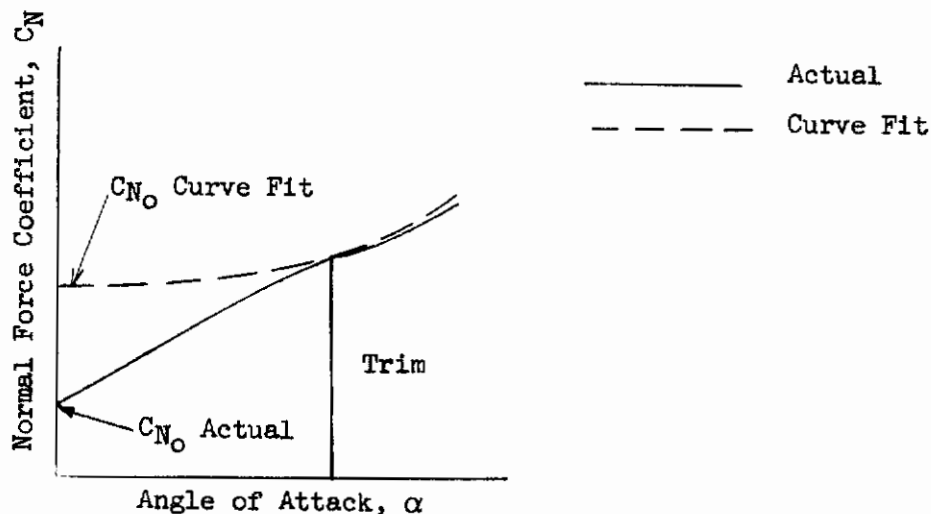
Figure 4.1 Curve Fit Non-Linear
Aerodynamic Characteristic

75

In this case, the C_{N_O} and C_{N_α} values used in the equation for C_N are obviously different from the actual values of these parameters.

A functional flow diagram for the solution of the aerodynamic forces and moments is presented in Figure (4.2). It should be noted that the actual machine programming will not necessarily follow the sequence shown since certain computer operations have been omitted in this description of the problem formulation.

Airframe Option (1) Controlled Aircraft - A controlled aircraft represents the most general case that will be considered. In order to account for the many component forces, it is necessary to make certain restricting assumptions. The assumptions will be made that the aircraft is confined to moderate variations in position angles and control deflections. Varying Mach number, center-of-gravity shift along the x-axis, and aerothermoelastic effects are included. The coefficients can then be expressed as shown in Block Number (1-7) of Figure (4.2). The functional computation sequence for this option proceeds from Block Number (1) to Block Number (1-7) in a straight-forward manner.

In the axial force coefficient equation, there is a provision for including the effects of variation in Reynolds number. This will be accomplished by supplying C_{A_O} as a function of unit Reynolds number and Mach number. A three-dimensional interpolation will be made to determine the value to be used in the equation.

The analyst will be provided the option of bypassing the aerothermoelastic calculations as indicated in Figure (4.2). The change in dynamic derivatives due to a change in the center-of-gravity location is programmed as a curve-read in order to avoid the complications of a transfer. It should be noted that either body-axis or wind-axis data can be supplied to these equations as the provision will be made to rotate wind-axis data into the body axis. The definition of α and β as applied to the SDF computer program is noted to be

$$\alpha = \text{Tan}^{-1}\left(\frac{w - w_W}{u - u_W}\right) \qquad \text{and} \qquad \beta = \text{Tan}^{-1}\left(\frac{v - v_W}{u - u_W}\right) \qquad (4.1)$$

Data supplied must correspond to this definition or an alternate computation of these angles must be formulated to agree with the method of data reduction.

Airframe Option (2) Point Mass - The consideration of the motion of a mass greatly simplifies the equations for the aerodynamic coefficients as no moments are considered. The additional restrictions that are imposed on this routine are that the vehicle is confined to moderate variations in position angles and control deflections. In addition, no consideration of aerothermoelastic effects, dynamic effects, and center-of-gravity shifts will be made. This reduces the equations to the form shown in Block Number (2-3) of Figure (4.2).

The forces calculated in this case will be in the wind-axes system rather than the body-axes system. This is in keeping with the solution of the equations of motion as noted in Paragraph 2.4.

FIGURE 4.2, SOLUTION OF AERODYNAMIC FORCES AND MOMENTS SUBPROGRAM

77

Airframe Option (3) Pitch-Up, Spin, and Similar Maneuvers of a Controlled
Aircraft - The study of a pitch-up, spin, or similar maneuvers of an aircraft
is normally restricted to particular conditions of velocity and altitude.
Aerothermoelastic effects and center-of-gravity shifts will be neglected.
Since large angles of attack and sideslip are expected, a four-dimensional table
look-up and interpolation of the coefficients as functions of angle of attack,
sideslip angle, and Mach number will be used. For this case, the parameters
$(C_A)_{\delta=0}$, $(C_N)_{\delta=0}$, $(C_y)_{\delta=0}$, $(C_l)_{\delta=0}$, $(C_m)_{\delta=0}$, and $(C_n)_{\delta=0}$ will be specified as
functions of α, β, and M_N. This allows the equations to be reduced to the form
indicated in Block Number (3-3) of Figure (4.2).

Airframe Option (4) Tumbling Re-entry Shapes - This option will have the
capability of accounting for the aerodynamic characteristics of a tumbling
re-entry shape that is rotationally symmetric about the longitudinal axis.
The Magnus forces and moments developed by a spinning motion about the longitud-
inal axes may be included. Restrictions on this case are: (a) no controls
are employed, (b) the center-of-gravity location is constant, and (c) aero-
thermoelastic effects are neglected. Each of the coefficients may then be
expressed as functions of the total angle of attack and Mach number. The
total angle of attack is defined in the following manner:

$$\alpha_T = \text{Tan}^{-1} \left(\frac{\sqrt{(w - w_w)^2 + (v - v_w)^2}}{(u - u_w)} \right) \qquad (4.2)$$

The aerodynamic coefficients required to describe the forces and moments
on such a vehicle are listed in Block Number (4-1) of Figure (4.2). A three-
dimensional interpolation must be performed for each coefficient together
with a rotation of the coefficients through the angle ϕ_A to the body axes
system. The aerodynamic roll angle, ϕ_A, is defined as:

$$\phi_A = \text{Tan}^{-1} \left(\frac{v - v_w}{w - w_w} \right) \qquad (4.3)$$

4.1.3 Error Constants - The use of error constants, designated by the
symbol ϵ_i, to modify the aerodynamic data characteristics is shown in Figure
(4.2). A detailed explanation of these error constants and their use is given
in Section 4.5.

4.2 Thrust and Fuel Flow Data - The techniques to be employed in the
introduction of the thrust and fuel-flow data into the solutions of the equa-
tions of motion are developed in an approach similar to that employed in
Paragraph 4.1, which considered aerodynamic data. An n-dimensional tabular
listing and interpolation technique is used, with the independent variables
being defined by the type of propulsion unit being considered. Equations are
developed to resolve the thrust forces into forces and moments in the vehicle
body-axes system. The provision to include error constants in the thrust and
fuel flow parameters is provided.

4.2.1 Data Inputs - The number of independent variables which affect
the thrust and fuel flow is determined by the type of propulsion unit being
considered. For the present formulation, the propulsion units are grouped

into the following options: (1) non-controlled-thrust rocket, (2) controlled-thrust rocket, and (3) air breathing engines. Options (2) and (3) require command information from an autopilot or flight plan programmer. Figure (4.3) presents a functional flow diagram for the computation of each of these three options for the case of a single nozzle (or propeller) engine. The data input techniques applicable to each option are outlined below.

Propulsion Option (1) Non-Controlled-Thrust Rocket - The thrust of a non-controlled-thrust rocket motor is assumed variable with time and altitude. The altitude effect is determined by the exit area of the nozzle, A_e, and the ambient pressure, P. If the thrust is specified for some constant ambient air pressure, the altitude correction can be calculated within the subprogram. In this subprogram, the vacuum thrust, in pounds, will be introduced by a tabular listing as a function of time, in seconds, and corrected as follows:

$$T = T_{VAC} - PA_e \tag{4.4}$$

The propellant consumption rate will be specified by a tabular listing, in slugs per second, as a function of time, in seconds. The vehicle mass can then be determined from the integrated propellant consumption rate and initial mass.

$$m = m_0 - \int_{t_0}^{t} \dot{m}_f \, dt \tag{4.5}$$

Note that $(d\,m/dt) = -\dot{m}_f$ for this definition of mass.

Propulsion Option (2) Controlled-Thrust Rocket - The controlled-thrust rocket differs from the non-controlled in that the propellant flow rate and the thrust at any given time and altitude may be varied by the flight programmer or autopilot subprograms of the computer program. It will be necessary, therefore, to specify the vacuum thrust as a function of propellant flow rate. The propellant flow rate must be obtained from an autopilot (or flight programmer) signal. The flow-rate command will then be used in the tabular listing of vacuum thrust. Correction of this thrust for altitude will be made by use of Equation (4.4). The vehicle mass is determined from an integration of the mass flow rate according to Equation (4.5).

Propulsion Option (3) Air Breathing Engines - An air-breathing engine is strongly affected by the environmental conditions under which it is operating. Engines which would be grouped in this classification are turbojets, ramjets, pulsejets, turboprops, and reciprocating machines. The parameters which will be considered of consequence in this program are:

(a) Altitude (h - ft)
(b) Mach number (M_N)
(c) Angle of attack (α - degrees), and
(d) Throttle setting (N - units defined by problem).

Both the thrust and fuel flow are functions of these variables. In order to accommodate these variables, a five-dimensional tabular listing and interpolation will be used to obtain both thrust and fuel flow. The thrust needs no further correction as the effects of all parameters are included in the interpolated value. The mass of the vehicle is determined from Equation (4.5).

The functional computation sequence for introducing these data is straight-forward as outlined in Figure (4.3). Also shown in Figure (4.3) is the computation required to resolve the engine force into body-axes or wind-axes components. This computation must be performed for all propulsion options and is, therefore, associated with the fixed portion of the computer program rather than with the thrust and fuel flow subprogram. The resolution is shown in Figure (4.3), however, since it is so closely associated with these forces.

4.2.2 <u>Component Forces and Moments</u> - All propulsion units are capable of introducing components of force and moment along each of the three coordinates of the vehicle body-axes system. These may be due to misalignments, position of installation, or vectoring of the thrust. A common method of control utilizes the thrust force to produce control moments by swiveling the exit nozzle. Since the equations of motion are derived on the basis of motion in the vehicle body-axes system for all options except the point-mass, it is necessary to resolve the forces and moments in the proper axes system. Defining the plane of swivel as a plane parallel to the x-axis and including the thrust vector, let ϕ_T be the angle of rotation of this plane from the x-y plane (y into z rotation is positive). Also let λ_T be the angle between the thrust vector and a line parallel to the x-axis in the plane of swivel $(0 < \lambda_T \leq 90^\circ)$. Then

$$T_x = T \cos \lambda_T$$
$$T_y = -T \sin \lambda_T \cos \phi_T \qquad (4.6)$$
$$T_z = -T \sin \lambda_T \sin \phi_T$$

where T_x, T_y, and T_z are the components of thrust in the vehicle body-axes system. (A positive T produces a positive $\dot{u}$.) These forces will introduce moments,

$$L_T = T_z (y_N - \Delta y_{C.G.}) - T_y (z_N - \Delta z_{C.G.})$$
$$M_T = T_x (z_N - \Delta z_{C.G.}) - T_z (x_N - \Delta x_{C.G.}) \qquad (4.7)$$
$$N_T = T_y (x_N - \Delta x_{C.G.}) - T_x (y_N - \Delta y_{C.G.})$$

Where L_T, M_T, and N_T are the thrust moments about the vehicle x, y, and z body axes respectively; x_N, y_N, and z_N are the distances of the point of swivel of the nozzle from the reference center of gravity and $\Delta x_{C.G.}$, $\Delta y_{C.G.}$, and $\Delta z_{C.G.}$ represent the shift in the center of gravity from the reference location. In the Six-Degree-of-Freedom Flight-Path Study computer program, consideration of the movement of the center of gravity will be confined to translation along the x-axis. This reduces the moment equations to the following form.

$$L_T = T_z y_N - T_y z_N$$
$$M_T = T_x z_N - T_z (x_N - \Delta x_{C.G.}) \qquad (4.8)$$
$$N_T = T_y (x_N - \Delta x_{C.G.}) - T_x y_N$$

80
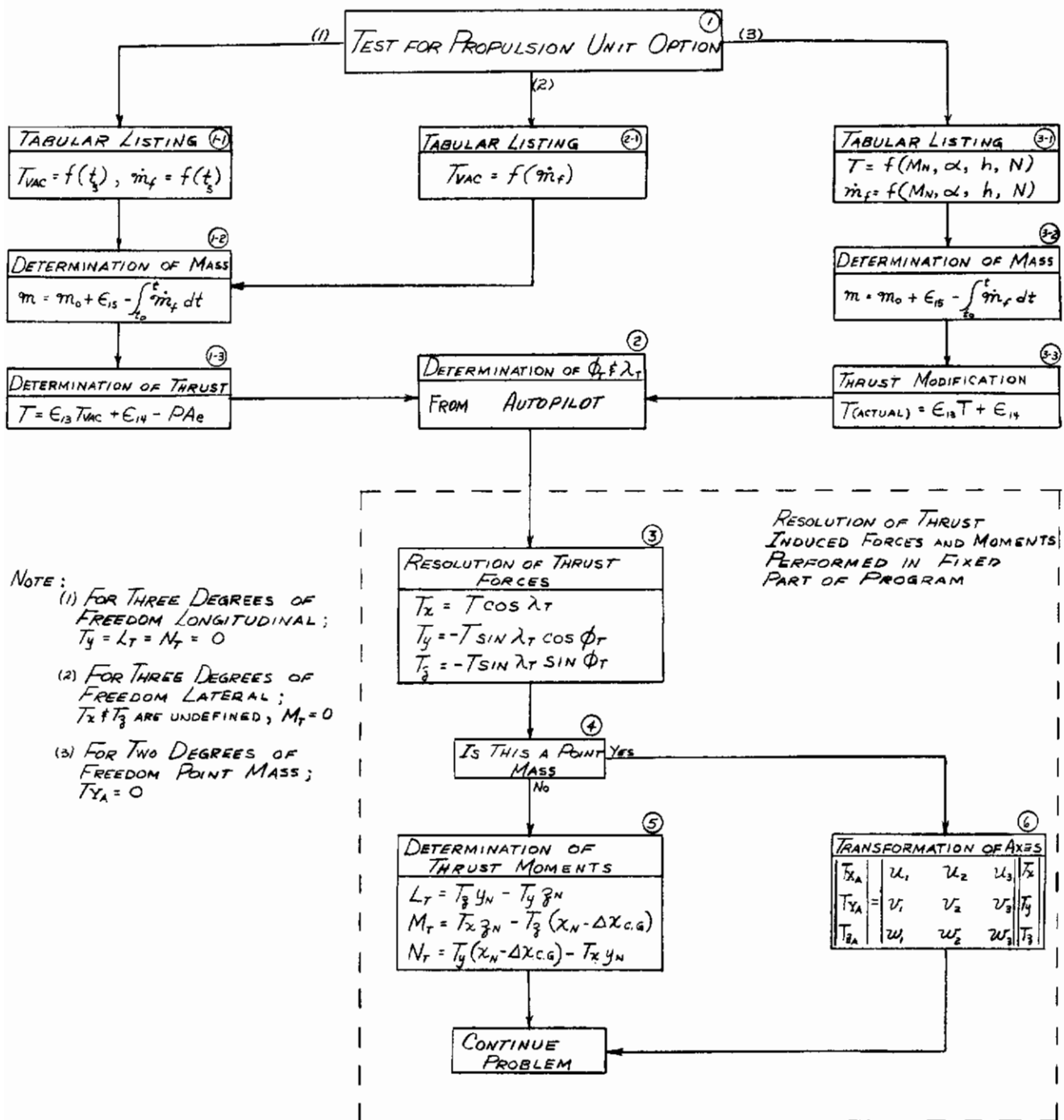
FIGURE 4.3, THRUST AND FUEL FLOW SUBPROGRAM

81

If more than one engine is used, or if a single engine with more than one exit nozzle is used, then the sum of the individual forces and moments must be obtained. In this case:

$$T_x = T_{x_1} + T_{x_2} + \ldots\ldots\ldots\ldots\ldots + T_{x_n} \qquad (4.9)$$

and similarly for T_y and T_z.

$$L_T = L_{T_1} + L_{T_2} + \ldots\ldots\ldots\ldots\ldots + L_{T_n}$$

$$M_T = M_{T_1} + M_{T_2} + \ldots\ldots\ldots\ldots\ldots + M_{T_n} \qquad (4.10)$$

$$N_T = N_{T_1} + N_{T_2} + \ldots\ldots\ldots\ldots\ldots + N_{T_n}$$

The functional flow diagram to incorporate a multiple engine configuration into the Six-Degree-of-Freedom Flight-Path Study computer program is outlined in Figure (4.4). However, the present subprogram will be limited to accounting for single-engine, single-nozzle operation only. More than one engine can be accounted for if the combined effects can be grouped into a single "effective" engine. Reassembly of the program deck will be required for multiple engine arrangements.

4.2.3 <u>Error Constants</u> - The use of error constants, designated by the symbol ϵ_i, to modify the thrust and fuel flow characteristics is shown in Figures 4.3 and 4.4. A detailed explanation of these error constants and their use is given in Section 4.5.

4.3 <u>Physical Characteristics</u> - The methods to be employed for the introduction of vehicle physical characteristics into the Six-Degree-of-Freedom Flight-Path Study computer program are outlined in this section. A table look-up and interpolation technique is used to determine those parameters which are variable. A provision is made for the introduction of error constants into several of the parameters.

4.3.1 <u>Categories of Physical Characteristics</u> - Physical characteristics are introduced into the computer program in two groups: (a) characteristics used in the general solution of the equations of motion, and (b) characteristics used only in specific, or auxiliary, subprograms. The physical characteristics used in the auxiliary subprograms (e.g. nose radius, wedge angle, skin thickness, skin density, and thermal conductivity used in the aerodynamic heating subprogram, Section 7.) will be specified as input data along with the introduction of the specific subprogram. The following items will be defined in the general vehicle characteristics subprogram:

(a) Initial mass of the vehicle (m_o),

(b) Reference area (S),

(c) Reference lengths (d_1, d_2),

(d) Reference center-of-gravity location ($x_{C.G._{ref}}$),

(e) Rotating machinery pitch angle (θ_r),

TABULAR LISTING
$T_{4VAC} = f(t)$
$\dot{m}_{f_4} = f(t)$

DETERMINATION OF THRUST
$T_4 = \epsilon T_{4VAC} + \epsilon - PAe_4$

DETERMINATION OF ϕ_{T_4} & λ_{T_4}
$\phi_{T_4} = \phi_{TC_4} + \epsilon$
$\lambda_{T_4} = \lambda_{TC_4} + \epsilon$

RESOLUTION OF THRUST FORCE
$T_{x_4} = T_4 \cos \lambda_{T_4}$
$T_{y_4} = -T_4 \sin \lambda_{T_4} \cos \phi_{T_4}$
$T_{3_4} = -T_4 \sin \lambda_{T_4} \sin \phi_{T_4}$

DETERMINATION OF MOMENTS
$L_{T_4} = T_{3_4} y_{N_4} - T_{y_4} 3_{N_4}$
$M_{T_4} = T_{x_4} 3_{N_4} - T_{3_4}(x_{N_4} - \Delta x_{C.G.})$
$N_{T_4} = T_{y_4}(x_{N_4} - \Delta x_{C.G.}) - T_{x_4} y_{N_4}$

TABULAR LISTING
$T_{3VAC} = f(t)$
$\dot{m}_{f_3} = f(t)$

DETERMINATION OF THRUST
$T_3 = \epsilon T_{3VAC} + \epsilon - PAe_3$

DETERMINATION OF ϕ_{T_3} & λ_{T_3}
$\phi_{T_3} = \phi_{TC_3} + \epsilon$
$\lambda_{T_3} = \lambda_{TC_3} + \epsilon$

RESOLUTION OF THRUST FORCE
$T_{x_3} = T_3 \cos \lambda_{T_3}$
$T_{y_3} = -T_3 \sin \lambda_{T_3} \cos \phi_{T_3}$
$T_{3_3} = -T_3 \sin \lambda_{T_3} \sin \phi_{T_3}$

DETERMINATION OF MOMENTS
$L_{T_3} = T_{3_3} y_{N_3} - T_{y_3} 3_{N_3}$
$M_{T_3} = T_{x_3} 3_{N_3} - T_{3_3}(x_{N_3} - \Delta x_{C.G.})$
$N_{T_3} = T_{y_3}(x_{N_3} - \Delta x_{C.G.}) - T_{x_3} y_{N_3}$

TABULAR LISTING
$T_{2VAC} = f(t)$
$\dot{m}_{f_2} = f(t)$

DETERMINATION OF THRUST
$T_2 = \epsilon T_{2VAC} + \epsilon - PAe_2$

DETERMINATION OF ϕ_{T_2} & λ_{T_2}
$\phi_{T_2} = \phi_{TC_2} + \epsilon$
$\lambda_{T_2} = \lambda_{TC_2} + \epsilon$

RESOLUTION OF THRUST FORCE
$T_{x_2} = T_2 \cos \lambda_{T_2}$
$T_{y_2} = -T_2 \sin \lambda_{T_2} \cos \phi_{T_2}$
$T_{3_2} = -T_2 \sin \lambda_{T_2} \sin \phi_{T_2}$

DETERMINATION OF MOMENTS
$L_{T_2} = T_{3_2} y_{N_2} - T_{y_2} 3_{N_2}$
$M_{T_2} = T_{x_2} 3_{N_2} - T_{3_2}(x_{N_2} - \Delta x_{C.G.})$
$N_{T_2} = T_{y_2}(x_{N_2} - \Delta x_{C.G.}) - T_{x_2} y_{N_2}$

TABULAR LISTING
$T_{1VAC} = f(t)$
$\dot{m}_{f_1} = f(t)$

DETERMINATION OF THRUST
$T_1 = \epsilon T_{1VAC} + \epsilon - PAe_1$

DETERMINATION OF ϕ_{T_1} & λ_{T_1}
$\phi_{T_1} = \phi_{TC_1} + \epsilon$
$\lambda_{T_1} = \lambda_{TC_1} + \epsilon$

RESOLUTION OF THRUST FORCE
$T_{x_1} = T_1 \cos \lambda_{T_1}$
$T_{y_1} = -T_1 \sin \lambda_{T_1} \cos \phi_{T_1}$
$T_{3_1} = -T_1 \sin \lambda_{T_1} \sin \phi_{T_1}$

DETERMINATION OF MOMENTS
$L_{T_1} = T_{3_1} y_{N_1} - T_{y_1} 3_{N_1}$
$M_{T_1} = T_{x_1} 3_{N_1} - T_{3_1}(x_{N_1} - \Delta x_{C.G.})$
$N_{T_1} = T_{y_1}(x_{N_1} - \Delta x_{C.G.}) - T_{x_1} y_{N_1}$

DETERMINATION OF MASS
$m = m_0 + \epsilon + \int_{t_0}^{t}(\dot{m}_{f_1} + \dot{m}_{f_2} + \dot{m}_{f_3} + \dot{m}_{f_4})dt$

DETERMINATION OF THRUST FORCES
$T_x = T_{x_1} + T_{x_2} + T_{x_3} + T_{x_4}$
$T_y = T_{y_1} + T_{y_2} + T_{y_3} + T_{y_4}$
$T_3 = T_{3_1} + T_{3_2} + T_{3_3} + T_{3_4}$

DETERMINATION OF MOMENTS
$L_T = L_{T_1} + L_{T_2} + L_{T_3} + L_{T_4}$
$M_T = M_{T_1} + M_{T_2} + M_{T_3} + M_{T_4}$
$N_T = N_{T_1} + N_{T_2} + N_{T_3} + N_{T_4}$

CONTINUE PROBLEM

FIGURE 4.4, THRUST AND FUEL FLOW SUBPROGRAM (MULTI-ENGINE ROCKET, UNCONTROLLED THRUST)

(f) Rotating machinery angular rate (ω_r),

(g) Rotating machinery moments of inertia (I_{x_r}, I_{y_r}, I_{z_r}),

(h) Vehicle center-of-gravity location ($x_{C.G.}$),

(i) Vehicle moments of Inertia (I_{xx}, I_{yy}, I_{zz}, I_{xy}, I_{xz}, I_{yz}), and

(j) Reference jet-damping lengths (l_y, l_z, l_l, l_m, l_n).

Items (a) through (g) will be constant throughout any stage. Items (h) through (j) will be variable during the stage due to the variation in mass caused by fuel consumption. Figure 4.5 presents a functional flow diagram defining the manner in which these characteristics are introduced into the computer program.

4.3.2 <u>Reference Weight</u> - The instantaneous mass is used in the computation of the body motion. The reference weight is obtained by:

$$W_T = m \ (32.174) \tag{4.11}$$

4.3.3 <u>Error Constants</u> - The use of error constants, designated by the symbol ϵ_i, to modify the general vehicle physical characteristics is shown in Figure 4.5. A detailed explanation of these error constants and their use is given in Section 4.5.

4.4 <u>Stages and Staging</u> - A problem common to missile performance analyses, and encountered frequently in airplane performance work, is that of staging or the release of discrete masses from the continuing airframe. The effect of dropping a booster rocket or fuel tanks is often great enough to require that the complete set of aerodynamic data be changed. Stage changes at constant weight, such as extending drag brakes or turning on afterburners, may also require revising the aerodynamic or physical characteristics of the vehicle. Another use of the staging technique is possible with the present computer program which does not involve physical changes to the configuration; this technique may be used to revise the aerodynamic descriptors as a function of aerodynamic attitude or Mach number. With this use of the stage concept, accurate descriptions of the forces and moments acting upon vehicle may be maintained over wide attitude ranges if required. Other applications of this stage technique are possible. Normally it is not practical to stop the computer and manually insert a new set of data. A better approach is to have the computer do this automatically. The loading of new data will be done automatically by the computer on the basis of whether a specified variable has exceeded or become less than a pre-selected value. For generality, it is possible to test on four values in each direction.

When the new data are read in, the conditions representing the last time step will be read in as initial conditions for the next stage. This avoids the discontinuity that would result from an infinite rate of change of center-of-gravity location. It also will cause the integration routine to be started over which will reduce the computer-induced transients due to staging.

84

```
┌─────────────────────────────────────────────────────────────┐
│                      DATA CONSTANTS                          │
│                                                             │
│  m_o,  S,  d_1,  d_2,   θ_r,   ω_r,  I_xr,  I_yr,  I_zr,  X_C.G._Ref │
└─────────────────────────────────────────────────────────────┘
```

$$m_o, \; S, \; d_1, \; d_2, \; \theta_r, \; \omega_r, \; I_{xr}, \; I_{yr}, \; I_{zr}, \; X_{C.G._{Ref}}$$

TABULAR LISTING

$$X_{C.G.} = f(m) + \epsilon_{18} \qquad\qquad I_{xy} = f(m) + \epsilon_{22}$$

$$I_{xx} = f(m) + \epsilon_{19} \qquad\qquad I_{xz} = f(m) + \epsilon_{23}$$

$$I_{yy} = f(m) + \epsilon_{20} \qquad\qquad I_{yz} = f(m) + \epsilon_{24}$$

$$I_{zz} = f(m) + \epsilon_{21}$$

TABULAR LISTING

$$l_y = f(X_{C.G.}) \qquad l_1 = f(X_{C.G.})$$

$$l_z = f(X_{C.G.}) \qquad l_m = f(X_{C.G.})$$

$$l_n = f(X_{C.G.})$$

TABULAR LISTING

$$\dot{I}_{xx} = f(t_s) \qquad\qquad \dot{I}_{xy} = f(t_s)$$

$$\dot{I}_{yy} = f(t_s) \qquad\qquad \dot{I}_{xz} = f(t_s)$$

$$\dot{I}_{zz} = f(t_s) \qquad\qquad \dot{I}_{yz} = f(t_s)$$

$$\Delta X_{C.G.} = X_{C.G.} - X_{C.G._{Ref}}$$

CONTINUE PROBLEM
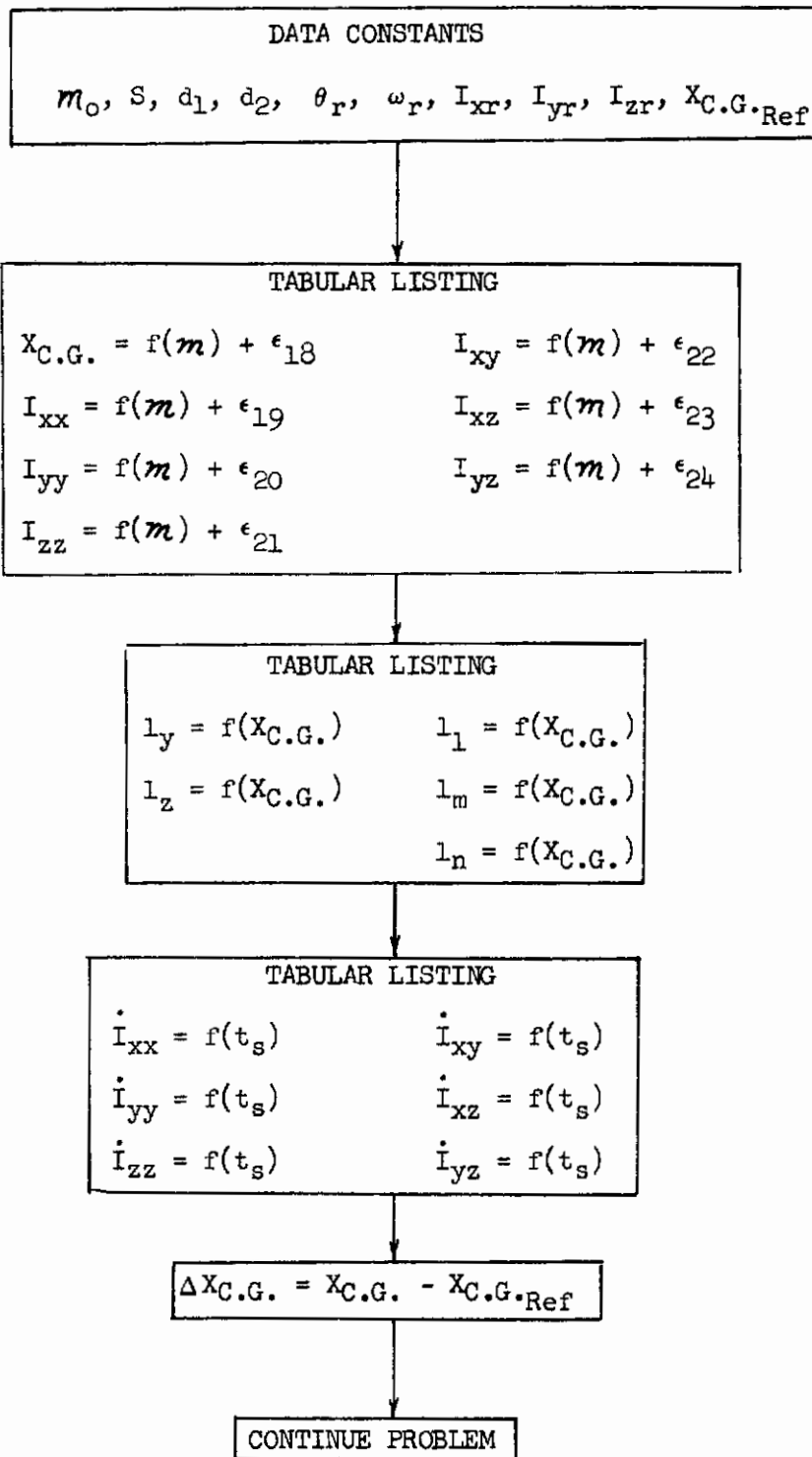
FIGURE 4.5   VEHICLE PHYSICAL CHARACTERISTICS SUBPROGRAM

85

4.5 <u>Error Analyses</u> - The Six-Degree-of-Freedom Flight-Path Study computer program will incorporate a provision for conveniently performing flight-path error and dispersion analyses by trajectory computation. This problem involves the determination of flight-path dispersion due to deviations of input quantities from their predicted nominal values. The usual approach to this type of problem requires that a series of trajectories be computed in which standard deviations, or errors, are systematically introduced for each parameter while the remaining parameters are held at their nominal values. These results are then combined to determine the" probable" dispersion. This approach will be implemented in the Six-Degree-of-Freedom Flight-Path Study computer program by providing a simple and efficient method of introducing the deviations. The capability of modifying a nominal value by either an error constant multiplier or an additive error constant is provided for many of the parameters as outlined below. The provision of these error constants will reduce substantially the number of tabular data listings that must be changed for an error analysis, thereby reducing the work of the analyst. The determination of the standard deviation of each of the parameters and the method of combining the trajectory variations are left to the analyst in view of multiplicity of combinations possible.

4.5.1 <u>Aerodynamic Data</u> - The provision to modify the aerodynamic coefficients through the use of error constants, ϵ_i, is outlined in Section 4.1. The constants are applied as follows:

$$n_F = (\epsilon_1 C_N + \epsilon_2) q^* S$$

$$a = (\epsilon_3 C_A + \epsilon_4) q^* S$$

$$y = (\epsilon_5 C_y + \epsilon_6) q^* S \tag{4.12}$$

$$l = (\epsilon_7 C_l + \epsilon_8) q^* S \ d_2$$

$$m = (\epsilon_9 C_m + \epsilon_{10}) q^* S \ d_1$$

$$n = (\epsilon_{11} C_n + \epsilon_{12}) q^* S \ d_2$$

These error constants allow the total aerodynamic coefficient to be modified to account for configuration modification, experimental or analytical error, or misalignments.

4.5.2 <u>Thrust and Fuel Flow Characteristics</u> - The provision to modify the thrust and mass characteristics, through the use of error constants, is outlined in Section 4.2. The constants are introduced as follows:

$$T = \epsilon_{13} T_{VAC} + \epsilon_{14} - PA_e$$

$$\mathcal{M} = \mathcal{M}_o + \epsilon_{15} + {}_{t_o}\int^t \dot{m}_f \ dt \tag{4.13}$$

An error-constant multiplier is not provided for the vehicle mass due to complications discussed in Paragraph 4.5.5.

4.5.3 <u>Vehicle Physical Characteristics</u> - The provision to modify some of the vehicle physical characteristics through the use of error constants is outlined in Section 4.3. The constants are applied as follows:

$$x_{C.G.} = f(m) + \epsilon_{18}$$

$$I_{xx} = f(m) + \epsilon_{19}$$

$$I_{yy} = f(m) + \epsilon_{20}$$

$$I_{zz} = f(m) + \epsilon_{21} \qquad (4.14)$$

$$I_{xy} = f(m) + \epsilon_{22}$$

$$I_{xz} = f(m) + \epsilon_{23}$$

$$I_{yz} = f(m) + \epsilon_{24}$$

4.5.4 <u>Autopilot Functions</u> - Error constants associated with an autopilot will necessarily be defined by the choice of autopilot. Section 6 presents a description of a typical control system which will be programmed for the Six-Degree-of-Freedom Flight-Path Study computer program. Although the constants are referred to as bias and drift constants, they are, in effect, error constants which serve to modify nominal values. These constants are applied in the following way:

<u>Bias on Control Surface Deflection and
Rate of Control Surface Deflection</u>

$$\dot{\delta}_n' = \dot{\delta}_n + B_{14_n}$$

$$\delta_n' = \int_o^t \dot{\delta}_n' \, dt + \delta_{n_o} \qquad (4.15)$$

<u>Bias and Drift on Attitude Sensors</u>

$$\Theta_{p'} = \Theta_p + B_{16} + B_{17}t$$

$$\Psi_{p'} = \Psi_p + B_{18} + B_{19}t \qquad (4.16)$$

$$\phi_{p'} = \phi_p + B_{12} + B_{13}t$$

<u>Bias on Rate Gyros</u>

$$p' = p + B_{20}$$

$$q' = q + B_{21} \qquad (4.17)$$

$$r' = r + B_{22}$$

87

In the application of error constants in the above equations, caution must be exercised to insure that the units are consistent. Each of the error constants will be assigned a nominal value which will be used when no other value is specified. The constants which are multipliers will have a nominal value of unity, while those that are additive will have a nominal value of zero.

4.5.5 <u>Additional Errors</u> - Not all of the system input constants can be modified for error analysis studies as indicated above. In certain cases, it may be found unrealistic to modify the input data through the use of error constants because the actual deviation would not appear as simply a constant increment or percentage change. An example of such a case would be the change in thrust-time history of a rocket due to temperature changes of the propellant since such a change affects both thrust level and burning time. For an accurate representation of such a case, it would be necessary to modify the entire tabular listing accordingly.

4.5.6 <u>Atmospheric Density Error</u> - An error constant has been incorporated in the computation of the atmospheric density in Option 6 only. The constants are applied as follows:

$$\rho' = \epsilon_{25}\rho + \epsilon_{26} \tag{4.18}$$

5. VEHICLE ENVIRONMENT

The models for simulating the environment in which a vehicle will operate are presented in this section. This environment includes the atmospheric wind, and the gravity field conditions associated with the planet over which the vehicle is moving. The shape of the planet and the conversion from geodetic to geocentric latitudes are also considered. In the discussions which follow, the descriptions of vehicle environment pertain to the planet Earth. The environmental simulation may be extended to any planet by replacing appropriate constants in the describing equations.

5.1 Atmospheres - The concept of a model atmosphere was introduced many years ago, and over the years several models have been developed. Reference (11) outlines the historical background of the gradual evolution of the ARDC model. The original (1956) ARDC model has been revised to reflect the density variation with altitude that was obtained from an analysis of artificial satellite orbit data. This revision is the 1959 ARDC Model Atmosphere.

The advantage of a model atmosphere is that it provides a common reference upon which performance calculations can be based. The model is not intended to be the "final word" on the properties of the atmosphere for a particular time and location. It must be realized that the properties of the atmosphere are quite variable and are affected by many parameters other than altitude. At the present time, the "state-of-the-art" is not advanced to the point where these parameters can be accounted for and it may be several years before the effects of some parameters can be evaluated.

5.1.1 1959 ARDC Model Atmosphere - The 1959 ARDC Model Atmosphere is specified in layers assuming either isothermal or linear temperature lapse-rate sections. This construction makes it very convenient to incorporate other atmospheres, either from specifications for design purposes or for other planets. The relations which mathematically specify the 1959 ARDC Model Atmosphere are as follows (Reference (12):

The 1959 ARDC Model Atmosphere is divided into 11 layers as noted in the table below.

Layer	H_b-Lower Altitude (Geopotential) Meters	Upper Altitude (Geopotential) Meters
1	0	11,000
2	11,000	25,000
3	25,000	47,000
4	47,000	53,000
5	53,000	79,000
6	79,000	90,000
7	90,000	105,000
8	105,000	160,000
9	160,000	170,000
10	170,000	200,000
11	200,000	700,000

For layers 1, 3, 5, 7, 8, 9, 10, and 11, a linear molecular-scale temperature lapse-rate is assumed and the following equations are used:

$$H_{gp} = \frac{.3048h}{1 + .3048h/6356766} \qquad \text{Meters} \qquad (5.1)$$

$$T_M = (T_M)_b \left[1 + K_1(H_{gp} - H_b) \right] \qquad {}^{\circ}R \qquad (5.2)$$

$$T = T_M \left[A - B \tan^{-1} \left(\frac{H_{gp} - C}{D} \right) \right] \qquad {}^{\circ}R \qquad (5.3)$$

$$P = P_b \left[1 + K_1(H_{gp} - H_b) \right]^{-K_2} \qquad \text{Lb./Ft.}^2 \qquad (5.4)$$

$$\rho = \rho_b \left[1 + K_1(H_{gp} - H_b) \right]^{-(1+K_2)} \qquad \text{Slugs/Ft.}^3 \qquad (5.5)$$

$$V_s = 49.020576(T_M)^{1/2} \qquad \text{Ft./Sec.} \qquad (5.6)$$

$$\nu = 0.0226988 \times 10^{-6} \left[\frac{T^{3/2}}{(T+198.72)\rho} \right] \qquad \text{Ft.}^2\text{/Sec.} \qquad (5.7)$$

For the isothermal layers 2, 4, and 6, the following changes are made in the above equations:

$$P = P_b e^{-K_3 (H_{gp} - H_b)} \qquad (5.8)$$

$$\rho = \rho_b e^{-K_3 (H_{gp} - H_b)} \qquad (5.9)$$

Values of the temperature, pressure, density, and altitude at the base of each altitude layer are listed below along with the appropriate values of K_1, K_2, and K_3.

Quantity	1	2	3	4	5	6
K_1	$-.225569^{-4}$	0	$.138466^{-4}$	0	$-.159202^{-4}$	0
K_2	-5.25612	-	11.3883	-	-7.59218	-
K_3	-	$.157689^{-3}$	-	$.120869^{-3}$	-	$.206234^{-3}$
T_b	518.688	389.988	389.988	508.788	508.788	298.188
P_b	2116.21695	472.73	51.979	2.5155	1.2181	2.1080^{-2}
ρ_b	2.37692^{-3}	7.0620^{-4}	7.7650^{-5}	2.8804^{-6}	1.39468^{-6}	4.1189^{-8}
H_b	0	11000.	25000.	47000.	53000.	79000.

Quantity	7	8	9	10	11
K_1	$.241458^{-4}$	$.886289^{-4}$	$.754341^{-5}$	$.350715^{-5}$	$.222129^{-5}$
K_2	8.54120	1.70824	3.41648	6.83296	9.76137
K_3	-	-	-	-	-
T_b	298.188	406.188	2386.188	2566.188	2836.188
P_b	2.1809^{-3}	1.5562^{-4}	7.5578^{-6}	5.8954^{-6}	2.9759^{-6}
ρ_b	4.261^{-9}	2.232^{-10}	1.845^{-12}	1.338^{-12}	6.113^{-13}
H_b	90000.	105000.	160000.	170000.	200000.

Values of the appropriate constants to be applied in the temperature equation (Equation (5.3)) are listed below.

H_{gp}(Km)	A	B	C	D
0-90	1.	0.	-	-
90-180	.759511	.174164	220	25
180-1200	.935787	.273966	180	140

5.1.2 <u>Limitations</u> - The validity of the 1959 ARDC model is limited to altitudes below 700 km., although the program is arranged to extrapolate the relationships to greater altitudes if desired. Extrapolation to greater altitudes is accomplished by altering the cutoff altitude.

At an altitude of 90 km (approximately 300,000 ft.) the subprogram normally ceases to calculate kinematic viscosity and speed of sound and assigns a value of zero to each of these parameters as an indication that the computation has stopped. This is done for the following reasons: (a) the molecular composition of the atmosphere is unknown, (b) the variation of the ratio of specific heats above 90 km. is not known, and (c) the numerical value of the speed of sound has little physical significance. The validity of Sutherland's empirical formula for viscosity is also reduced because of the extremely low pressures which exist.

5.1.3 <u>Accuracy</u> - Due to a lack of knowledge of the rounding-off procedures used to evaluate the constants in Reference (11), it was impossible to obtain exact agreement between the subprogram and the values tabulated in Reference (11). A comparison of the results over an altitude range of 0 - 1,000,000 ft. revealed that the deviation of the computed from the reference values never exceeded one tenth of one percent and in most cases was less than one half of this value.

5.2 <u>Winds Aloft</u> - The winds-aloft subprogram provides for three separate methods of introducing the wind vector - as a function of altitude, a function of range, and a function of time. This will facilitate the investigation of wind effects for the conventional performance studies. The wind vector will be approximated by a series of straight line segments for each of the methods mentioned above. Statistically derived profiles of the type presented in Reference (13) can be represented by this approach and it is presumed that the analyst will resort to sources of this type to obtain the wind input data. The present subprogram will not be particularly concerned with the method used to determine the wind vector, as this is a separate problem outside the scope of the Six-Degree-of-Freedom Flight-Path Study computer program.

Four options will be used to define the wind vector in the SDF computer program. The three components of the wind vector in a geodetic horizon coordinate system will be specified as tabular listings with linear interpolations (curve reads) in the following options.

<u>Wind Option (0)</u> - In this option the wind vector is zero throughout the problem. This will allow the analyst the option of evaluating performance without the effects of wind. This option causes the winds-aloft subprogram to be bypassed in the computational sequence.

<u>Wind Option (1)</u> - In this option the components of the wind vector will be specified as a function of time for the estimated cruise altitude. Wind speed will be specified in feet per second and time will be specified in seconds.

<u>Wind Option (2)</u> - The three components of the wind vector will be introduced as a function of altitude in this option. Wind speed will be specified in feet per second and altitude will be specified in feet.

<u>Wind Option (3)</u> - In this option the components of the wind vector will be introduced as a function of range for the estimated cruise altitude. Wind speed will be specified in feet per second and range will be specified in nautical miles. The range utilized in this computation will be the great-circle range.

By staging of the wind option, it will be possible to switch from one method of reading wind data to another during the computer run. Care must be exercised in this operation, however, as the switching will introduce sharp-edged gusts if there are sizeable differences in the wind vector from one option to another at the time of switching. This effect should be avoided except in cases where gust effects are being studied.

Figure (5.1) presents a functional flow diagram of the winds-aloft subprogram. Note that the inertial components of the wind are not determined in this subprogram. This wind, which is due to the rotation of the atmosphere with the planet, is determined in the winds-aloft resolution. Only local-geocentric components of wind, as noted by an observer at a fixed location, are considered by the winds-aloft subprogram.
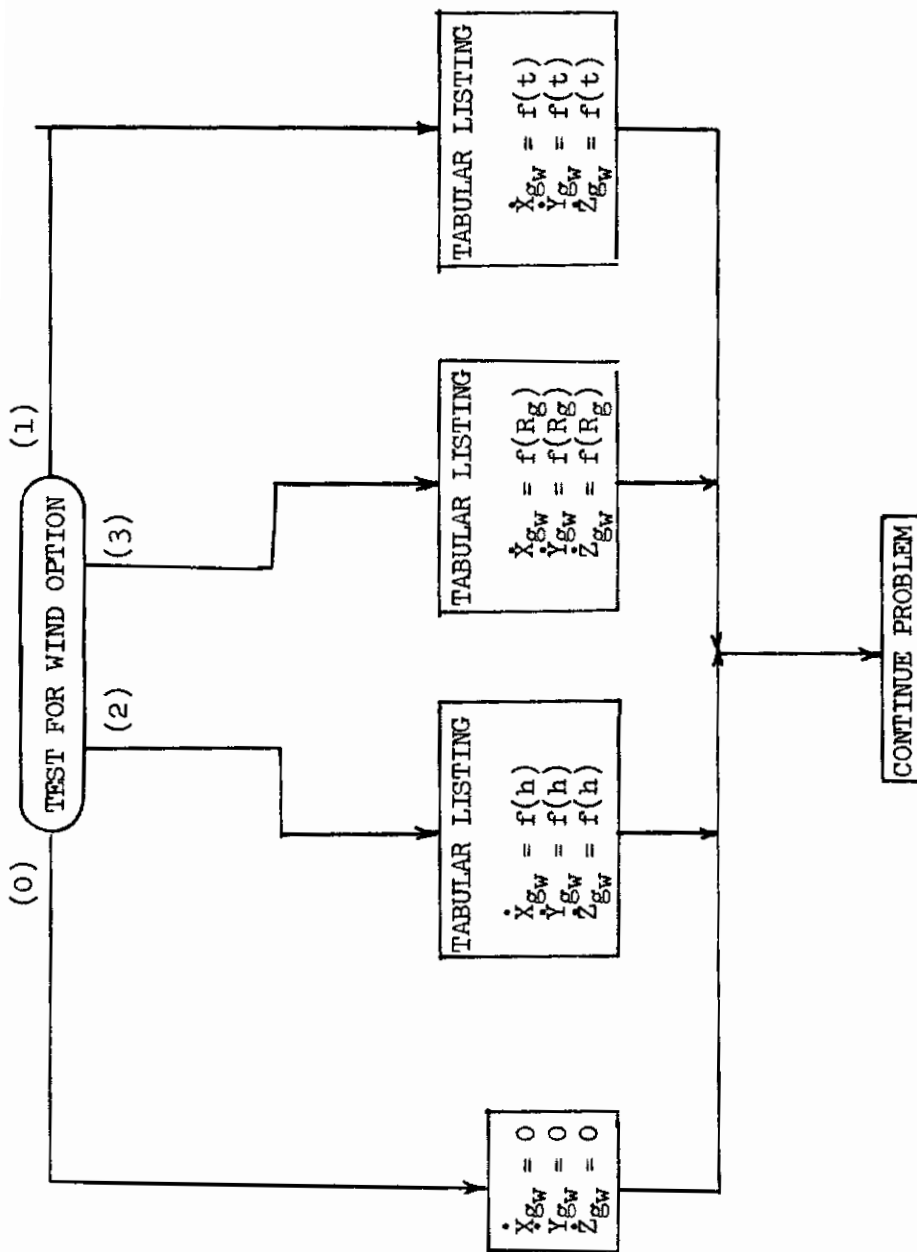
Figure 5.1 Functional Flow Diagram - Winds-Aloft Subprogram

Wind effects will be included in the formulation of the six-degree-of-freedom, the three-degree-of-freedom longitudinal, and the three-degree-of-freedom lateral options. The reduced degrees of freedom of the latter two options will allow the deletion of unnecessary components of the wind vector. Since wind effects are not normally of interest in the point-mass option, the winds-aloft subprogram will be bypassed automatically when this option is selected.

5.3 <u>Gravity</u> - This section presents the equations necessary for the introduction of the gravity components into the equations of motion. These components were determined by taking partial derivatives of the gravity potential equation. The potential equation adopted has been recommended for use in the Six-Degree-of-Freedom Flight-Path Study computer program by AFCRC. Constants for the potential equation were determined from References (14), (15) and (16).

Spherical harmonics are normally used to define the gravity potential field of the Earth, References (17) through (20). Each harmonic term in the potential is due to a deviation of the potential from that of a uniform sphere. In the present analysis the second-, third-, and fourth-order terms are considered. The first-order term, which would account for the error introduced by assuming that the mass center of the Earth is at the origin of the geocentric coordinate system, is assumed to be zero. With this assumption

$$U = \frac{\mu}{R}\left[1 + \frac{J}{3}\left(\frac{R_e}{R}\right)^2 P_2 + \frac{H}{5}\left(\frac{R_e}{R}\right)^3 P_3 + \frac{K}{30}\left(\frac{R_e}{R}\right)^4 P_4 + \dots\right] \quad (5.10)$$

where P_2, P_3, and P_4 are Legendre functions of geocentric latitude ϕ_L expressed as

$$
\begin{aligned}
P_2 &= 1 - 3\sin^2\phi_L \\[6pt]
P_3 &= 3\sin\phi_L - 5\sin^3\phi_L \\[6pt]
P_4 &= 3 - 30\sin^2\phi_L + 35\sin^4\phi_L
\end{aligned}
\quad (5.11)
$$

The gravitational acceleration along any line is the partial derivative of U along that line. At this point, it should be noted that the three mutually perpendicular directions in the spherical coordinate system are identical (other than sign) to those in the local-geocentric-horizon coordinate system which is defined in Section 3.1.5. Therefore, the acceleration in the ϕ_L direction is identical to g_{X_g} and the acceleration in the R direction is identical to $-g_{Z_g}$. Or in the equation form:

$$
g_{Z_g} = -\frac{\partial U}{\partial R} = -\frac{\mu}{R}\left[-\frac{2J}{3}\left(\frac{R_e^2}{R^3}\right) P_2 - \frac{3H}{5}\left(\frac{R_e^3}{R^4}\right) P_3 - \frac{4K}{30}\left(\frac{R_e^4}{R^5}\right) P_4\right] \\
+ \frac{\mu}{R^2}\left[1 + \frac{J}{3}\left(\frac{R_e}{R}\right)^2 P_2 + \frac{H}{5}\left(\frac{R_e}{R}\right)^3 P_3 + \frac{K}{30}\left(\frac{R_e}{R}\right)^4 P_4\right]
\quad (5.12)
$$

$$gX_g = \frac{1}{R}\frac{\partial U}{\partial \phi_L} = \frac{\mu}{R^2}\left[\frac{J}{3}\left(\frac{R_e}{R}\right)^2 (-6 \sin \phi_L \cos \phi_L) \right.$$

$$+ \frac{H}{5}\left(\frac{R_e}{R}\right)^3 (3 \cos \phi_L - 15 \sin^2 \phi_L \cos \phi_L)$$

$$\left. + \frac{K}{30}\left(\frac{R_e}{R}\right)^4 (-60 \sin \phi_L \cos \phi_L + 140 \sin^3 \phi_L \cos \phi_L) \right] \qquad (5.13)$$

Collecting terms:

$$gZ_g = \frac{\mu}{R^2}\left[1 + J\left(\frac{R_e}{R}\right)^2 P_2 + \frac{4H}{5}\left(\frac{R_e}{R}\right)^3 P_3 + \frac{K}{6}\left(\frac{R_e}{R}\right)^4 P_4 \right] \qquad (5.14)$$

$$gX_g = \frac{\mu}{R^2}\left[-2J\left(\frac{R_e}{R}\right)^2 P_5 + \frac{3H}{5}\left(\frac{R_e}{R}\right)^3 P_6 + \frac{2K}{3}\left(\frac{R_e}{R}\right)^4 P_7 \right] \qquad (5.15)$$

where

$$P_5 = \sin \phi_L \cos \phi_L$$

$$P_6 = \cos \phi_L (1 - 5 \sin^2 \phi_L) \qquad (5.16)$$

$$P_7 = \sin \phi_L \cos \phi_L (-3 + 7 \sin^2 \phi_L)$$

Equations (5.14) and (5.15) are used in the gravity subroutine with the following values recommended for the constants.

$$\mu = 1.407698 \times 10^{16} \text{ ft.}^3/\text{sec.}^2$$

$$R_e = 20,925,631. \text{ ft.}$$

$$J = 1623.41 \times 10^{-6}$$

$$H = 6.04 \times 10^{-6}$$

$$K = 6.37 \times 10^{-6}$$

It should be noted that these constants and equations pertain to the planet Earth; however, it is possible to use these same equations for any other planet. For this reason, the values of these constants will be programmed as an input to the program so that the applicable constants may be inserted for the planet under consideration. Due to limited knowledge of the gravitational fields of other planets, it is probable that zero values would be assigned to some of the harmonic coefficients when the program is used for entry studies on other planets.

The above equations are applicable to a non-rotating planet as the centrifugal relieving effects caused by the planet's rotation are included in the equations of motion. In addition, the effects of local anomalies must be added if it is desired to make a weight-to-mass conversion based on a measured weight.

95

5.4 <u>Local-Geocentric to Geodetic Coordinates</u> - Positions on the planet
are specified in terms of geodetic latitude and altitude (for a given longitude)
while the motion of the body is computed in a planetocentric system which is
independent of the surface. In the central program, the flight-path angle γ
and the heading angle σ are calculated with respect to the local-geocentric
coordinates. By definition γ and σ are angles measured with respect to the
local geodetic. Although the maximum difference that can exist between the
two coordinate system is 11 minutes of arc, it may be desirable to know γ and
σ more accurately than is obtained when measured from the local geocentric.

5.4.1 <u>Latitude</u> - It will be necessary to resolve the geocentric latitude
to geodetic latitude for an accurate determination of position. Figure (5.2)
presents the geometry required for describing the position of a point in a
meridian plane of an oblate spheroid.

Figure 5.2 Planet-Oblateness Effect on Latitude and Altitude

It is apparent from this figure that the most significant difference between the
geocentric referenced position and the geodetic position is the distance $\overline{AB}$
on the surface of the reference spheroid. This distance can be defined by a
knowledge of the angle ϕ_L, the geocentric <u>latitude</u>; ϕ_g, the geodetic latitude;
the corresponding radii; and the distance $\overline{OC}$.

The relationship between the geocentric and geodetic latitude of a point on
the surface of a planet which is an oblate spheroid is obtained as follows:
The equation for the surface in a meridian plane is

$$\frac{X^2}{R_e^2} + \frac{Z^2}{R_p^2} = 1 \tag{5.17}$$

96

The tangent of the geodetic latitude can be found by determining the negative reciprocal of the slope of a tangent to this ellipse. The expression for this tangent is

$$\text{Tan } \phi_g = -\frac{1}{\left.\dfrac{d(-Z)}{dX}\right|_B} = -\frac{R_e^2 \, Z_B}{R_p^2 \, X_B} \qquad (5.18)$$

Note that Z_B is a negative number in the northern hemisphere.

The tangent of the geocentric latitude of point B is

$$\text{Tan } \phi_{Lg} = -\frac{Z_B}{X_B} \qquad (5.19)$$

Substituting Equation (5.19) into Equation (5.18) gives the required relation

$$\text{Tan } \phi_g = \frac{R_e^2}{R_p^2} \text{ Tan } \phi_{Lg} \qquad (5.20)$$

The expression for the radius of the planet at point B in terms of the geocentric latitude of the point and the equatorial and polar radii is obtained by the rectangular to polar coordinate transformation

$$-Z_B = R\phi_{Lg} \text{ Sin } \phi_{Lg} \qquad (5.21)$$

$$X_B = R\phi_{Lg} \text{ Cos } \phi_{Lg} \qquad (5.22)$$

and, solving for $R\phi_{Lg}$ by substituting Equations (5.21) and (5.22) into Equation (5.17), gives

$$R\phi_{Lg} = \sqrt{\frac{R_e \, R_p}{R_p^2 \, \text{Sin}^2 \, \phi_{Lg} + R_e^2 \, \text{Cos}^2 \, \phi_{Lg}}} \qquad (5.23)$$

The distance $R\phi_g$ is determined in terms of $R\phi_{Lg}$, ϕ_{Lg}, and ϕ_g using the law of sines to be

$$R\phi_g = R\phi_{Lg} \left(\frac{\text{Sin } \phi_{Lg}}{\text{Sin } \phi_g}\right) \qquad (5.24)$$

The distance $\overline{OC}$ is calculated by subtracting the projections on the X-axis of $R\phi_{Lg}$ and $R\phi_g$.

$$\overline{OC} = R\phi_{Lg} \text{ Cos } \phi_{Lg} - R\phi_g \text{ Cos } \phi_g \qquad (5.25)$$

The point P represents the vehicle position for which it is desired to determine the geodetic latitude, knowing the geocentric latitude and distance from the center of the planet. Expressing the Cartesian coordinates of the vehicle in

97

terms of the geodetic latitude, altitude (h), and the characteristic dimensions $R\phi_g$ and $\overline{OC}$ defines the required relation between the geocentric latitude and geodetic latitude to be

$$\text{Tan } \phi_L = \frac{-Z_p}{X_p} = \frac{(R\phi_g + h) \text{ Sin } \phi_g}{(R\phi_g + h) \text{ Cos } \phi_g + \overline{OC}}$$

or

$$\text{Tan } \phi_L = \frac{(R\phi_g + h) \text{ Sin } \phi_g}{h \text{ Cos } \phi_g + R\phi_{Lg} \text{ Cos } \phi_{Lg}} \tag{5.26}$$

This equation, being transcendental, is inconvenient for the solution of geodetic latitude when the geocentric latitude is known. Although solution is possible, the complication involved would be uneconomical in view of the fact that the calculation is a small correction to the working coordinate, the geocentric latitude. The solution is relatively simple when the geodetic is taken as the independent variable. The results of such a computation are presented in Figure (5.3) for the planet Earth where the maximum difference between the two latitudes is shown to be on the order of 11 minutes of arc at the surface of the spheroid at 45 degrees latitude. This amounts to approximately 11 nautical miles error which should be accounted for. The results of Figure (5.3) have been approximated by a curve fit of the form

$$\phi_g - \phi_L = \Delta\phi = (k_0 + k_1 h^* + k_2 h^{*2} + k_3 h^{*3}) \text{ Sin } 2\phi_L \tag{5.27}$$

where $\qquad h^* = \dfrac{h'}{1,000,000}$

and

k_0	=	11.591437	Sec.	or k_0	=	.1931906	Deg.
k_1	=	-.54061508	Sec./Ft.	k_1	=	-.009010251	Deg./Ft.
k_2	=	.020308362	Sec./Ft.^{2}	k_2	=	.000338472	Deg./Ft.^{2}
k_3	=	-.0003723074	Sec./Ft.^{3}	k_3	=	-.00000621179	Deg./Ft.^{3}

The error incurred by the use of Equation (5.27) instead of the exact solution of Equation (5.26) is shown by the symbols in Figure (5.3). (The maximum error is on the order of .004 minute.) The solution has been extended to 20,000,000 feet altitude, or approximately one Earth's radius. This altitude is sufficient for the problems to be considered by the SDF computer program for the planet Earth. Greater altitudes than this must consider such other effects as solar radiation pressures, planetary perturbations, and the effects of the orbital properties of the planet and may, therefore, be handled by other programs such as an interplanetary trajectory program discussed in Section 8.
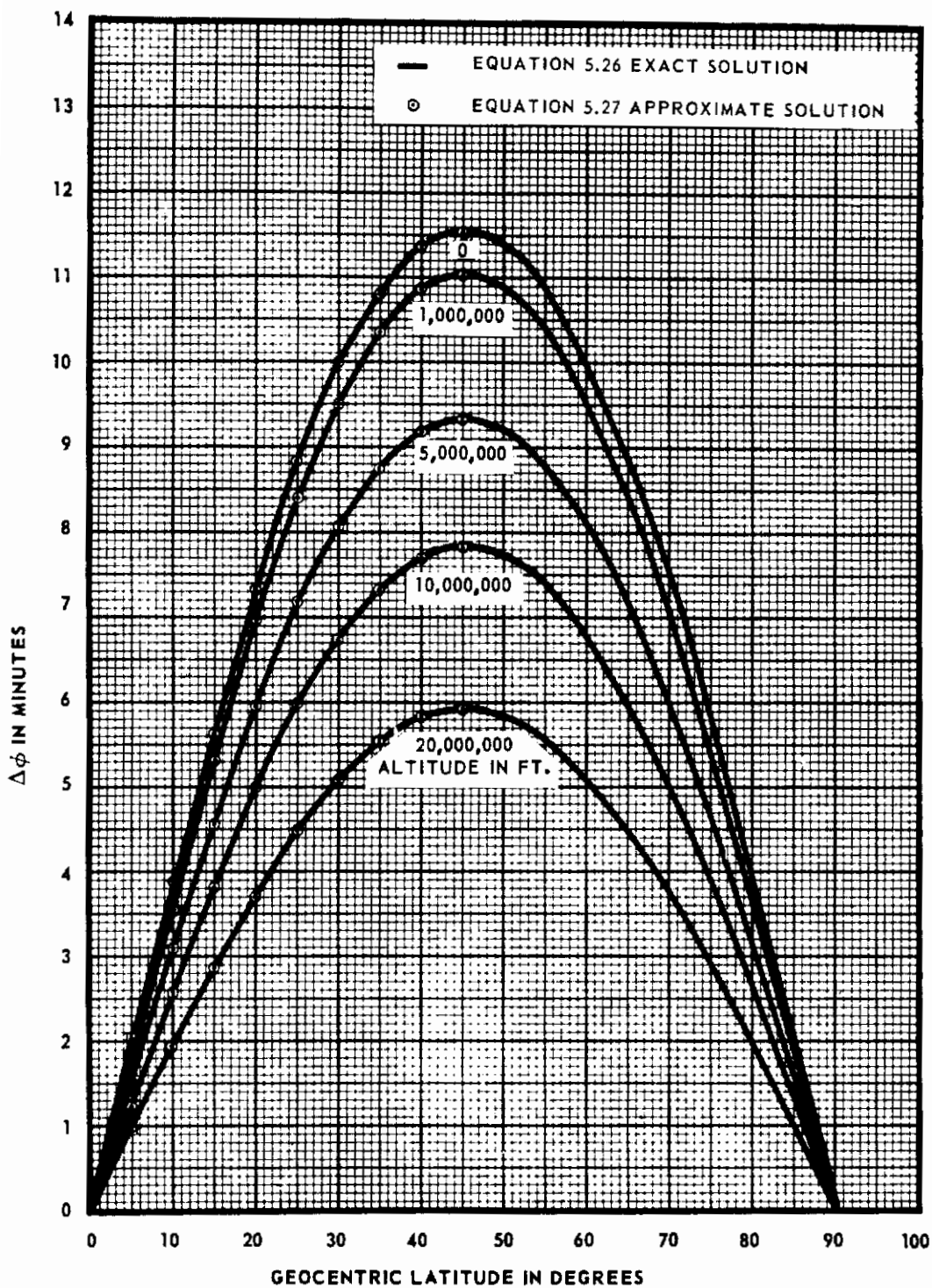
FIGURE 5.3, DIFFERENCE BETWEEN GEODETIC AND GEOCENTRIC LATITUDES
AS A FUNCTION OF GEOCENTRIC LATITUDE AND ALTITUDE

99

5.4.2 <u>Flight-Path Angles</u> - Knowing geodetic latitude for any geocentric latitude and local-geocentric components of velocity it is possible to get the components of velocity in local-geodetic coordinates X_{g_1}, Y_{g_1}, and Z_{g_1}, (See Figure (5.4).)
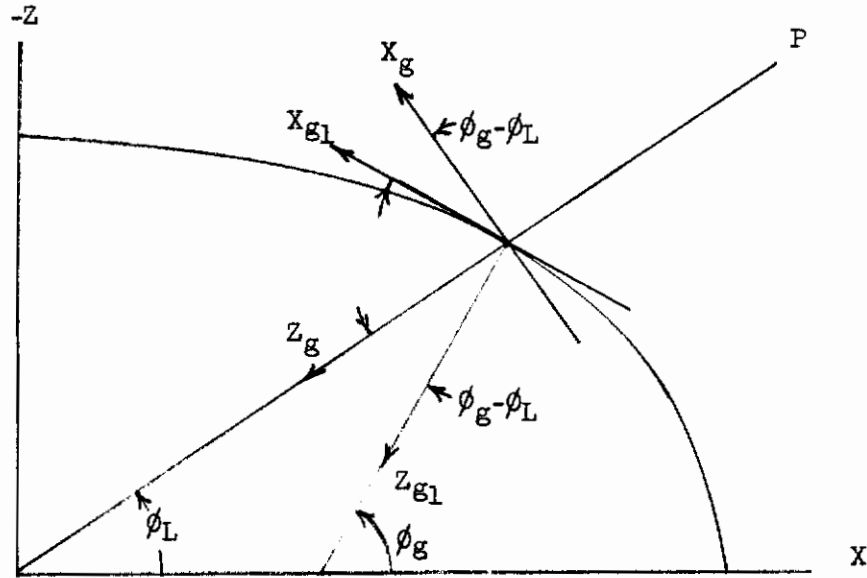
Figure 5.4 Relation of Geodetic and Geocentric Horizons

The transformation is given by:

$$
\begin{vmatrix} \dot{X}_{g_1} \\ \dot{Y}_{g_1} \\ \dot{Z}_{g_1} \end{vmatrix}
=
\begin{vmatrix} \cos(\phi_g - \phi_L) & 0 & \sin(\phi_g - \phi_L) \\ 0 & 1 & 0 \\ -\sin(\phi_g - \phi_L) & 0 & \cos(\phi_g - \phi_L) \end{vmatrix}
\begin{vmatrix} \dot{X}_g \\ \dot{Y}_g \\ \dot{Z}_g \end{vmatrix}
\tag{5.28}
$$

As noted above, the maximum difference between the geodetic latitude and the geocentric latitude is 11 minutes of arc, which occurs at 45 degrees geodetic latitude. The small-angle approximation is valid and

$$\text{Sin} (\phi_g - \phi_L) = \phi_g - \phi_L \text{ in radians} \tag{5.29}$$

$$\text{Cos} (\phi_g - \phi_L) = 1 \tag{5.30}$$

100

and substituting Equations (5.29) and (5.30) into matrix (5.28) gives:

$$
\begin{vmatrix} \dot{X}_{g1} \\ \dot{Y}_{g1} \\ \dot{Z}_{g1} \end{vmatrix} = \begin{vmatrix} 1 & 0 & (\phi_g - \phi_L)\text{rad.} \\ 0 & 1 & 0 \\ -(\phi_g - \phi_L)\text{rad.} & 0 & 1 \end{vmatrix} \begin{vmatrix} \dot{X}_g \\ \dot{Y}_g \\ \dot{Z}_g \end{vmatrix}
\tag{5.31}
$$

The flight-path angle and heading angle corrected to the local-geodetic latitude are computed by

$$
\gamma_D = \text{Sin}^{-1}\left(\frac{-\dot{Z}_{g1}}{V_{g1}}\right) = \text{Sin}^{-1}\left(\frac{-\{\dot{Z}_g - \dot{X}_g(\phi_g - \phi_L)\text{ rad.}\}}{V_g}\right)
\tag{5.32}
$$

since the magnitude of vector V_g, is equal to the magnitude of vector V_{g1}.

and

$$
\sigma_D = \text{Sin}^{-1}\left(\frac{\dot{Y}_g}{\sqrt{\dot{X}_{g1}{}^2 + \dot{Y}_{g1}{}^2}}\right) = \text{Sin}^{-1}\left(\frac{\dot{Y}_g}{\sqrt{\{\dot{X}_g + \dot{Z}_g(\phi_g-\phi_L)\text{rad.}\}^2 + \dot{Y}_g{}^2}}\right)
\tag{5.33}
$$

The angles γ and σ may be computed in local-geocentric coordinates by Equations (3.69 and 3.70).

$$
\gamma = \text{Sin}^{-1}\left(\frac{-\dot{Z}_g}{V_g}\right)
$$

and

$$
\sigma = \text{Sin}^{-1}\left(\frac{\dot{Y}_g}{\sqrt{\dot{X}_g{}^2 + \dot{Y}_g{}^2}}\right)
$$

or by setting $(\phi_g - \phi_L)$ equal to zero in Equations (5.32) and (5.33).

5.4.3 Geodetic Altitude - The geodetic, or true altitude (h), will be approximated by the altitude (h') by the relation (reference Figure (5.2)).

$$
h \cong h' = R - R\phi_L
\tag{5.34}
$$

The error incurred by this approximation has been investigated and determined to be of the order of $1 - \cos \epsilon_g$. Numerical evaluation of the error using the relations of Equation (5.34) and the exact solution is summarized below.

True Altitude (h) in feet	Error (h' - h) to the nearest foot
50,000	1
100,000	1
150,000	1
200,000	3
250,000	3
500,000	4
1,000,000	6
2,000,000	11
3,000,000	16
4,000,000	20
5,000,000	24
10,000,000	39
20,000,000	59

6. AUTOPILOTS AND FLIGHT-PLAN PROGRAMMERS

The autopilot and flight-plan programmer are mechanisms by which the vehicle motion or trajectory are regulated or controlled. For use in the SDF computer program, an autopilot is defined as that portion of the program which determines the vehicle control-surface or thrust vector deflections. This definition applies for computation options which permit any combination of the rotational degrees of freedom. This portion of the program may range in sophistication from simple curve-read functions of control surface deflection with time to a linear-differential-equations simulation of a multiloop autopilot containing corrective networks, servo systems, gyros, etc. which is commanded by steering equations developed from an inertial navigation system. A flight-plan programmer is a device, similar in operation to an autopilot but restricted to computation options which exclude the rotational degrees of freedom. This is done because, for the most part, flight-plan programmers arbitrarily assign rotational attitude.

6.1 <u>Typical Autopilot</u> - Since the autopilot for a particular vehicle is a highly specialized device, formulation of a library of autopilot subprograms will not be attempted. Rather, a typical vehicle autopilot is treated in the following section which employs most of the elements normally used in this device. This autopilot is considered as an example formulation to demonstrate the techniques required in the digital simulation of autopilot networks in general.

6.1.1 <u>Description of Flight Control System</u> - The flight-control system (See Figure (6.1)) to be programmed for the SDF computer program has three control channels: pitch attitude, azimuth attitude, and roll rate. The pitch and azimuth attitude control channels each contain inner and outer feedback loops. The inner attitude rate loop is used to improve the damping characteristics of the missile and to provide dynamic stability. The body angular rates, q and r, are sensed by body-mounted rate gyros and are roll resolved to obtain the pitch and azimuth attitude rates required in the inner feedback loops of the pitch and azimuth control channels respectively. During a certain portion of the flight, the inner feedback loop signal is obtained by resolving the sum of corresponding components of the acceleration and angular velocity measured by the rate gyros and body-mounted accelerometers. The forward portion of each inner loop contains a lag (or lead, depending on the constants used) network to improve dynamic stability and a notch filter to attenuate the aeroelastic oscillations sensed by the rate gyros. The outer feedback signals of both the azimuth and pitch control channels are the attitudes obtained from a servo repeater driven by the platform gimbals. The yaw-and pitch-attitude commands are summed with the appropriate repeater output. The resultant error signal is multiplied by a constant gain to provide the inner-loop rate command. The total pitch-attitude command is the sum of a predetermined attitude program and the output of a pressure control loop. The pressure control loop generates a pitch attitude error signal proportional to the difference in the stagnation-pressure command and the measured stagnation pressure. The effects of temperature limiting may be incorporated in a manner analogous to the pressure control loop. A temperature control loop has been devised which will determine the change in pitch and/or azimuth attitude required to avoid a critical heating condition. The computation of this command modification is discussed in Section 6.3.

FIGURE 6.1, CONTROL SYSTEM FUNCTIONAL BLOCK DIAGRAM

The roll-control channel consists of a feedback from a body-mounted roll-rate gyro which is summed with the roll-rate command. The resultant error signal is passed through a network which improves the loop transient response and from thence to the control surfaces. There are four independently actuated control surfaces mounted 90° apart. The roll-resolved outputs of the pitch and azimuth channels are presented to the appropriate pair of diametrically opposed control surfaces. The output of the roll-control channel is to each of the four control surfaces. Opposing control surfaces move as a unit for pitch and azimuth control and differentially for roll control.

6.1.2 <u>Control System Input Data Simulations</u> - The flight data measured by the gyros, repeaters, and accelerometers must be calculated or obtained from other sections of the program. The functional block diagram (Figure (6.1)) illustrates the sources of input data for the control system computer simulation. The steering functions provide the steering signals (commands) for the control system. For this particular application, the commands are determined from several two-dimensional curve read-out subroutines where time is the independent variable. The steering functions must also specify the changes in computations corresponding to the position of the switches A-B-C-D. These switches are used to modify the control system for various phases of the flight, and the position of the switches is dependent on a time reference.

The platform portion of the fixed program computes the missile attitude angles (Section 3.2) in a coordinate system representing a stable platform. The platform gimbals for this application are arranged in the yaw-pitch-roll sequence and the platform will be aligned initially with the local geodetic vertical. The platform will be inertially fixed in its orientation at the time of launch. (See Section 3.2 for the coordinate transformations.)

The rigid-body angular rates, p-q-r, that would be measured by the body-mounted rate gyros, are calculated in the equations of motion. If the effect of aeroelasticity on the control system is to be investigated, the appropriate normalized bending modes, damping ratios, and natural frequencies must be supplied to the aeroelastic computational block which in turn computes the aeroelastic body-bending angular rates, r_A and q_A. These aeroelastic body rates will then be summed with the appropriate angular rates from the rigid-body equations of motion to provide the rate gyro signals. Appendix Six presents a method by which the aeroelastic body-bending rates may be simulated by a second-order differential equation.

The indication of two body-mounted accelerometers whose sensitive axes are aligned with the body y- and z-axes must also be determined for this program. These accelerations may be taken directly from the summation of the forces and moments subprogram.

6.1.3 <u>Pitch Control Channel</u> - A stagnation-pressure command generated in the steering functions tabulation will be compared with the pressure behind a normal shock wave (P_{2_T}), and the difference multiplied by the gain factor K_A. The gain, K_A, is a predetermined function of time and is obtained from a curve-read subroutine. Thus,

$$(P_{2_{T_c}} - P_{2_T})\, K_A \;=\; E_1 \tag{6.1}$$

105

The total pressure behind a normal shock may be approximated by the relation

$$P_{2_T} = (.455 + 1.29 M_N^2) P \tag{6.2}$$

The error signal, E_1, is modified by a compensation network whose transfer function is:

$$\frac{\tau_1 S + 1}{(\tau_2 S + 1)(\tau_3 S + 1)} = \frac{\Theta_r}{E_1} \tag{6.3}$$

This transfer function is converted to differential equation form by the method outlined in Appendix Five; Transfer Function Number (3) of Table 5.1. The solutions of the following first-order differential equations for Θ_{r_1} and Θ_{r_2} are required for the digital simulation of the pressure loop compensation network.

$$\dot{\Theta}_{r_1} \tau_2 + \Theta_{r_1} = E_1$$
$$\dot{\Theta}_{r_2} \tau_3 + \Theta_{r_2} = E_1 \tag{6.4}$$

The output of the compensation network is calculated by summing functions of Θ_{r_1} and Θ_{r_2}

$$\Theta_r = \left[\frac{\tau_2 - \tau_1}{\tau_2 - \tau_3} \right] \Theta_{r_1} + \left[\frac{\tau_3 - \tau_1}{\tau_3 - \tau_2} \right] \Theta_{r_2} \tag{6.5}$$

The pitch attitude of the vehicle, (Θ_p) with respect to platform coordinates, is obtained from the platform subprogram. It may be desirable to investigate the effect of drift on the attitude sensors. This drift may be simulated by adding $B_{16} + B_{17}t$ to the pitch attitude, Θ_p, calculated in the platform subprogram

$$\Theta_p' = \Theta_p + B_{16} + B_{17}t \tag{6.6}$$

A pitch repeater is used to develop an electrical signal proportional to the angular displacement of the pertinent gimbals. The transfer function representing this repeater is a second-order system; the repeater output may be obtained by solving the following differential equation, Transfer Function Number (1) of Table 5.1.

$$\frac{\ddot{\Theta}_m}{\omega_1^2} + \frac{2\zeta_1 \dot{\Theta}_m}{\omega_1} + \Theta_m = \Theta_p' \tag{6.7}$$

The pitch-attitude command generated by the steering functions is summed with $-\Theta_r$, $-\Theta_m$, and Θ_T (Θ_T is a temperature limiting attitude command, see Section 6.3) and the sum is multiplied by a constant gain K_B. For switch D in the closed position

$$(\Theta_c' + \Theta_T - \Theta_r - \Theta_m)K_B = E_2 \tag{6.8}$$

If pressure control is not required during a part of the flight, switch D is opened for that portion of the flight. For switch D open, the summation of Equation (6.7) reduces to:

$$(\Theta_c' + \Theta_T - \Theta_m)K_B = E_2 \tag{6.9}$$

The limiter may be represented by a simple logic element. If L_1 is the limiting value, the logical questions are:

$$\text{If} \quad |E_2| < |L_1| \qquad \text{Then} \quad \dot{\Theta}_c = E_2$$
$$\text{If} \quad |E_2| > |L_1| \qquad \text{Then} \quad \dot{\Theta}_c = L_1 \tag{6.10}$$

where the sign of limit must correspond to the sign of $\dot{\Theta}_c$.

The error signal E_3 depends upon the position of the switch A. If switch A is closed,

$$(\dot{\Theta}_c - \dot{\Theta}_H)K_c = E_3 \tag{6.11}$$

and if switch A is open, the signal E_3 is simply

$$-\dot{\Theta}_H K_c = E_3 \tag{6.12}$$

(The generation of the attitude rate, $\dot{\Theta}_H$, is discussed in Paragraph 6.1.5.)

The signal E_3 is modified by a simple lag (or lead) network. The equations required to compute the output of this network are given in Appendix Five, Transfer Function Number (2).

$$\tau_s \dot{E4}_1 + E4_1 = E_3 \tag{6.13}$$

$$E4 = (\tau_4/\tau_5)E_3 + \left[\frac{\tau_5 - \tau_4}{\tau_5}\right] E4_1 \tag{6.14}$$

The output of the lag network is directed to the notch filter which may be used to attenuate a certain aeroelastic body-bending frequency band. The output of this filter may be represented by the differential equations of Transfer Function Number (7) Table 5-1. The output, E_5, is:

$$E_5 = E4 - 2E4_2 + 2E4_3 \tag{6.15}$$

where $E4_2$ and $E4_3$ are determined from the solution of the following differential equations:

$$\tau_{16} \dot{E4}_2 + E4_2 = E4 \tag{6.16}$$

$$\tau_{16}^2 \ddot{E4}_3 + 2\tau_{16} \dot{E4}_3 + E4_3 = E4 \tag{6.17}$$

107

6.1.4 __Azimuth Control Channel__ - The elements of the azimuth control channel are identical to those of the pitch control channel with the single exception that the azimuth channel contains no pressure control loop. The equations representing the azimuth control channel are analogous to Equations (6.6) through (6.17) and are presented in a corresponding order below.

__Bias__

$$\psi_p' \;=\; \psi_p + B_{18} + B_{19}t \tag{6.18}$$

__Repeater__

$$\frac{\ddot{\psi}_m}{\omega_1^2} \;+\; \frac{2\zeta_1\,\dot{\psi}_m}{\omega_1} \;+\; \psi_m \;=\; \psi_p' \tag{6.19}$$

__Outer Loop Summation__

$$(\psi_c' + \psi_T - \psi_m)K_D \;=\; E_6 \tag{6.20}$$

__Limiter__

$$\begin{aligned}
&\text{If} \quad |E_6| < |L_2| \qquad (\dot{\psi}\cos\Theta)_c = E_6\\
&\text{If} \quad |E_6| > |L_2| \qquad (\dot{\psi}\cos\Theta)_c = L_2
\end{aligned} \tag{6.21}$$

__Inner Loop Summation__

$$\left[(\dot{\psi}\cos\Theta)_c - (\dot{\psi}\cos\Theta)_m\right] K_E = E_7 \qquad \text{Switch A Closed} \tag{6.22a}$$

$$(-\dot{\psi}\cos\Theta)_m K_E = E_7 \qquad \text{Switch A Open} \tag{6.22b}$$

__Lag Network__

$$\begin{aligned}
&\tau_7\,\dot{E}_{8_1} + E_{8_1} = E_7\\
&E_8 = \frac{\tau_6\,E_7}{\tau_7} + \left[\frac{\tau_7 - \tau_6}{\tau_7}\right]E_{8_1}
\end{aligned} \tag{6.23}$$

__Notch Filter__

$$\begin{aligned}
&E_9 = E_8 - 2E_{8_2} + 2E_{8_3}\\
&\tau_{16}\,\dot{E}_{8_2} + E_{8_2} = E_8\\
&\tau_{16}^2\,\ddot{E}_{8_3} + 2\tau_{16}\,\dot{E}_{8_3} + E_{8_3} = E_8
\end{aligned} \tag{6.24}$$

108

The roll attitude of the missile is required to resolve the body components of angular velocity to pitch and azimuth attitude rates. The roll attitude simulated by the platform subprogram is modified to include a bias and a drift.

$$\phi'_p = \phi_p + B_{12} + B_{13}t \qquad (6.25)$$

This modified roll attitude is converted to an electrical signal by an attitude repeater similar to the repeaters used in the pitch and yaw channels. The output of the repeater is determined from the solution of the following differential equation.

$$\frac{\ddot{\phi}_m}{\omega_1^2} + \frac{2\,\zeta\dot{\phi}_m}{\omega_1} + \phi_m = \phi'_p \qquad (6.26)$$

The pitch and azimuth servo commands E_5 and E_9 are roll resolved to obtain body components of the servo commands.

$$\delta_{qc} = E_5 \cos \phi_m + E_9 \sin \phi_m$$
$$\delta_{rc} = E_9 \cos \phi_m - E_5 \sin \phi_m \qquad (6.27)$$

6.1.5 <u>Body Angular Rates and Accelerations</u> - The body angular rates, p, q, and r, sensed by the three body-mounted rate gyros, are calculated in the equations of motion. A bias on the rate gyros will be included by adding a constant to each of the calculated rates,

$$p' = p + B_{20}$$
$$q' = q + B_{21} \qquad (6.28)$$
$$r' = r + B_{22}$$

to simulate physical imperfections in the instrument. If the effect of aero-elasticity on the stability of the control system is to be investigated, the additional motion of a rate gyro due to body bending is computed in the aero-elastic modification operation and summed with the rigid-body rates calculated in Equation (6.28) to simulate the total signal generated by the body rate gyros, (q_m' and r_m').

If switch B is placed in the closed position, an additional signal is summed with q_m' and r_m'. This signal is developed from the output of two body-mounted accelerometers whose sensitive axes are aligned with the y- and z-body axis. The y- and z-components of acceleration may be obtained from the body components of the externally applied forces.

$$a_y = \frac{F_y}{m} - g_y$$
$$a_z = \frac{F_z}{m} - g_z \qquad (6.29)$$

109

where F_y and F_z are body components of the summation of the externally appl...
forces and the weight. The output of the accelerometer is obtained by modify-
ing the true body components of acceleration with a transfer function that
describes the behavior of the accelerometer. The error signal E_{10} is then
obtained by multiplying the accelerometer output by the constant gain K_F.
The differential equations are

$$\frac{\ddot{E}_{10}}{\omega_2^2} + \frac{2\zeta_2\dot{E}_{10}}{\omega_2} + E_{10} = K_F\, a_z$$

$$\frac{\ddot{E}_{11}}{\omega_2^2} + \frac{2\zeta_2\dot{E}_{11}}{\omega_2} + E_{11} = K_F\, a_y$$

(6.30)

For the switch B closed, the input to the resolver is:

$$q_m = q_m' - E_{10}$$

$$r_m = r_m' + E_{11}$$

$(6.31a)$

whereas if switch B is open:

$$q_m = q_m'$$

$$r_m = r_m'$$

$(6.31b)$

The resolutions of the body components of inertial rotation to attitude
rates would be mechanized in the actual control system by a roll resolver
and is simulated by

$$\dot{\theta}_H = q_m \cos\phi_m - r_m \sin\phi_m$$

$$(\dot{\psi}\cos\theta)_m = r_m \cos\phi_m + q_m \sin\phi_m$$

(6.32)

These attitude rates are then summed with command signals in the pitch
and azimuth control channels described in Paragraphs 6.1.3 and 6.1.4.

6.1.6 **Roll Rate Channel** - The roll-rate command generated by the steer-
ing functions subprogram is compared with the measured roll rate as computed
in the equations of motion and biased according to Equation (6.27). A time-
varying gain, K_G, is developed by a two-dimensional curve-read subroutine.
The error signal, E_{12}, is given by

$$E_{12} = (p_c - p')K_G$$

(6.33)

110

The frequency characteristics of E_{12} are modified by a network in order to improve the transient response of the closed loop. The output of the network, δ_{pc}, is given by Transfer Function Number (5), Table 5-1, as

$$\delta_{pc} = A_3 \, \delta_{pc_1} + B_3 \, \delta_{pc_2} + C_3 \, \delta_{pc_3} \qquad (6.34)$$

where: δ_{pc_1}, δ_{pc_2}, and δ_{pc_3} are determined by solving the following differential equations.

$$\tau_{13} \, \dot{\delta}_{pc_1} + \delta_{pc_1} = E_{12}$$

$$\tau_{14} \, \dot{\delta}_{pc_2} + \delta_{pc_2} = E_{12} \qquad (6.35)$$

$$\tau_{15} \, \dot{\delta}_{pc_3} + \delta_{pc_3} = E_{12}$$

and the coefficients are defined as:

$$A_3 = \frac{(\tau_{13} - \tau_{11})(\tau_{13} - \tau_{12})}{(\tau_{13} - \tau_{14})(\tau_{13} - \tau_{15})}$$

$$B_3 = \frac{(\tau_{14} - \tau_{11})(\tau_{14} - \tau_{12})}{(\tau_{14} - \tau_{13})(\tau_{14} - \tau_{15})} \qquad (6.36)$$

$$C_3 = \frac{(\tau_{15} - \tau_{11})(\tau_{15} - \tau_{12})}{(\tau_{15} - \tau_{13})(\tau_{15} - \tau_{14})}$$

6.1.7 Control-Surface Deflections - For switch C in the closed position, the control-surface commands developed in the pitch, azimuth, and roll-rate channels are summed to provide the control-deflection commands for the four surfaces.

$$\delta_{1c} = \delta_{qc} + \delta_{pc}$$

$$\delta_{2c} = \delta_{rc} + \delta_{pc}$$

$$\delta_{3c} = -\delta_{qc} + \delta_{pc} \qquad (6.37)$$

$$\delta_{4c} = -\delta_{rc} + \delta_{pc}$$

The servo response will be represented by a first-order lag network, and the actual control-surface deflections are given by the solution of the following equations.

$$\tau_{10} \, \dot{\delta}_n + \delta_n = \delta_{nc}$$

or $\qquad (6.38)$

$$\dot{\delta}_n = \frac{1}{\tau_{10}} (\delta_{nc} - \delta_n)$$

111

There is a limit on the rate of control-surface deflection due to the physical limitations of the control-surface servo system. There also may be a bias, B_{14}; on the rate of control-surface deflections. The effects described above will be simulated by the following equations.

$$\dot{\delta}_n = \frac{1}{\tau_{10}} \left[\delta_{nc} - \delta_n \right] + B_{14n}$$

$$\text{If} \qquad \left| \dot{\delta}_n \right| < \left| L_3 \right| \qquad \dot{\delta}'_n = \dot{\delta}_n \qquad\qquad (6.39)$$

$$\text{If} \qquad \left| \dot{\delta}_n \right| > \left| L_3 \right| \qquad \dot{\delta}'_n = L_3$$

where the sign of L_3 corresponds to the sign of $\dot{\delta}_n$. The integration of the four deflection rates defined in Equation (6.39), for $n = 1,2,3,4$ is performed for each of the four control surfaces. These computed deflections must be limited, since the actual missile control-surface has some maximum possible displacement, L_4. There also may be a bias on the control-surface deflections due to mechanical misalignment, δ_{n_o}. The control-surface deflections are given by the following equations.

$$\delta'_n = \int_0^t \dot{\delta}'_n \, dt + \delta_{no}$$

$$\text{If} \qquad \left| \delta'_n \right| < \left| L_4 \right| \qquad \delta_n = \delta'_n \qquad\qquad (6.40)$$

$$\text{If} \qquad \left| \delta'_n \right| > \left| L_4 \right| \qquad \delta_n = L_4$$

The four control surface deflections calculated above must be resolved into the three effective control deflections δ_p, δ_q, and δ_r. The deflections computed above are defined in terms of their position with respect to body axes as shown in Figure (6.2). The positive direction of each surface would produce a rotational velocity vector into the missile.

The effective rolling moment deflection is the average of the four δ's computed above.

$$\delta_p = (1/4)(\delta_1 + \delta_2 + \delta_3 + \delta_4)$$

δ_q and δ_r are defined as positive rotations about axes parallel to the body y and z axes respectively. Therefore, from Figure (6.2),

$$\delta_q = (\delta_3 - \delta_1)(1/2) \qquad \delta_r = (\delta_4 - \delta_2)(1/2)$$
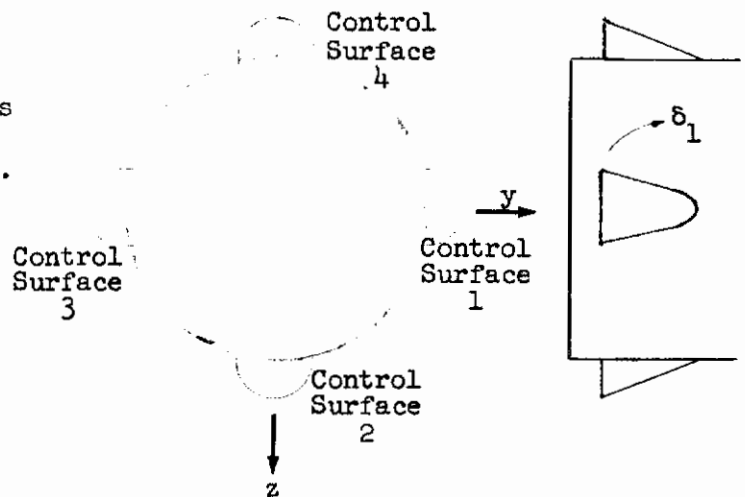
Figure 6.2 Control-Surface Arrangement and Definition of Surface Deflections

112

6.1.8 <u>Computational Flow Diagram</u> - The equations representing the typical control system have been derived in Paragraphs 6.1.3 through 6.1.7 by tracing the channels of the control system functional diagram (Figure (6.1)). Since the indicated numerical operations must proceed sequentially in the digital computer, the same equations have been arranged in a chronological order in the computational flow diagram of Figure (6.3).

6.2 <u>Flight-Plan Programmer</u> - A flight-plan programmer subprogram has been incorporated into the SDF computer program which allows a selection of several types of functions for trajectory control of the point-mass reduced-degrees-of-freedom options. The flight-plan control sequences outlined in this section permit a selection of 6 control options, with 4 of these having a selection of 3 independent variables against which to program the control functions. Five of these programmers are contained in one subprogram; the other is contained in an alternate subprogram (Section 6.2.3).

6.2.1 <u>Flight-Plan Programmer Control Commands</u> - The flight-plan programmer, as defined for the SDF computer program, is the means by which the trajectory is controlled for the point-mass options. This feature of the point-mass problem corresponds to the steering functions for an autopilot used in the options which permit the rotational degrees of freedom. Use of the flight-plan programmer is restricted to the point-mass options since it permits vehicle motion without regard to rotational inertia (e.g. absolute specification of angle of attack versus Mach number or time). Since there are several flight-plan methods that are used extensively during preliminary design and development of a particular vehicle, a number of control methods have been selected as a preliminary library of flight-plan programs of the SDF computer program. As such, these methods of control are available at the option of the analyst by appropriate specification of input data. The flight-plans that will be included are:

(1) Programmed lift coefficient C_L, side-force coefficient C_Y, and drag coefficient C_D.

(2) Programmed angle of attack α, and/or angle of sideslip, β.

(3) Programmed body-axes attitude angles ψ and Θ (local Euler angles), with a dynamic pressure feed-back.

(4) Programmed wind-axes normal load factor, n_γ and n_σ, with thrust included.

(5) Programmed flight-path angle γ, versus altitude h, with $\beta = 0$.

The first four flight-plan commands will be curve-read functions of the independent variables time t, Mach number M_N, or airspeed V_a. Flight-plans (1), (2), and (3) represent "exact" flight-plan control commands in that the forces acting upon the vehicle are dictated by the programmed control. (Flight-plan (3) has a feed-back loop but is considered an exact flight-plan control.) Flight-plans (4) and (5) approximate the action of an autopilot by employing an error function and a gain to alter the forces acting upon the body. This results in a trajectory that approximates the desired trajectory depending on the form of the command terms and the value of the gain factor selected.
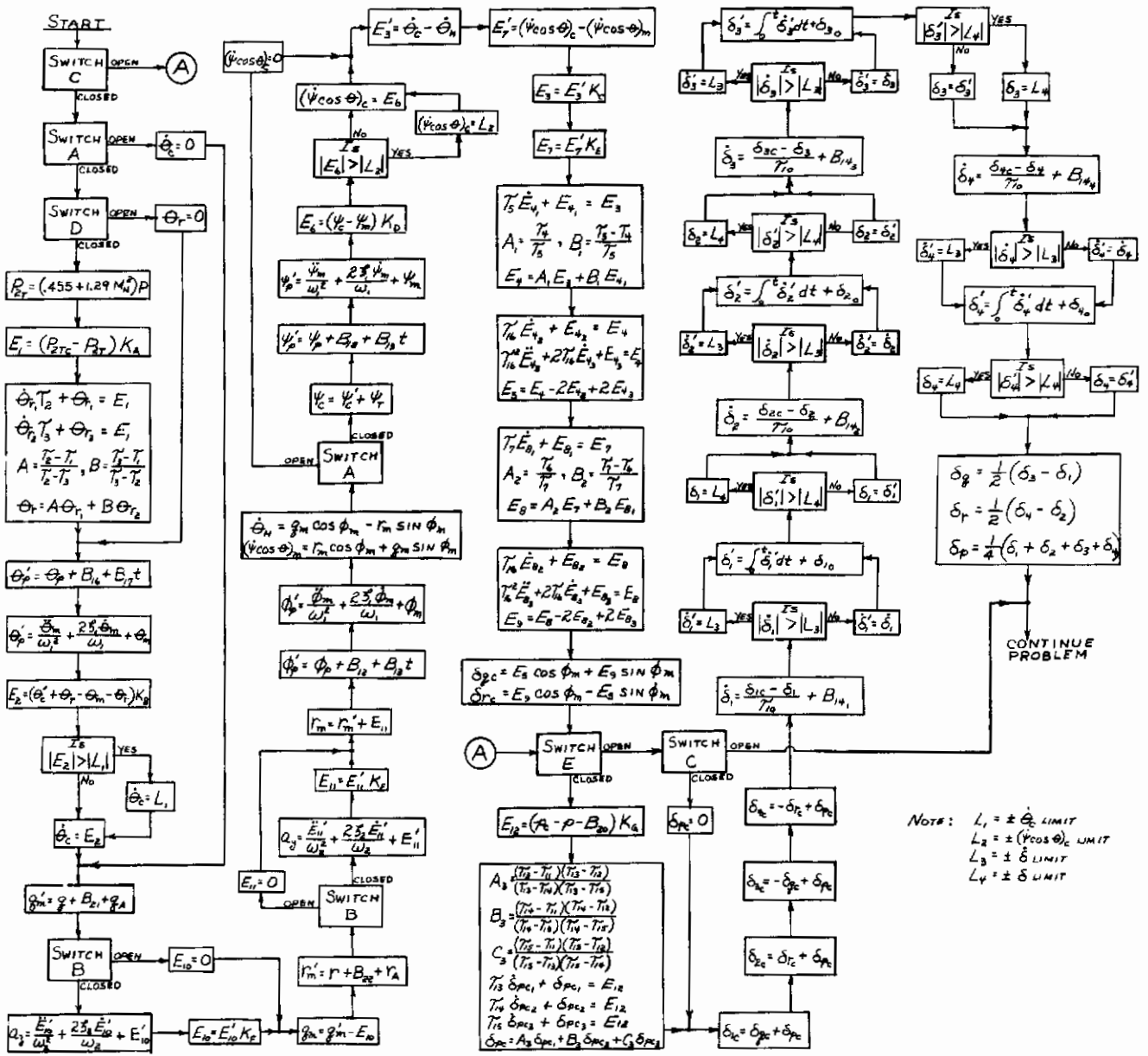
FIGURE 6.3. CONTROL SYSTEM COMPUTATIONAL FLOW DIAGRAM

114

Under normal conditions this method will give a realistic flight-path that follows the commanded values very closely. A preliminary analyses has been performed to determine how closely the computed load factors follow the commanded values (Flight-plan (4)) and is discussed in later paragraphs to show the comparison. This method is considered preferable to an iteration procedure to get a simultaneous convergence of several quantities since it results in a substantial saving of machine running time to solve the problem.

6.2.2 <u>Discussion of Selected Flight-Plan Sequences</u> - Flow diagrams for the 5 flight-plan control programs are shown in Figure (6.4). Individual explanations of the data required and the sequence of operations are given below.

<u>Flight Plan (1) Programmed Lift, Drag, and Side Force Coefficients</u> - This flight-plan is the simplest considered and is intended for use with gliding or coasting bodies without thrust. The data required for this control program are the parameters time, Mach number, or airspeed, one of which will be used as the independent variable for the command functions. Also required is the dynamic pressure, q^*, and the reference area, S. The technique is to obtain C_{L_c}, C_{Y_c}, and C_{D_c} from linear interpolations of tabular listings, and calculate the forces L, Y, and D by multiplying by q^*S. The problem is continued without entrance to the aerodynamic data subprogram. A control word is set up by the executive program such that when this flight-plan program is used, the aero subprogram will be bypassed. This control method may be used for obtaining the glide trajectory for a vehicle, the decay trajectory of a satellite, or the re-entry trajectory of a ballistic missile.

<u>Flight Plan (2) Programmed Angle of Attack and Sideslip</u> - This flight-plan is similar to Plan (1) above with the exception that the attitude of the body, with respect to the trajectory, is known (i.e. specified). Such knowledge allows the inclusion of thrust forces and a determination of thrust components parallel and normal to the flight path. The data required for this control mode are the parameters time, Mach number, or airspeed against which the command functions of angle of attack, α_c, and sideslip, β_c, are programmed. The commands α_c and β_c are introduced as tabular listings of the desired parameter. With α_c and β_c given the problem is continued in the normal manner. The aerodynamic forces are computed in the aerodynamic subprogram and the motion is then determined on the basis of these forces. This flight-plan programmer may be used for the ballistic trajectory by programming α_c and β_c equal to zero. This is done automatically within the flight-plan programmer subprogram initialization subroutine such that if using the point-mass option with no flight programmer specified, it implies that α_c and β_c are zero, or that the trajectory is ballistic. A particular lift-to-drag ratio may be followed by programming the appropriate angle of attack and/or sideslip.

<u>Flight Plan (3) Programmed Body-Axis Attitude Angles, ψ and θ, With Dynamic-Pressure Feed-Back</u> - This flight-plan program provides feedback loop control which is especially useful in the analysis of certain boost-phase trajectories and hypervelocity glide trajectories. This control is accomplished by modifying the attitude command according to the difference between the computed and desired dynamic pressure corrected for planet rotation effect. The desired dynamic pressure is specified in terms of the desired altitude-velocity profile. In the case of glide trajectories, the feedback loop provides a method of controlling the skips which occur if the correct flight-path angle is not selected at the start of the computation.

<p style="text-align:center">115</p>

FLIGHT PLAN (1)   PROGRAMMED LIFT, DRAG, AND SIDE FORCE COEFFICIENTS

| DATA REQUIRED FROM CENTRAL PROGRAM t, M_N, V_a, q^*, S | → | PROGRAM C_L, C_D AND C_Y AS $f(t)$ OR $f(M_N)$ OR $f(V_a)$ BY A TABULAR LISTING | → | CALCULATE: $L = C_L q^* S$ $D = C_D q^* S$ $Y = C_Y q^* S$ | → | CONTINUE PROBLEM |

FLIGHT PLAN (2)   PROGRAMMED ANGLE OF ATTACK AND SIDESLIP

| DATA REQUIRED FROM CENTRAL PROGRAM t, M_N OR V_a | → | PROGRAM α_c & β_c AS $f(t)$ OR $f(M_N)$ OR $f(V_a)$ BY A TABULAR LISTING | → | CONTINUE PROBLEM |

FLIGHT PLAN (3)   PROGRAMMED BODY-AXIS ATTITUDE ANGLES, ψ AND θ, WITH DYNAMIC PRESSURE FEEDBACK

| DATA REQUIRED FROM CENTRAL PROGRAM $t, M_N, V_a, q^*, h, \gamma, \sigma$, $V, R, g_{a_g}, \Delta\theta_{c_2}$ FROM HTLS | → | GAIN FACTOR C_q^* | → | PROGRAM ψ_c & θ_c AS $f(t), f(M_N)$ OR $f(V_a)$ BY A TABULAR LISTING NOTE: ψ_c MAY BE COMMANDED EQUAL TO σ | → | PROGRAM $h_c = f(V_a)$ WANTED FOR A NON-ROTATING PLANET CONDITION, i.e. C.F. COMPONENT COMPUTED USING V_a | → | CALCULATE ρ_{c_1} TO CORRECT C.F. COMPONENT FOR INITIAL VELOCITY IN TERMS OF DENSITY REQUIRED $\rho_{c_1} = \rho_c \left[\dfrac{g_{a_g} R - V^2}{g_{a_g} R - V_a^2} \right]$ WHERE $\rho_c = f(h_c)$ |

COMPUTE α & β
$$\alpha = \theta_{c_1} - \tan^{-1}\left[\frac{\tan\gamma}{\cos(\psi_c - \sigma)} \right]$$
$$\beta = \tan^{-1}\left\{ \frac{\cos\gamma \sin(\psi_c - \sigma)}{\cos\gamma \cos\theta_{c_1} \cos(\psi_c - \sigma) + \sin\gamma \sin\theta_{c_1}} \right\}$$

TEST $\psi_c = 0$ → NO → ← $\theta_c = \theta_{c_1} + \Delta\theta_{c_1} + \Delta\theta_{c_2}$ ← CALCULATE $\Delta\theta_{c_1}$ $\Delta\theta_{c_1} = C_q^*(q^* - q_c^*)$ ← CALCULATE q_c^* $q_c^* = \frac{1}{2}\rho_{c_1} V_a^2$

TEST → YES → $\alpha = \theta_{c_1} - \gamma$ $\beta = 0$ → CONTINUE PROBLEM

FLIGHT PLAN (4)   PROGRAMMED WIND-AXES NORMAL LOAD FACTOR, n_γ & n_σ, WITH THRUST INCLUDED

| DATA REQUIRED FROM CENTRAL PROGRAM $t, M_N, V_a, n_\gamma, n_\sigma, m$ L, Y, T | → | UPPER & LOWER LIMITS OF α & β | → | INITIAL OR PREVIOUS VALUES OF α & β | → | PROGRAM OF n_{γ_c} & n_{σ_c} AS $f(t), f(M_N)$ OR $f(V_a)$ USING A TABULAR LISTING |

| CONTINUE PROBLEM | ← | CHECK LIMIT VALUES OF α & β. IF GREATER SET $\alpha = \alpha_{LIMIT}$ AND $\beta = \beta_{LIMIT}$ | ← | $\alpha_n = \alpha_{n-1} + \Delta\alpha$ $\beta_n = \beta_{n-1} + \Delta\beta$ | ← | COMPUTE $\Delta\alpha$ & $\Delta\beta$ $\Delta\alpha = C_\alpha (n_{\gamma_c} - n_\gamma)$ $\Delta\beta = C_\beta (n_{\sigma_c} - n_\sigma)$ | ← | COMPUTE C_α & C_β $C_\alpha = \dfrac{m\, g_{REF}}{L/\alpha + T\cos\alpha}$ $C_\beta = \dfrac{-m\, g_{REF}}{-Y/\beta + T\cos\beta}$ |

FLIGHT PLAN (5)   PROGRAMMED FLIGHT PATH ANGLE γ, VERSUS ALTITUDE h, WITH SIDESLIP β, EQUAL TO ZERO

| DATA REQUIRED FROM CENTRAL PROGRAM $\gamma, \dot\gamma, h, T, L, m$ | → | UPPER & LOWER LIMIT OF γ | → | INITIAL & PREVIOUS VALUE OF γ | → | PROGRAM $\gamma_c = f(h)$ BY A TABULAR LISTING |

| COMPUTE α_n $\alpha_n = \alpha_{n-1} + \Delta\alpha$ | ← | COMPUTE $\Delta\alpha$ $\Delta\alpha = C_\gamma(\gamma_c - \gamma) + C_{\dot\gamma}(\dot\gamma_c - \dot\gamma)$ | ← | COMPUTE C_γ & $C_{\dot\gamma}$ $C_{\dot\gamma} = C_\gamma = m V_a \left[\dfrac{1}{T\cos\alpha + L/\alpha} \right]$ | ← | COMPUTE $\dot\gamma_c$ $\dot\gamma_c = \left[\dfrac{\gamma_{c_n} - \gamma_{c_{n-1}}}{h_n - h_{n-1}} \right] V \sin\gamma$ |

| CHECK ON LIMIT VALUE OF α. IF GREATER SET $\alpha = \alpha_{LIMIT}$ | → | CONTINUE PROBLEM |

FIGURE 6.4,   SIX-DEGREE-OF-FREEDOM FLIGHT-PATH STUDY
FLIGHT PROGRAMMER SUBPROGRAM CONTROL FUNCTIONS

116

The following quantities must be computed prior to beginning the flight-plan programmer calculations: altitude, h, dynamic pressure, q*, inertial velocity, V, radius from the center of the planet, R, local radial gravitational attraction, gZ_g, horizontal and vertical flight-path angle σ and γ, and time, airspeed, or Mach number, whichever is to be considered the independent variable for the body-attitude angles, ψ and Θ. The body-attitude angles for the specified maneuver and the velocity-altitude profile desired for a non-rotating planet condition are introduced as tabular listings. The computation proceeds as follows: From the commanded altitude, h_c, the density, ρ_c, is determined from the atmosphere subprogram. This altitude and density are the desired quantities the vehicle should have at the computed airspeed if no planet rotation existed, (i.e., the centrifugal relieving effect being computed using airspeed, V_a, which is also the inertial speed, V, under these conditions). Planet rotation changes the situation, making the airspeed greater or less than the inertial speed (depending on the azimuth direction) with V_a in general being greater than V when the vehicle is moving against the planet rotation (westward in the case of the Earth). The method used to correct this is as follows:

Assume that equilibrium flight existed over a non-rotating planet. Then

$$C_L \ 1/2 \ \rho_c \ V_a^2 \ = \ W_T \left[1 - \frac{V_a^2}{gZ_g \ R} \right] \tag{6.41}$$

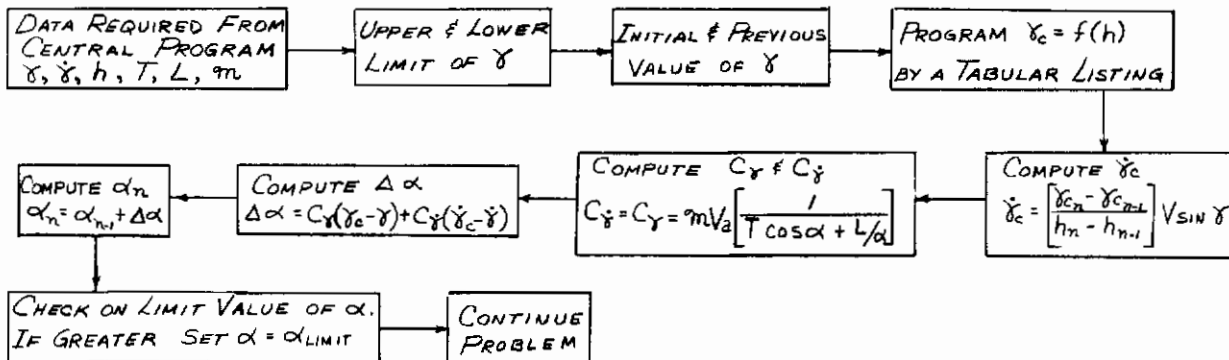For the same airspeed, and assuming the same C_L is wanted, the condition existing if the planet were rotating would be,

$$C_L \ 1/2 \ \rho_{c_1} \ V_a^2 \ = \ W_T \left[1 - \frac{V^2}{gZ_g \ R} \right] \tag{6.42}$$

Solving the above equations for ρ_{c_1}, which is the desired density in terms of the commanded density ρ_c obtained from the h_c versus V_a curve, results in,

$$\rho_{c_1} \ = \ \rho_c \left[\frac{gZ_g \ R - V^2}{gZ_g \ R - V_a^2} \right] \tag{6.43}$$

The commanded dynamic pressure is therefore

$$q_c^* \ = \ 1/2 \ \rho_{c_1} \ V_a^2 \tag{6.44}$$

and is used to revise the pitch attitude by $\Delta\Theta_c$ determined as

$$\Delta\Theta_c \ = \ C_q^* \ (q^* - q_c^*) \tag{6.45}$$

The commanded attitude is then modified by

$$\Theta_{c_1} \ = \ \Theta_c + \Delta\Theta_c \tag{6.46}$$

The value of the gain coefficient, C_q*, must be determined empirically according to the configuration being considered; however, studies on a low-lift vehicle have indicated a value of 0.02 degrees per unit $\Delta q*$ is of the correct order of magnitude. The vertical flight-path angle is resolved to the pitch plane of the vehicle by

$$\text{Tan } \gamma' = \frac{\text{Tan } \gamma}{\text{Cos } (-\psi_c + \sigma)} \tag{6.47}$$

from which the aerodynamic angle of attack is computed as

$$\alpha = \Theta_{c_1} - \gamma' \tag{6.48}$$

The angle of sideslip, β, is computed from the same resolution as above by

$$\text{Tan } \beta = \frac{\text{Cos } \gamma \text{ Sin } (-\psi_c + \sigma)}{\text{Cos } \gamma \text{ Cos } \Theta_{c_1} \text{ Cos } (-\psi_c + \sigma) + \text{Sin } \gamma \text{ Sin } \Theta_{c_1}} \tag{6.49}$$

With the aerodynamic angles, α and β, known, the aerodynamic forces are computed in the normal manner and used in the solution of the equations of motion.

If it is desired to eliminate the feedback control, the value of C_q* is specified as zero. The corrected pitch attitude, Θ_{c_1}, may also include an attitude correction based upon the equilibrium stagnation temperature or thin-skin temperature computed by the temperature monitoring subprogram, Section 6.3. A great-circle trajectory which is unaffected by lateral aerodynamic forces may be computed by making $\psi_c = \sigma$.

Flight-Plan (4) Programmed Wind-Axes Normal Load Factors, n_γ and n_σ, With Thrust Included - The data required from the preceding part of the program are the parameters, time, Mach number, or airspeed, against which the commanded vertical wind-axes normal load factors, n_{γ_c} and n_{σ_c}, are programmed, and the computed values of n_γ, n_σ, lift L, and side force Y. The thrust T and mass are also required. The analyst will also specify the upper and lower limits which will be allowed for angle of attack and sideslip. To start the program, initial values of α and β will be specified which are compatible with the initial n_{γ_c} and n_{σ_c} commanded. The load factors are introduced as a tabular listing versus the parameters time, Mach number, or airspeed. The C_α and C_β gains are computed using the equations specified which are derived as follows: The wind-axes normal load factor, n_γ, is defined as

$$n_\gamma = \frac{L + T \text{ Sin } \alpha}{m \, g_{ref}} = \frac{C_{L_\alpha} \alpha \, q*S + T \text{ Sin } \alpha}{m \, g_{ref}} \tag{6.50}$$

The derivative of n_γ with respect to α is

$$\frac{dn_\gamma}{d\alpha} = \frac{C_{L_\alpha} q*S}{m \, g_{ref}} + \frac{T}{m \, g_{ref}} \text{ Cos } \alpha \tag{6.51}$$

118

Assume that C_{L_α} can be expressed as

$$C_{L_\alpha} \cong \frac{C_L}{\alpha} \tag{6.52}$$

Then

$$\frac{dn_\gamma}{d\alpha} = \frac{C_L \, q^*S}{m \, g_{ref} \, \alpha} + \frac{T}{m \, g_{ref}} \, \cos \alpha$$

$$= \frac{L}{m \, g_{ref} \, \alpha} + \frac{T}{m \, g_{ref}} \, \cos \alpha \tag{6.53}$$

The gain factor C_α is therefore $\dfrac{1}{\dfrac{dn_\gamma}{d\alpha}}$ or

$$C_\alpha = \frac{m \, g_{ref}}{\dfrac{L}{\alpha} + T \, \cos \alpha} \tag{6.54}$$

Using a similar technique for C_β

$$C_\beta = \frac{-m \, g_{ref}}{-\dfrac{Y}{\beta} + T \, \cos \beta} \tag{6.55}$$

The corrections to the angle of attack and sideslip, $\Delta\alpha$ and $\Delta\beta$, are computed using the gains C_α and C_β multiplied by the difference between n_{γ_c} and n_γ, and n_{σ_c}, and n_σ, respectively.

This technique of control has been investigated as to the stability of the solution and the accuracy with which the commanded load factor is followed. The results[1] are shown in Figure (6.5), for two typical command functions. Considering the fact that one-second time increment was taken as the computation interval, the results are considered in good agreement with the commanded values. The advantage of this method of control, compared to the normal iterative solution, is the reduction in computing time required since every cycle through the computation advanced the vehicle along the trajectory.

---

(1) It should be noted that this investigation was run on a supplementary program with typical inertia and aerodynamic characteristics of an airframe. Very large time increments were used to test the stability of the solution. Results of actual computations using the SDF computer program should be greatly improved over those shown.
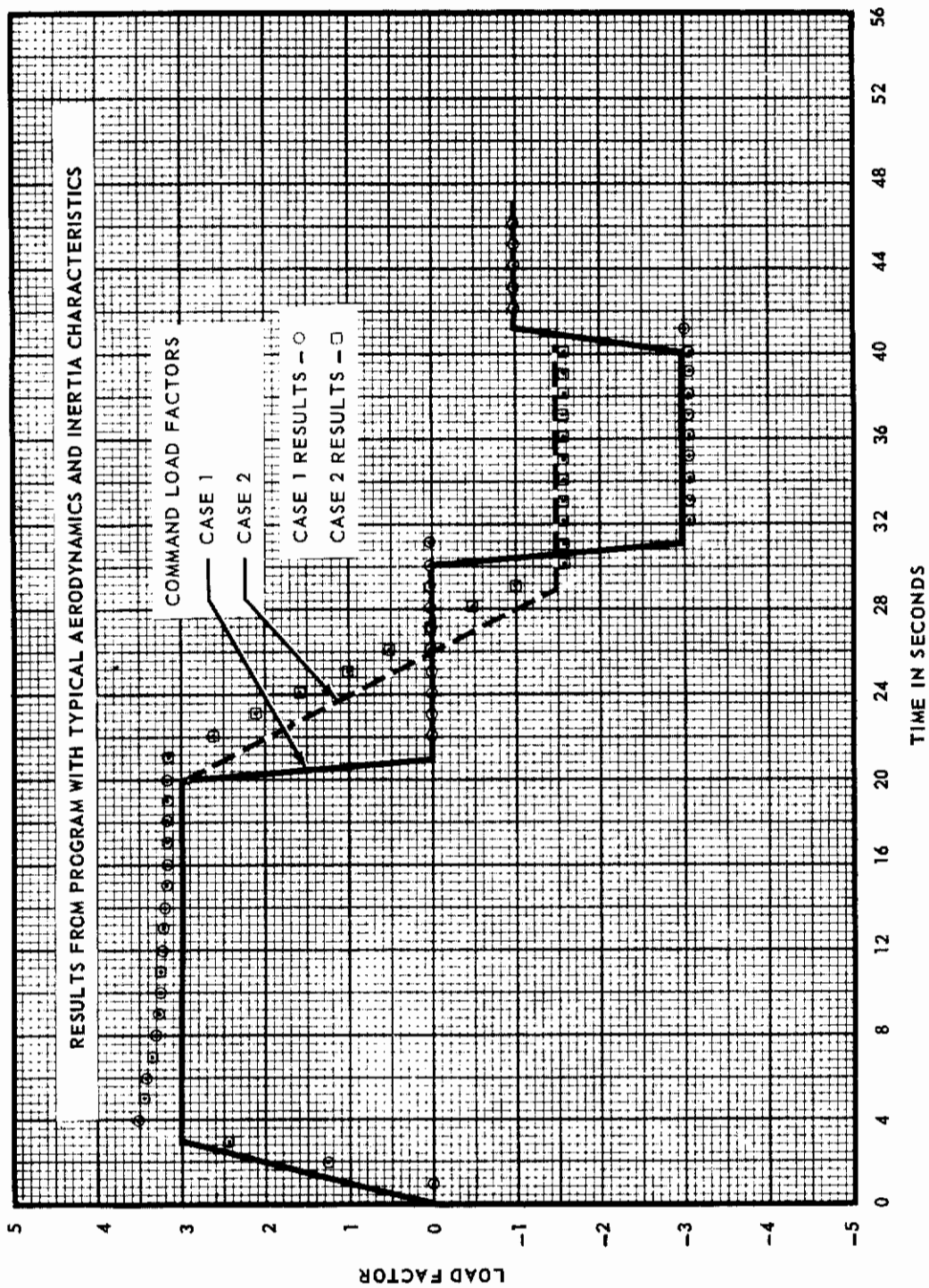
FIGURE 6.5, FLIGHT PLAN (4) PROGRAMMED WIND-AXIS NORMAL LOAD FACTOR

120

Flight Plan (5) Programmed Flight-Path Angle γ Versus Altitude h, With Sideslip Angle β Equal to Zero. - The data required from the central program are altitude, vehicle mass, thrust, lift, and instantaneous value of the vertical flight-path angle and its time derivative. Also required for this program are the upper and lower limits which the angle of attack may have. To start the program an initial angle of attack **a** will be specified which is compatible[1] with the γ_c versus h profile desired. A tabular listing of the γ_c versus h profile desired is the command input. The problem is to find the angle of attack which will provide the necessary forces to follow the commanded flight-path angle at the altitude computed. From the relation

$$m \, V_g \frac{d\gamma}{dt} = T \, Sin \, \alpha + L_\alpha \, \alpha - m \, g_{ref} \, Cos \, \gamma$$

the expression

$$\dot{\gamma} = \frac{T \, Sin \, \alpha + L_\alpha \, \alpha - m \, g_{ref} \, Cos \, \gamma}{m \, V_g} \tag{6.56}$$

is obtained. Differentiating with respect to the angle of attack gives

$$\frac{d\dot{\gamma}}{d\alpha} = \frac{T \, Cos \, \alpha + L_\alpha}{m \, V_g} \tag{6.57}$$

and the change in angle of attack required to correct for an error in commanded flight-path angle rate of change is

$$\Delta\alpha_{\dot{\gamma}} = \frac{m \, V_g}{T \, Cos \, \alpha + L_\alpha} \, (\gamma_c - \gamma) \tag{6.58}$$

Changes in flight-path angle are produced by timewise application of flight-path angle rates according to the relation

$$d\gamma = \dot{\gamma} \, dt$$

Therefore

$$\frac{d\gamma}{d\alpha} = \frac{d\dot{\gamma}}{d\alpha} \, dt \tag{6.59}$$

and substituting the expression previously obtained for $d\dot{\gamma}/d\mathbf{a}$ gives the result

$$\frac{\Delta\gamma}{\Delta\alpha} = \left[\frac{T \, Cos \, \alpha + L_\alpha}{m \, V_g} \right] \Delta t \tag{6.60}$$

---

(1) Actually any initial **a** will suffice, however, the nearer to that actually required the more exactly the resulting flight path will follow that commanded since this is an approximation program.

Therefore the change in flight-path angle for a given change in angle of attack is proportional to the same factor as the time rate of change of flight-path angle and

$$\Delta\alpha_\gamma = \left(\frac{m\ V_g}{T\ \cos\ \alpha + L_\alpha}\right)(\gamma_c - \gamma) \tag{6.61}$$

The total change in angle of attack may be obtained by

$$\Delta\alpha = \left(\frac{m\ V_g}{T\ \cos\ \alpha + L_\alpha}\right)\left[g\ (\dot\gamma_c - \dot\gamma) + (\gamma_c - \gamma)\right] \tag{6.62}$$

where g is a gain factor on the time rate of change.

The new angle of attack may be computed from a knowledge of the existing angle of attack and the increment $\Delta\alpha$ defined above. An investigation in which the characteristics of an airframe were approximated has been made and the results are presented in Figure (6.6) which shows the solution using the above feedback corrections to be stable and to approximate closely the desired flight-path angle.

    6.2.3 _Flight Plan Programmer 10 - Programmed Torquing Commands to Pitch Rate Gyro with Drift and Bias_ - Flight Plan Programmer 10 is an alternate subprogram which permits the calculation of dispersion associated with gyro errors and winds for vehicles employing three single-axis, rate integrating gyros as the basic attitude reference. This flight plan programmer was designed for the execution of a dispersion analysis of a boost and glide mission. The pitch attitude of the vehicle during boost is specified by a stored gyro torque program; the pitch rate integrating gyro is deleted during the glide phase. Yaw and roll torque programs which nominally maintain sideslip and bank angle zero are simulated. This flight plan programmer develops the angle of attack, angle of sideslip and bank angle associated with non-nominal winds and errors in the rate integrating gyros.

    In developing the flight plan programmer, the following basic assumptions were made.

    a.   The vehicle follows the rate integrating gyro error signal immediately. This implies a perfect control system and a vehicle with no moment of inertia.

    b.   The instrument errors and winds which introduce changes in the angle of attack, angle of sideslip, and bank angle are small so that the total angular change is the sum of the effects of the individual perturbing errors.

    c.   The xz body plane coincides with local vertical plane and contains the relative wind velocity vector during the nominal (no errors) flight.
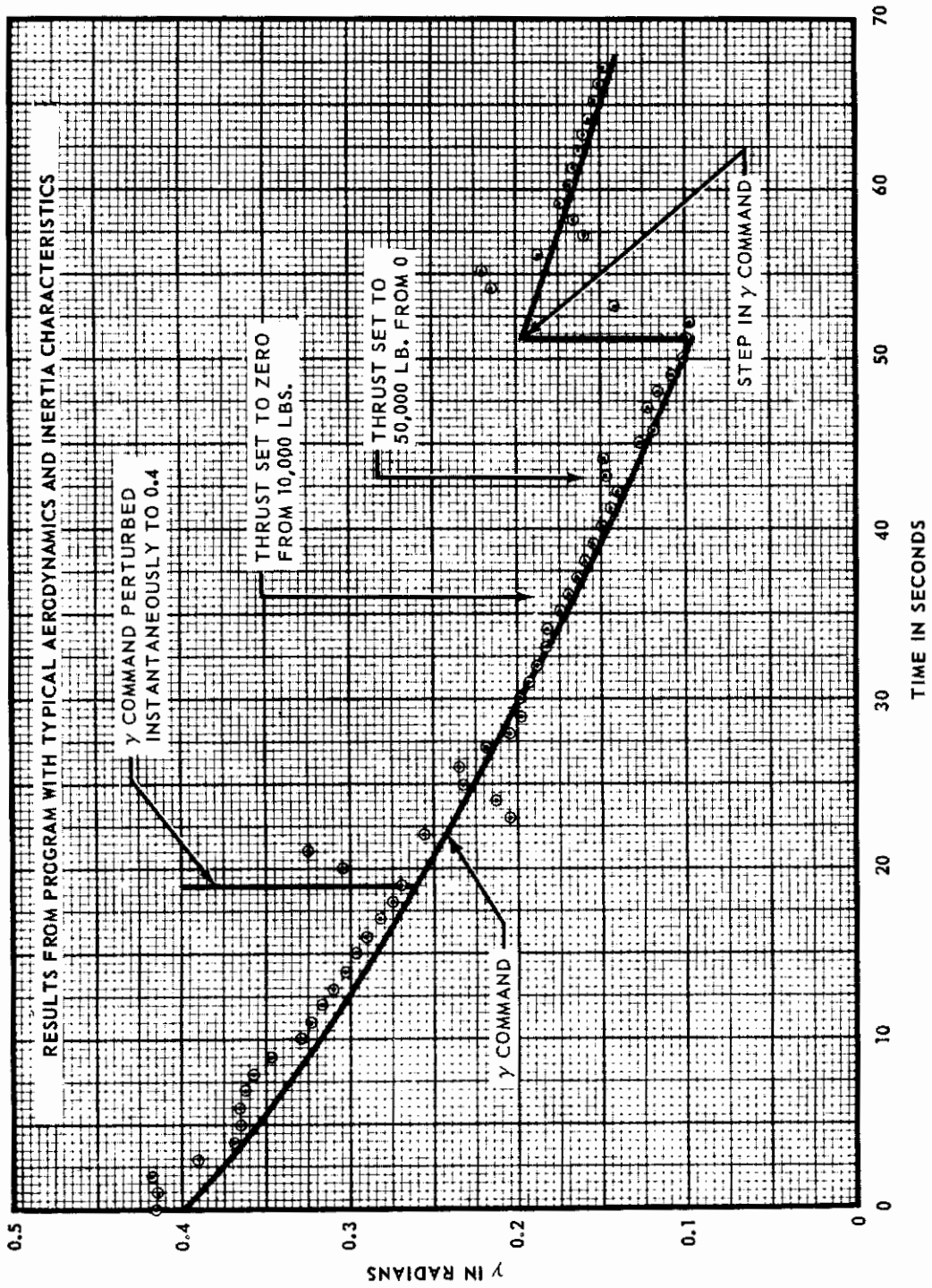
Approved for Public Release

FIGURE 6.6, FLIGHT PLAN (5) — PROGRAMMED FLIGHT-PATH ANGLE

123

Winds - The effect of winds can be considered in the point mass options if the vehicle attitude is specified by a control system. The vehicle is thereby restrained from reaching a trim condition, and the resulting angles of attack and sideslip can be ascertained. An expression for the angle of attack, α, and the angle of sideslip, β_W, is obtained below.

In Figure 6.7, σ and γ are the flight path angles relative to the unperturbed wind coordinates $X_A'-Y_A'-Z_A'$. The angles σ_A and γ_A define the airspeed vector and the perturbed wind coordinates $X_A Y_A Z_A$. Applying the law of sines to triangle x_N-Z_g-M gives an expression for the angle of sideslip due to winds.

$$\frac{\sin (\sigma_A - \sigma)}{\sin \beta_W} = \frac{\sin d}{\cos \Theta} \qquad (6.63)$$

The angle d can be expressed in terms of known parameters by applying the law of cosines.

$$\cos d = -\sin (\sigma_A - \sigma) \sin \Theta$$

The feasibility of utilizing the approximation sin d = 1 in equation (6.63) will be investigated by determining the maximum value of $\sigma_A - \sigma$ which causes sin d to differ from unity by one percent. The value of cos d (.139) which corresponds to sin d = .99 is inserted in the above equation with sin Θ at its maximum value of unity. The results indicate that a $\sigma_A - \sigma$ of eight degrees or less will introduce an error of one percent or less in Equation 6.63.

Applying this approximation to Equation 6.63, the following expression for β_W is obtained.

$$\beta_W = \mathrm{Sin}^{-1} \left[\mathrm{Cos}\,\Theta \, \mathrm{Sin}\,(\sigma_A - \sigma) \right] \qquad (6.64)$$

The angle of attack can be determined by applying the law of sines to the spherical triangle y_N-X_A-A

$$\frac{\mathrm{Sin}\,\gamma'}{\mathrm{Sin}\,\gamma_A} = \frac{\mathrm{Sin}\,f}{\mathrm{Cos}\,(\sigma_A - \sigma)}$$

Utilizing the approximation sin f = unity and solving for γ' in the above equation gives the following result.

$$\gamma' = \sin^{-1} \left[\frac{\mathrm{Sin}\,\gamma_A}{\mathrm{Cos}\,(\sigma_A - \sigma)} \right] \qquad (6.65)$$

The angle of attack is obtained by subtracting γ' from the pitch attitude Θ specified by the control system. Thus

$$\alpha = \Theta - \mathrm{Sin}^{-1} \left[\frac{\mathrm{Sin}\,\gamma_A}{\mathrm{Cos}\,(\sigma_A - \sigma)} \right] \qquad (6.66)$$

When the pitch-rate-integrating gyro is deleted from the control system (at end of boost), the angle of attack is assumed to equal its trim value, modified to

GEOMETRY USED TO DETERMINE EFFECTS
OF WIND AND PITCH GYRO ERRORS

FIGURE 6.7

125
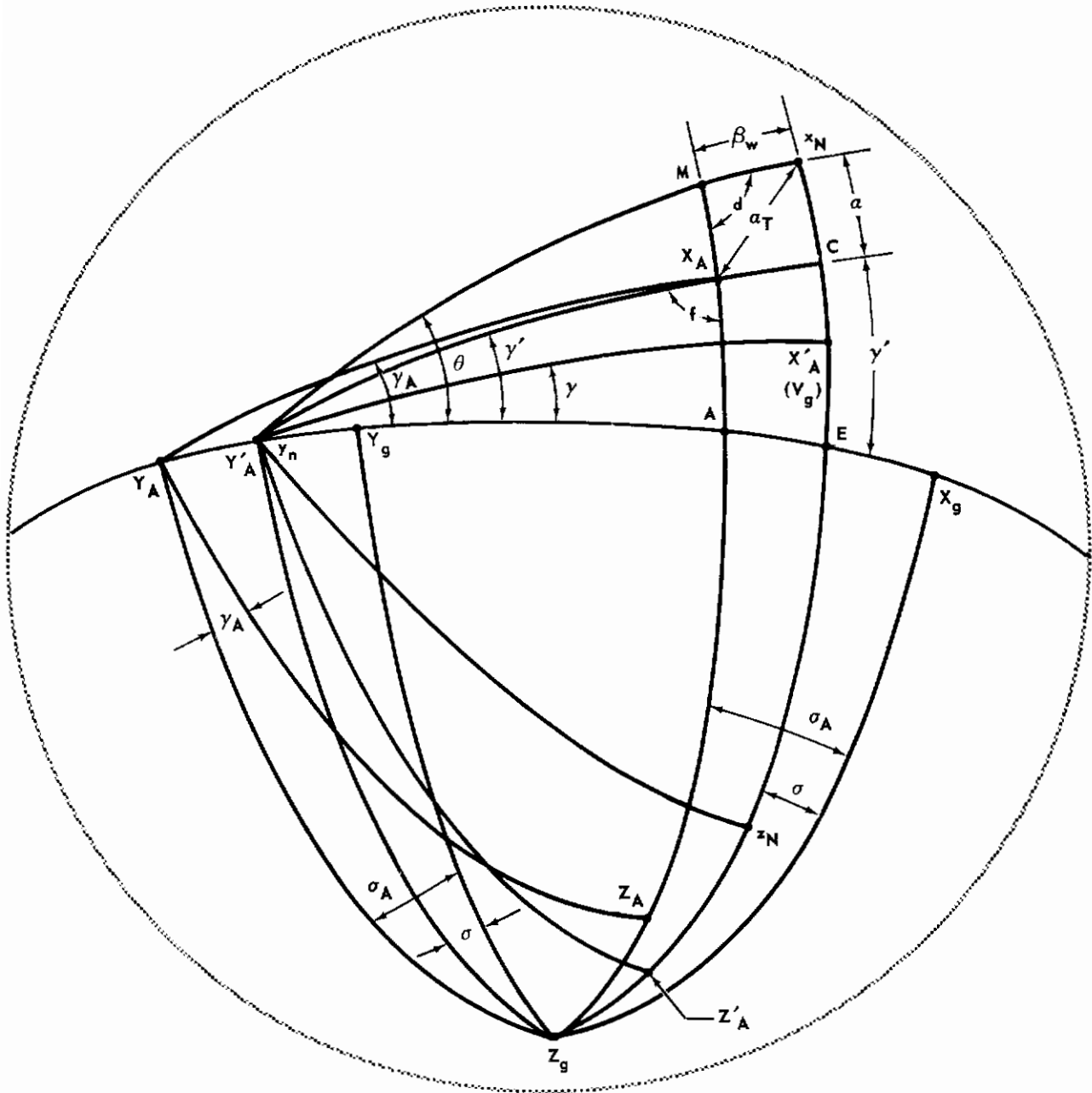
include any deviations from its expected value. The nominal trim angle of attack (α_0) is introduced as a function of Mach number in a tabular listing (FTAB02). Deviations in trim angle of attack (α) are obtained by varying K_{26} from its nominal value of one where

$$\alpha = K_{26}\, \alpha_0 \tag{6.67}$$

The pitch attitude is obtained by solving for θ in Equation (6.66).

Pitch Rate-Integrating Gyro - The pitch attitude of the vehicle is controlled by torquing the pitch rate integrating gyro at some prescribed rate, q_c. The pitch attitude error is given by:

$$\theta_E = \int_0^t (q_c - q)\, dt$$

However, in this program, it is assumed that the above error is corrected instantaneously by the control system. Therefore, the pitch attitude at any time may be written as

$$\theta = \theta_{initial} + \int_0^t q_c\, dt \tag{6.68}$$

where q_c is a table (FTAB01) of pitch rate commands as a function of time. Errors in the pitch program and/or errors in the rate integrating gyro are introduced by including error constants in Equation (6.68) as shown below.

$$\theta = \theta_{initial} + \int_0^t K_{21}\, q_c\, dt + K_{22} + K_{24} + K_{25}\, t + K_{23}\, \frac{RNTP}{|RNTP|} \tag{6.69}$$

where K_{21} = torque constant, nominal value of one
K_{22} = pitch gyro bias, degrees
K_{24} = error in initial pitch alignment, degrees
K_{25} = pitch gyro drift rate, degrees/second
K_{23} = one half pitch dead-band width, degrees
$\frac{RNTP}{|RNTP|}$ = direction of perturbing pitch force due to misalignment of thrust and/or asymmetric aerodynamics

Yaw Rate-Integrating Gyro - The yaw rate integrating gyro errors will cause a rotation of the vehicle about the body z axis and thus introduce a sideslip angle. The resultant force acting on the vehicle will alter the direction of the velocity vector so as to reduce this sideslip angle. The geometry involved is presented in Figure 6.7. The nominal orientation of the body axis is $x_n y_n z_n$; X_{AN} is the nominal velocity vector. The azimuth angle between the $x_n z_n$ plane and the local geocentric system ($X_g Y_g Z_g$) is the nominal azimuthal vehicle attitude, ψ_0. An error in the yaw rate integrating gyro introduces a rotation, ζ, about the body z axis as defined below.

$$\zeta = K_{11} + K_{17} + K_{12}\, t + K_{18}\, (RNTY/|RNTY|) \tag{6.70}$$

126

where K_{11} = yaw gyro bias, degrees
 K_{17} = error in initial yaw alignment, degrees
 K_{12} = yaw gyro drift rate, degrees/second
 K_{18} = one half yaw dead-band width, degrees
 $\dfrac{RNTY}{|RNTY|}$ = direction of perturbing yaw force due to misalignment of thrust and/or asymmetric aerodynamics

The contribution to ζ associated with imperfect zero torquing of the gyro required to maintain zero angle of sideslip is neglected. This contribution can be approximated as an equivalent gyro drift.

The change in azimuth flight path angle associated with vehicle lateral maneuvering reduces the resulting angle of sideslip by ξ, that is

$$\beta_r = \xi - \zeta \tag{6.71}$$

where ξ can be obtained as follows from the geometry of Figure 6.8. By applying the law of sines to the spherical triangle Z_g-M-x_n one obtains

$$\frac{\sin \xi}{\sin (\sigma - \psi_0)} = \frac{\cos \Theta}{\sin d}$$

Again for small β, the sin of d is approximately unity as shown in the discussion of the effect of sinds. The above expression then simplifies to

$$\sin \xi = \cos \Theta \sin (\sigma - \psi_0) \tag{6.72}$$

where ψ_0 is tabulated versus time and is equal to σ of the nominal trajectory.

 Roll Rate-Integrating Gyro - A similar investigation of the lateral displacements due to the roll rate integrating gyro errors is presented below.

The roll angle is developed from the expression:

$$\phi = K_{13} + K_{19} + K_{14} t + K_{20} (RNTR/|RNTR|) \tag{6.73}$$

where K_{13} = roll gyro bias, degrees
 K_{19} = error in initial roll alignment, degrees
 K_{14} = roll gyro drift rate, degrees/second
 K_{20} = one half roll dead-band width, degrees
 $\dfrac{RNTR}{|RNTR|}$ = direction of perturbing roll force due to misalignment of thrust and/or asymmetric aerodynamics

The contribution to ϕ associated with imperfect zero torquing of the gyro required to maintain zero angle of sideslip and bank angle is neglected. These contributions can be approximated as an equivalent gyro drift. The roll angle arising from the roll gyro error will in general introduce a bank angle B_A and a sideslip β_p. The geometry involved is given in Figure 6.9. The velocity X_A is located in an arbitrary position to simulate lateral departures from nominal which have previously accrued. The bank angle can be expressed in terms of the angles b and c as follows:

$$B_A = c - b \tag{6.74}$$

127

GEOMETRY USED TO DETERMINE EFFECT
OF YAW GYRO ERRORS
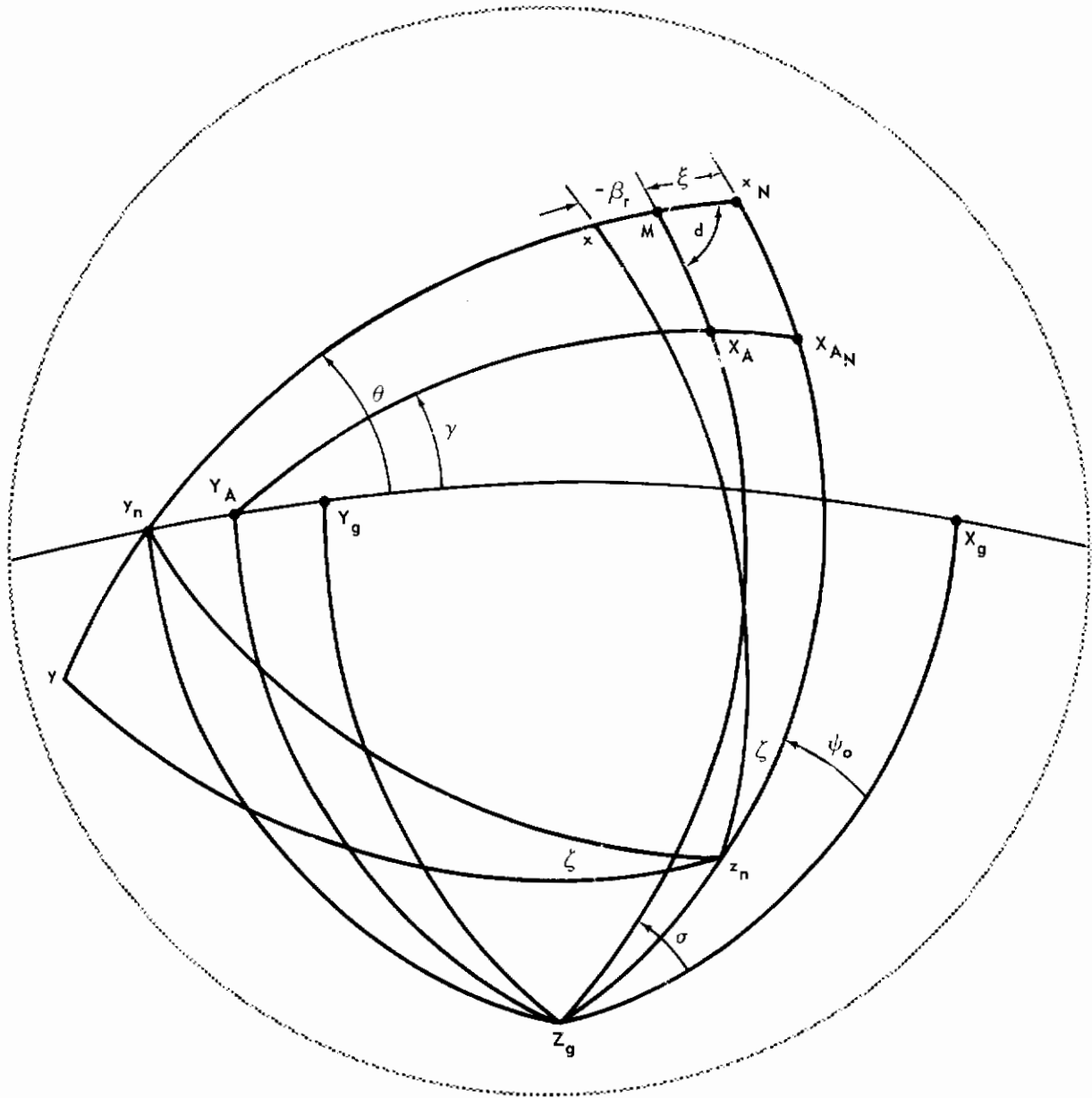
128

GEOMETRY USED TO DETERMINE EFFECT OF ROLL GYRO ERRORS
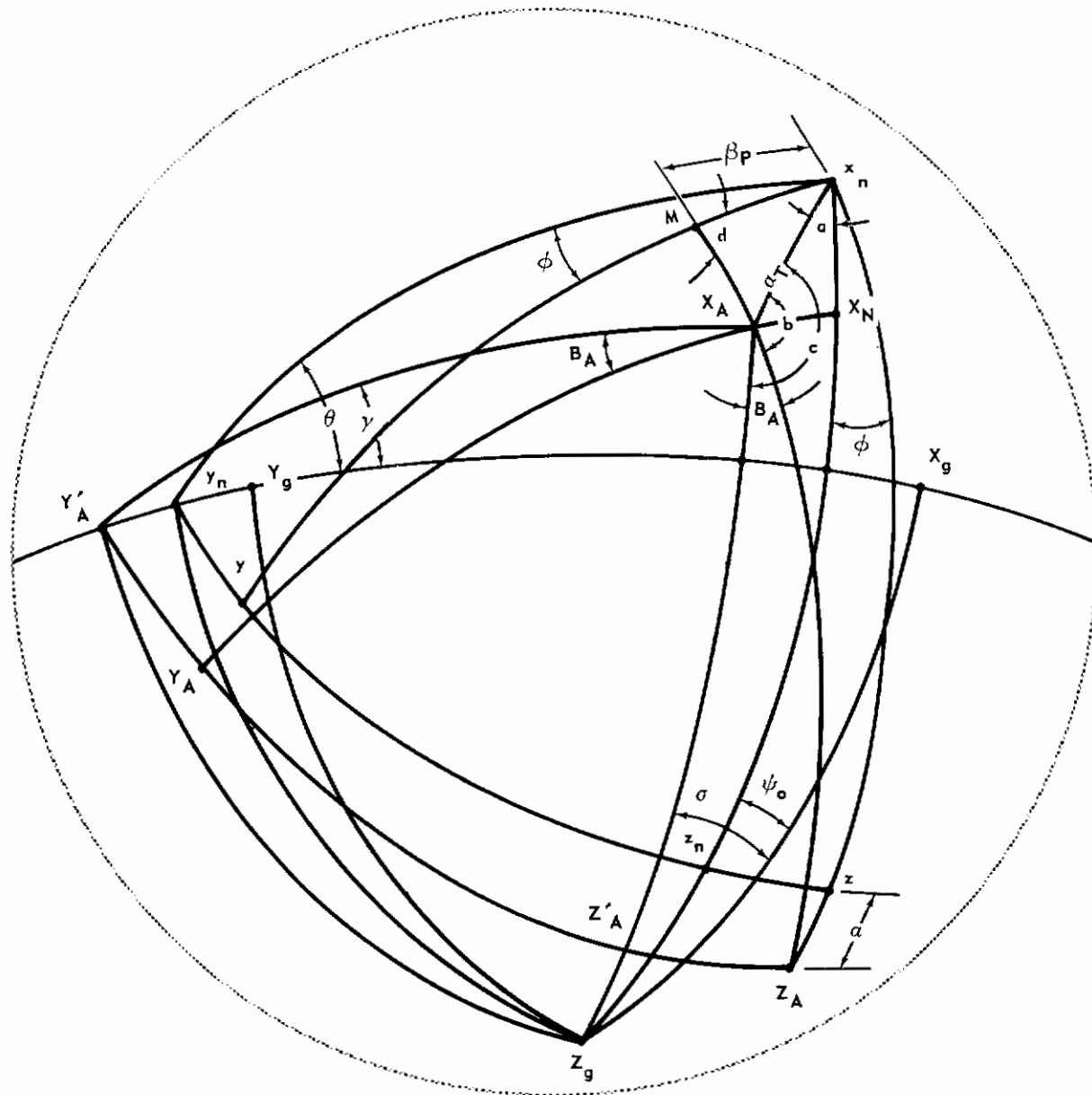
FIGURE 6.9

The angle c may be determined by using the law of sines on the spherical triangle $Z_g X_A x_n$

$$\frac{\sin c}{\cos \Theta} = \frac{\sin (\sigma - \psi_0)}{\sin \alpha_T} \tag{6.75}$$

In order to specify the correct quadrant of the angle c, the tangent of c is also required. The cosine of c is needed and is:

$$\cos c = \frac{-\sin \Theta + \cos \alpha_T \sin \gamma}{\sin \alpha_T \cos \gamma} \tag{6.76}$$

Dividing (6.75) by (6.76), the desired tangent function is obtained.

$$\tan c = \frac{\sin (\sigma - \psi_0) \cos \Theta \cos \gamma}{-\sin \Theta + \cos \alpha_T \sin \gamma} \tag{6.77}$$

The angle b is found in a similar manner from triangle $Z_A X_A x_n$

$$\sin b = \cos \alpha \sin (a + \phi) \tag{6.78}$$

$$\cos b = -\sin \alpha / \sin \alpha_T \tag{6.79}$$

and finally:

$$\tan b = \frac{\sin (a + \phi) \cos \alpha \sin \alpha_T}{-\sin \alpha} \tag{6.80}$$

The angle a is needed in (6.80) and again the tangent function must be used. The sine and cosine of a are required and are determined from triangle $x_n X_A Z_g$ as:

$$\cos a = \frac{-\sin \gamma + \cos \alpha_T \sin \Theta}{\sin \alpha_T \cos \Theta} \tag{6.81}$$

$$\sin a = \frac{\cos \gamma \sin (\sigma - \psi_0)}{\sin \alpha_T} \tag{6.82}$$

Dividing (6.82) by (6.81), the tangent of a is obtained.

$$\tan a = \frac{\cos \gamma \sin (\sigma - \psi_0) \cos \Theta}{-\sin \gamma + \cos \alpha_T \sin \Theta} \tag{6.83}$$

When the total angle of attack is zero, angle a is undefined and the bank angle equals the roll angle. When this occurs, the computation sequence is directed to bypass the bank angle computations presented above, and the bank angle is set equal to the roll angle.

The angle of sideslip associated with vehicle roll is determined from triangle $X_A - M - x_n$.

130

The angle d is again assumed to be 90°. Using this approximation, the expression for β_p is:

$$\text{Sin } \beta_p = \text{Sin } \alpha_T \text{ Sin b} \tag{6.84}$$

The total angle of sideslip due to winds, as well as the roll and yaw gyro errors, is:

$$\beta = \beta_w + \beta_r + \beta_p \tag{6.85}$$

This completes the development of the flight plan programmer which provides expressions for angle-of-attack, angle of sideslip and bank angle which are associated with specified winds and instrument errors. A functional flow diagram of the flight plan programmer is shown in Figure 6.10.

6.3 <u>Structural Temperature Limiting</u> - A subprogram is formulated which will override or modify the commanded functions from an autopilot or flight-plan programmer according to computed structural temperatures and thus alter the trajectory to relieve the aerodynamic heating. The temperature control function is of the form:

Total command = programmed command + Σcommand corrections due to temp-

erature + Σcommand corrections due to temperature time rate of change.

The command parameters may be any term that can be controlled by either the autopilot or flight-plan programmer, but must have the capability to increase (or decrease) the altitude, change the attitude, or to decelerate the vehicle. Several temperatures may be used, each contributing its effect to change the trajectory and relieve the local heating. Since the trajectory change to provide a relief of the temperature at one local point may, in many instances, aggravate the temperature at some other point, the trajectory obtained with the temperature limit functions will represent a compromise between the several controlling temperatures used.

6.3.1 <u>Temperature Limiting Problem Formulation</u> - The method for accomplishing a temperature limiting control, while computing the trajectory, is to modify the command functions generated by the autopilot or flight-plan programmer by incremental commands which are functions of a temperature, or its time derivative. Assuming that pitch attitude is the flight parameter to be controlled, a typical block diagram of the flight-plan programmer (or steering functions for an autopilot) may be as shown on the following page:

131

FUNCTIONAL FLOW DIAGRAM
FLIGHT PLAN PROGRAMMER 10

$$t < t_1$$

Y branch:

$$\theta = \int_o^t K_{21}\, q_c\, dt + K_{22} + K_{24}$$
$$+ K_{25} t + K_{23} \frac{RNTP}{|RNTP|} + \theta_{INITIAL}$$

$$a = \theta - \sin^{-1}\left[\frac{\sin \gamma_A}{\cos(\sigma_A - \sigma)}\right]$$

N branch:

$$a = K_{26}\, a_o$$
$$\theta = a + \sin^{-1}\left[\frac{\sin \gamma_A}{\cos(\sigma_A - \sigma)}\right]$$

$$\beta_w = \sin^{-1}[\cos \theta \sin(\sigma_A - \sigma)]$$
$$\zeta = K_{11} + K_{17} + K_{12} t + K_{18}\frac{RNTY}{|RNTY|}$$
$$\phi = K_{13} + K_{19} + K_{14} t + K_{20}\frac{RNTR}{|RNTR|}$$

$$\text{IF } |\zeta| < K_{15},\ \zeta = 0$$
$$|\phi| < K_{16},\ \phi = 0$$

$$\xi = \sin^{-1}[\cos \theta \sin(\sigma - \psi_o)]$$
$$\beta_r = \xi - \zeta$$

$$a = \tan^{-1}\left[\frac{\cos \gamma \sin(\sigma - \psi_o)\cos \theta}{-\sin \gamma + \cos a_T \sin \theta}\right]$$

$$\beta_p = \sin^{-1}[\sin a_T \sin b]$$

$$b = \tan^{-1}\left[\frac{\sin(a + \phi)\cos a \sin a_T}{-\sin a}\right]$$

$$c = \tan^{-1}\left[\frac{\sin(\sigma - \psi_o)\cos \theta \cos \gamma}{-\sin \theta + \cos a_T \sin \gamma}\right]$$

$$\beta = \beta_w + \beta_r + \beta_p$$

$$\tan^2 a_T = \tan^2 a + \tan^2 \beta$$

$$\text{IS } a_T = 0?$$

N

Y

$$B_A = c - b$$

FPPSF

$$B_A = \phi$$
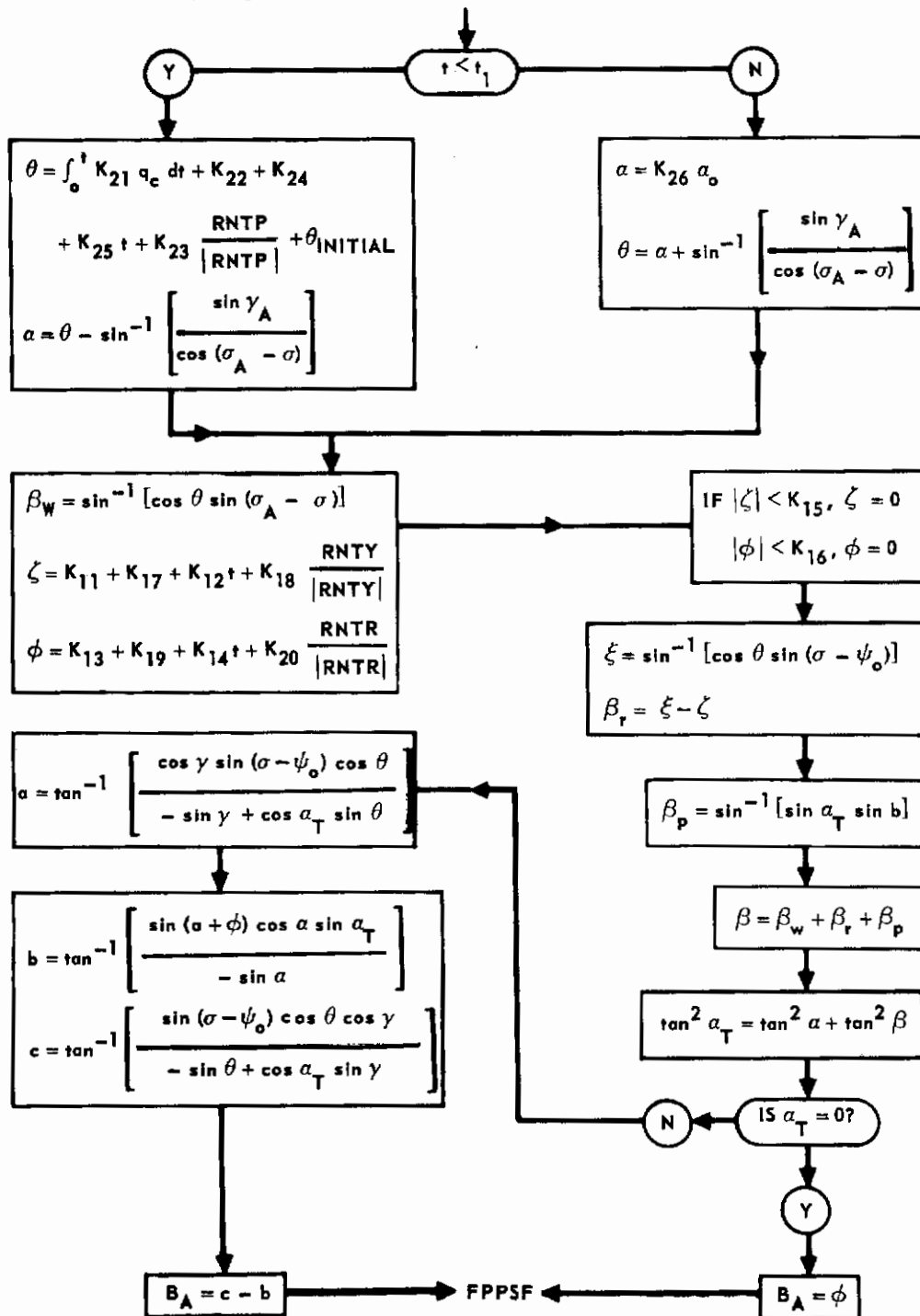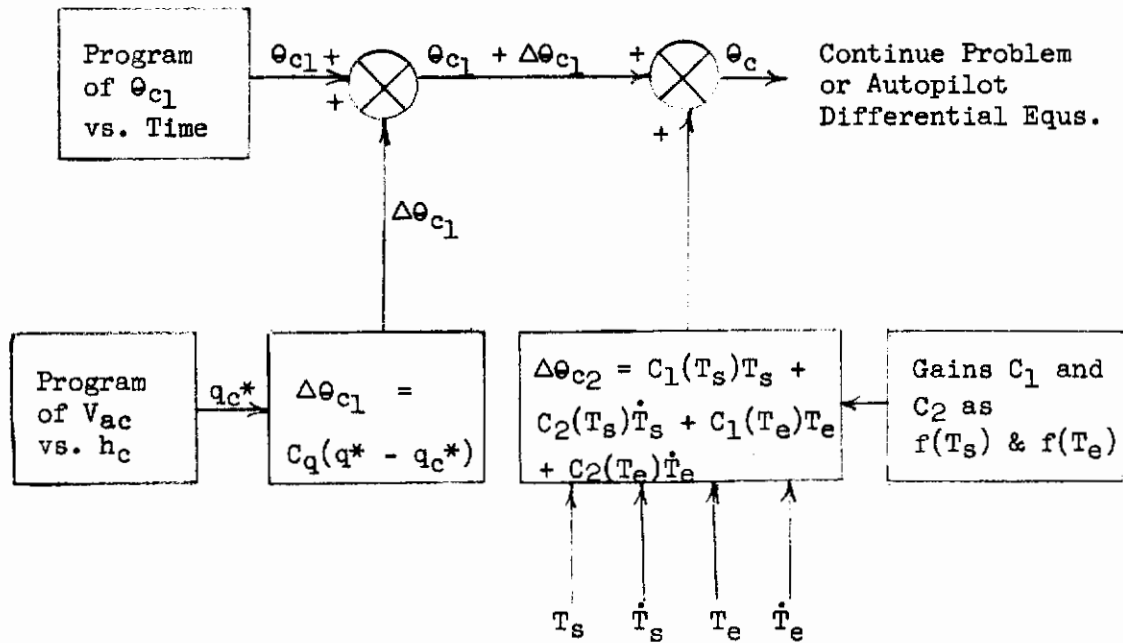
FIGURE 6.10

Figure 6.11 Typical Steering Command
Function Modified by Dynamic Pressure
Error and Structural Heating Limit Feedback

Here, the desired program of Θ versus time is modified by an error in dynamic
pressure and a temperature limiting function which is the subject of the present
analysis. The temperature limiting subprogram is, therefore, a feedback loop
which overrides a programmed command function. The gain factors $C_1(T_s)$, $C_2(T_s)$,
$C_1(T_e)$, and $C_2(T_e)$ are empirical functions of the structural or equilibrium
stagnation temperature which increase in magnitude as the limiting temperature
is approached. The values of the gain factors are selected so that the temp-
erature-limiting subprogram exercises no control when the temperatures are
not critical but completely overrides the basic pitch-attitude command, together
with the corrections due to errors in dynamic pressure, when the temperatures
are close to the limit. The total pitch-attitude command is given by

$$\Theta_c = \Theta_{c_1} + \Delta\Theta_{c_1} + \Delta\Theta_{c_2} = \Theta_{c_1} + C_{q^*}(q^* - q_c^*) + C_1(T_s) T_s$$

$$+ C_2(T_s) \dot{T}_s + C_1(T_e) T_e + C_2(T_e) \dot{T}_e \tag{6.36}$$

For the example case, it is assumed that Θ must be reduced to lower the
structural temperature, T_s. It is further assumed that increasing Θ to get
the missile to a higher altitude will reduce the stagnation-point temperature,
T_e.

133

The gain factors are introduced into the program as tabular listing of temperature. The form and magnitude of these gain factors will be considered in the discussion of an example problem, Paragraph 6.3.2. The temperatures, and their time derivatives, used as intelligence for the temperature limiting loop are computed in the temperature monitoring subprogram which is described in Section 7.

The control quantities which can be modified by the temperature limiting subprogram may be any parameter which, when altered by the flight-plan programmer or the autopilot, will change the trajectory to relieve the temperatures. Typical command parameters may be

(a) Angle of Attack, α

(b) Lift Coefficient, C_L

(c) Aerodynamic Roll Angle, ϕ_A

(d) Pitch Control-Surface Deflection, δ_q

as well as the pitch attitude example used in the explanation above. The value and form of the gain factor functions selected will depend upon the parameter which they are modifying and, until more experience is gained with this type of control, will have to be determined experimentally. It should be further noted that several structural or equilibrium stagnation-point temperatures may be used to compute the temperature limiting correction instead of only one, as used in the original explanation. Each temperature would have its own gain factors in this case.

Figure (6.12) presents a functional flow diagram of the temperature-limiting subprogram computation for the flight-plan programmer shown in Figure (6.11). The computation of the dynamic pressure feedback correction is not considered part of the present analysis and is, therefore, omitted. It is further assumed, for the diagram of Figure (6.12), that lateral aerodynamic forces are to be kept very small and that the body yaw angle is commanded to be the instantaneous azimuth angle. The operation of the flight-plan programmer is explained in Section 6.2.

6.3.2 <u>Example Formulation</u> - An example formulation of a temperature limiting program, as applied to a body-attitude-angle flight-plan programmer, is now presented with particular attention given to the method of determining the gain factors C_1, C_2, etc. The values of the gain factors should be such that, as T_s approaches the allowable upper limit, the commanded angle of attack (related to the pitch angle, Θ) should go to zero. Also, as T_e approaches its upper limit, angle of attack should be increased to give a climb into less dense atmosphere. The corrections provided by these two temperatures are in opposition to each other and will, therefore, produce a pitch command which will hunt for a compromise attitude angle. Since Θ is related to α through the flight-path angle, γ, an instantaneous change in Θ effectively changes α. Assume, for example, that the allowable structure and equilibrium stagnation temperatures are $1000^\circ R$ and that the maximum angle of attack anticipated from the commanded pitch attitude is on the order of 10 degrees. A typical

134

INPUT DATA FOR TEMPERATURE LIMITING SUBPROGRAM

T_s, $\dot{T}_s$ FROM THIN SKIN PROGRAM

T_e, $\dot{T}_e$ FROM EQUILIBRIUM STAGNATION TEMP-
ERATURE PROGRAM

TABULAR LISTING OF $C_1(T_s)$ AND $C_2(T_s)$ AS $f(T_s)$

TABULAR LISTING OF $C_1(T_e)$ AND $C_2(T_e)$ AS $f(T_e)$

COMPUTE $\Delta\theta_{C_2}$

$$\Delta\theta_{C_2} = C_1(T_s)T_s + C_2(T_s)\dot{T}_s + C_1(T_e)T_e + C_2(T_e)\dot{T}_e$$

TRANSFER TO FLIGHT PROGRAMMER

COMMAND

$\theta_{C_1} = f(t, M_N, \text{ or } V_a)$

$\psi_C = \sigma$

NO DYNAMIC PRESSURE FEEDBACK

COMPUTE θ_C

$$\theta_C = \theta_{C_1} + \Delta\theta_{C_2}$$

COMPUTE α

CONTINUE
PROBLEM

FIGURE 6.12   FUNCTIONAL FLOW DIAGRAM - TEMPERATURE LIMITING PROGRAM
COMBINED WITH COMMANDED BODY ATTITUDE ANGLES FLIGHT PROGRAMMER

135

example of the form of $C_1(T_s)$ is shown in Figure (6.13).
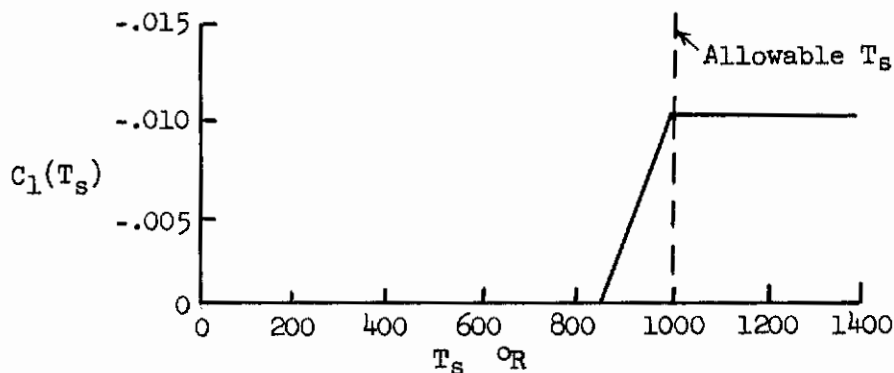
Figure 6.13 Gain Factor $C_1(T_s)$ as a Function of T_s

The gain factor $C_1(T_s)$ shown here has the property that as the skin temperature reaches $850^\circ R$, the attitude angle starts decreasing proportional to $C_1(T_s) \times T_s$, and is reduced by 10 degrees as the allowable structural temperature is approached. From then on, the decrease is directly proportional to the temperature, T_s. The gain factor $C_1(T_e)$ might have a similar form as shown in Figure (6.14).
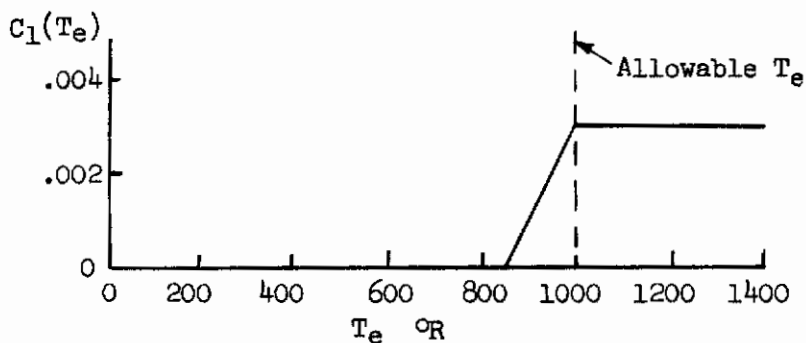
Figure 6.14 Gain Factor $C_1(T_e)$ as a Function of T_e

This gain factor function would increase the attitude angle by 3 degrees as the allowable equilibrium stagnation temperature is approached.

The form of the gain factors that multiply the temperature derivatives are similar to the factors discussed previously, but are slightly more complicated to derive. These factors, in effect, must anticipate the temperature gradient and start corrective action that will take into account the response time required to provide a relief. Assume that 10 seconds are required for corrective action to be felt by the vehicle and that the maximum temperature rate to be expected is on the order of 20 degrees per second. At this rate, in 10 seconds, a temperature rise of 200 degrees would occur. Therefore, if

this rate is encountered when the temperature is already 800 degrees corrective action must be occurring. Assuming further that only about a 3 degrees change in angle will be sufficient to start the corrective action, typical $C_2(T_s)$ and $C_2(T_e)$ gain functions would be as shown in Figures (6.15) and (6.16).
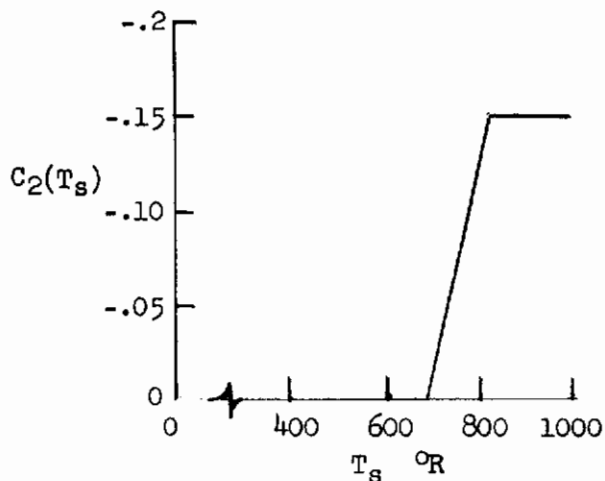
Figure 6.15 Gain Factor $C_2(T_s)$
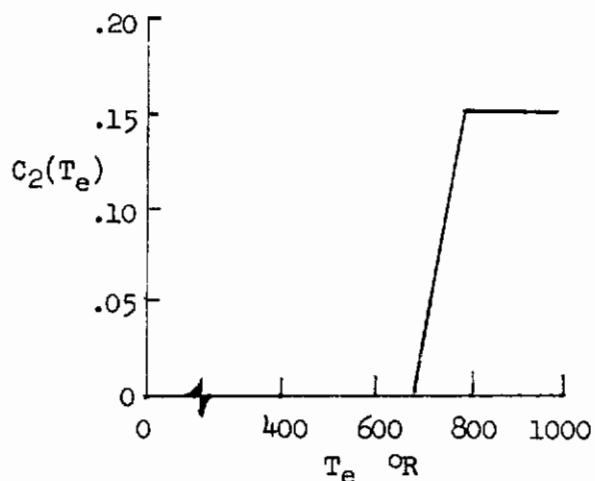
Figure 6.16 Gain Factor $C_2(T_e)$

6.3.3 <u>Discussion</u> - It should be noted that the preceding explanation is only an example of the problem solution philosophy to be used. The actual form of the gain-factor functions will have to be determined empirically and will depend upon the aerodynamic, thermodynamic, and inertia characteristics of the vehicle, the control used, and the anticipated flight path.

The temperature computation subprogram of Section 7 is an approximate solution of the thin-skin temperature of a two-dimensional flat plate and of the equilibrium stagnation-point temperature. This computation is used in lieu of a more exact program due to machine storage limitations and computation time. Since the temperatures computed are not exact, the allowable temperature used in specifying the gain factors should account for the approximations involved.

Special flight conditions and/or particular combinations of allowable skin and stagnation-point temperatures may preclude temperature limiting by the method outlined. An example situation may occur when the vehicle is in a vertical climb with the equilibrium stagnation-point temperature reaching its allowable limit. In such a case, the normal correction command would be to increase the angle of attack, but the particular flight attitude is such that the maximum relieving action may be occurring. Unless the increase in angle of attack produced a substantial increase in drag, and therefore a deceleration, the corrective action given by the present program may not produce the desired results. Another situation which may occur is when the allowable temperatures are specified so low that, regardless of the maneuver of the vehicle, the limiting temperatures will be exceeded. It is necessary, therefore, to examine the physical situation of the flight and the control requested before the temperature limiting program is used.

137

7. AERODYNAMIC HEATING SUBPROGRAMS

The SDF computer program includes a subprogram to monitor a characteristic structural temperature or aerodynamic heating rate. In addition to providing a knowledge of the heating parameter, or temperatures, the aerodynamic heating subprogram also provides input information for an alternate flight-path control program so that the degree of heating may be partially controlled. The aerodynamic heating subprogram may also provide a reference temperature to the aerodynamic data input subprogram for use in modifying aerodynamic coefficients for the effects of structural temperature on static aeroelasticity.

To satisfy the auxiliary requirements of the aerodynamic heating program requires a problem formulation which will account for the variation in local flow properties with angle of attack, boundary-layer type, Mach number, altitude, and type of structure. However, the problem of aerodynamic heating is a complicated one and a detailed analysis of the temperatures in an actual structure requires an extensive computation. In view of the extensive computations associated with the SDF computer program, it is necessary to simplify the aerodynamic heating subprogram as much as possible while retaining those features of the solution required for the rest of the program.

The aerodynamic heating subprogram formulation outlined in this section is made up of two parts; one of which computes the thin-skin temperature of a flat surface at angle of attack assuming two-dimensional flow with an attached shock wave; and the second which computes the equilibrium stagnation temperature on a hemispherical, or hemicylinder, nose. The combination of these two problem formulations provides temperatures with the required properties which are of sufficient accuracy for the monitoring and control purposes of this program. More exact analyses of the heating of particular structures must, of course, be performed with more sophisticated heating problem formulations which are beyond the scope of this analysis.

7.1 <u>Thin-Skin Temperature of Arbitrary Wedge at Angle of Attack</u>. - The computation of the thin-skin temperature of a two-dimensional flat surface at angle of attack, as applied to the aerodynamic heating subprogram of the SDF computer program, is developed as follows:

Ignoring conduction into the structure, the basic heat energy-balance equation for an element of skin is:

$$Q_c - Q_r = Q_s \qquad (7.1)$$

which states that the heat energy stored in the skin is the difference between the convective heat input and the heat radiated to space. Basic definitions of the three quantities involved may be expressed as:

$$Q_c = \frac{h}{c_p} \ (H_{aw} - H_s) \qquad (7.2)$$

$$Q_r = \sigma \epsilon_s (T_s^4 - T_r^4) \qquad (7.3)$$

$$Q_s = \delta_s \rho_s c_{p_s} \dot{T}_s \qquad (7.4)$$

138

Although relatively simple in appearance, the resulting differential equation has non-linear coefficients thereby complicating the solution when classical methods are used. However, the predictor-corrector integration subroutine used in the SDF computer program allows the problem to be solved with a reasonable amount of computation effort.

Solving for $\dot{T}_s$ gives

$$\dot{T}_s = \frac{h}{\delta_s \rho_s c_{p_s} c_p} (H_{aw} - H_s) - \frac{\sigma \epsilon_s}{\delta_s \rho_s c_{p_s}} (T_s^4 - T_r^4) \qquad (7.5)$$

where c_{p_s} and ϵ_s are properties of the skin material and surface coating, and h, c_p, and H_s are properties of the air flowing over the point on the body under consideration, both of which are functions of T_s, the skin temperature.

The auxiliary functions defining the properties noted above will now be defined. The method of defining the heat transfer properties is based upon the reference enthalpy method outlined by Eckert in Reference (21). The convective heat input to the skin depends upon the heat transfer coefficient, which is defined by Reference (21) as:

$$Nu = \frac{h l_H}{K^*} = K_H (R_N^*)^{Y_H} (P_r^*)^{1/3}$$

The notation (*) signifies that the quantities are based upon the reference enthalpy. Letting $K^* = c_p^* \mu^* / P_r^*$ and solving for the heat transfer coefficient, h, gives

$$h = \frac{K_H c_p^* \mu^*}{l_H} (R_N^*)^{Y_H} (P_r^*)^{-2/3} \qquad (7.6)$$

The polynomial

$$H = D_1 + D_2 T + D_3 T^2 \qquad (7.7)$$

approximates, the curve of enthalpy as a function of temperature given by Keenan and Kaye, Reference (22). The constants are:

$$D_1 = -94.38$$

$$D_2 = 0.2331$$

$$D_3 = 8.4 \times 10^{-6}$$

Equation (7.7) may be used to compute the enthalpy of the air at the skin temperature, T_s, or the enthalpy of the flow outside the boundary layer corresponding to the local flow temperature, T_2. The inverse relation between enthalpy and temperature is given by:

$$T = D_4 + D_5 H + D_6 H^2 \qquad (7.8)$$

139

where

$$D_4 = 400$$

$$D_5 = 3.829$$

$$D_6 = -1.978 \times 10^{-4}$$

Equations (7.7) and (7.8) are valid for the Keenan and Kaye enthalpy temperature variation to approximately 8000°R but disregard the effects of dissociation or ionization. These real gas effects become apparent at approximately 4000°R, see Figure (7.1). However, within the range of temperatures (either local or structural) which are tolerable by aircraft of the foreseeable future, the effects of dissociation are negligible and the Keenan and Kaye curve is considered valid. For this reason the effects of pressure are omitted from the relations for enthalpy, Equations (7.7) and (7.8). The reference enthalpy is empirically defined in Reference (21) as:

$$H^* = H_2 + 0.5(H_s - H_2) + 0.22(H_{aw} - H_2) \tag{7.9}$$

The adiabatic wall temperature is given by

$$H_{aw} = H_2 + \frac{r_H V_2^2}{2Jg_{ref}} = H_2 + \frac{r_H V_2^2}{5.012 \times 10^4} \tag{7.10}$$

The constants K_H and Y_H, used in Equation (7.6) and the recovery factor r_H, used in Equation (7.10), depend upon the local Reynolds number of the point on the surface under consideration. If R_{N_2} is less than $R_{N_{critical}}$, the flow is assumed to be laminar and the constants have the values:

$$K_H = 0.332$$

$$Y_H = 0.500$$

$$r_H = 0.850$$

If R_{N_2} is greater than $R_{N_{critical}}$, the flow is assumed to be turbulent and the constants are accordingly revised to

$$K_H = 0.0296$$

$$Y_H = 0.800$$

$$r_H = 0.900$$

The heat capacity and emissivity characteristics of the skin are functions of the skin temperature, so that

$$\epsilon_s = f_1(T_s) \tag{7.11}$$

and

$$c_{p_s} = f_2(T_s) \tag{7.12}$$

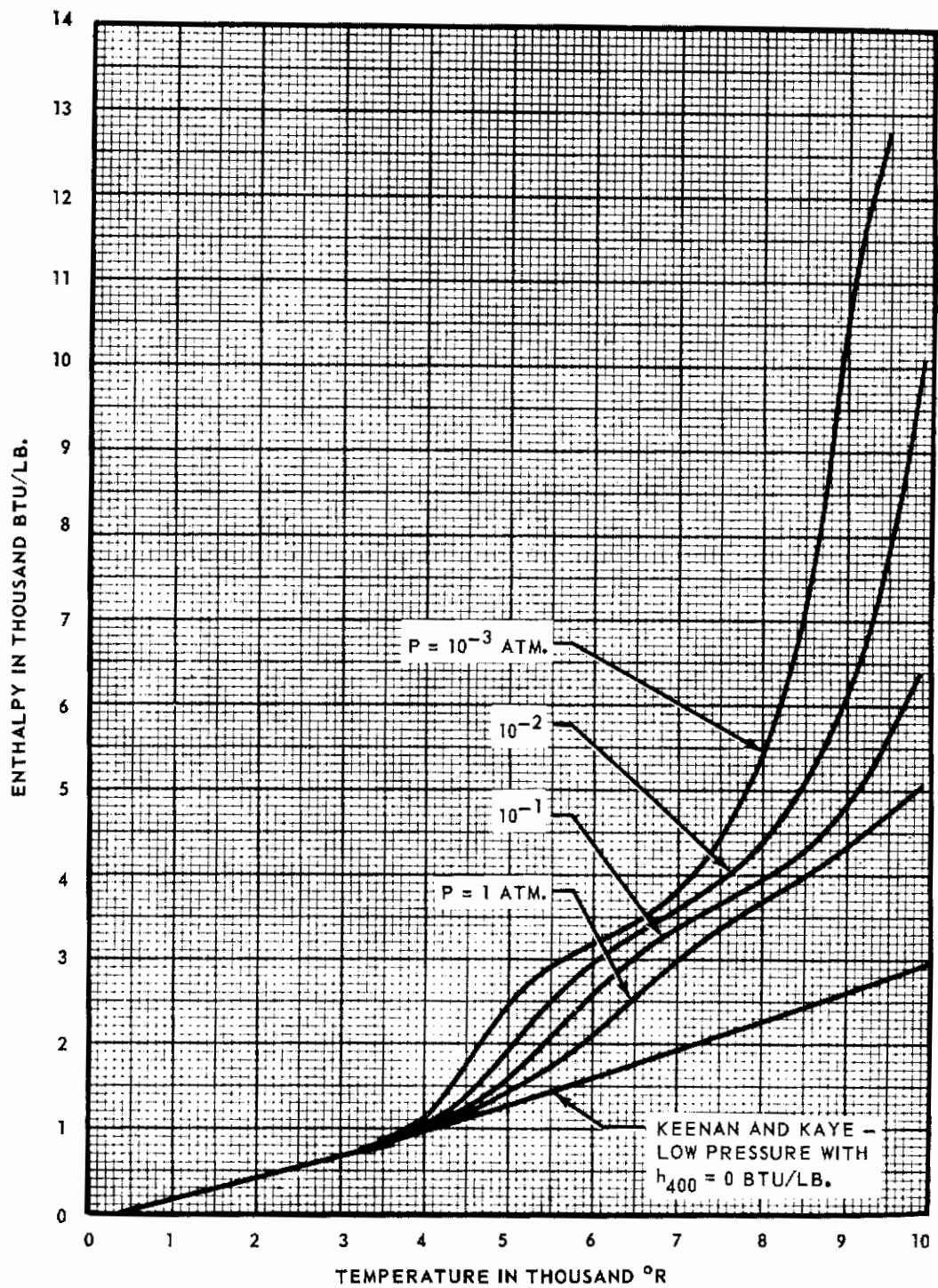will be introduced as two-dimensional interpolations of tabular listings.

FIGURE 7.1, ENTHALPY OF DISSOCIATED AND IONIZED AIR PER AEDC-TN-56-12

141

The viscosity variation with temperature has been taken as Sutherland's relation

$$\mu^* = 1.18 \times 10^{-5} \left(\frac{716}{T_H{}^* + 216} \right) \left(\frac{T_H{}^*}{500} \right)^{3/2} \tag{7.13}$$

which also neglects the effects of dissociation.

The temperature $T_H{}^*$ may be computed by Equation (7.8) when H is H*. The local flow parameters, based upon the reference enthalpy, are defined by

$$\rho^* = \frac{P_2}{53.3 \ T_H{}^*} \tag{7.14}$$

$$R_N{}^* = \frac{\rho^* V_2 l_H}{\mu^*} \tag{7.15}$$

A functional flow diagram outlining the sequence of computations to perform the entire analysis, including the computation of local flow conditions discussed in Section 7.3, is shown in Figure 7.2.

The thin-skin temperature computation formulated in this section is probably limited to angles of attack less than 30 degrees because of inadequacies in the computation of the convective heat transfer coefficient and the limit at which the shock wave is attached. At higher angles of attack the coefficient computed by the present method is considered to be too low. However, it is the purpose of the present analysis to provide a program to the SDF computer program which will (a) monitor the gross effects of aerodynamic heating, (b) implement the aerothermo-elasticity tie-in of the aerodynamic characteristics, and (c) provide a temperature feedback reference for the corrective action portion of the autopilot program. Detailed aerodynamic heating computations may be performed by more sophisticated methods using the present formulation as an indication of trajectories on flight conditions for which aerodynamic heating considerations are important.

7.2 Equilibrium Stagnation-Point Temperature. – The stagnation-point equilibrium temperature is obtained by equating the convective heat flux to the heat flux radiated to space. The heat flux to the stagnation-point of a hemisphere can be predicted by the empirical method of Reference (23) which is based on the analytical solution of Reference (24) and has been successfully correlated with test data. Use of the method of Reference (23) results in heat transfer rates[1] which are slightly higher than those predicted by the theory of Reference (24) for Mach numbers less than 18, and is employed because of its simplicity.

---

(1) The heat transfer coefficients predicted by Reference (23) are approximately 6 per cent higher than those given by the theory of Reference (24) for Mach numbers on the order of 9 and for the altitude range of 100,000 to 250,000 feet.

Initial Heating Input Data and Constants

ℓ_H, RN_{crit}, δ_s, ρ_s, σ, P^*, T_r, D_7 Initial Skin Temperature T_{sn-1}

Input Data From Central Program M_N, V_a, P, T, ρ, α

Compute $\alpha_H = (D_7 + \alpha)'$ Deg. Change α_H to Radians

$$C_p = 2\alpha_H^2\left(0.6 + \sqrt{0.36 + \frac{1}{(M_N\alpha_H)^2}}\,\right)$$

$$\frac{P_2}{P} = 0.7\,C_p M_N^2 + 1 \quad \therefore \quad P_2 = \left(\frac{P_2}{P}\right)P$$

$$\frac{\rho_2}{\rho} = \frac{6(P_2/P)+1}{6 + P_2/P} \quad \therefore \quad \rho_2 = \left(\frac{\rho_2}{\rho}\right)\rho(32.174)\,Lb/Ft^3$$

$$\frac{T_2}{T} = \frac{P_2/P}{\rho_2/\rho} \quad \therefore \quad T_2 = \left(\frac{T_2}{T}\right)T$$

Compute:

$$M_N = \sqrt{\sqrt{\frac{6}{7}}\left(\frac{P_2}{P}\right) + \frac{1}{7}}$$

$$\beta = Sin^{-1}\left(\frac{M_{N_n}}{M_N}\right)$$

$$M_{N_2} = \left(\frac{5}{6(\rho_2/\rho)-1}\right)^{1/2}\frac{1}{Sin(\beta-\alpha_H)}$$

$$V_2 = M_{N_2}\,49.1\sqrt{T_2}$$

Compute:

$$\mu_2 = 1.18 \times 10^{-5}\left(716/(T_2+216)\right)\left((T_2/500)^{3/2}\right)$$

$$RN_2 = (\rho_2 V_2 \ell_H)/\mu_2$$

→ (A)

Compare $RN_2 \longrightarrow RN_{crit}$

If $RN_2 \geq RN_{crit}$ Then

$K_H = 0.0296$
$Y_H = 0.8000$
$r_H = 0.9000$

If $RN_2 < RN_{crit}$ Then

$K_H = 0.332$
$Y_H = 0.500$
$r_H = 0.850$

Compute

$$H_2 = D_1 + D_2 T_2 + D_3 T_2^2$$

$$H_{AW} = H_2 + \left(\frac{r_H V_2^2}{5.012 \times 10^4}\right)$$

→ (B)

$$\dot{T}_s = \frac{K_H \mu^*}{\ell_H \delta_s \rho_s C_{ps}} * Y_H (RN_N^*)^{-2/3} (P_r^*)(H_{AW}-H_S) - \frac{\sigma \epsilon_s}{\delta_s \rho_s C_{ps}}(T_S^4 - T_r^4)$$

Solve Equation for T_S

Auxiliary Defining Equations as Functions of T_S are:

$$H_S = D_1 + D_2 T_S + D_3 T_S^2$$

$$H^* = H_2 + 0.5(H_S - H_2) + 0.22(H_{AW} - H_2)$$

$$T_H^* = D_4 + D_5 H^* + D_6 H^{*2}$$

$$\mu^* = 1.18 \times 10^{-5}\left(\frac{716}{T_H^*+216}\right)\left(\frac{T_H^*}{500}\right)^{3/2}$$

$$\rho^* = \frac{P_2}{53.3\,T_H^*}$$

$$RN_N^* = \frac{\rho^* V_2 \ell_H}{\mu^*}$$

$$C_{ps} = f_1(T_S) \quad \text{(Tabular Listing)}$$

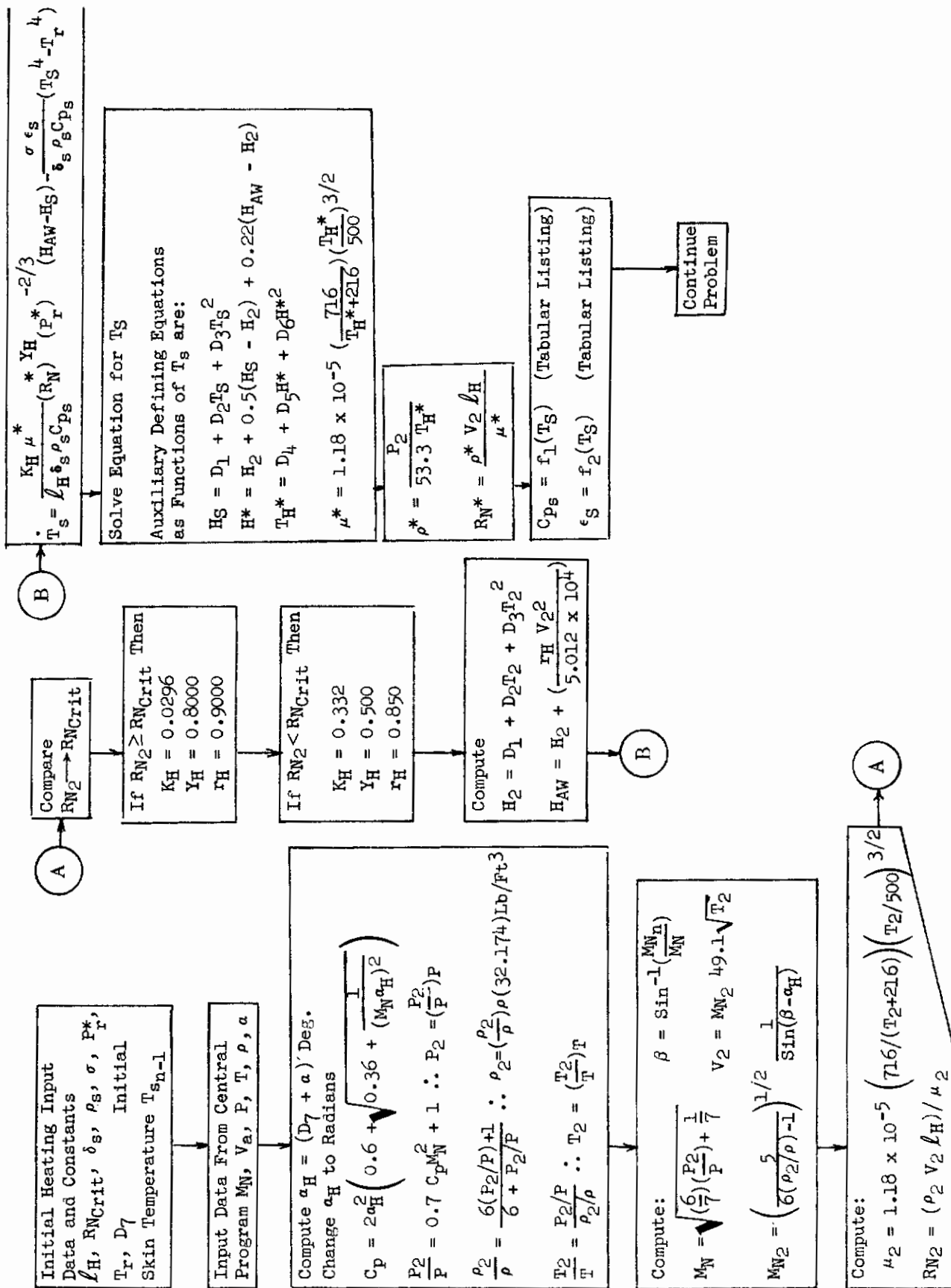$$\epsilon_S = f_2(T_S) \quad \text{(Tabular Listing)}$$

→ Continue Problem

FIGURE 7.2 FUNCTIONAL FLOW DIAGRAM – SKIN TEMPERATURE OF A WEDGE AT ANGLE OF ATTACK

143

The method assumes conditions of equilibrium dissociation behind the normal shock wave and expresses the stagnation-point heat-flux rate by the following empirical equation:

$$Q_c = \frac{17600}{\sqrt{r_n}} \sqrt{\frac{\rho}{\rho_{SL}}} \left(\frac{V_a}{26000}\right)^{3.15} \left(\frac{H_T - H_e}{H_T - H_{ref}}\right) \tag{7.16}$$

where H_e is given by Equation (7.7) substituting T_e for the temperature and H_T is given by

$$H_T = H_o + \frac{V_a^2}{5.012 \times 10^4} \tag{7.17}$$

The heat flux radiated to space is

$$Q_r = \sigma \epsilon_e \left(T_e^4 - T_r^4\right) \tag{7.18}$$

so that a quartic equation is obtained for the equilibrium temperature. A closed solution exists for the roots of this equation but the manipulations are rather tedious, involving the extraction of both cube and square roots. If a linear variation of the emissivity, ϵ_e, is assumed, the equation is of fifth-order and solvable only by iterative techniques. For this reason the following linearization is adopted. (An approximation for the emissivity, ϵ_e, is also made later in the analysis.) If the equilibrium temperature for the current instant of time is related to a previous solution by

$$T_{e_n} = T_{e_{n-1}} + \Delta T_e \tag{7.19}$$

then the quantity

$$T_{e_n}^4 = (T_{e_{n-1}} + \Delta T_e)^4$$

can be expanded to a polynomial in the equilibrium temperature. The expansion gives

$$T_{e_n}^4 = T_{e_{n-1}}^4 + 4T_{e_{n-1}}^3 \Delta T_e + 6T_{e_{n-1}}^2 \Delta T_e^2 + 4T_{e_{n-1}} \Delta T_e^3 + \Delta T_e^4$$

which may be approximated by

$$T_{e_n}^4 = T_{e_{n-1}}^4 + 4T_{e_{n-1}}^3 \Delta T_e$$

since the change in equilibrium temperature is small compared to the temperature itself. The heat radiated may then be approximated by

$$Q_r = \epsilon_{e_{(n-1)}} \left(4T_{e_{n-1}}^3 T_{e_n} - 3T_{e_{n-1}}^4 - T_r^4\right) \tag{7.20}$$

where ϵ_e is approximated by the value at the last known temperature T_e. This equation, linear in the equilibrium temperature, may be used in the solution of the problem. Since the change in equilibrium temperature is small compared to the absolute value of the temperature from the last solution, the above approximation results in only a small error in most cases. If an iteration is used in conjunction with this linearization, the error is further reduced.

144

An alternate equation will be obtained for the enthalpy, since the curve fit of Equation (7.7) is other than linear, thereby complicating the solution for T_e. Therefore

$$H_e = H_{e_{n-1}} + \Delta He$$

but, by definition,

$$H_b - H_a = \int_{Ta}^{Tb} c_p \, dT$$

Therefore, if $\bar{c}_p$ is the average specific heat between T_e and $400^\circ R$, then

$$H_e = \bar{c}_p (T_e - 400)$$

where the constant 400 is included to adjust the absolute value of the enthalpy at a given temperature. This constant is consistent with the reference enthalpy curve of Reference (22) and Figure (7.1).

Then

$$H_{e_{n-1}} = \bar{c}_{p_{n-1}} (T_{e_{n-1}} - 400)$$

and

$$H_{e_n} = \bar{c}_{p_n} (T_{e_n} - 400)$$

The enthalpy variation with temperature is nearly linear, so that

$$\bar{c}_{p_{n-1}} = \bar{c}_{p_n}$$

when ΔT is small. Then the enthalpy may be written

$$H_{e_n} = \frac{H_{e_{n-1}}}{(T_{e_{n-1}} - 400)} (T_{e_n} - 400) \qquad (7.21)$$

Equating Equations (7.16) and (7.20), substituting Equation (7.21) for enthalpy and solving for T_{e_n}, the relation

$$T_{e_n} = \frac{\dfrac{17600}{\sqrt{r_n}} \sqrt{\dfrac{\rho}{\rho_{SL}}} \left[\dfrac{V_a}{26000}\right]^{3.15} \left[\dfrac{H_T + \dfrac{400}{T_{e_{n-1}} - 400} (D_1 + D_2 T_{e_{n-1}} + D_3 T_{e_{n-1}}^2)}{H_T - H_{ref}} \right] + \sigma \epsilon_{e_{n-1}}(3T_{e_{n-1}}^4 + T_r^4)}{\dfrac{17600}{\sqrt{r_n}} \sqrt{\dfrac{\rho}{\rho_{SL}}} \left[\dfrac{V_a}{26000}\right]^{3.15} \left[\dfrac{(D_1 + D_2 T_{e_{n-1}} + D_3 T_{e_{n-1}}^2)}{(H_T - H_{ref})(T_{e_{n-1}} - 400)} \right] + 4 \sigma \epsilon_{e_{n-1}} T_{e_{n-1}}^3}$$

is obtained.

$$(7.22)$$

145

A functional flow diagram outlining the sequences of computations required is shown in Figure (7.3). The values of the constant parameters have been combined with the empirical constants in the convective heat flux equation. Note that an interation loop is provided to improve accuracy if considered necessary by the analyst.

This computation may be made applicable to the stagnation line of a yawed hemicylinder, approximating a swept-wing leading edge, by suitably altering Equation (7.22) for the revised definition of convective heat input, Equation (7.16), to the following:[2]

$$Q_c = \frac{17600}{\sqrt{r_n}} \sqrt{\frac{\rho}{\rho_{SL}}} \left(\frac{V_a}{26000}\right)^{3.15} \left(\frac{H_{T_1} - H_e}{H_{T_1} - H_{ref}}\right) \left(\sqrt{\frac{3}{4}} \, \cos \lambda_{LE}\right) \quad (7.23)$$

where

$$H_{T_1} = H_T - (H_T - H)(1 - r_H) \, \sin^2 \lambda_{LE}$$

or

$$H_{T_1} = H_T - 0.15(H_T - H) \, \sin^2 \lambda_{LE}$$

7.3 Local Flow Conditions. - Sections 7.1 and 7.2 describe the skin temperature computation except for the determination of the local flow conditions - P_2, ρ_2, T_2, M_{N2}, μ_2, and R_{N2}. These parameters must be computed using trajectory quantities obtained from the remainder of the program. The two-dimensional pressure on a wedge with an attached shock wave (Reference (25) is correlated by the similarity parameter $M_N \sin (\alpha_H)$ as shown in Figure (7.4). Also shown in this figure is the pressure predicted by the Tsien hypersonic similarity relation given in Reference (26), Page 263, which is

$$C_p = \alpha_H^2 \left[0.6 + \sqrt{.36 + \frac{1}{(M_N \, \alpha_H)^2}} \right] \quad (7.24)$$

where C_p is defined as the pressure coefficient for the pressure ratio across the oblique shock wave and α_H is the total angle of attack of the surface (i.e., the sum of the angle of attack and the surface wedge angle).

$$C_p = \frac{1}{0.7 \, M_N^2} \left[\frac{P_2 - P}{P} \right] \quad (7.25)$$

$$\alpha_H = D_7 + \alpha \quad (7.26)$$

---

(2) At the higher Mach numbers the variation of Q_c with sweep back is more nearly proportional to $\cos^{3/2} \lambda_{LE}$.

INITIAL HEATING INPUT DATA σ, ϵ_e, T_R, H_{REF}, r_n
ESTIMATE OF INITIAL NOSE STAGNATION TEMPERATURE T_{en-1}

INPUT DATA FROM CENTRAL PROGRAM V_a, T, ρ

COMPUTE:

$$H = D_1 + D_2 T + D_3 T^2 \qquad H_T = H + (V_a^2/5.012 \times 10^4)$$

$$H_{en-1} = D_1 + D_2 T_{en-1} + D_3 T_{en-1}^2 \qquad \epsilon_{en-1} = f(T_{en-1}) \text{ TABULAR LISTING}$$

$$T_{en} = \frac{\sigma \epsilon_{en-1}(3T_{en-1}^4 + T_R^4) + 361000\left(\dfrac{\rho}{r_n}\right)^{1/2}\left(\dfrac{V_a}{26000}\right)^{3.15}\dfrac{(H_T - H_{REF})}{(T_{en-1} - 400)}H_{en-1} + 144400000\left(\dfrac{\rho}{r_n}\right)^{1/2}\left(\dfrac{V_a}{26000}\right)^{3.15}\dfrac{(H_T - H_{REF})}{(T_{en-1} - 400)}H_{en-1}}{4\,\sigma \epsilon_{en-1}T_{en-1}^3 + 361000\left(\dfrac{\rho}{r_n}\right)^{1/2}\left(\dfrac{V_a}{26000}\right)^{3.15}\dfrac{(H_T - H_{REF})}{(T_{en-1} - 400)}H_{en-1}}$$

FIRST TIME ONLY OR IF REQUESTED

$\dfrac{|T_{en} - T_{en-1}|}{T_{en}} < 0.005$

NO → $T_{en-1} = T_{en}$
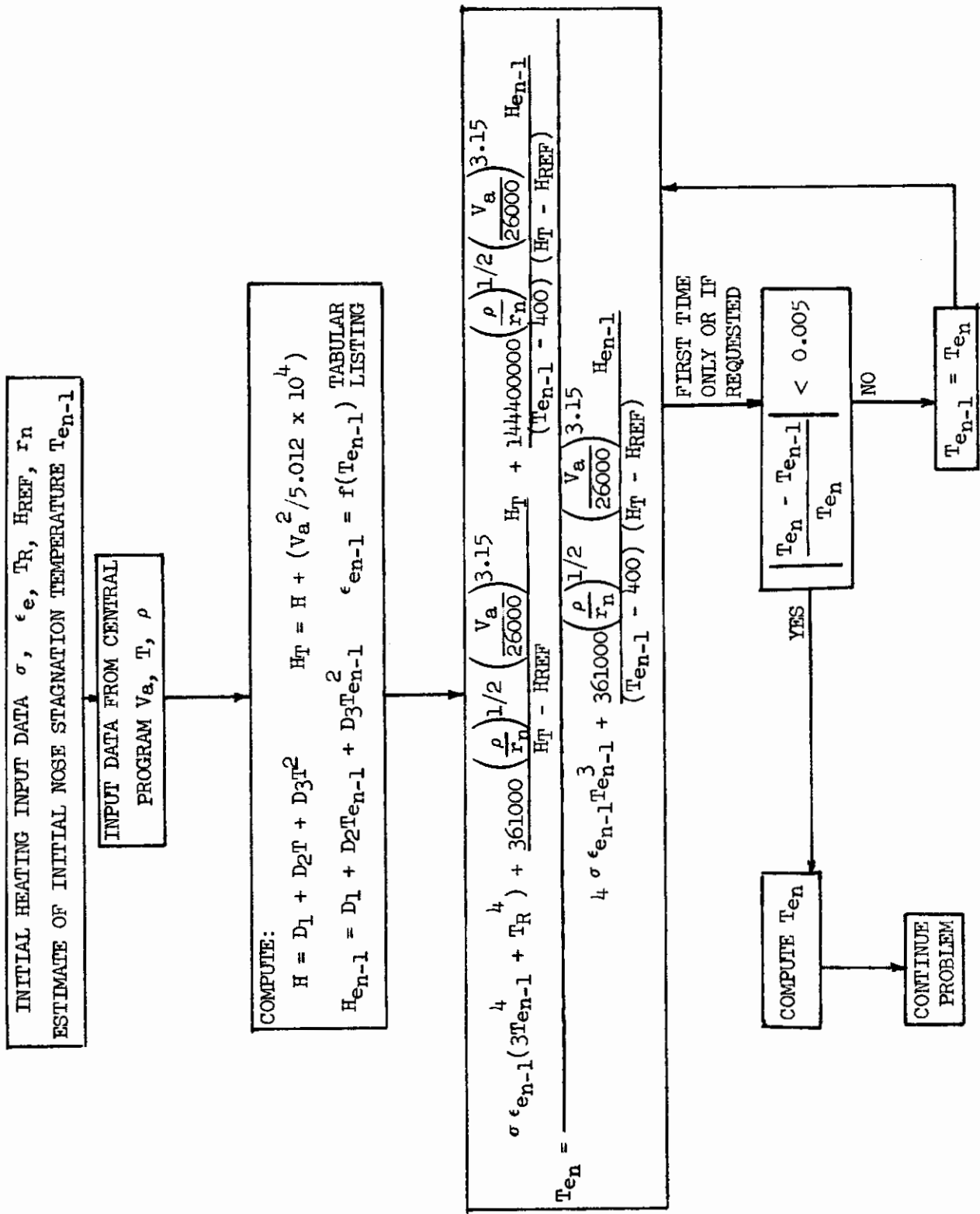
YES → COMPUTE T_{en} → CONTINUE PROBLEM

FIGURE 7.3 FUNCTIONAL FLOW DIAGRAM
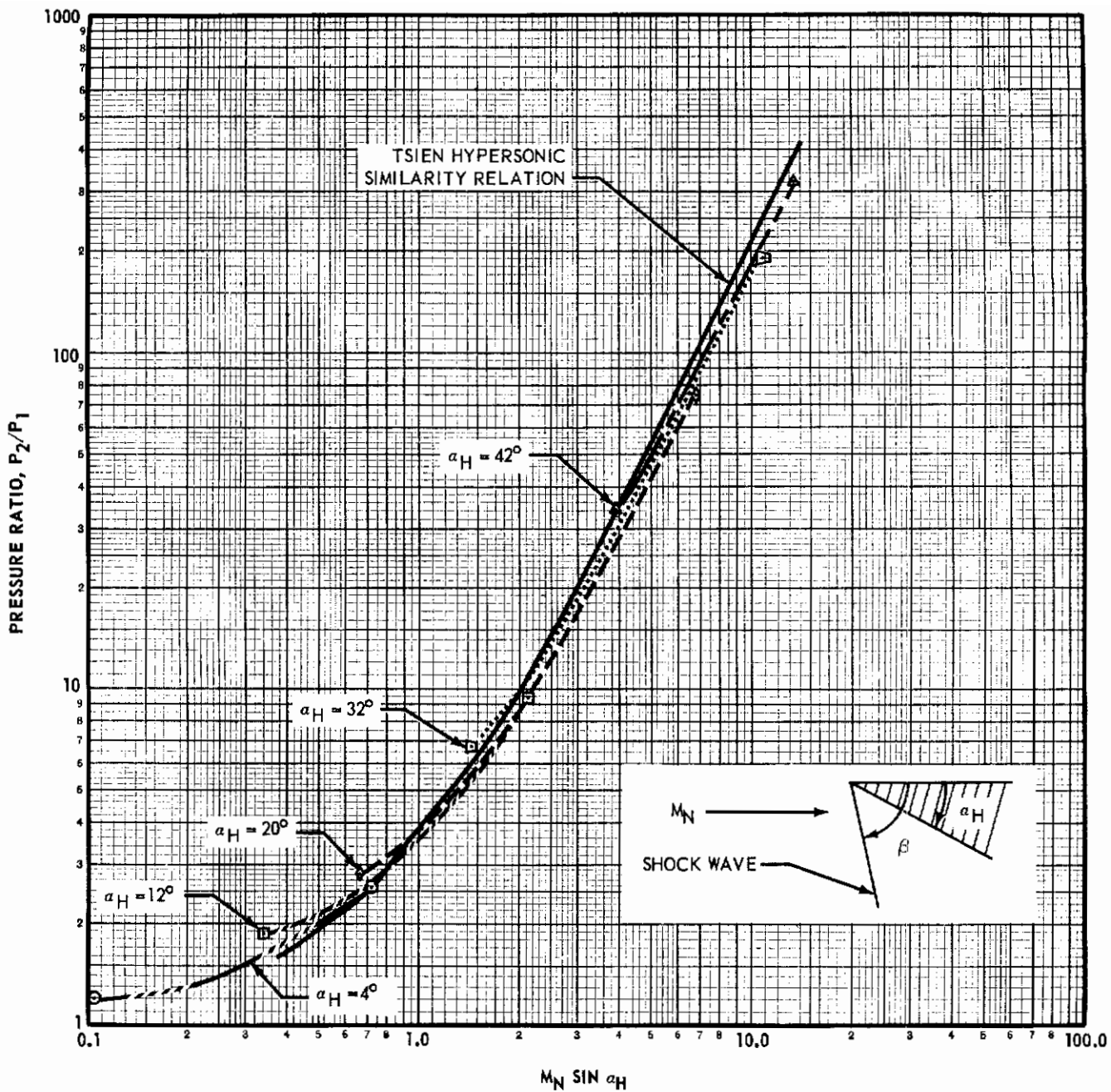EQUILIBRIUM STAGNATION TEMPERATURE ON A HEMISPHERICAL NOSE

FIGURE 7.4, COMPARISON OF PRESSURE RATIO ON A TWO-DIMENSIONAL WEDGE
CORRELATED BY THE SIMILARITY PARAMETER $M_N \sin \alpha_H$
AND BY THE TSIEN HYPERSONIC SIMILARITY RELATION

148

The pressure ratio is therefore

$$\frac{P_2}{P} = C_p \; 0.7 \; M_N^2 + 1 \qquad (7.27)$$

The density ratio across the shock can be expressed as a function of the pressure ratio using the Rankine-Hugoniot relations and is, for air,

$$\frac{\rho_2}{\rho} = \left[\frac{6\left(\frac{P_2}{P}\right) + 1}{6 + \frac{P_2}{P}} \right] \qquad (7.28)$$

The temperature ratio follows directly from the equation of state

$$\frac{T_2}{T} = \frac{P_2/P}{\rho_2/\rho} \qquad (7.29)$$

To find V_2 requires the computations of M_{N_2} from the relation, for air,

$$M_{N_2} = \left[\frac{5}{6(P_2/P) - 1} \right]^{1/2} \left[\frac{1}{\sin(\beta - \alpha H)} \right] \qquad (7.30)$$

The shock wave angle can be determined from

$$\beta = \sin^{-1} \left[\frac{M_{N_n}}{M_N} \right] \qquad (7.31)$$

where M_N is the free-stream Mach number and M_{N_n} is the component of the free-stream Mach number normal to the shock wave. A relation between the pressure ratio across a normal shock and the Mach number normal to the shock is given by

$$\frac{P_2}{P} = \frac{7 \; M_{N_n}^2 - 1}{6} \qquad (7.32)$$

for air, which may be solved for M_{N_n}. Substituting Equation (7.32) into Equation (7.31) gives

$$\sin \beta = \frac{\sqrt{(6 \; P_2/P + 1)/7}}{M_N} \qquad (7.33)$$

149

With the shock-wave angle known, the local Mach number may be calculated from Equation (7.30) and the local flow velocity V_2 may be calculated

$$V_2 = M_{N_2} \sqrt{T_2} \quad 49.1 \tag{7.34}$$

The coefficient of viscosity, μ_2, and the local Reynolds number R_{N_2} may be computed by

$$\mu_2 = 1.18 \times 10^{-5} \left(\frac{716}{T_2 + 216} \right) \left[\frac{T_2}{500} \right]^{3/2} \tag{7.35}$$

and

$$R_{N_2} = \frac{\rho_2 \, V_2 \, l_H}{\mu_2} \tag{7.36}$$

respectively.

The SDF computer program may be used in conjunction with interplanetary trajectory computer programs to continue the trajectory of a space vehicle following its arrival at close proximity to a planet, or to determine the near-planet trajectory injection conditions for interplanetary flight. Interplanetary trajectory computer programs usually consider the planets as point masses, positioned by the published ephemerides, and possessing gravitational fields which may be expressed by gravitational potential functions. From these data the resultant magnitude and direction of the gravitational field are computed at the position of the space vehicle. When the trajectory comes close to the surface of a planet, the effects of the atmosphere and planet's oblateness must be considered and the position and velocity relative to a point on the surface of the rotating central body may be desired. For these reasons the SDF computer program has been designed to perform the following computations in coordination with interplanetary computer programs.

(a) Determine the boost-phase trajectory for a vehicle embarking upon a space flight.

(b) Determine the re-entry and landing maneuver for a vehicle returning from a space flight.

(c) Calculate that portion of space flight which is near enough to the surface of the central body that those effects of atmosphere or planet's oblateness which are not included in the interplanetary trajectory computer program may be considered if necessary.

These computations may be performed with either the six-degree-of-freedom or three-degree-of-freedom point-mass options. Coordination of the two programs is effected by a semiautomatic tie-in. When transferring from the SDF computer program to the interplanetary trajectory computer program, a deck of cards is punched which may be used to prepare the input tape for the interplanetary computer program. The SDF computer program will accept similarly prepared cards when the transfer is from the interplanetary trajectory program.

The coordinate transformation required to transfer from one program to the other is included in the SDF computer program. A derivation of the transformation is given in Section 3.4. The computations and data input necessary to initialize the SDF computer program from an interplanetary trajectory computer program are contained in Part II of this report.

Transfer from one program to another is made on an altitude criterion. The transfer altitude specification is left to the analyst. Figures (8.1) and (8.2) show the accelerations due to aerodynamic drag, gravitational perturbations of the sun and moon, radiation pressure (for a vehicle loading of one slug per square foot of radiated area), and the Earth's oblateness. At an altitude of 600,000 feet the accelerations due to airloads (in this case drag) are reduced to the order of the perturbation accelerations produced by the sun and moon which is approximately one part in one million.
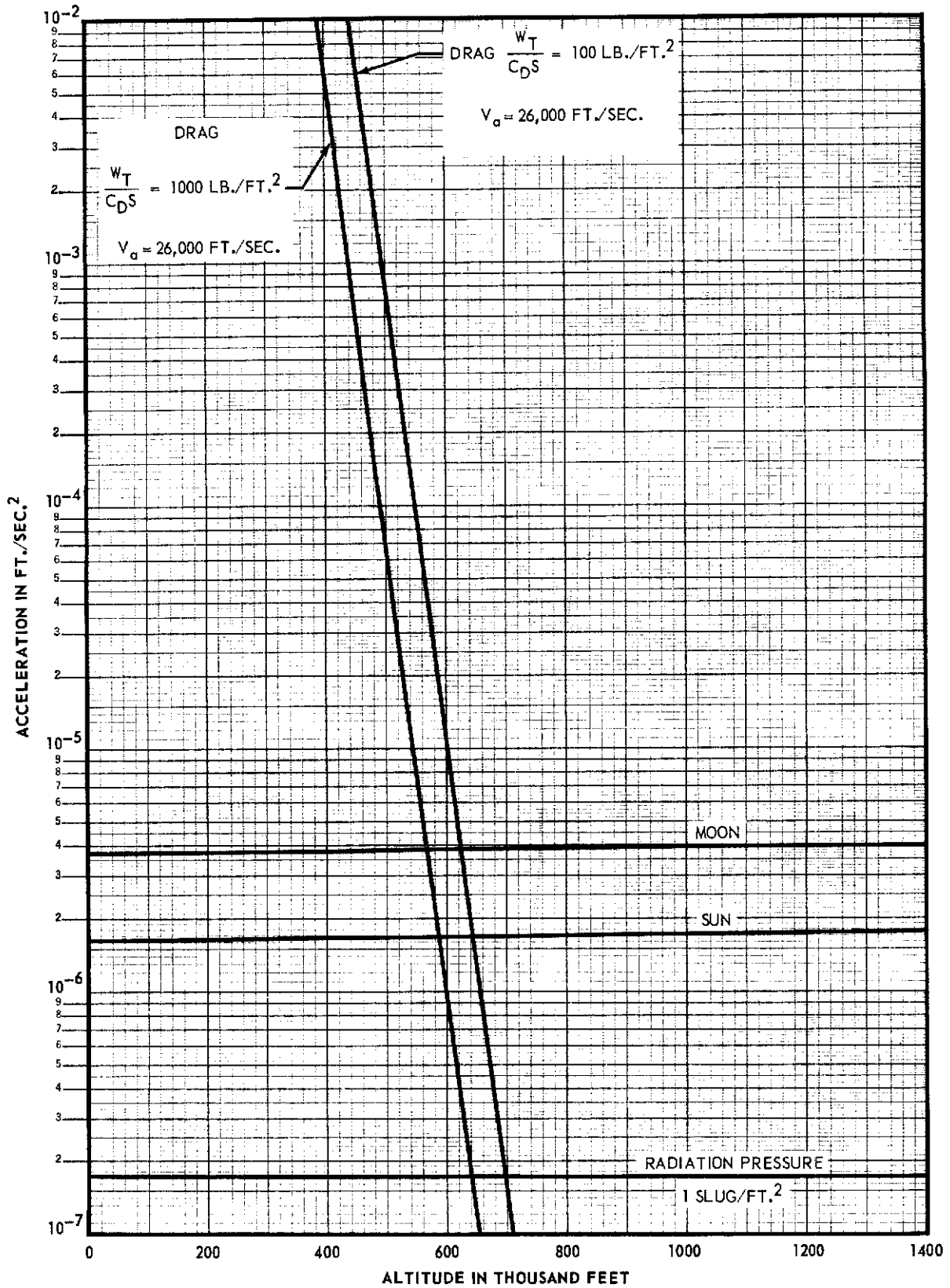
FIGURE 8.1, ACCELERATIONS DUE TO AERODYNAMIC DRAG, RADIATION PRESSURE, MOON AND SUN GRAVITATIONAL ATTRACTION
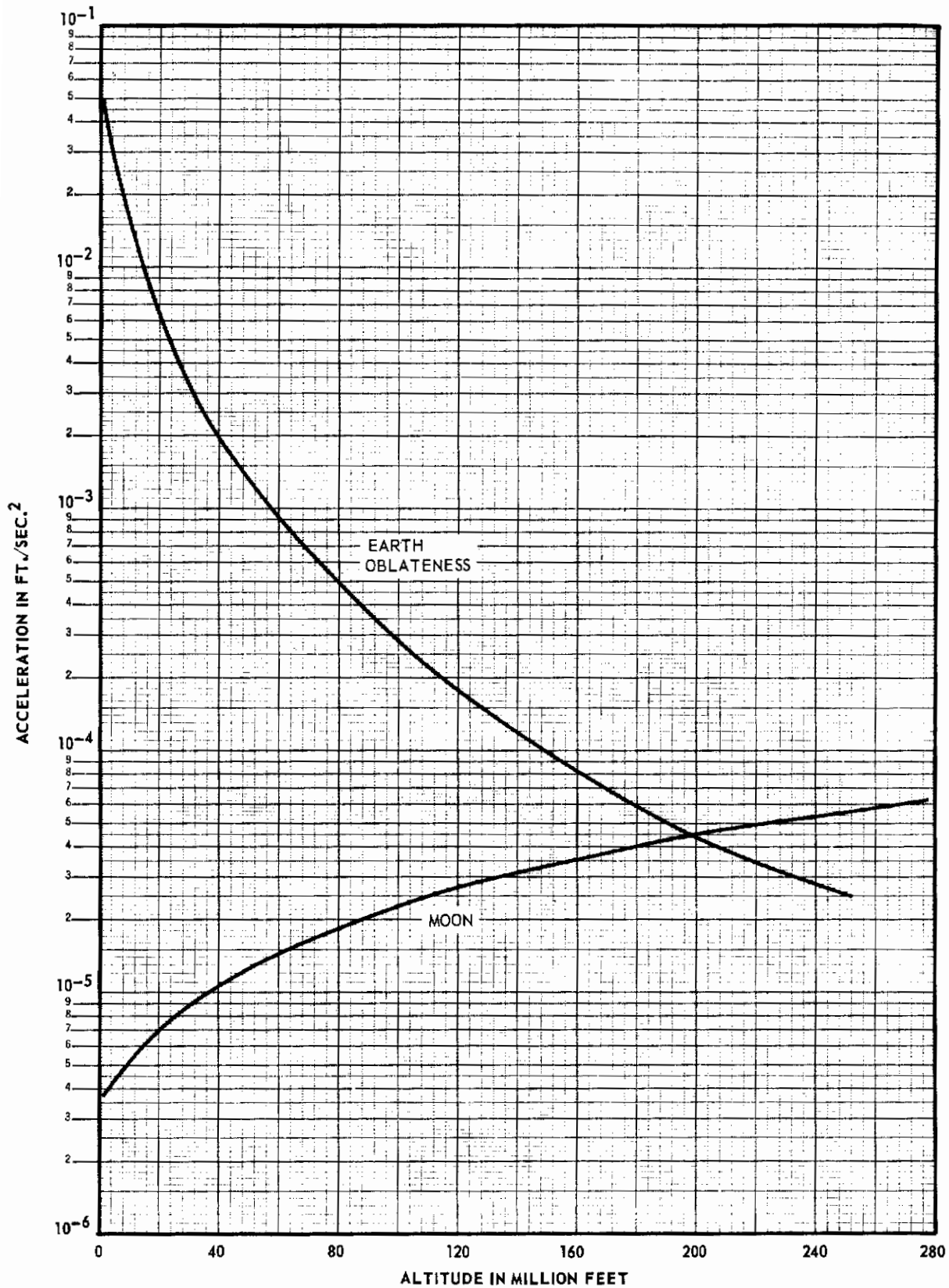
152

FIGURE 8.2, ACCELERATIONS DUE TO EARTH'S OBLATENESS AND
MOON GRAVITATIONAL ATTRACTION

153

Accelerations due to oblateness are on the order of 0.025 feet per second per second at 600,000 feet which is a considerable error. A suggested criterion for transfer is based on the maximum accuracy of existing accelerometers which is on the order of 3.2×10^{-4} feet per second per second. Figure (8.2) shows that the effect of Earth's oblateness reduces to this value at approximately 90,000,000 feet altitude. If the interplanetary trajectory computer program used has considered the effects of oblateness then the lower altitude may be used without accumulating this error.

9. AUXILIARY COMPUTATIONS

In addition to the computations which can be made from the problem formulation as presented in other sections, several other computed quantities are optional calculations:

(a) planet - surface reference range, R_D
(b) great - circle range, R_g
(c) down and cross range
(d) theoretical burnout velocity, V_{theo}
(e) velocity losses, V_P, V_{grav}, and V_D

9.1 Planet-Surface Referenced Range - The total distance traveled over the surface of the planet is computed as the integrated surface range. If the distance traveled by the vehicle over a given portion of the trajectory is:

$$R'_D = \int_{t_1}^{t_2} V_G \, dt \tag{9.1}$$

then the curvilinear planet surface referenced range is

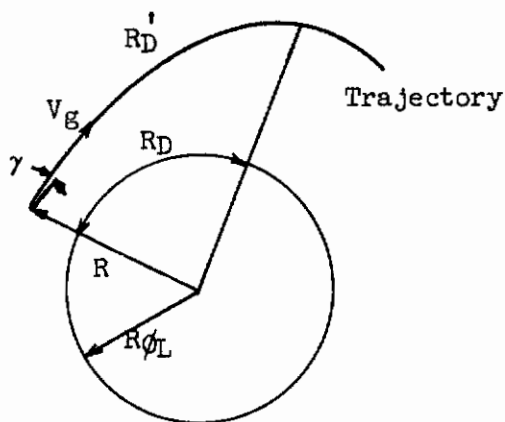$$R_D = \int_{t_1}^{t_2} \frac{R\phi_L}{R} V_G \cos \gamma \, dt \tag{9.2}$$

Figure 9.1 Relation Between Distance Along Trajectory and Surface-Referenced Range

The flight-path angle, γ, may be referenced to local-geocentric coordinates or corrected for the difference between local geocentric and local geodetic latitudes (see Paragraph 5.4) for this computation. When the motion is assumed to occur over a flat, non-rotating planet, the quantities $R\phi_L$ and R in Equation (9.2) are undefined and the surface-reference range must be re-defined as

$$R_D = \int_{t_1}^{t_2} V \cos \gamma \, dt \tag{9.3}$$

9.2 Great-Circle Range. - The great-circle distance from the launch point to the instantaneous vehicle position, R_g, may also be required. Expressions for this distance are derived as follows:

By spherical trigonometry, (see Figure (9.2))

$$\cos \frac{R_g}{R'} = \cos(90-\phi_L)\cos(90-\phi_{L_0}) + \sin(90-\phi_L)\sin(90-\phi_{L_0})(\cos(\theta_L-\theta_{L_0})) \tag{9.4}$$

155

or simplifying

$$\text{Cos} \, \frac{R_g}{R'} = \text{Sin} \, \phi_L \, \text{Sin} \, \phi_{L_O} + \text{Cos} \, \phi_L \, \text{Cos} \, \phi_{L_O} \, \text{Cos} \, (\theta_L - \theta_{L_O}) \tag{9.5}$$

Therefore,

$$R_g = R' \, \text{Cos}^{-1} \left[\text{Sin} \, \phi_L \, \text{Sin} \, \phi_{L_O} + \text{Cos} \, \phi_L \, \text{Cos} \, \phi_{L_O} \, \text{Cos} \, (\theta_L - \theta_{L_O}) \right] \tag{9.6}$$

Figure 9.2 Great-Circle Range

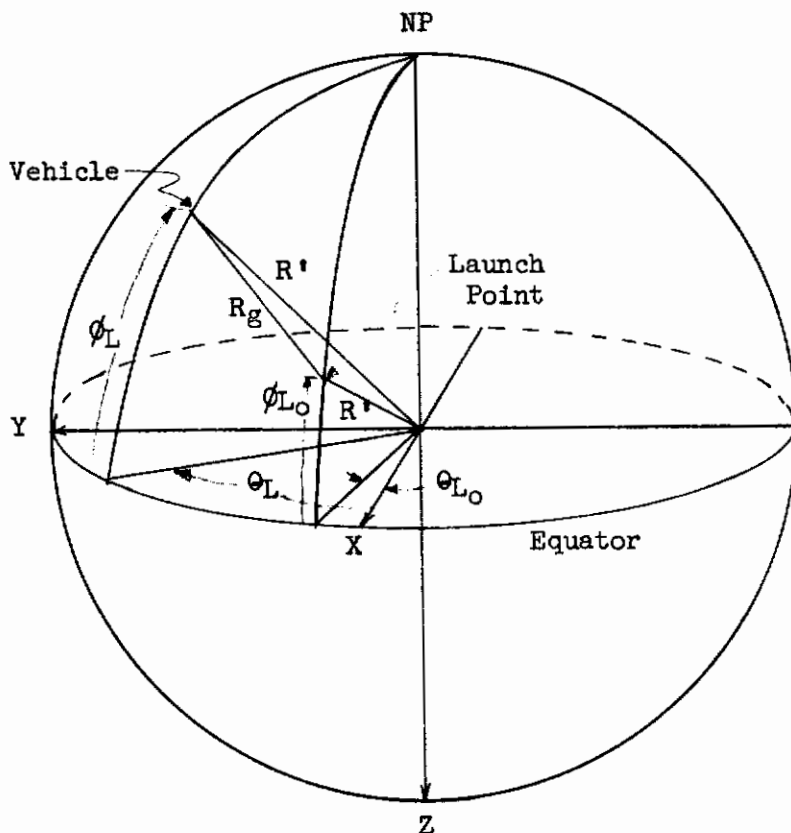However, since the planets are generally oblate spheroids, R' is not a constant radius. An approximation may be obtained by averaging the planet's radius at the launch point and at the vehicle's position. Therefore, define the average radius, R', as

$$R' \cong \frac{R_{\phi_L} + R_{\phi_{L_O}}}{2} \tag{9.7}$$

and the surface-referenced great-circle range from the launch point to the vehicle is

$$R_g \cong \left[\frac{R\phi_L + R\phi_{L_O}}{2}\right] \cos^{-1}\left[\sin \phi_L \sin \phi_{L_O} + \cos \phi_L \cos \phi_{L_O} \cos(\Theta_L - \Theta_{L_O})\right] \quad (9.8)$$

For the flat-planet option the range from the launch point must also be re-defined (see explanation preceding Equation (9.3)). Therefore

$$R_g = \sqrt{(X_g - X_{g_O})^2 + (Y_g - Y_{g_O})^2} \quad (9.9)$$

9.3 <u>Down and Cross Range</u> - To determine at any time the lateral distance from the initial great circle, an optional computation can be made in the three-degree point mass option and in the full six-degree-of-freedom trajectory over an oblate earth. The initial great circle is defined by the initial heading at the initial latitude and longitude. Then the crossrange of a particular trajectory point is defined as the perpendicular distance from the point to the initial great circle. The downrange is then the distance along the initial great circle from the initial point to the point at which the crossrange is measured. From the spherical triangle, Figure 9.3, the great circle range, LF, to the point F, is computed by Equation (9.8). The heading, ζ, of this great circle at the initial point is computed from the spherical triangle, L-N-F.

$$\tan \zeta = \frac{\sin(\Theta_L - \Theta_{L_O}) \cos \phi_L \cos \phi_{L_O}}{\sin \phi_L - \sin \phi_{L_O} \cos LF} \quad (9.10)$$

The right spherical triangle LPF is then solved for the downrange, X_D, and the crossrange, Y_D.

$$X_D = R' \cos^{-1}\left(\frac{\cos LF}{\cos(\sin^{-1}(\sin LF \sin \xi))}\right) \quad (9.11)$$

$$Y_D = R' \sin^{-1}(\sin LF \sin \xi) \quad (9.12)$$

where

$$\xi = \zeta - \sigma_o$$
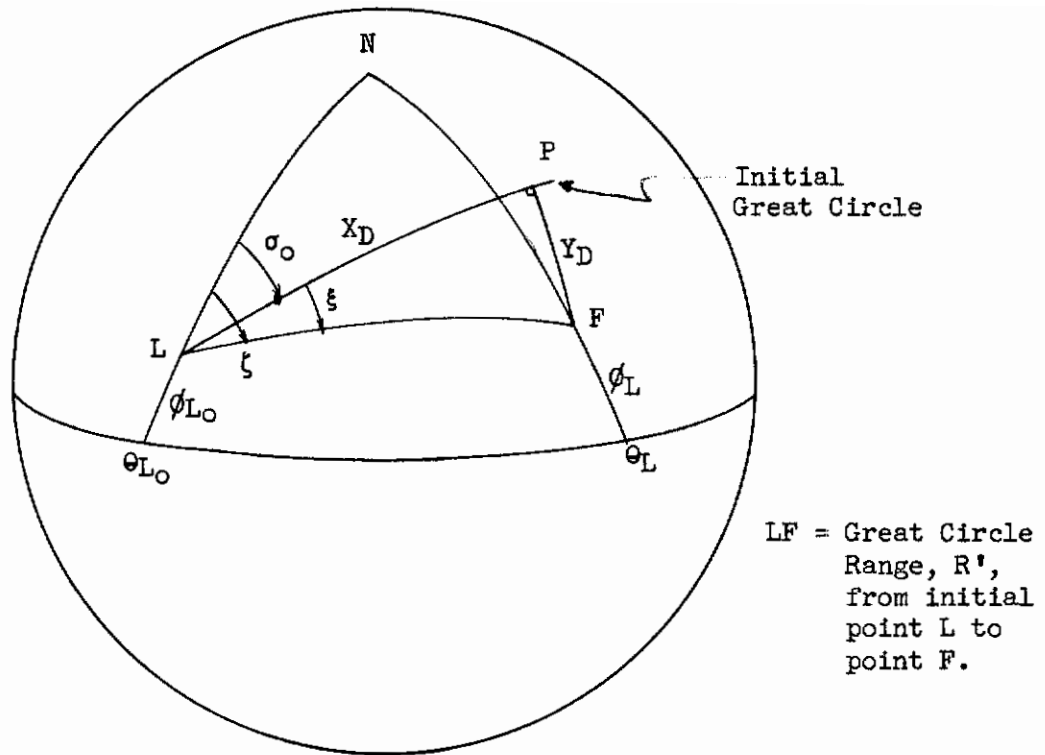
R' is defined by Equation (9.7)

157

Figure 9.3 Downrange and Crossrange Geometry

9.4 <u>Theoretical Burnout Velocity and Losses</u>. - For trajectory and performance optimization studies it is convenient to know the theoretical burnout velocity possible and the velocity losses due to gravity, aerodynamic drag, and atmospheric back pressure upon the engine nozzle. These quantities may be computed as follows:

<u>Theoretical Velocity</u>

$$V_{theo} = \int_{t_1}^{t_2} \frac{T_{vac}}{m}\, dt \qquad\qquad (9.13)$$

<u>Velocity Loss Due To Gravity</u>

$$V_{grav} = \int_{t_1}^{t_2} -g_{Z_g} \sin \gamma_D \, dt \qquad\qquad (9.14)$$

Velocity Loss Due to Aerodynamic Drag

$$V_D = \int_{t_1}^{t_2} -\frac{D}{m} \, dt \tag{9.15}$$

Velocity Loss Due to Atmospheric Back Pressure Upon The Engine Nozzle

$$V_P = \int_{t_1}^{t_2} -\frac{P_{A_e}}{m} \, dt \tag{9.16}$$

The resultant velocity V_g' is obtained by adding the components computed,

$$V_g' = V_{theo} + V_{grav} + V_D + V_P \tag{9.17}$$

and should compare closely to the surface-referenced speed, V_g, obtained from the trajectory computation, when any initial speed is included in the theoretical velocity.

10. INITIALIZATION AND COMPUTATION

Beginning a calculation with the generalized computer program requires not only the introduction of certain initial conditions and the necessary tabular values of the vehicle characteristics but also special machine computations to prepare the initial conditions data for use in the subsequent solution. The initial conditions as introduced by the analyst must be in a form which are readily available and not redundant.

Initial data which must be specified for every computation is of three types: (1) identification (remarks, case number, security classification, stage); (2) integration (integration time interval, integration method, print interval, initial time); and (3) atmospheric and gravitational reference data. In addition, the position, velocity, and vehicle attitude and angular rates must be specified. However, the form of this data is dependent upon the option calculation being made. For the convenience of the analyst certain auxiliary calculations can also be made if specified by input data. Because of the multiple possibilities available, a detailed listing of the input data is contained in the User's Manual. To simplify the preparation of the data cards, nominal values have been assigned to all input data except that which requires symbolic names as data and for tabular listings. The computational flow diagrams of the various calculations are also contained in the User's Manual.

11. REVERSE OPTION

A reverse option of computation is incorporated into the SDF computer program whereby known trajectory and motion information may be introduced into the program to compute unknown aerodynamic forces and moments.

11.1 <u>Trajectory Data from Fixed Radar Station and Measured Body Rates</u>. - The Six-Degree-of-Freedom reverse-option program computation sequence is constructed as follows: Considering first the method to be used when the trajectory position data are referenced to a fixed radar station, the data are assumed to be in terms of a Cartesian coordinate system oriented at some point on the earth. Signify these data by x_m, y_m, z_m, and $\dot{x}_m$, $\dot{y}_m$, and $\dot{z}_m$ for position and velocity, respectively. The origin of this system is located at the longitude of the radar reference point, (which is also the initial longitude of the inertial X-axis), at the geocentric latitude of the radar reference point, and at an altitude, h_o, above the reference ellipsoid.

The geocentric latitude of the location of the origin of the measured data (ϕ_{L_0}), the altitude of the origin above the reference ellipsoid (h_o), and the azimuth angle (A) of the x_m-axis are specified for the problem, Figure 11.1. Next the calculation of the inertial-axis position of the origin of the measured data is made. The analysis of Section 5.4 discusses the acceptable approximation that the geocentric altitude is equal to the geodetic altitude, h_o. Preparatory to the transformation of the measured trajectory data from the earth-reference axes system to the inertial coordinate system, the a-b-c set of direction cosines are computed. The transformation matrix which orients a platform axes to the inertial axes (see Section 3.2) is directly applicable to the required transformation providing the inertial angle B_p is set equal to $-\omega_p t$. The measured position and linear velocity data (or specified data, if the reverse program is being used as a design problem) are introduced in the earth-referenced coordinates and transformed to inertial coordinates.

This completes the portion of the solution sequence peculiar to the use of earth-reference trajectory data such as radar data. The measured inertial components of position and velocity, referenced to the inertial coordinate system, are the standard form required for all methods of operating the present reverse-option program. Alternate methods of operation are discussed in Paragraph 11.2.

Since the equations of motion, of necessity, are solved in a body-axes coordinate system, the inertial components of inertial velocity must be transformed to body components of inertial velocity. This transformation is made by the l-m-n set of direction cosines, see Section 3.1. (This transformation matrix is computed by two methods depending upon whether the problem is being computed the first time or has been running for several steps. In the discussion which follows, it will be assumed that the problem is being initialized. The solution sequence will lead to the alternate procedure through the time up-dating technique.) The geocentric latitude and longitude are computed along with the radial position from the center of the planet and the inertial angle B. The i-j-k direction cosines, which transform quantities in local-geocentric-horizon coordinates to inertial coordinates, are computed for subsequent use.

161

The measured body angular rates are introduced. From here the problem proceeds along the sequence marked "first time only". The initial values of ψ, Θ, and ϕ are introduced, from which the d-e-f set of direction cosines are computed, see Section 3.2. The required initial values of the l-m-n direction cosines, the original measured trajectory information is transformed from the inertial components to the required body-axes components.

This completes the first initializing pass through the problem, having obtained the initial body angular rates, p_m, q_m, and r_m; and the body components of velocity, u_m, v_m, and w_m. The problem leads through the up-dating operation and thence for the second time through the computation for B up to the computation of the l-m-n direction cosines. The l-m-n set of direction cosines are now obtained allowing transformation to body components of velocity to be made and goes through the up-dating loop a second time. The third cycle is identical to the second cycle through the calculation of the body-axes component. The body components of acceleration at point (n-1), using the average slope between the n-2 and n data points, are then computed. To allow this computation to proceed requires the n-2 point, which was the reason for the initializing passes through the first part of the problem. It should be noted, then, that the subsequent computation applies to the (n-1), or proceeding, time step.

The measured wind data are introduced into the computation, transferred to inertial wind components, and thence to body components. The airspeed is computed by the normal definition (e.g., see Section 3.3).

The gravitation terms are computed and transformed to body-axes components. The measured atmospheric properties, or the standard values, are introduced. Mach number and reference dynamic pressure are computed. Other forces and moments, given as functions of time, in body coordinates, are introduced together with the vehicle physical data.

This leads the problem sequence to the equations of motion, which solves for the forces and moments using the body components of acceleration, velocity, and angular rates obtained from the preceeding analysis. These forces and moments are reduced to the aerodynamic coefficients, C_A, C_y, C_N, C_l, C_m, and C_n. After computing the angles of attack and sideslip, the sequence again up-dates the time and starts the program solution of the next known point.

11.2 Alternate Methods of Data Input and Solution. - Several alternate methods of operating the reverse program option may be devised depending upon the trajectory information which is available. Some of these techniques are considered in the following paragraphs. It should be noted, however, that only the formulation of Section 11.1 has been prepared in the computer program.

When measured acceleration data, obtained from accelerometers mounted on an inertial platform oriented to the launch point vertical and flight azimuth, are used in place of measured radar data, the computations indicated in Figure 11.1 would be replaced. The alternate computation would begin with the orientation of the inertial platform, the initial conditions, and proceed to the main sequence the first-time through. The problem re-enters the acceleration sequence where the trajectory acceleration data are stored. Resolving the measured acceleration data, to inertial axes data and subtracting that due to gravity, provides the inertial acceleration. Integrate at time steps equal to the time intervals of the measured data and the solution sequence continues as before.

Other methods of operating the reverse option program could employ position data obtained from radar observations and the linear velocities from platform mounted accelerometers. In this case parts of both of the data input programs discussed above would be used to introduce the known trajectory. Also accelerometer data may be introduced from an inertial platform which has been torqued according.to a particular program. In this case the torquing program would be incorporated along with the coordinate transformations, see Section 3.2. In some cases measured body inertial angular rates (p_m, q_m, r_m) may not be available. An alternate method of introducing the required orientation would be to observe the Euler angles of the body from photographic records as a function of time and differentiate to get the p_m, q_m, and r_m. Also data may be obtained from an inertial platform, in which case the information required to compute l-m-n set of direction cosines is available directly.

11.3 Non-Rotating Body Axes Coordinate System - The aerodynamic coefficients (Section 11.1) are referenced to a rotating body-axes coordinate system. However, if the body is rolling as a function of time and an incorrectly measured roll rate, p, is used, the body attitude and consequently, aerodynamic forces computed on the rolling vehicle, will be in error. The coefficient of the force which is actually supporting the vehicle may be continuing in a well behaved fashion and may be quite accurate. Thus the following simple coordinate transformation converts all the force coefficients to a non-rotating body axes coordinate system which removes errors in the roll attitude of the vehicle. Errors in pitch and yaw do not introduce the type of errors noted above and hence are not considered in the present transformation.

Assuming a yaw-pitch-roll rotation sequence to define the local-geocentric-referenced body Euler angles ψ -θ-ϕ, respectively, the roll angle may be determined from

$$\tan \phi = \frac{m_1 \, l_3 + m_2 j_3 + m_3 k_3}{n_1 \, l_3 + n_2 j_3 + n_3 k_3}$$

(11.1)

The values of m_1, m_2, m_3, n_1, n_2, n_3, l_3, j_3, and k_3 are available at the appropriate times in the problem from the l-m-n and the i-j-k direction cosines. The derivation of Equation (11.1) is obtained according to the procedure outlined in Sections 3.2.2, 3.2.3, and 3.2.4. The force coefficients will be transformed as follows:

Local Geocentric
Vertical Plane
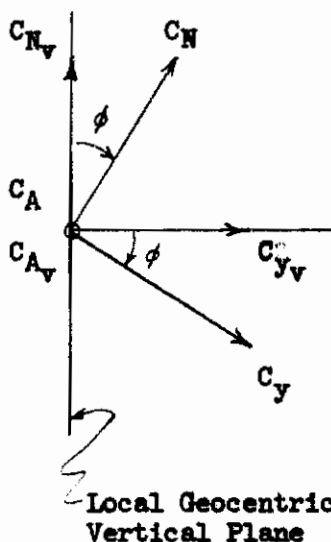
$$C_{A_V} = C_A$$

$$C_{y_V} = C_y \cos \phi + C_N \sin \phi$$

$$C_{N_V} = C_N \cos \phi - C_y \sin \phi$$

or in matrix form (11.2)

$$\begin{bmatrix} C_{A_V} \\ C_{y_V} \\ C_{N_V} \end{bmatrix} = \begin{bmatrix} 1 & 0 & 0 \\ 0 & \cos \phi & \sin \phi \\ 0 & -\sin \phi & \cos \phi \end{bmatrix} \begin{bmatrix} C_A \\ C_y \\ C_N \end{bmatrix}$$

163

The moment coefficients are transformed by

$$
\begin{bmatrix} C_{1_V} \\ C_{m_V} \\ -C_{n_V} \end{bmatrix} = \begin{bmatrix} \phi \end{bmatrix} \begin{bmatrix} C_1 \\ C_m \\ -C_n \end{bmatrix}
\tag{11.3}
$$

where $\begin{bmatrix} \phi \end{bmatrix}$ is the transformation matrix defined in Equation (11.2). The aerodynamic angles, α_V and β_V are consistent with transformed aerodynamic force and moment coefficients, and are defined as follows:

$$
\tan \alpha_V = \frac{(w-w_W)_V}{(u-u_W)} \quad \text{and} \quad \tan \beta_V = \frac{(v-v_W)_V}{(u-u_W)}
\tag{11.4}
$$

since $(u-u_W) = (u-u_W)_V$

The required velocity components are calculated by

$$
\begin{bmatrix} (u-u_W)_V \\ (v-v_W)_V \\ -(w-w_W)_V \end{bmatrix} = \begin{bmatrix} \phi \end{bmatrix} \begin{bmatrix} (u-u_W) \\ (v-v_W) \\ -(w-w_W) \end{bmatrix}
\tag{11.5}
$$

The functional flow diagram for the coordinate transformation is shown in Figure 11.1.

11.4 <u>Limitations on Reverse Option</u> - There are several aspects of the reverse program option which should be noted since they limit the applicability of the method.

(a) The reverse-program option may be generally applied only to the six-degree-of-freedom analysis. The three-degree-of-freedom longitudinal motion may be considered, but analysis is restricted to motion in the planet's equatorial plane or to a non-rotating spherical planet. Reverse options could be set up using other equations of motion, however under some conditions (e.g., the point mass trajectory analysis with thrust forces) the normal trajectory information available is insufficient for a reverse option solution.

(b) All input data should be corrected for zero shift, instrument error, etc., and should be smooth. The smoothing of the data must actually portray the path of the vehicle. Smoothing flight-test data by a least squares method or a direct polynominal fit might not be adequate, and further smoothing by inspection or by more powerful mathematical methods may be required. The aerodynamic force data obtained will, of course, be only as good as the trajectory data introduced.

(c) The radar data coordinate system orientation on the earth (usually the launch point) is required. The positive x_m axis will be measured along the firing azimuth, the positive z_m axis down along the geocentric radius, and the positive y_m axis will be measured to the right to make a right-hand Cartesian system.
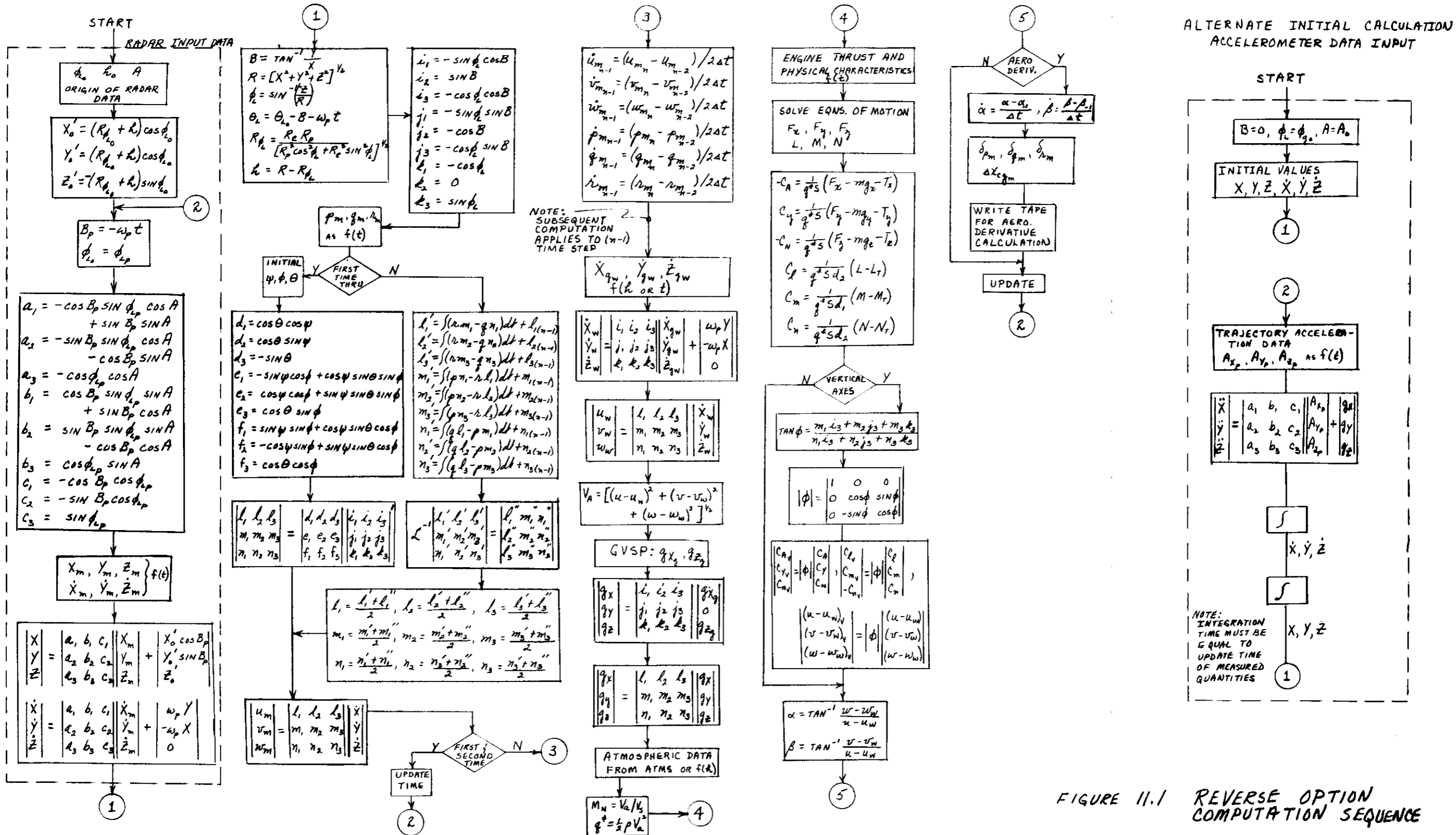
164

REVERSE OPTION COMPUTATION SEQUENCE

FIGURE 11.1 REVERSE OPTION COMPUTATION SEQUENCE

165

(d) The body angular rates, p_m, q_m, r_m, should be obtained by direct measurement.

(e) All data other than aerodynamic forces and moments required in the equations of motion should be given. This includes the mass and inertia characteristics, and engine forces and moments.

11.5 <u>Aerodynamic Derivatives</u> - The aerodynamic coefficients computed by the reverse option are related to the aerodynamic derivatives. One method of determining the relationship between several independent variables and a dependent variable is the multiple regression technique, Reference (27), Section 7.3; Reference (28), Section 37.3; and Reference (29). If the aerodynamic coefficients are assumed to be summations of the products of independent variables and the corresponding aerodynamic derivatives, then the aerodynamic equations as shown in Table 1 may be written in the form:

$$Y'_v = C_0 + C_1 X_1 + C_2 X_2 + \ldots + C_i X_i \ldots + C_k X_k \tag{11.6}$$

where:

Y' denotes the dependent variable as computed from Eq. (11.6)
X_i denotes the independent variable
C_i denotes the corresponding aerodynamic derivative
Y denotes the measured dependent variable (aerodynamic coefficient)
subscript v denotes the index of the set of values ($v = 1,2, \ldots n$)
subscript i denotes the particular independent variable ($i = 1,2, \ldots k$)
subscript j denotes an independent variable different from i

The solution of this type of equation is done by the method of least squares, Reference (27), p. 130. The maximum likelihood estimates of the constants, C_i, are the values which minimize the sum of the squares of the residuals,

$$\sum_{v=1}^{n} (Y_v - Y'_v)^2 , \quad \text{where the regression equation is evaluated}$$

in the form:

$$Y'_v = \beta_0 + \beta_1 x_{1v} + \beta_2 x_{2v} \ldots \beta_i x_{iv} \ldots + \beta_k x_{kv} \tag{11.7}$$

where:

$$x_{iv} = X_{iv} - \bar{X}_i$$
$$\bar{X}_i = \frac{1}{n} \sum_{v=1}^{n} X_{iv}$$

The coefficients of equation 11.7 are related to the original aerodynamic derivatives of equation 11.6:

$$C_0 = \beta_0 - \beta_1 \bar{X}_1 - \beta_2 \bar{X}_2 \ldots - \beta_i \bar{X}_i \ldots - \beta_k \bar{X}_k$$
$$C_i = \beta_i \tag{11.8}$$

The maximum likelihood estimates, denoted by an asterisk, are determined by the solution of the normal equations, Reference (27), p. 131, or by Cramer's Rule, Reference (28), p. 552.

TABLE 1

AERODYNAMIC EQUATIONS

Cycle		LINEAR TERMS	RATE TERMS	SQUARE TERMS
1	$C_A =$	$C_{A_o} + C_{A_\alpha}|\alpha| + C_{A_\beta}|\beta| + C_{A_{\delta_{\xi}}}|\delta_{\xi}|$		$+ C_{A_{\alpha^2}}\alpha^2 + C_{A_{\beta^2}}\beta^2 \qquad + C_{A_{\delta_{\xi}^2}}\delta_{\xi}^2$
2	$C_N =$	$C_{N_o} + C_{N_\alpha}\alpha + C_{N_\beta}|\beta| + C_{N_{\delta_{\xi}}}$	$+ C_{N_q}\dfrac{qd_1}{2V_a} \qquad + C_{N_{\dot\alpha}}\dfrac{\dot\alpha d_1}{2V_a}$	$+ C_{N_{\alpha^2}}\alpha|\alpha| + C_{N_{\beta^2}}\beta^2 \qquad + C_{N_{\delta_{\xi}^2}}\delta_{\xi}|\delta_{\xi}|$
3	$C_Y =$	$C_{Y_o} + C_{Y_\alpha}|\alpha| + C_{Y_\beta}\beta \qquad + C_{Y_{\delta_r}}\delta_r$	$+ C_{Y_r}\dfrac{rd_2}{2V_a} \qquad + C_{Y_{\dot\beta}}\dfrac{\dot\beta d_2}{2V_a}$	$+ C_{Y_{\alpha^2}}\alpha^2 + C_{Y_{\beta^2}}\beta|\beta| \qquad + C_{Y_{\delta_r^2}}\delta_r|\delta_r|$
4	$C_\ell =$	$C_{\ell_o} + C_{\ell_\alpha}|\alpha| + C_{\ell_\beta}|\beta| + C_{\ell_{\delta_p}}\delta_p$	$+C_{\ell_p}\dfrac{pd_2}{2V_a} \qquad +C_{\ell_r}\dfrac{rd_2}{2V_a}$	$+ C_{\ell_{\alpha^2}}\alpha^2 + C_{\ell_{\beta^2}}\beta^2 + C_{\ell_{\delta_p^2}}\delta_p|\delta_p|$
5	$C_m =$	$C_{m_o} + C_{m_\alpha}\alpha + C_{m_\beta}|\beta| + C_{m_{\delta_{\xi}}}$	$+ C_{m_q}\dfrac{qd_1}{2V_a} \qquad + C_{m_{\dot\alpha}}\dfrac{\dot\alpha d_1}{2V_a}$	$+ C_{m_{\alpha^2}}\alpha|\alpha| + C_{m_{\beta^2}}\beta^2 \qquad + C_{m_{\delta_{\xi}^2}}\delta_{\xi}|\delta_{\xi}|$
6	$C_n =$	$C_{n_o} + C_{n_\alpha}|\alpha| + C_{n_\beta}\beta \qquad + C_{n_{\delta_r}}\delta_r$	$+C_{n_r}\dfrac{rd_2}{2V_a} \qquad + C_{n_{\dot\beta}}\dfrac{\dot\beta d_2}{2V_a}$	$+ C_{n_{\alpha^2}}\alpha^2 + C_{n_{\beta^2}}\beta|\beta| \qquad +C_{n_{\delta_r^2}}\delta_r|\delta_r|$

CROSS-COUPLED TERMS	CENTER-OF-GRAVITY TERMS
$+ C_{A_{\alpha\beta}}|\alpha\beta| \qquad + C_{A_{\alpha\delta_{\xi}}}|\alpha\,\delta_{\xi}| + C_{A_{\beta\delta_{\xi}}}|\beta\,\delta_{\xi}|$	
$+ C_{N_{\alpha\beta}}\alpha|\beta| \qquad + C_{N_{\alpha\delta_{\xi}}}|\alpha|\delta_{\xi} + C_{N_{\beta\delta_{\xi}}}|\beta|\delta_{\xi}$	$+ C_{N_{\dot\alpha x}}\Delta X_{cg}\dfrac{\dot\alpha d_1}{2V_a} \qquad + C_{N_{qx}}\Delta X_{cg}\dfrac{qd_1}{2V_a}$
$+ C_{Y_{\alpha\beta}}|\alpha|\beta \qquad\qquad + C_{Y_{\alpha\delta_r}}|\alpha|\delta_r + C_{Y_{\beta\delta_r}}|\beta|\delta_r$	$+C_{Y_{\dot\beta x}}\Delta X_{cg}\dfrac{\dot\beta d_2}{2V_a} \qquad + C_{Y_{rx}}\Delta X_{cg}\dfrac{rd_2}{2V_a}$
$+ C_{\ell_{\alpha\beta}}|\alpha\beta| + C_{\ell_{\alpha\delta_p}}|\alpha|\delta_p + C_{\ell_{\beta\delta_p}}|\beta|\delta_p$	$+ C_{\ell_{rx}}\Delta X_{cg}\dfrac{rd_2}{2V_a}$
$+ C_{m_{\alpha\beta}}\alpha|\beta| \qquad + C_{m_{\alpha\delta_{\xi}}}|\alpha|\delta_{\xi} + C_{m_{\beta\delta_{\xi}}}|\beta|\delta_{\xi}$	$+ C_{m_{\dot\alpha x}}\Delta X_{cg}\dfrac{\dot\alpha d_1}{2V_a} \qquad + C_{m_{qx}}\Delta X_{cg}\dfrac{qd_1}{2V_a} \qquad - \dfrac{C_N \Delta x_{cg}}{d_1}$
$+ C_{n_{\alpha\beta}}|\alpha|\beta \qquad\qquad + C_{n_{\alpha\delta_r}}|\alpha|\delta_r + C_{n_{\beta\delta_r}}|\beta|\delta_r$	$+C_{n_{\dot\beta x}}\Delta X_{cg}\dfrac{\dot\beta d_2}{2V_a} \qquad + C_{n_{rx}}\Delta X_{cg}\dfrac{rd_2}{2V_a} \qquad - \dfrac{C_Y \Delta x_{cg}}{d_2}$

167

$$\beta_o^* = \bar{Y} = \frac{1}{n} \sum_{v=1}^{n} Y_v$$

$$\beta_1^* = \frac{1}{L} \sum_{i=1}^{k} l_{oj} L_{ij} \qquad (i=1,2, \dots k) \qquad (11.9)$$

where:

$$l_{ij} = \frac{1}{n} \sum_{v=1}^{n} x_{iv} x_{jv}$$

$$l_{oj} = \frac{1}{n} \sum_{v=1}^{n} y_v x_{jv}$$

$$y_v = Y_v - \bar{Y}$$

$$L = \begin{vmatrix} l_{11} & \cdots & l_{1k} \\ \vdots & & \vdots \\ l_{k1} & \cdots & l_{kk} \end{vmatrix}$$

$$L_{ij} = \text{cofactor of } l_{ij} = (-1)^{i+j} \left| \text{minor}_{ij} \right|$$

$\left| \text{minor}_{ij} \right|$ is formed by striking out the i row and j column of the L determinant

The desired aerodynamic derivatives are obtained by evaluating equation 11.8 with the results of equation 11.9.

The standard deviation, s, of the curve-fit is defined (Reference 28, Eq. 37.3.3):

$$s^2 = \frac{1}{n} \sum_{v=1}^{n} (z_v)^2 \qquad (11.10)$$

where:

$$z_v = (Y_v - Y'_v) = \text{residual}$$

11.5.1 <u>Superfluous Terms</u> - The form of the regression curve, equation 11.6, must be known to compute the aerodynamic derivatives. The aerodynamic equations presented in Table 1 are the equations used in the basic SDF program. However, some of the power terms and cross-coupling terms are not necessary for particular aerodynamic configurations. Thus, for simplicity, this computer program has been formulated to use the linear terms plus those other terms specified by the analyst for individual problems. However, for program simplicity, it is necessary to add the terms in blocks, i.e.: the rate terms, the square terms, the cross-coupled terms and the center of gravity terms.

In the event of doubt of the need for a specific block of terms, an analysis of the variance may test the significance of the additional terms, Reference (29), p. 403. The data must be fitted twice: (1) by the regression equation without the additional terms and (2) with the additional terms. The F-distribution ratio can then be obtained from the computation:

$$F = \frac{\text{mean square of additional variance due to added terms}}{\text{mean square of variation around regression with added terms}}$$

$$= \frac{\dfrac{1}{m-k}\left[\displaystyle\sum_{i=1}^{m}\left(c_i \sum_{v=1}^{n} y_v x_{iv}\right) - \sum_{i=1}^{k}\left(c_i \sum_{v=1}^{n} y_v x_{iv}\right)\right]}{\dfrac{1}{n-m-1}\left[\displaystyle\sum_{v=1}^{n} y_v^2 - \sum_{i=1}^{m}\left(c_i \sum_{v=1}^{n} y_v x_{iv}\right)\right]} \qquad (11.11)$$

where: m-k = number of added terms

Comparison of the F-ratio with a F-ratio distribution, Reference (29), Table 23.5, provides a test of the probability that the added terms provide a significantly better fit of the data than the initial regression equation. The numerator has m-k degrees of freedom and the denominator has n-m-1 degrees of freedom. The computation of the F-ratio is included in the computer program as an optional feature. The significance is then left to the analyst to determine. If the computed F-ratio is larger than the tabular distribution, then the probability is less than 1 percent (or 5 percent) that the regression of yield upon the additional terms in the universe were really zero. Or, more simply, if the computed F-ratio is greater than the tabulated distribution, the additional terms provide a significantly better representation of the relationship between the aerodynamic coefficients and the aerodynamic derivatives than the reduced equation.

11.5.2 Autocorrelation - To determine if a trend in the data exists which is gradually shifting the mean, the mean square successive difference, δ^2, is compared to the variance, s^2, of the data including the effect of the trend, Reference 30 . This ratio is computed:

$$\frac{\delta^2}{s^2} = \frac{\dfrac{1}{n-1}\displaystyle\sum_{v=1}^{n-1}(z_{v+1} - z_v)^2}{\dfrac{1}{n}\displaystyle\sum_{v=1}^{n} z_v^2} \qquad (11.12)$$

The computed value, δ^2/s^2, is then compared to a significance table for Von Neumann's ratio, Reference (29), Table 20.5, for a particular probability, chosen here as 5 percent. As an example, if n (number of observations in the sample) = 18, the δ^2/s^2 must fall between K = 1.3405 and K' = 2.8948 to reject the hypothesis that the residuals are significantly autocorrelated. If the computed ratio is less than the critical value, K, it is indicative of positive autocorrelation. For flight test data, this might mean, for example, that the Mach effect on the aerodynamic derivatives is appreciable within the sample. The apparent solution to such an undesireable situation is to divide the original sample into two samples with different mean values, and repeat the computations of the aerodynamic derivatives and Von Neumann's ratio for the smaller samples. This subdivision of the sample cannot be continued when the number, n, of observations in the sample becomes so small that the degrees of freedom reduce below one, and should not approach this limit too closely since the confidence interval of the basic calculations will become excessive. The degrees of freedom are n-k-1; therefore:

169

$$n \geq k+2 \tag{11.13}$$

For the convenience of the analyst, the computer program will provide alternate choices for the selection of the initial sample size, i.e., (1) Mach segment; pre-selected Mach segments by the analyst or (2) maximum fixed sample size.

11.5.3 <u>Confidence Limits</u> - The confidence interval on an individual aerodynamic derivative can be obtained in the following manner, Reference (28), Sec. 37.3:

$$t = (n-k-1)^{1/2} \frac{s_i}{s} \ (\beta_i^* - \beta_i) \tag{11.14}$$

where t is the value of the Student's t distribution, Reference 28, Table 4, with n-k-1 degrees of freedom for a specified confidence coefficient.

From Eq. 37.3.4, Reference (28):

$$s_i^2 = \frac{L}{L_{ii}} \tag{11.15}$$

Thus by substitution of Equations 11.5 and 11.10 into Equation 11.14 and rearranging, the confidence interval may be evaluated in the following relationship:

$$\beta_i^* + \frac{t \ s}{(n-k-1)^{1/2}} s_i \ \leq \ \beta_{i_{true}} \ \leq \ \beta_i^* - \frac{t \ s}{(n-k-1)^{1/2}} s_i \tag{11.16}$$

11.5.4 <u>Multiple Correlation</u> - The coefficient of multiple correlation (R_y) indicates the degree of the variance of the dependent variable that is explained by the k terms of the regression equation. A value of one for the coefficient would denote perfect correlation of all the independent variables with the estimated values.

Coefficient of multiple correlations, Reference (29), p. 191:

$$R_y^2 = \frac{\beta_1^* \ (\sum_{v=1}^{n} y_v x_{1v}) + \beta_2^* \ (\sum_{v=1}^{n} y_v x_{2v}) + \ldots + \beta_k^* \ (\sum_{v=1}^{n} y_v x_{kv})}{\sum_{v=1}^{n} y_v^2} \tag{11.17}$$

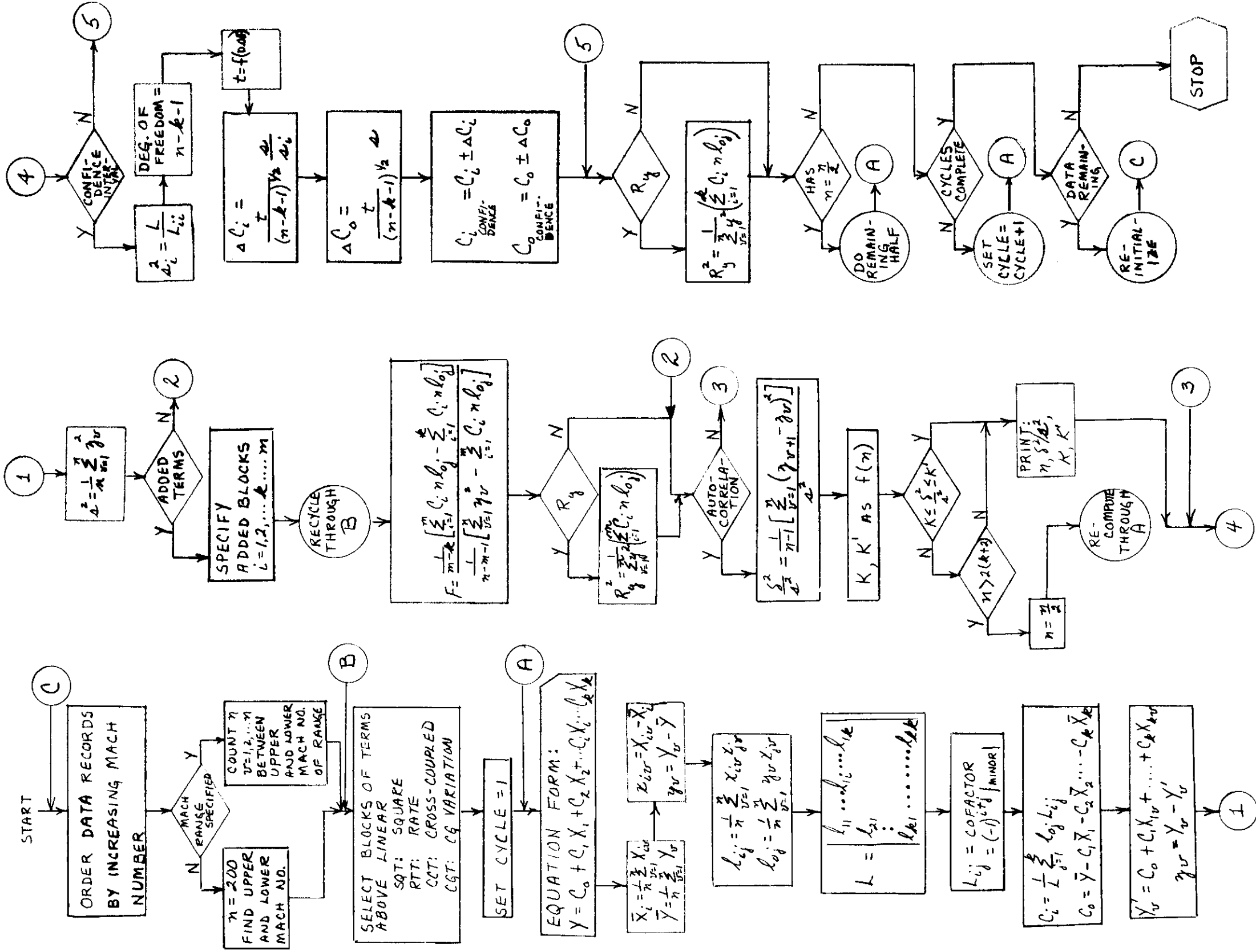A functional flow chart of the aerodynamic derivatives computations is shown in Figure 11.2.

AERODYNAMIC DERIVATIVE COMPUTATION SEQUENCE

FIGURE 11.2 FUNCTIONAL FLOW CHART — AERODYNAMIC DERIVATIVES

171

1. Perkins, C. D., and Hage, R. E., <u>Airplane Performance Stability and Control</u>, John Wiley & Sons, Inc., New York 1949, Chapters 10 and 11.

2. BuAer Report AE-61-4, "Fundamentals of Design of Piloted Aircraft Flight Control Systems," Vol. II, <u>Dynamics of the Airframe</u>, February 1953.

3. Hausner, G. W., and Hudson, D. E., <u>Applied Mechanics Dynamics</u>, D. Van Nostrand Company, Inc., New York, 1950.

4. Becker, R. A., <u>Introduction to Theoretical Mechanics</u>, McGraw-Hill Book Co., Inc., New York, 1954.

5. Webster, A. G., <u>The Dynamics of Particles and of Rigid, Elastic, and Fluid Bodies</u>, Hafner Publishing Company, Inc., New York, 1949.

6. Slater, J. C., and Frank, N. H., <u>Mechanics</u>, McGraw-Hill Book Co., Inc., 1947.

7. Seely, F. B., and Ensign, N. E., <u>Analytical Mechanics for Engineers</u>, John Wiley & Sons, Inc., New York, 1941, p. 391.

8. Page, Leigh, <u>Introduction to Theoretical Physics</u>, D. Van Nostrand Co., Inc., New York.

9. Doolin, Brian F., N.A.C.A. TN 3968, "The Application of Matrix Methods to Coordinate Transformations Occurring in Systems Involving Large Motions of Aircraft", dated May 1957.

10. "The 1960 American Ephemeris and Nautical Almanac", Superintendent of Documents, U.S. Printing Office, Washington 25, D.C.

11. Champion, K. S. W., Minzner, R. A., and Pond, H. T., AFCRC-TR-59-267, "The ARDC Model Atmosphere, 1959", August 1959.

12. Minzner, R. A., and Ripley, W. S., ARCRC-TN-56-204, "The ARDC Model Atmosphere", December 1956.

13. "Handbook of Geophysics for Air Force Designers", U.S. Air Force Cambridge Research Center, Geophysics Research Directorate, Cambridge, Massachusetts, 1957.

14. Herrick, S., Baker, R. M. L., and Hilton, U.C.L.A. Astronomical Papers, Vol. I, No. 24, 1957, "Gravitational and Related Constants for Accurate Space Navigation".

15. O'Keefe, S., Eckels, A., and Squires, R., ARS Paper 873-59, June 1959, "The Gravitational Field of the Earth".

16. Baker, Hilton, et. al., Interim Report, Task 5, Project Mercury Contract NAS 1-204, 1959.

17. Heiskanen, W., and Mainesz, Vening, The Earth and Its Gravity Field, McGraw-Hill Book Co., Inc., New York, 1958.

18. Jeffreys, H., The Earth, Fourth Edition, Cambridge University Press, New York, 1959.

19. O'Keefe, J. A., Eckels, A., and Squires, R. K., "Vanguard Measurements Give Pear-Shaped Component of Earth's Figure", Science, Vol. 129, p. 565.

20. Wilson, R. H., Jr., "A Gravitational Force Function for the Earth Representing All Deviations From a Spherical Geoid", Journal of Franklin Institute, November 1959.

21. Eckert, Ernest R. G., "Survey of Heat Transfer at High Speeds", WADC TR 54-70, April 1954.

22. Keenan, J. H., and Kaye, J., Thermodynamic Properties of Air, John Wiley & Sons, New York, 1945.

23. Detra, R. W., Kemp, N. H., and Riddell, F. R., "Addendum to Heat Transfer to Satellite Vehicles Re-Entering the Atmosphere", Jet Propulsion, December 1957.

24. Fay, J. A., and Riddell, F. R., Journal of Aeronautical Sciences, "Theory of Stagnation Point Heat Transfer in Dissociated Air", February 1958.

25. Ames Research Staff, "Equations, Tables, and Charts for Compressible Flow", NACA TR 1135, 1953.

26. Liepmann, H. W., and Rosko, A., Elements of Gasdynamics, John Wiley & Sons, Inc., New York, 1957.

27. Hoel, P. G., Introduction to Mathematical Statistics, Second Edition, John Wiley & Sons, New York, 1954.

28. Cramer, Harold, Mathematical Methods of Statistics, Princeton University Press, Princeton, 1946.

29. Ezekiel, Mordecai, and Fox, Karl, Methods of Correlation and Regression Analysis, Linear and Curvilinear, Third Edition, John Wiley & Sons, New York, 1959.

30. Von Neumann, J., et. al., "The Mean Square Successive Difference", The Annals of Mathematical Statistics, Vol. 12.

APPENDICES

Appendices One through Seven have been added to this report in order that a certain amount of detail may be included for particular portions of the problem formulation without interrupting the overall development being considered. The following topics are discussed in the appendices which follow.

Appendix One Derivation of Jet Damping Force and Moments

Appendix Two Rotating Machinery Terms in the Equations of Motion

Appendix Three An Orthogonality Constraint

Appendix Four A Method of Including Aerothermoelasticity

Appendix Five The Method of Converting Complex Transfer Functions to Real-Time Differential Equations

Appendix Six A Second-Order Simulation of the Effects of Aeroelasticity on Autopilot Behavior

Appendix Seven Geophysical and Engineering Constants for the Six-Degree-of-Freedom Flight-Path Study Computer Program.

APPENDIX I

DERIVATION OF THE JET-DAMPING FORCE AND MOMENT

Introduction - This appendix presents the derivation of relations for the jet-damping forces and moments caused by the expelling of the burnt fuel under conditions of angular rotation (References (One-1), (One-2), and (One-3)). The equations derived are applicable to a rocket, ram-jet, or turbo-jet engine. However, the contributions derived for a ram-jet or turbo-jet are only part of the engine flow forces since the change in momentum of the air flow, in addition to the fuel flow, must be considered. This contribution is assumed here to be accounted for in the aerodynamics of the body.

The equations are derived for a vehicle symmetrical about the x-z plane with motion restricted to this plane. These equations are then extended to consideration of motion in the horizontal plane using the same assumptions. This neglects the cross-coupling terms between planes, but since the jet-damping terms are small corrections to the general equations of motion, the omission of these effects is considered permissible in view of the complication required for their inclusion.

Jet Damping Force - A particle of fuel Δm within the missile is ejected out the nozzle in Δt time (reference Figure (1)).
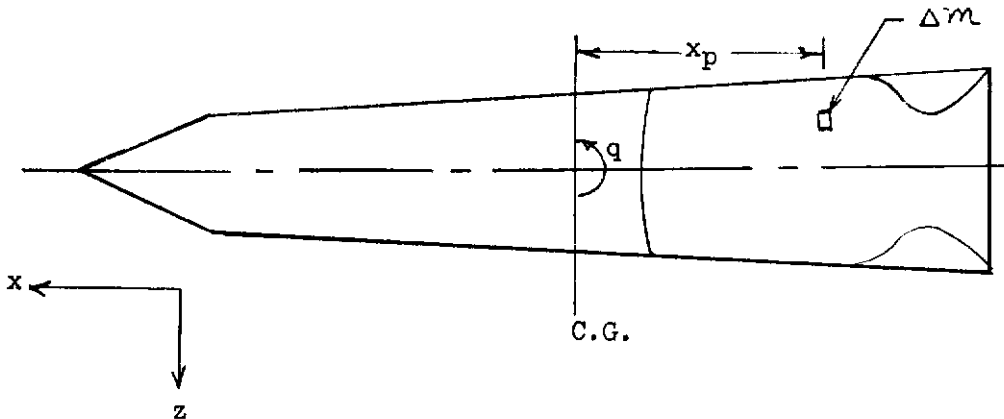

Figure 1 - Body Geometry for
Thrusting Rocket
With Changing Mass

The increment of force in the x direction is:

$$\Delta F_x = \Delta m \ddot{x}_p \tag{I.1}$$

where x_p is the distance from the center of gravity to the particle Δm. This force is the thrust term which is considered on the left side of the equations in the sum of the forces, and hence need not be considered here.

175

The increment of force in the z-direction due to the motion of a Δm particle of fuel is:

$$\Delta F_{z_D} = -2\Delta m \dot{x}_p \, q - \Delta m x_p \, \dot{q} \tag{I.2}$$

which is obtained from the general expression for acceleration, Equation (2.6), given in Section 2 of this report by assuming the particle of fuel travels only in the x-direction and the motion of the body is restricted to the x-plane. Summing over the total particles ejected

$$F_{z_D} = -2 \sum_j \Delta m_j \dot{x}_p \, q - \sum_j \Delta m_j x_p \, \dot{q} \tag{I.3}$$

Since $\dot{x}_p \, q$ will be large compared to $x_p \, \dot{q}$ only the first term in the above equation will be retained. Now writing Δm as

$$\Delta m = \rho \Delta x_p \Delta A \tag{I.4}$$

we have

$$F_{z_D} = -2q \int_x \int_A \rho \, \dot{x}_p \, dA \, dx_p \tag{I.5}$$

Assume all particles at a given x_p are moving at the same velocity and have the same density so that

$$F_{z_D} = -2q \int_x \rho A \, \dot{x}_p \, dx_p \tag{I.6}$$

Also assume that all particles being expelled originate from the same point in the body (say l_1)[1] so that

$$\rho A \, \dot{x}_p = \dot{m} \tag{I.7}$$

Then

$$F_{z_D} = -2q \, \dot{m} \int_{l_1}^{l_2} dx_p$$

or

$$F_{z_D} = -2q \, \dot{m} (l_2 - l_1) \tag{I.8}$$

---

(1) For solid-propellant radially-burning rockets, l_1 coincides with the center of gravity of the propellant grain. For end-burning rockets l_1 is a variable with time being the location of the reacting surface. For liquid propellant rockets, l_1 may be approximated as the location of the propellant free-surface center of area in the tank where a weighted average of fuel and oxidizer locations must be used.

It should be noted that the $\dot{m}$ term is the mass flow rate of the particles leaving the body and is equal to the negative of the body mass rate of change with time. Also the distances associated with x_p have a negative value measured aft of the center of gravity and the effective distance traveled by the particles is designated l_z representing a characteristic distance. The term to add to the F_z term due to jet damping is therefore

$$F_{z_D} = 2\,\dot{m}\,q\,l_z \qquad (I.9)$$

is the rate of change of mass of the body and l_z is a characteristic distance perpendicular to the z-axis along the x-axis, negative if extending aft of the center of gravity. In most cases, the change in mass will be the fuel flow and, from the definition of the vehicle mass given in Section 8.2.

$$\frac{d m}{dt} = -\dot{m}f \qquad (I.10)$$

Using the same analysis in the yaw plane, the jet damping term becomes;

$$F_{y_D} = -2\,\dot{m}\,r\,l_y \qquad (I.11)$$

$\dot{m}$ is the rate of change of mass of the body and l_y is the characteristic distance perpendicular to the y-axis, along the x-axis, negative if extending aft of the center of gravity.

Jet Damping Moment - Assume that the missile is pitching about the instantaneous center of gravity. The moment of the incremental force ΔF_{z_D} described above is

$$\Delta M_D = -2\Delta m\,x_p\,\dot{x}_p\,q - \Delta m\,x_p^2\,\dot{q} \qquad (I.12)$$

Making the same assumptions and following the same general development as used to determine the jet-damping force gives

$$M_D = -\dot{m}\,q\,(l_{m_2}^2 - l_{m_1}^2) \qquad (I.13)$$

Similarly for jet damping about the yaw and roll axes, the moments are

$$L_D = -\dot{m}\,(l_{l_2}^2 - l_{l_1}^2)\,p$$
$$N_D = -\dot{m}\,(l_{n_2}^2 - l_{n_1}^2)\,r \qquad (I.14)$$

Let

$$l_{l_2}^2 - l_{l_1}^2 = l_l^2$$
$$l_{m_2}^2 - l_{m_1}^2 = l_m^2$$
$$l_{n_2}^2 - l_{n_1}^2 = l_n^2 \qquad (I.15)$$

where l_l, l_m, and l_n are considered characteristic distances with the exponent retained as an aid to identification. The substitution is made to conserve machine storage space.

APPENDIX II

ROTATING-MACHINERY TERMS IN THE EQUATIONS OF MOTION

This appendix presents a derivation of the moment contributions due to the gyroscopic effects of rotating machinery aboard the flight vehicle. An accounting of such moments, in completely general terms, is exceedingly complicated and lengthy such that a number of simplifying restrictions are entirely justified. For this reason the principal gyroscopic moments which will arise for several types of rotating machinery are derived here with an explanation of the approximations made. The three types of vehicles to which this derivation is applicable are:

(1) A conventional turbojet or propeller driven aircraft.

(2) A convertiplane in which the engine or propeller is rotated during transition from vertical to forward flight (or vice versa).

(3) A satellite in which motors are being started and stopped (by proper selection of coordinate systems).

The general derivation of the rotating-machinery contributions is outlined for reference should a particular future application require inclusion of the terms omitted in the present application.

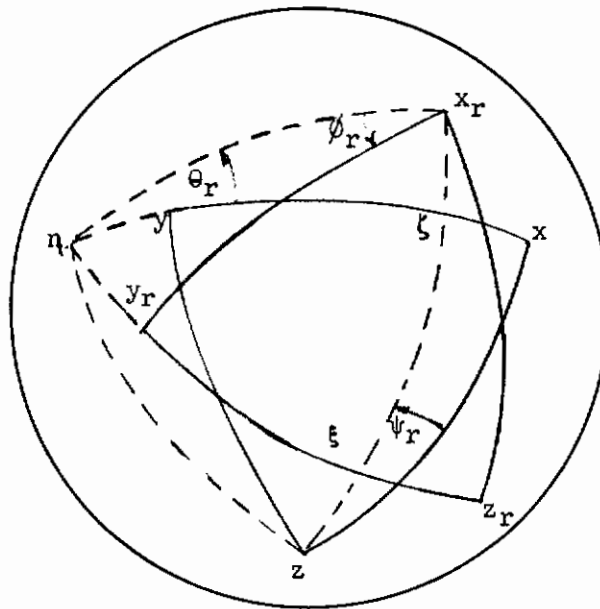Figure (1) aids in the description of the rotating-machinery axes system.

Figure 1 - Rotating-Machinery Axes System

Let the axes system of the rotating machinery be designated as x_r-y_r-z_r where x_r is along the shaft and y_r, z_r are perpendicular to x_r in a normal right-handed manner so that y_r crossed into z_r describes a positive rotation vector in the positive x_r-direction. The shaft is canted with respect to the body x-axes at an angle ψ_r in the x-y plane and pitched at an angle Θ_r which is perpendicular to the body x-y plane. A positive ψ_r rotation is clockwise when viewed in the positive z-direction. Positive Θ_r rotation is nose up. The angle ϕ_r is the rotation angle of the shaft and is equal to

$$\phi_r = \int_0^t \omega_r dt$$

where ω_r is the rotation rate of the shaft.

In matrix notation (see References (Two-1) and (Two-2)) the coordinate transformation from the body axes to the rotating-machinery axes is:

$$\begin{vmatrix} x_r \\ y_r \\ z_r \end{vmatrix} = \begin{vmatrix} \phi_r \end{vmatrix} \begin{vmatrix} \Theta_r \end{vmatrix} \begin{vmatrix} \psi_r \end{vmatrix} \begin{vmatrix} x \\ y \\ z \end{vmatrix} \tag{II.1a}$$

or, transforming from the machinery axes back to the body axes

$$\begin{vmatrix} x \\ y \\ z \end{vmatrix} = \begin{vmatrix} -\psi_r \end{vmatrix} \begin{vmatrix} -\Theta_r \end{vmatrix} \begin{vmatrix} -\phi_r \end{vmatrix} \begin{vmatrix} x_r \\ y_r \\ z_r \end{vmatrix} \tag{II.1b}$$

Moments in the body-axes system due to moments in the rotating-machinery axes system can be expressed as:

$$\begin{vmatrix} L \\ M \\ N \end{vmatrix} = \begin{vmatrix} -\psi_r \end{vmatrix} \begin{vmatrix} -\Theta_r \end{vmatrix} \begin{vmatrix} -\phi_r \end{vmatrix} \begin{vmatrix} L_r \\ M_r \\ N_r \end{vmatrix} \tag{II.2}$$

However, moments of the engine L_r, M_r, and N_r are functions of the total shaft rates, p_r, q_r, and r_r and their derivatives $\dot{p}_r$, $\dot{q}_r$, $\dot{r}_r$.

The total shaft rates are functions of the body rates, rotational speed of the shaft, and rotation of the shaft axes system with respect to the body. The rotation is

179

$$\begin{vmatrix} p_r \\ q_r \\ r_r \end{vmatrix} = \begin{vmatrix} \omega_r \\ 0 \\ 0 \end{vmatrix} + \begin{vmatrix} \phi_r \end{vmatrix}\begin{vmatrix} \theta_r \end{vmatrix}\begin{vmatrix} \psi_r \end{vmatrix} \begin{vmatrix} p - \dot\theta_r \sin\psi_r \\ q + \dot\theta_r \cos\psi_r \\ r + \dot\psi_r \end{vmatrix} \qquad (II.3)$$

The components, L, M, and N due to the rotating machinery can be obtained by substituting the expressions for p_r, q_r, r_r, $\dot p_r$, $\dot q_r$, and $\dot r_r$ into the general equations for L_r, M_r, and N_r and then performing the indicated coordinate transformation into the body axes. However, this procedure can be simplified somewhat by an examination of the physical situation. Any machinery which has a moment of momentum which is large enough to produce significant gyroscopic moments will probably be dynamically balanced and the products of inertia will be zero. The motor or engine shaft will have a fixed mass and geometry so that all time rate of change of inertia terms will also be zero. Due to the symmetry of the rotating mass the inertias I_{yr} and I_{zr} will be equal. Further, because of the restrictions of the bearing system the rotation of the shaft in the machinery axes will all occur about the x_r axes as noted in the coordinate transformation above. With these simplifications the contributions of the rotating machinery are:

$$L_r = I_{xr}\,\dot p_r$$
$$M_r = I_{yr}\,\dot q_r + (I_{xr} - I_{zr})\,p_r r_r \qquad (II.4)$$
$$N_r = I_{zr}\,\dot r_r + (I_{yr} - I_{xr})\,p_r q_r$$

I_{xr}, I_{yr}, and I_{zr} are moments of inertia in the x_r, y_r, and z_r-axes. The moments in the body axes due to the rotating machinery are:

$$L = L_r \cos\theta_r \cos\psi_r + M_r(\sin\phi_r \sin\theta_r \cos\psi_r - \cos\phi_r \sin\psi_r)$$
$$+ N_r(\cos\phi_r \sin\theta_r \cos\psi_r + \sin\phi_r \sin\psi_r)$$
$$M = L_r \cos\theta_r \sin\psi_r + M_r(\sin\phi_r \sin\theta_r \sin\psi_r + \cos\phi_r \cos\psi_r) \qquad (II.5)$$
$$+ N_r(\cos\phi_r \sin\theta_r \sin\psi_r - \sin\phi_r \cos\psi_r)$$
$$N = -L_r \sin\theta_r + M_r \sin\phi_r \cos\theta_r + N_r \cos\phi_r \cos\theta_r$$

Expanding Equation (II.3) for the total turning rates of the rotating machinery gives

$$p_r = \omega_r + p\cos\theta_r \cos\psi_r + q\cos\theta_r \sin\psi_r - (r + \dot\psi_r)\sin\theta_r$$
$$q_r = (p\cos\psi_r + q\sin\psi_r)\sin\theta_r \sin\phi_r + (q\cos\psi_r - p\sin\psi_r)\cos\phi_r$$
$$+ \dot\theta_r \cos\phi_r + (r + \dot\psi_r)\sin\phi_r \cos\theta_r$$
$$r_r = (p\cos\psi_r + q\sin\psi_r)\cos\phi_r \sin\theta_r + (p\sin\psi_r - q\cos\psi_r)\sin\phi_r$$
$$- \dot\theta_r \sin\phi_r + (r + \dot\psi_r)\cos\phi_r \cos\theta_r \qquad (II.6)$$

Significant simplification of these relations can be made by considering the relative magnitudes of the several terms. In general the cant angle ψ_r is very small and, except for some problems in dynamic aeroelasticity where the geometry of the aircraft is not fixed, the rate of turning, $\dot{\psi}_r$, is zero. The present analysis will assume that ψ_r and its derivatives are zero. The Θ_r-terms have been retained to account for the moments generated by a converti-plane during transition from vertical to forward flight (or vice versa). Also, the rotational rate of the machinery will be much greater than the body rates p, q, and r. Within the limitations of these assumptions, the following expressions for the rotational rates are obtained. It should be noted that the relative magnitude of q_r and r_r is much smaller than p_r. Therefore, to obtain reasonable approximations for these rates requires the retention of terms which are negligible for p_r.

$$p_r \simeq \omega_r$$

$$q_r \simeq p \sin \phi_r \sin \Theta_r + (q + \dot{\Theta}_r) \cos \phi_r + r \sin \phi_r \cos \Theta_r \qquad (II.7)$$

$$r_r \simeq p \cos \phi_r \sin \Theta_r - (q + \dot{\Theta}_r) \sin \phi_r + r \cos \phi_r \cos \Theta_r$$

The derivatives of the total rotational rates p_r, q_r, and r_r are also required. The Equation (II.6) should be used for this operation. The derivatives are presented assuming ψ_r and its derivatives to be zero.

$$\dot{p}_r = \dot{\omega}_r + \dot{p} \cos \Theta_r - p \dot{\Theta}_r \sin \Theta_r - \dot{r} \sin \Theta_r - r \dot{\Theta}_r \cos \Theta_r$$

$$\dot{q}_r = p \dot{\phi}_r \sin \Theta_r \cos \phi_r + (p \dot{\Theta}_r + \dot{r}) \sin \phi_r \cos \Theta_r + (\dot{p} - r \dot{\Theta}_r) \sin \Theta_r \sin \phi_r$$
$$\quad - (q + \dot{\Theta}_r) \dot{\phi}_r \sin \phi_r + (\dot{q} + \ddot{\Theta}_r) \cos \phi_r + r \dot{\phi}_r \cos \Theta_r \cos \phi_r$$
$$\qquad\qquad (II.8)$$

$$\dot{r}_r = -p \dot{\phi}_r \sin \Theta_r \sin \phi_r + (p \dot{\Theta}_r + \dot{r}) \cos \phi_r \cos \Theta_r + (\dot{p} - r \dot{\Theta}_r) \sin \Theta_r \cos \phi_r$$
$$\quad - (q + \dot{\Theta}_r) \dot{\phi}_r \cos \phi_r - (\dot{q} + \ddot{\Theta}_r) \sin \phi_r - r \dot{\phi}_r \cos \Theta_r \sin \phi_r$$

However, $\dot{\phi}_r$ is ω_r and by the same reasoning which resulted in the simplifica-tion of Equation Set II.6 to Equation Set II.7, the differentials are reasonably approximated by

$$\dot{p}_r \simeq \dot{\omega}_r + \dot{p} \cos \Theta_r - p \dot{\Theta}_r \sin \Theta_r - \dot{r} \sin \Theta_r - r \dot{\Theta}_r \cos \Theta_r$$

$$\dot{q}_r \simeq p \omega_r \sin \Theta_r \cos \phi_r - (q + \dot{\Theta}_r) \omega_r \sin \phi_r + r \omega_r \cos \Theta_r \cos \phi_r$$

$$\dot{r}_r \simeq -p \omega_r \sin \Theta_r \sin \phi_r - (q + \dot{\Theta}_r) \omega_r \cos \phi_r - r \omega_r \cos \Theta_r \sin \phi_r$$
$$\qquad\qquad (II.9)$$

The moments in the machinery axes are obtained by substituting Equations (II.7) and (II.9) into Equation (II.4)

$$L_r = I_{xr} (\dot{\omega}_r + \dot{p} \cos \Theta_r - p \dot{\Theta}_r \sin \Theta_r - \dot{r} \sin \Theta_r - r \dot{\Theta}_r \cos \Theta_r)$$

$$M_r = I_{yr} \left[p \, \omega_r \, \mathrm{Sin} \, \Theta_r \, \mathrm{Cos} \, \phi_r - (q + \dot{\Theta}_r) \, \omega_r \, \mathrm{Sin} \, \phi_r + r \, \omega_r \, \mathrm{Cos} \, \Theta_r \, \mathrm{Cos} \, \phi_r \right]$$

$$+ (I_{xr} - I_{zr}) \, \omega_r \left[p \, \mathrm{Cos} \, \phi_r \, \mathrm{Sin} \, \Theta_r - (q + \dot{\Theta}_r) \, \mathrm{Sin} \, \phi_r + r \, \mathrm{Cos} \, \phi_r \, \mathrm{Cos} \, \Theta_r \right]$$

$$N_r = I_{zr} \left[-p \, \omega_r \, \mathrm{Sin} \, \Theta_r \, \mathrm{Sin} \, \phi_r - (q + \dot{\Theta}_r) \, \omega_r \, \mathrm{Cos} \, \phi_r - r \, \omega_r \, \mathrm{Cos} \, \Theta_r \, \mathrm{Sin} \, \phi_r \right]$$

$$+ (I_{yr} - I_{xr}) \, \omega_r \left[p \, \mathrm{Sin} \, \phi_r \, \mathrm{Sin} \, \Theta_r + (q + \dot{\Theta}_r) \, \mathrm{Cos} \, \phi_r + r \, \mathrm{Sin} \, \phi_r \, \mathrm{Cos} \, \Theta_r \right]$$

$$\text{(II.10)}$$

Substituting the expressions of Equation (II.10) into the coordinate transformation of Equation (II.5), the moments L, M, and N are obtained.

$$L = I_{xr}(\dot{\omega}_r + \dot{p} \, \mathrm{Cos} \, \Theta_r - p \, \dot{\Theta}_r \, \mathrm{Sin} \, \Theta_r - \dot{r} \, \mathrm{Sin} \, \Theta_r - r \, \dot{\Theta}_r \, \mathrm{Cos} \, \Theta_r) \, \mathrm{Cos} \, \Theta_r$$

$$+ I_{yr} \left[p \, \omega_r \, \mathrm{Cos} \, \phi_r \, \mathrm{Sin}^2 \, \Theta_r \, \mathrm{Sin} \, \phi_r - (q + \dot{\Theta}_r) \, \omega_r \, \mathrm{Sin}^2 \, \phi_r \, \mathrm{Sin} \, \Theta_r \right.$$

$$\left. + r \, \omega_r \, \mathrm{Cos} \, \phi_r \, \mathrm{Cos} \, \Theta_r \, \mathrm{Sin} \, \phi_r \, \mathrm{Sin} \, \Theta_r \right] + (I_{xr} - I_{zr}) \, \omega_r \left[p \, \mathrm{Cos} \, \phi_r \, \mathrm{Sin}^2 \, \Theta_r \, \mathrm{Sin} \, \phi_r \right.$$

$$\left. - (q + \dot{\Theta}_r) \, \mathrm{Sin}^2 \, \phi_r \, \mathrm{Sin} \, \Theta_r + r \, \mathrm{Cos} \, \phi_r \, \mathrm{Cos} \, \Theta_r \, \mathrm{Sin} \, \phi_r \, \mathrm{Sin} \, \Theta_r \right]$$

$$+ I_{zr} \left[-p \, \omega_r \, \mathrm{Sin} \, \phi_r \, \mathrm{Sin}^2 \, \Theta_r \, \mathrm{Cos} \, \phi_r - (q + \dot{\Theta}_r) \, \omega_r \, \mathrm{Cos}^2 \, \phi_r \, \mathrm{Sin} \, \Theta_r \right.$$

$$\left. - r \, \omega_r \, \mathrm{Sin} \, \phi_r \, \mathrm{Cos} \, \Theta_r \, \mathrm{Cos} \, \phi_r \, \mathrm{Sin} \, \Theta_r \right] + (I_{yr} - I_{xr}) \, \omega_r \left[p \, \mathrm{Sin} \, \phi_r \, \mathrm{Sin}^2 \, \Theta_r \, \mathrm{Cos} \, \phi_r \right.$$

$$\left. + (q + \dot{\Theta}_r) \, \mathrm{Cos}^2 \, \phi_r \, \mathrm{Sin} \, \Theta_r + r \, \mathrm{Sin} \, \phi_r \, \mathrm{Cos} \, \Theta_r \, \mathrm{Cos} \, \phi_r \, \mathrm{Sin} \, \Theta_r \right]$$

As noted earlier, the inertias I_{yr} and I_{zr} will be assumed to be equal, therefore

$$L = I_{xr}(\dot{\omega}_r + \dot{p} \, \mathrm{Cos} \, \Theta_r - p \, \dot{\Theta}_r \, \mathrm{Sin} \, \Theta_r - \dot{r} \, \mathrm{Sin} \, \Theta_r - r \, \dot{\Theta}_r \, \mathrm{Cos} \, \Theta_r) \, \mathrm{Cos} \, \Theta_r$$

$$- I_{xr} \, \omega_r \, (q + \dot{\Theta}_r) \, \mathrm{Sin} \, \Theta_r$$

and similarly for M, and N

$$M = I_{xr} \, \omega_r \, (p \, \mathrm{Sin} \, \Theta_r + r \, \mathrm{Cos} \, \Theta_r) \qquad \text{(II.11)}$$

$$N = -I_{xr} \, (\dot{\omega}_r + \dot{p} \, \mathrm{Cos} \, \Theta_r - p \, \dot{\Theta}_r \, \mathrm{Sin} \, \Theta_r - \dot{r} \, \mathrm{Sin} \, \Theta_r - r \, \dot{\Theta}_r \, \mathrm{Cos} \, \Theta_r) \, \mathrm{Sin} \, \Theta_r$$

$$- I_{xr} \, (q + \dot{\Theta}_r) \, \omega_r \, \mathrm{Cos} \, \Theta_r$$

The predominate terms of this contribution are:

$$L = -I_{xr} \, \omega_r \, (q + \dot{\Theta}_r) \, \mathrm{Sin} \, \Theta_r$$

$$M = I_{xr} \, \omega_r \, (p \, \mathrm{Sin} \, \Theta_r + r \, \mathrm{Cos} \, \Theta_r)$$

$$N = -I_{xr} \, (q + \dot{\Theta}_r) \, \omega_r \, \mathrm{Cos} \, \Theta_r$$

and are the terms normally considered for the types of aircraft considered in the present derivation. These contributions are programmed into the SDF computer program for normal operation. The derivation of the lesser terms has been indicated, however, and may be extended in greater degrees of sophistication by the user should the particular application require them.

APPENDIX III

AN ORTHOGONALITY CONSTRAINT

Introduction - The direction consines relating body coordinates and inertial coordinates will be evaluated by solving the nine simultaneous differential equations noted in Equation (3.12), Section 3.1. The numerical integration of Equation (3.12) will produce errors in the resultant direction cosines which in turn will cause the resolved components of a given vector to be non-orthogonal. This appendix presents the constraint equations that may be used to improve the orthogonality of the transformation between body and inertial coordinates. The results of a digital computer study, designed to evaluate the constraint equations, are also presented. The constraints developed in the following analysis were suggested by the memorandum of Reference (Three-1).

Computation of the Direction Cosines - The direction cosines to be considered relate body and inertial coordinates and are defined by Equation (3.1) from Section 3.1.

$$
\begin{vmatrix} X \\ Y \\ Z \end{vmatrix}
=
\begin{vmatrix} l_1 & m_1 & n_1 \\ l_2 & m_2 & n_2 \\ l_3 & m_3 & n_3 \end{vmatrix}
\begin{vmatrix} x \\ y \\ z \end{vmatrix}
\qquad (III.1)
$$

The direction cosines in Equation (III.1) are given by the solution of the following nine simultaneous differential equations (see Equation (3.12), Section 3.1 for derivation).

$$\dot{l}_1 = rm_1 - qn_1$$

$$\dot{l}_2 = rm_2 - qn_2$$

$$\dot{l}_3 = rm_3 - qn_3$$

$$\dot{m}_1 = pn_1 - rl_1$$

$$\dot{m}_2 = pn_2 - rl_2 \qquad (III.2)$$

$$\dot{m}_3 = pn_3 - rl_3$$

$$\dot{n}_1 = ql_1 - pm_1$$

$$\dot{n}_2 = ql_2 - pm_2$$

$$\dot{n}_3 = ql_3 - pm_3$$

Let the matrix of direction cosines evaluated at a given time, by the numerical integration of Equation (3.12), be defined as the A_c matrix;

183

$$A_c = \begin{vmatrix} 1_{1_c} & m_{1_c} & n_{1_c} \\ 1_{2_c} & m_{2_c} & n_{2_c} \\ 1_{3_c} & m_{3_c} & n_{3_c} \end{vmatrix} \qquad\qquad (III.3)$$

The true orthogonal matrix of direction cosines at the same time will be defined as the A matrix;

$$A = \begin{vmatrix} 1_1 & m_1 & n_1 \\ 1_2 & m_2 & n_2 \\ 1_3 & m_3 & n_3 \end{vmatrix} \qquad\qquad (III.4)$$

Since A is orthogonal, the value of A, as a determinant, is unity, and each term in A is equal to its cofactor. For example,

$$m_1 = 1_3 n_2 - 1_2 n_3$$

Constraint Equations - A method of preventing divergence in the numerical integration of the nine direction cosine rates will be developed. Only errors that tend to cause divergence will be considered. It is assumed that a constant error, α, is introduced at every time step such that each direction cosine is modified by $1 + \alpha$, thus

$$A_c = (1 + \alpha) A \qquad\qquad (III.5)$$

It will be shown that this type of error may be greatly diminished by averaging the matrix of calculated direction cosines with the transposed inverse of the matrix of calculated direction cosines.

The inverse of the computed matrix, A_c, is equal to the reciprocal of the determinant of A_c times the transposed cofactors of A_c. Recalling that each term in the orthogonal A matrix is equal to its cofactor and that the determinant of A is unity, the inverse of A_c is written from Equation (III.5)

$$A_c^{-1} = \frac{1}{1 + \alpha} A_T \qquad\qquad (III.6)$$

where the superscript -1 indicates the inverse of a matrix and the subscript T denotes the transpose of a matrix. For $\alpha \ll 1$ the Maclaurin series expansion of $1/(1 + \alpha)$ converges rapidly, and terms of order two and higher may be neglected.

$$\frac{1}{1 + \alpha} = 1 - \alpha + \alpha^2 - \alpha^3 + \ldots \qquad\qquad (III.7)$$

Substituting Equation (III.7) into Equation (III.6) gives:

$$A_c^{-1} = (1 - \alpha) A_T \tag{III.8}$$

The transpose of Equation (III.8) is:

$$A_{c_T}^{-1} = (1 - \alpha) A \tag{III.9}$$

The average of corresponding terms in the $A_{c_T}^{-1}$ and A_c matrices eliminates the assumed error, since

$$1/2 \left[A_{c_T}^{-1} + A_c \right] = A \left[\frac{1 - \alpha}{2} + \frac{1 + \alpha}{2} \right] = A \tag{III.10}$$

Other types of errors are introduced through numerical integration which are not necessarily eliminated by this averaging process. Therefore, this constraint is not intended to improve the accuracy of the direction cosines but rather is used to prevent divergence and maintain an orthogonal transformation.

The computer equations required to mechanize the constraint are presented below. The determinant of A_c is:

$$\Delta = l_{1_c} m_{2_c} n_{3_c} + l_{3_c} m_{1_c} n_{2_c} + l_{2_c} m_{3_c} n_{1_c}$$
$$- l_{3_c} m_{2_c} n_{1_c} - l_{2_c} m_{1_c} n_{3_c} - l_{1_c} m_{3_c} n_{2_c} \tag{III.11}$$

The inverse of the transpose of A_c is

$$A_{c_T}^{-1} = \frac{1}{\Delta} \begin{vmatrix} (m_{2_c} n_{3_c} - n_{2_c} m_{3_c}) & (n_{2_c} l_{3_c} - l_{2_c} n_{3_c}) & (l_{2_c} m_{3_c} - m_{2_c} l_{3_c}) \\ (n_{1_c} m_{3_c} - m_{1_c} n_{3_c}) & (l_{1_c} n_{3_c} - n_{1_c} l_{3_c}) & (m_{1_c} l_{3_c} - l_{1_c} m_{3_c}) \\ (m_{1_c} n_{2_c} - n_{1_c} m_{2_c}) & (n_{1_c} l_{2_c} - n_{2_c} l_{1_c}) & (l_{1_c} m_{2_c} - m_{1_c} l_{2_c}) \end{vmatrix} \tag{III.12}$$

For convenience let $A_{c_T}^{-1}$ be written as

$$A_{c_T}^{-1} = \begin{vmatrix} l_1' & m_1' & n_1' \\ l_2' & m_2' & n_2' \\ l_3' & m_3' & n_3' \end{vmatrix} \tag{III.13}$$

Then $1/2(A_{c_T}^{-1} + A_c)$, the matrix of direction cosines with the error, α, attenuated, may be written as

$$A = 1/2 \begin{vmatrix} (l_{1_c} + l'_c) & (m_{1_c} + m'_1) & (n_{1_c} + n'_1) \\ (l_{2_c} + l'_2) & (m_{2_c} + m'_2) & (n_{2_c} + n'_2) \\ (l_{3_c} + l'_3) & (m_{3_c} + m'_3) & (n_{3_c} + n'_3) \end{vmatrix} \qquad \text{(III.14)}$$

Equations (III.11) through (III.14) are required to employ the orthogonality constraint. The matrix of Equation (III.14) contains the corrected direction cosines relating body and inertial coordinates.

Evaluation of the Constraint - To evaluate the effectiveness of the constraint, Equation (III.2) was solved simultaneouly using Modified Euler integration with a time step of 0.01 second. The body angular rates, p, q, and r, were selected so that the body coordinates were rotated at one revolution per second about an axis fixed with respect to inertial coordinates. Therefore, at the end of each second, the direction cosine matrix relating the two coordinate systems is a unit matrix. The accuracy of the individual direction cosines may easily be determined at the end of each second.

The criterion used to evaluate the orthogonality of the direction cosines is to multiply the computed matrix of direction cosines by its transpose. For an orthogonal transformation, a unit matrix is the correct result of this multiplication. The elements of the product of the computed matrix with its transpose is compared with corresponding elements of a unit matrix. This comparison is used as a criterion for evaluating the orthogonality of the computed matrix of direction cosines with its transpose produced a matrix with numbers along the main diagonal that differed from unity by about 3×10^{-4}. The off-diagonal numbers which should have been zero were about 6×10^{-6}. After the same number of revolutions with the constraint developed above employed, the product of the computed matrix with its transpose produced numbers along the main diagonal which differed from unity by 2×10^{-8}. The off-diagonal numbers were about 8×10^{-10}. From these results we may conclude that the orthogonality of the transformation is markedly improved by using the constraint with Modified Euler integration.

APPENDIX IV

A METHOD OF INCLUDING AEROTHERMOELASTICITY

Aerothermoelastic Effects - The effect of static aerothermoelasticity on the aerodynamic coefficients will be accounted for in some of the aerodynamic subprograms. This effect results from the deflection and distortion of the heated structure under loading. Considerable theoretical work has been devoted to the problem of static aeroelasticity. Typical examples are References (Four-1), (Four-2), and (Four-3). The magnitude of effects is dependent upon the amount of deflection of the structure which is, in turn, a function of the structural rigidity.

A development of the static aerothermoelastic terms to be included in the program follows. Let F represent any one of the orthogonal components of aerodynamic force or moment acting on a rigid airframe at a given flight condition, and let F' represent the force or moment acting on the elastic airframe under the same conditions. Then:

$$F' = F + \sum \Delta F_i \qquad (IV.1)$$

where ΔF_i represents the incremental force (or moment) contribution of the i-th member of the airframe due to its structural deflection, δ_i, under load. Assuming linear deflection-load characteristics,

$$\Delta F_i = \frac{dF_i}{d\delta_i} \delta_i \qquad (IV.2)$$

The i-th member will deflect in a given plane due to both inertia loads, n, and aerodynamic loads, N, on the member in that plane so that

$$\delta_i = \frac{\partial \delta_i}{\partial n} n + \frac{\partial \delta_i}{\partial N_i} N_i' \qquad (IV.3)$$

and since

$$N_i' = N_i + \frac{dN_i}{d\delta_i} \delta_i \qquad (IV.4)$$

we have

$$\delta_i = \frac{\frac{\partial \delta_i}{\partial n} n + \frac{\partial \delta_i}{\partial N_i} N_i}{1 - \frac{\partial \delta_i}{\partial N_i} \frac{dN_i}{d\delta_i}} \qquad (IV.5)$$

Substituting Equations (IV.2) and (IV.5) into Equation (IV.1), and noting that $n = N'/W_T$, we obtain

$$F' = F + \sum \frac{dF_1}{d\delta_1} \left[\frac{\frac{\partial \delta_1}{\partial n} \frac{N'}{W_T} + \frac{\partial \delta_1}{\partial N_1} N_1}{1 - \frac{\partial \delta_1}{\partial N_1} \frac{dN_1}{d\delta_1}} \right] \qquad \text{(IV.6)}$$

or

$$F' = F + N' \sum \left[\frac{\frac{dF_1}{d\delta_1} \frac{\partial \delta_1}{\partial n} \frac{1}{W_T}}{1 - \frac{\partial \delta_1}{\partial N_1} \frac{dN_1}{d\delta_1}} \right] + N \sum \left[\frac{\frac{dF_1}{d\delta_1} \frac{\partial \delta_1}{\partial N_1} \frac{dN_1}{dN}}{1 - \frac{\partial \delta_1}{\partial N_1} \frac{dN_1}{d\delta_1}} \right] \qquad \text{(IV.7)}$$

To solve for N' let $F' = N'$, $F = N$. Then

$$N' = N + N' \sum \left[\frac{\frac{dN_1}{d\delta_1} \frac{\partial \delta_1}{\partial n} \frac{1}{W_T}}{1 - \frac{\partial \delta_1}{\partial N_1} \frac{dN_1}{d\delta_1}} \right] + N \sum \left[\frac{\frac{dN}{d\delta_1} \frac{\partial \delta_1}{\partial N_1} \frac{dN_1}{dN}}{1 - \frac{\partial \delta_1}{\partial N_1} \frac{dN_1}{d\delta_1}} \right] \qquad \text{(IV.8)}$$

and

$$N'/N = \left(1 + \sum \left[\frac{\frac{dN_1}{d\delta_1} \frac{\partial \delta_1}{\partial N_1} \frac{dN_1}{dN}}{1 - \frac{\partial \delta_1}{\partial N_1} \frac{dN_1}{d\delta_1}} \right] \right) \bigg/ \left(1 - \sum \left[\frac{\frac{dN_1}{d\delta_1} \frac{\partial \delta_1}{\partial n} \frac{1}{W_T}}{1 - \frac{\partial \delta_1}{\partial N_1} \frac{dN_1}{d\delta_1}} \right] \right) \qquad \text{(IV.9)}$$

It is normally more convenient to work with coefficients, rather than forces or moments, therefore

$$\frac{dF}{d\delta_1} = \frac{dC_F}{d\delta_1} \quad q^*S \qquad \text{(IV.10)}$$

$$\frac{dF_1}{d\delta_1} = \frac{dC_{F_1}}{d\delta_1} \quad q^*S \qquad \text{(IV.11)}$$

The effect of a change in the modulus of elasticity from the reference-temperature value, E_O, can be introduced in the following way:

$$\frac{\partial \delta_1}{\partial F_1} = \left(\frac{\partial \delta_1}{\partial F_1} \right)_{E_O} \left(\frac{E_O}{E} \right)_1 \qquad \text{(IV.12)}$$

188

$$\frac{\partial \delta_1}{\partial n} = \left(\frac{\partial \delta_1}{\partial n}\right)_{E_O} \left(\frac{E_O}{E}\right)_1 \tag{IV.13}$$

Introducing these expressions into Equation (IV.9), we obtain

$$N'/N = \cfrac{1 + \sum \left[\cfrac{\left(\frac{dC_{N_1}}{d\delta_1}\right)(q^*S)\left(\frac{\partial \delta_1}{\partial N_1}\right)_{E_O}\left(\frac{E_O}{E}\right)_1 \frac{dN_1}{dN}}{1 - \left(\frac{\partial \delta_1}{\partial N_1}\right)_{E_O}\left(\frac{E_O}{E}\right)_1\left(\frac{dC_{N_1}}{d\delta_1}\right)(q^*S)}\right]}{1 - \sum \left[\cfrac{\left(\frac{dC_{N_1}}{d\delta_1}\right)(q^*S)\left(\frac{\partial \delta_1}{\partial n}\right)_{E_O}\left(\frac{E_O}{E}\right)_1 \frac{1}{W_T}}{1 - \left(\frac{\partial \delta_1}{\partial N_1}\right)_{E_O}\left(\frac{E_O}{E}\right)_1\left(\frac{dC_{N_1}}{d\delta_1}\right)(q^*S)}\right]} \tag{IV.14}$$

An analysis of the structure under the influence of various temperature distributions will yield the parameters necessary to evaluate the above equation for a constant dynamic pressure. Repeated applications, with varying dynamic pressure, will result in the functional dependence of the (aeroelastic/rigid) load ratio upon the temperature distribution and dynamic pressure. A complete analysis would require that the effect of each of the independent variables considered in the determination of the aerodynamic coefficients, $(\alpha, \beta, \delta_p, \delta_q, \delta_r, M_N, T_s)$, be evaluated. However, the scope of such an analysis is beyond that desired for this program. A program which could accomplish this analysis would require more machine space than that required by the SDF computer program.

It therefore becomes necessary to make certain simplifying assumptions in the above analysis. Since the primary object of the SDF computer program is to evaluate performance and not highly specialized design problems, these assumptions are justifiable. This philosophy is consistent with that followed in the aerodynamic heating program, where the calculations are limited to 2 or 3 monitoring temperatures. The determination of the temperature distribution throughout the structure is beyond the scope of the program.

In view of this, let us make the following assumption,

$$\left(\frac{E_O}{E}\right)_1 = \left(\frac{E_O}{E}\right) \tag{IV.15}$$

It is now possible to group some of the terms in Equation (IV.14) into constants (for a particular Mach number), and the equation becomes

$$N'/N = \cfrac{1 + \cfrac{q^*}{E}\sum\left[\cfrac{K_1}{1 - K_2(q^*/E)}\right]}{1 - \cfrac{q^*}{E}\sum\left[\cfrac{K_3}{1 - K_2(q^*/E)}\right]} \tag{IV.16}$$

189

where

$$K_1 = E_o \, S \, \frac{dC_{N_1}}{d\delta_1} \, \frac{\partial \delta_1}{\partial N_1} \, \frac{dN_1}{dN} \qquad \text{(IV.17)}$$

$$K_2 = E_o \, S \, \frac{\partial \delta_1}{\partial N_1} \, \frac{dC_{N_1}}{d\delta_1} \qquad \text{(IV.18)}$$

$$K_3 = E_o \, S \, \frac{dC_{N_1}}{d\delta_1} \, \frac{\partial \delta_1}{\partial n} \, \frac{1}{W_T} \qquad \text{(IV.19)}$$

Equation (IV.16) may be written in the following way:

$$N'/N = \frac{1 + x}{1 - y} \qquad \text{(IV.20)}$$

The denominator may be expanded by the binomial theorem to give

$$\frac{1}{1 - y} = (1 - y)^{-1} = 1 + y + y^2 + y^3 + \dots \qquad \text{(IV.21)}$$

which is approximately given by

$$\frac{1}{1 - y} \simeq 1 + y \qquad \text{(IV.22)}$$

when y is small relative to unity. Then

$$N'/N = (1 + x)(1 + y) \qquad \text{(IV.23)}$$

or, again retaining only first-order terms in x and y,

$$N'/N = 1 + x + y \qquad \text{(IV.24)}$$

Now

$$x = \frac{q^*}{E} \sum \frac{K_1}{1 - K_2(q^*/E)} \qquad \text{(IV.25)}$$

If this equation is also expanded in a binomial series, and only the first-order terms retained, we obtain:

$$x = \frac{q^*}{E} \sum K_1 \left(1 + \frac{K_2 q^*}{E}\right) \qquad \text{(IV.26)}$$

Similarly

$$y = \frac{q^*}{E} \sum K_3 \left(1 + \frac{K_2 \, q^*}{E}\right) \qquad \text{(IV.27)}$$

Substituting Equations (IV.26) and (IV.27) into Equation (IV.24)

190

$$N'/N = 1 + \frac{q*}{E}\left[\sum K_1\left(1 + \frac{K_2\,q*}{E}\right) + \sum K_3\left(1 + \frac{K_2\,q*}{E}\right)\right] \quad (IV.28)$$

or

$$N'/N = 1 + \left(\sum K_1 + \sum K_3\right)\frac{q*}{E} + \left(\sum K_1 K_2 + \sum K_3 K_2\right)\left(\frac{q*}{E}\right)^2$$

The term $(q*/E)$ may be represented in the following way

$$\frac{q*}{E} = \frac{q*}{E_o}\;\frac{E_o}{E} \quad (IV.30)$$

Making this substitution into Equation (IV.29), we obtain

$$N'/N = 1 + \left(\sum K_1 + \sum K_3\right)\left(\frac{q*}{E_o}\right)\left(\frac{E_o}{E}\right) + \left(\sum K_1 K_2 + \sum K_3 K_2\right)\left(\frac{q*}{E_o}\right)^2\left(\frac{E_o}{E}\right)^2 \quad (IV.31)$$

Typical examples of the (E_o/E) ratio for various materials are presented as a function of temperature in Figure (1). In this subprogram an (E_o/E) ratio will be input as a function of a reference structural temperature. The ratio is to be representative of the entire structure, as indicated in Equation (IV.15). The reference structural temperature variation will be determined in the aerodynamic heating subprogram. Utilizing the interpolated (E_o/E) ratio, Equation (IV.31) may be expressed as

$$N'/N = 1 + A_1 q*\left(\frac{E_o}{E}\right) + A_2 q*^2\left(\frac{E_o}{E}\right)^2 \quad (IV.32)$$

where

$$A_1 = \left(\sum K_1 + \sum K_3\right)/E_o \quad (IV.33)$$

$$A_2 = \left(\sum K_1 K_2 + \sum K_3 K_2\right)/E_o^2 \quad (IV.34)$$

Equation (IV.34) will be evaluated for the following force and moment derivatives: C_{A_α}, $C_{A\delta_q}$, $C_{N\alpha}$, $C_{N\delta_q}$, C_{y_β}, $C_{y\delta_r}$, C_{l_α}, $C_{l\delta_p}$, C_{m_α}, $C_{m\delta_q}$, C_{n_α}, and $C_{n\delta_r}$.

A typical example is

$$C_{A_\alpha}' = C_{A_\alpha}\left[1 + A_1 q*\left(\frac{E_o}{E}\right) + A_2 q*^2\left(\frac{E_o}{E}\right)^2\right] \quad (IV.35)$$

Figure (2) gives an indication of the dynamic pressure effect on the elastic control derivative, $C_{M\delta_q}$, at various Mach numbers. The points denoted by symbols have been computed by the "exact" method which accounts for the load and temperature distribution through an actual structure. The solid line is a second-degree curve fit of these points which demonstrates very acceptable accuracy. The first-order approximation to the second-order curve fit and a straight-line least-squares curve fit are also shown in this figure. In certain cases the straight-line curve fit gives small incremental errors, but large percentage errors because of the magnitude of the derivative. For this reason the second order term will be retained in the above equations. With these assumptions and limitations, the aerothermo-elastic effects are introduced as indicated by the equation flow diagram. It will be required to input one curve of (E_o/E) versus temperature, and twenty-four curves consisting of an individual curve versus Mach number for each of the A values.
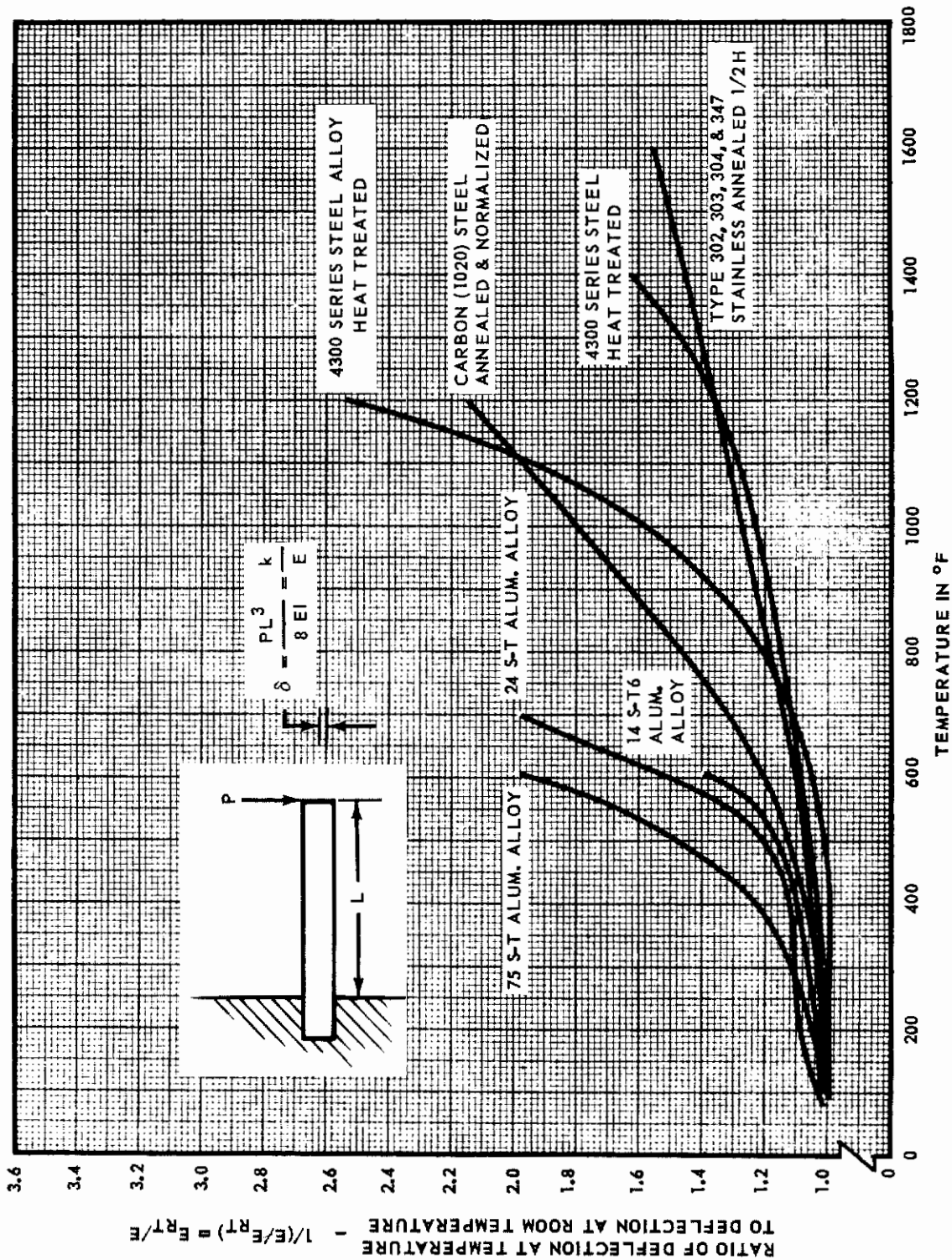
FIGURE 1, APPENDIX FOUR   COMPARISON OF DEFLECTIONS OF A CANTILEVER BEAM
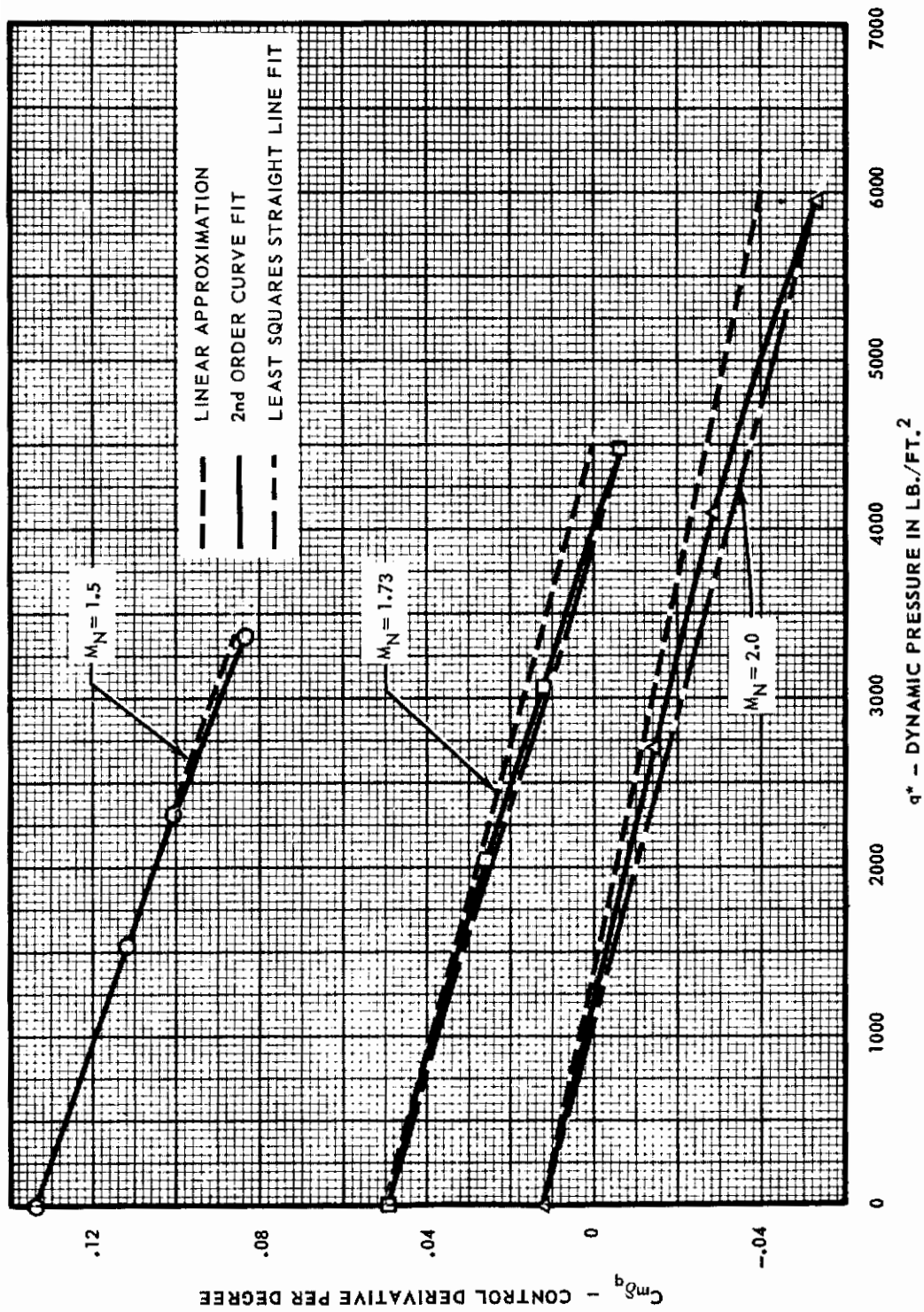AT ELEVATED TEMPERATURE FOR SEVERAL MATERIALS

192

FIGURE 2, APPENDIX FOUR   VARIATION OF THE EFFECT OF STATIC AEROELASTICITY
ON THE CONTROL DERIVATIVE OF A TYPICAL MISSILE WITH DYNAMIC PRESSURE

THE METHOD OF CONVERTING COMPLEX TRANSFER FUNCTIONS
TO REAL TIME DIFFERENTIAL EQUATIONS

The transfer functions representing control-system corrective networks, filters, servos, etc., are usually specified as functions of the complex frequency, s. A transfer function may be illustrated in block-diagram form as:
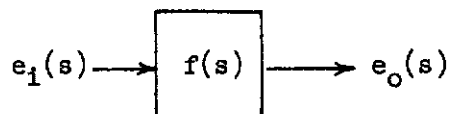
$$e_i(s) \longrightarrow \boxed{f(s)} \longrightarrow e_o(s)$$

which is interpreted as:

$$f(s) = \frac{e_o(s)}{e_i(s)} \tag{V.1}$$

The above notation indicates that the frequency spectrum of the input signal $e_i(s)$ is modified by the transfer function $f(s)$ to describe the output, $e_o(s)$. Since computations in this digital program are performed in the time domain, it will be necessary to determine the transient response by solving the differential equations representing the pertinent transfer functions.

Transfer functions containing only poles are easily converted to differential equation, form by recalling that multiplication by s in the frequency domain corresponds to differentiation in the time domain when initial conditions are zero. (See Transfer Function 1, Table V-1). However, if zeros are present in a transfer function, a solution for the output will involve a derivative of the input signal. This derivative would have to be evaluated by a programmed differentiation operation. This undesirable operation may be avoided by first expanding the transfer function into partial fractions. Each partial fraction represents a simple first-order differential equation; the output of a given transfer function may be determined by summing the solutions of each of the first-order equations, according to the partial fraction expansion. The differential equations representing a transfer function with two real zeros and two real poles will be developed as an example.

$$\frac{e_o(s)}{e_i(s)} = \frac{(\tau_1 s+1)(\tau_2 s+1)}{(\tau_3 s+1)(\tau_4 s+1)} \tag{V.2}$$

The partial fraction expansion is obtained by using the procedures outlined in Reference (Five-1).

$$\frac{e_o(s)}{e_i(s)} = \frac{\tau_1\,\tau_2}{\tau_3\,\tau_4} + \frac{C}{\tau_3 s+1} + \frac{D}{\tau_4 s+1} \tag{V.3}$$

where

$$C = \frac{(\tau_3-\tau_1)(\tau_3-\tau_2)}{\tau_3(\tau_3-\tau_4)} \qquad\qquad D = \frac{(\tau_4-\tau_1)(\tau_4-\tau_2)}{\tau_4(\tau_4-\tau_3)} \tag{V.4}$$

194

TABLE V-1,
CONVERSION OF COMPLEX TRANSFER FUNCTIONS TO REAL TIME DIFFERENTIAL EQUATIONS

No.	Transfer Function	Description	Partial Fraction Expansion	Definition of Constants	Differential Equation	Output
1.	$\dfrac{e_o}{e_i} = \dfrac{1}{T_1 s^n + T_2 s^{n-1} + \cdots + T_n s + 1}$	Real or Complex Poles, No Zeros	Not Required	Not Required	$T_1 \dfrac{d^n e_o}{dt^n} + T_2 \dfrac{d^{n-1} e_o}{dt^{n-1}} + \cdots + T_n \dfrac{de_o}{dt} + e_o = e_i$	Obtained From Direct Solution of The Differential Eq.
2.	$\dfrac{e_o}{e_i} = \dfrac{T_2 s + 1}{T_1 s + 1}$	1 Real Pole, 1 Real Zero	$\dfrac{e_o}{e_i} = \dfrac{T_2}{T_1} + \dfrac{T_1 - T_2}{T_1}\left(\dfrac{1}{T_1 s + 1}\right)$	Not Required	$\dot{y}_1 T_1 + y_1 = e_i$	$e_o = \dfrac{T_2}{T_1} e_i + \dfrac{(T_1 - T_2)}{T_1} y_1$
3.	$\dfrac{e_o}{e_i} = \dfrac{T_2 s + 1}{(T_3 s + 1)(T_4 s + 1)}$	2 Real Poles, 1 Real Zero	$\dfrac{e_o}{e_i} = \dfrac{A}{T_3 s + 1} + \dfrac{B}{T_4 s + 1}$	$A = \dfrac{T_2 - T_3}{T_4 - T_3}$, $B = \dfrac{T_2 - T_4}{T_3 - T_4}$	$\dot{y}_2 T_3 + y_2 = e_i$ $\dot{y}_3 T_4 + y_3 = e_i$	$e_o = A y_2 + B y_3$
4.	$\dfrac{e_o}{e_i} = \dfrac{(T_1 s + 1)(T_2 s + 1)}{(T_3 s + 1)(T_4 s + 1)}$	2 Real Poles, 2 Real Zeros	$\dfrac{e_o}{e_i} = \dfrac{T_1 T_2}{T_3 T_4} + \dfrac{C}{T_3 s + 1} + \dfrac{D}{T_4 s + 1}$	$C = \dfrac{(T_3 - T_1)(T_3 - T_2)}{T_3(T_3 - T_4)}$, $D = \dfrac{(T_4 - T_1)(T_4 - T_2)}{T_4(T_4 - T_3)}$	$\dot{y}_2 T_3 + y_2 = e_i$ $\dot{y}_3 T_4 + y_3 = e_i$	$e_o = \dfrac{T_1 T_2}{T_3 T_4} + C y_2 + D y_3$
5.	$\dfrac{e_o}{e_i} = \dfrac{(T_1 s + 1)(T_2 s + 1)}{(T_4 s + 1)(T_5 s + 1)(T_6 s + 1)}$	3 Real Poles, 2 Real Zeros	$\dfrac{e_o}{e_i} = \dfrac{E}{T_4 s + 1} + \dfrac{F}{T_5 s + 1} + \dfrac{G}{T_6 s + 1}$	$E = \dfrac{(T_4 - T_1)(T_4 - T_2)}{(T_4 - T_5)(T_4 - T_6)}$ $F = \dfrac{(T_5 - T_1)(T_5 - T_2)}{(T_5 - T_4)(T_5 - T_6)}$ $G = \dfrac{(T_6 - T_1)(T_6 - T_2)}{(T_6 - T_4)(T_6 - T_5)}$	$\dot{y}_5 T_4 + y_5 = e_i$ $\dot{y}_6 T_5 + y_6 = e_i$ $\dot{y}_7 T_6 + y_7 = e_i$	$e_o = E y_5 + F y_6 + G y_7$
6.	$\dfrac{e_o}{e_i} = \dfrac{(T_1 s + 1)(T_2 s + 1)(T_3 s + 1)}{(T_4 s + 1)(T_5 s + 1)(T_6 s + 1)}$	3 Real Poles, 3 Real Zeros	$\dfrac{e_o}{e_i} = \dfrac{T_1 T_2 T_3}{T_4 T_5 T_6} + \dfrac{H}{T_4 s + 1} + \dfrac{J}{T_5 s + 1} + \dfrac{K}{T_6 s + 1}$	$H = \dfrac{(T_4 - T_1)(T_4 - T_2)(T_4 - T_3)}{T_4(T_4 - T_5)(T_4 - T_6)}$ $J = \dfrac{(T_5 - T_1)(T_5 - T_2)(T_5 - T_3)}{T_5(T_5 - T_4)(T_5 - T_6)}$ $K = \dfrac{(T_6 - T_1)(T_6 - T_2)(T_6 - T_3)}{T_6(T_6 - T_4)(T_6 - T_5)}$	$\dot{y}_5 T_4 + y_5 = e_i$ $\dot{y}_6 T_5 + y_6 = e_i$ $\dot{y}_7 T_6 + y_7 = e_i$	$e_o = \dfrac{T_1 T_2 T_3}{T_4 T_5 T_6} + H y_5 \\ + J y_6 + K y_7$
7.	$\dfrac{e_o}{e_i} = \dfrac{T_1^2 s^2 + T_2 s + 1}{(T_1 s + 1)^2}$	Notch Filter, T is Real	$\dfrac{e_o}{e_i} = 1 - \dfrac{B}{T_1 s + 1} + \dfrac{2}{(T_1 s + 1)^2}$	Not Required	$\dot{y}_8 T + y_8 = e_i$ $\ddot{y}_9 T^2 + 2T\dot{y}_9 + y_9 = e_i$	$e_o = e_i - 2 y_8 + 2 y_9$
8.	$\dfrac{e_o}{e_i} = \dfrac{T_1 s^2 + T_2 s + 1}{T_3 s^2 + T_4 s + 1}$	Filter	$\dfrac{e_o}{e_i} = \dfrac{T_1}{T_3} + \dfrac{(T_2 - \frac{T_1 T_4}{T_3})s + (1 - \frac{T_1}{T_3})}{T_3 s^2 + T_4 s + 1}$	$L = \dfrac{T_1}{T_3}$ $M = T_2 - \dfrac{T_1 T_4}{T_3}$ $N = 1 - \dfrac{T_1}{T_3}$	$T_3 \ddot{y}_{10} + T_4 \dot{y}_{10} + \int y_{10}\,dt = e_i$ $T_3 \ddot{y}_{11} + T_4 \dot{y}_{11} + y_{11} = e_i$	$e_o = A e_i + B y_{10} + C y_{11}$

and the term $\tau_1\tau_2/\tau_3\tau_4$ is the value of the transfer function as s approaches infinity.

The output of this transfer function may be written as:

$$e_o(s) = \frac{\tau_1\tau_2}{\tau_3\tau_4} \ e_1(s) + C \ y_2(s) + D \ y_3(s) \qquad (V.5)$$

where y_2 and y_3 are defined as follows:

$$y_2(s) = \frac{e_1(s)}{\tau_3 s + 1} \qquad (V.6)$$

$$y_3(s) = \frac{e_1(s)}{\tau_4 s + 1}$$

The differential equations represented by Equation (V.6) are:

$$\tau_3 \ \dot{y}_2(t) + y_2(t) = e_1$$

$$\tau_4 \ \dot{y}_3(t) + y_3(t) = e_1 \qquad (V.7)$$

The output of the transfer function is given by substituting the values of $y_2(t)$ and $y_3(t)$ into the following time-domain equation:

$$e_o(t) = \frac{\tau_1\tau_2}{\tau_3\tau_4} \ e_1(t) + C \ y_2(t) + D \ y_3(t) \qquad (V.8)$$

A representative group of transfer functions and the corresponding time domain equations have been developed in a similar fashion and are tabulated in Table V-1.

APPENDIX VI

A SECOND-ORDER SIMULATION OF THE EFFECT
OF AEROELASTICITY ON AUTOPILOT BEHAVIOR

A method of approximating the effect of aeroelasticity on the dynamic behavior of an autopilot in the SDF computer program will be developed in this appendix. The computations required for the simplified aeroelastic study are presented in order that they may be incorporated into a particular autopilot subprogram if such a study is desired. Such an aeroelastic modification was indicated in the typical autopilot formulation. However, these corrections have not been included in the computer program assembled to demonstrate the operation of that autopilot.

The purpose of this analysis is to generate an expression for the aeroelastic vibrations that would be sensed by body-mounted rate gyros. The equations are developed with the following assumptions.

1. The vibrations are excited only by control forces.

2. Only longitudinal and lateral vibrations are considered.

3. The amplitude of a given point may be represented by a second-order differential equation.

4. The aeroelastic angular rates at a given point may be directly superimposed upon the rigid-body angular rates.

The input data required for this study are:

1. The normalized lateral and longitudinal body-bending mode shapes for the first, second, and third modes.

2. The natural frequency and structural damping ratio of each mode.

3. Generalized force inputs, Z_i and Y_i, for the i-th mode in the x-z and x-y planes respectively.

The complex frequency expression for the instantaneous deflection of the point to which the normalized body bending curve is referenced may be written as:

$$z_i = \frac{Z_i}{s^2 + 2\zeta_{z_i}\,\omega_{z_i} + \omega_{z_i}^2} \qquad\qquad (VI.1)$$

$$y_i = \frac{Y_i}{s^2 + 2\zeta_{y_i}\,\omega_{y_i} + \omega_{y_i}^2}$$

197

where: ζ_{z_i}, ζ_{y_i} Structural damping ratio x-z and x-y planes respectively.

ω_{z_i}, ω_{y_i} Natural frequency, x-z and x-y planes respectively.

z_i, y_i Displacement of point to which the mode shape is normalized, x-z and x-y planes respectively.

The deflections z_i and y_i are obtained by solving the differential equations corresponding to (VI.1) and (VI.2).

The derivation which follows is based on the analyses of Reference (Six-1). Two body-mounted rate gyros have been arbitrarily located on the typical normalized body bending mode shapes of Figure (1). The objective of the derivation are to determine an expression for the aeroelastic body angular rates at the rate gyro body station. This will be accomplished by first determining the slope of the normalized bending curve at the rate gyro station. The actual slope at any instant is then obtained by the normalizing factors z_i and y_i. The rate of change of the actual slope is approximately equal to the aeroelastic body angular rate at the rate-gyro station.
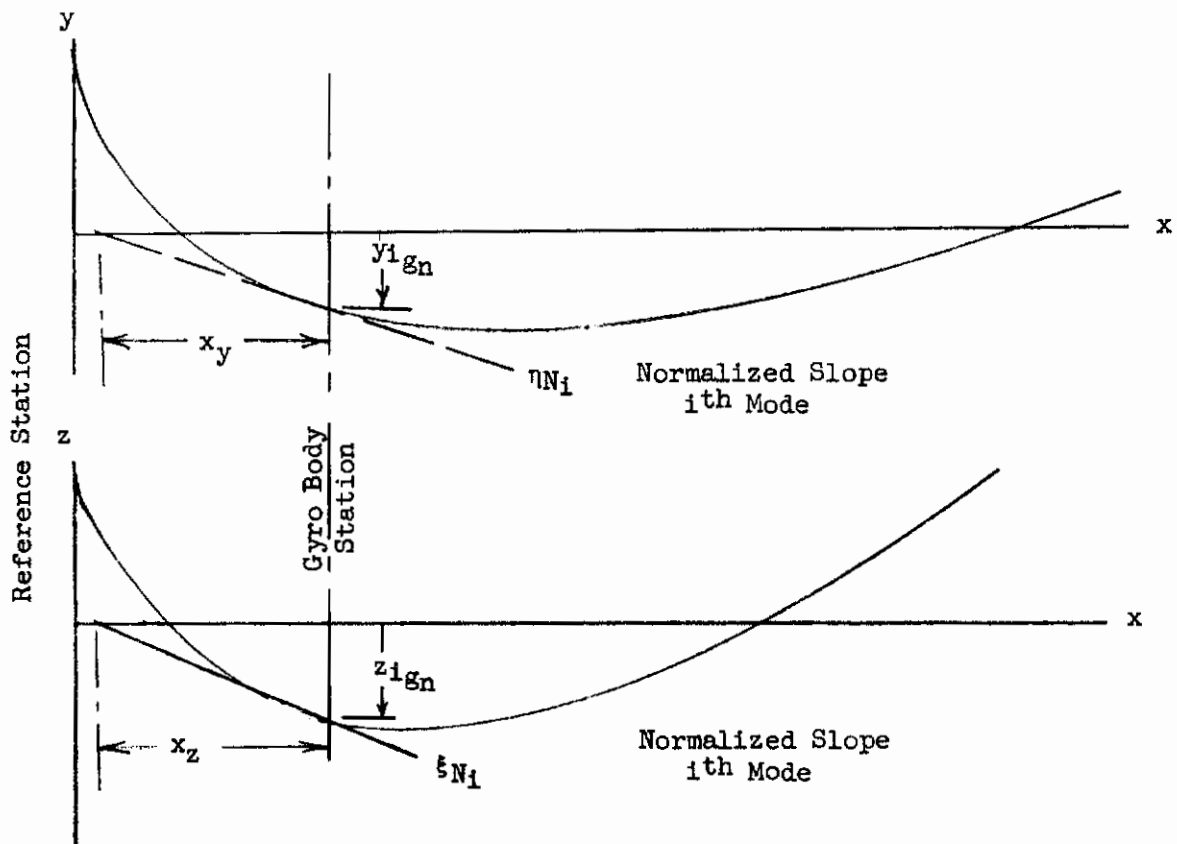

Figure 1 - Normalized Body-Bending Shapes

$z_{i_{gN}}$ and $y_{i_{gN}}$ represent the normalized displacement of the gyro body station in the x-z and x-y planes respectively. The instantaneous deflection of the gyro body stations may be determined by multiplying the normalized displacements by the deflection of the reference point as computed in Equations (VI.1) and (VI.2).

$$z_{i_g} = z_{i_{gN}} z_i \tag{VI.3}$$

$$y_{i_g} = y_{i_{gN}} y_i \tag{VI.4}$$

The slope of the normalized bending curve at the gyro station is:

$$\eta_{N_i} = \frac{y_{i_{gN}}}{x_y} \tag{VI.5}$$

$$\xi_{N_i} = \frac{z_{i_{gN}}}{x_z} \tag{VI.6}$$

The actual slope at any instant is obtained by combining Equations (VI.3) with (VI.6) and (VI.4) with (VI.5).

$$\eta_i = \frac{y_{i_g}}{x_y} = \eta_{N_i} y_i \tag{VI.7}$$

$$\xi_i = \frac{z_{i_g}}{x_z} = \xi_{N_i} z_i$$

The rate of change of the actual instantaneous slopes is:

$$\dot{\eta}_i = \eta_{N_i} \dot{y}_i \tag{VI.9}$$

$$\dot{\xi}_i = \xi_{N_i} \dot{z}_i \tag{VI.10}$$

For small amplitudes of oscillation, the slope of the tangent is approximately equal to the angle the tangent makes with the reference x-axis. Therefore, the aeroelastic angular body rates at the rate-gyro stations are:

$$q_{A_i} = \dot{\xi}_i \tag{VI.11}$$
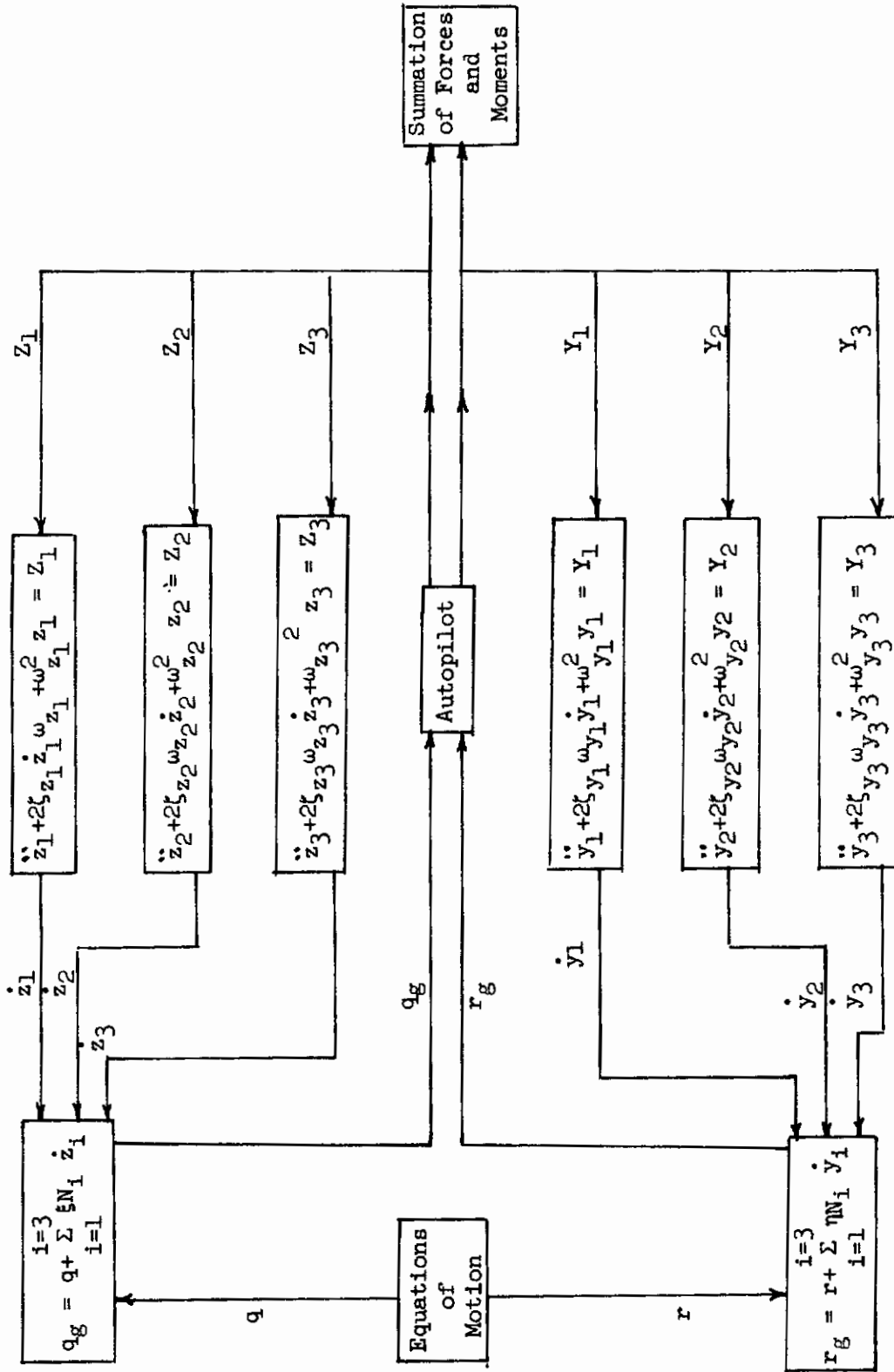
$$r_{A_i} = \dot{\eta}_i \tag{VI.12}$$

The output of the rate gyros are determined by adding the aeroelastic rates given in Equations (VI.11) and (VI.12) to the respective rigid-body angular rates, q and r

$$q_g = q + \sum_{i=1}^{i=3} \xi_{N_i} \dot{z}_i \tag{VI.13}$$

$$r_g = r + \sum_{i=1}^{i=3} \eta_{N_i} \dot{y}_i \tag{VI.14}$$

The computational flow sequence for the aeroelastic study is shown in Figure (2) on the following page.

Appendix Six, Figure 2   AEROELASTIC FUNCTIONAL BLOCK DIAGRAM

GEOPHYSICAL AND ENGINEERING CONSTANTS FOR THE
SIX-DEGREE-OF-FREEDOM FLIGHT-PATH STUDY COMPUTER PROGRAM

The geophysical and general engineering constants which have been incorporated in the SDF computer program design are summarized in the following table. References for these constants are also presented. Specific constants which are associated with a particular subprogram are discussed with that subprogram.

TABLE VII-1

ITEM AND SYMBOL	VALUE	UNITS	REFERENCE
Mathematical Constants			
π	3.14159265	-	Seven-1
e	2.71828183	-	Seven-1
Radian Measure			
$\pi/180$	0.01745329	Radian/Degree	Seven-1
$180/\pi$	57.2957795	Degree/Radian	Seven-1
Length			
International Nautical Mile	6076.1	Feet	Seven-2
Statute Mile	5280.0	Feet	Seven-2
1-Foot	0.3048	Meters	Seven-2
1 Meter	3.28083333	Feet	Seven-3
Properties of Planet Earth			
Rotational Angular Velocity = ω_p	$7.29211508 \times 10^{-5}$	Radian/Second	Seven-3
Equatorial Radius = R_{ea}	20,925,631.	Feet	Seven-3
Effective Radius at Latitude 45°32'33"	6,356,766.0	Meters	Seven-2
Properties of Reference Spheroid			
Equatorial Radius = R_e	20,926,428	Feet	Seven-1
Polar Radius = R_p	20,855,965	Feet	Seven-1
Gravitational Constants			
Reference Gravitational Acceleration = g_{ref}	32.174	Feet/Second^2	Seven-2
Geocentric Gravitational Constant = μ	1.407698×10^{16}	Feet^3/Second^2	Seven-3
Second Harmonic Coefficient = J	1623.41×10^{-6}	-	Seven-3
Third Harmonic Coefficient = H	6.04×10^{-6}	-	Seven-3
Fourth Harmonic Coefficient = K	6.37×10^{-6}	-	Seven-3
Miscellaneous Constants			
Stefan-Boltzman Constant = σ	$.4758 \times 10^{-12}$	BTU/(Sec-°R^4-Ft^2)	Seven-1
Degrees Rankine	1.8	°K	Seven-2
1 Astronomical Unit	9.289742538×10^7	Statute Miles	

REFERENCES FOR APPENDICES

One-1 Rosser, J. B., Newton, R. R., and Gross, G. L., <u>Mathematical Theory of Rocket Flight</u>, McGraw-Hill Book Co., Inc., New York, 1947.

One-2 Davis, L., Jr., Follin, J. W., Jr., and Blitzer, L., <u>The Exterior Ballistics of Rockets</u>, D. Van Nostrand Co., Princeton, N.J., 1958.

One-3 Barton, M. V., "Equations of Motion for Varying Mass Missiles", Texas University Report UT/DRL 79, 5 September 1946.

Two-1 Doolin, Brian F., "The Application of Matrix Methods to Coordinate Transformations Occurring in Systems Studies Involving Large Motions of Aircraft", NACA TN 3968, May 1957.

Two-2 Lass, H., <u>Vector and Tensor Analysis</u>, McGraw-Hill Book Co., Inc., 1950.

Three-1 TN-4065-51, U.S. Naval Ordnance Test Station, China Lake, California.

Four-1 BOCA Symposium Paper, "Aeroelastic Effects for a Wing Control Missile", Presented at NOTS, Pasadena, California, 13 May 1952.

Four-2 Fung, Y. C., <u>The Theory of Aeroelasticity</u>, John Wiley & Sons, Inc., New York, 1955.

Four-3 Bisplinghoff, R., Ashley, H., and Hoffman, R., <u>Aeroelasticity</u>, Addison-Wesley Pub., Co., Cambridge, Massachusetts, 1955.

Five-1 Truxall, John G., <u>Control System Synthesis</u>, McGraw-Hill Book Co., Inc., 1955.

Six-1 Honeywell Missile Development Lab Progress Report No. 4, "NASA Scout Guidance and Control", dated 15 July 1959.

Seven-1 Forsythe, W. E., "Smithsonian Physical Tables", 9th Ed., Smithsonian Institution, Washington, D.C., 1954.

Seven-2 Champion, K. S. W., Minzner, R. A., and Pond, H. T., "The ARDC Model Atmosphere, 1959", AFCRC-TR-59-267, August 1959.

Seven-3 Interim Report, Task 5, Project Mercury Contract NAS 1-204, 1959, Baker, Hilton, and others.